F 1503/2

BULETINUL INSTITUTULUI POLITEHNIC DIN IAȘI

Tomul XXXV (XXXIX)

Fasc. 1–2

Secția II

CHIMIE
ȘI
INGINERIE CHIMICĂ

1989

BULETINUL INSTITUTULUI POLITEHNIC DIN IAŞI

MŰSZAKI EGYETEM KÖZPONTI KÖNYVTÁRA 1893 MISKOLC

Tomul XXXV (XXXIX)

Fasc. 1–2

L: 041641

Secţia II

CHIMIE ŞI INGINERIE CHIMICĂ

1989

COLEGIUL DE REDACȚIE

Prof. dr. chim. **CAMELUȚA BELDIE** (președinte)
Prof. dr. ing. **ADRIAN RADU**
Prof. dr. ing. **M. GAFIȚANU**
Conf. dr. ing. **D. LIUȚE**
Prof. dr. doc. **D. MANGERON**
Prof. dr. ing. **GH. MAXIM**
Acad. prof. dr. doc. **CRISTOFOR SIMIONESCU**
Prof. dr. doc. **GH. CHIRIȚĂ**
Prof. dr. doc. **VALERIU BLIDARU**

Această fascicolă a apărut și cu sprijinul material al comitetului sindical și consiliului U.A.S.C.R. al Institutului politehnic din Iași

COMITETUL DE REDACȚIE AL SECȚIEI

II. **CHIMIE ȘI INGINERIE CHIMICĂ**

Prof. dr. doc. **RADU TUDOSE**
Prof. dr. **ANGELA POPA**
Prof. dr. ing. **I. ROȘCA**
Conf. dr. ing. **SPIRIDON OPREA**

REDACȚIA

Prof. dr. doc. **D. MANGERON**
(redactor responsabil)

Prof. dr. ing. **HUGO ROSMAN**
(secretar)

Conf. dr. ing. **VICTOR BULACOVSCHI**
(redactor)

ECATERINA IRIMIEA
(tehnoredactor)

BULETINUL INSTITUTULUI POLITEHNIC DIN IAŞI
BULLETIN OF THE POLYTECHNIC INSTITUTE OF JASSY
ИЗВЕСТИЯ ЯССКОГО ПОЛИТЕХНИЧЕСКОГО ИНСТИТУТА
Tomul XXXV (XXXIX), Fasc. 1–2 1989

Secţia II

CHIMIE ŞI INGINERIE CHIMICĂ

SUMAR

Pag.

N. CALU, M. BANGOURA şi I. BERDAN, Studiul sistemului de reacţie Al(III) — hemateină (franc., rez. rom.) 1
D. BÎLBĂ, N. BÎLBĂ, A. BOLD şi I. BERDAN, Separarea ionilor de Al(III), Ga(III), In(III) şi Tl(III) pe celuloze fosfat prin cromatografie pe coloană (franc., rez. rom.) 7
A. BOLD, A. POPA, M. GĂBURICI, E. POPOVICI şi M. CRUCEANU, Site moleculare NaX faze staţionare în cromatografia pe strat subţire (III) (engl., rez. rom.) 13
T. ONOFREI, Sorbţia şi separarea Sr(II) şi Ba(II) pe 4(4′-azobenzilceluloza) 1-hidroxi-2-carboxibenzen (engl., rez. rom.) 19
A. TARHON şi GH. IONESCU, Eliminarea catalitică a oxigenului din amestecul azot—hidrogen—oxigen utilizat în sinteza amoniacului (engl., rez. rom.) 23
T. ONOFREI, V. DULMAN, L. ODOCHIAN şi V. ŞUNEL, Determinarea gravimetrică a trietilentetraaminei (engl., rez. rom.) 29
I. CURIEVICI, V. NICU, ŞT. UNGUREANU, C. PETRILĂ, R. DIACONESCU, M. NICU, E. IONESCU şi S. MATACHE, Modelul matematic al instalaţiei de fabricare a acidului adipic (I) (franc., rez. rom.) 35
I. CURIEVICI, V. NICU, C. PETRILĂ, ŞT. UNGUREANU, R. DIACONESCU, M. NICU, E. IONESCU şi S. MATACHE, Modelul matematic al instalaţiei de fabricare a acidului adipic (II) (franc., rez. rom.) . . . 43
F. MUSTAŢĂ, R. TUDOSE şi E. COSTEA, Studiul experimental al transferului termic la curgerea în filme subţiri de lichide nenewtoniene (engl., rez. rom.) 53
I. SIMINICEANU, Selectarea şi proiectarea compresoarelor pentru industria amoniacului (engl., rez. rom.) 59
C. HAGIU, Îngrăşăminte ureo-fosfatice, (engl., rez. rom.) 65
ST. PETRESCU, C. CALISTRU şi AL. SZÉP, Cinetica dizolvării KCl în soluţie de sulfat de amoniu (engl., rez. rom.) 71
S. IFRIM, C. LUCHIAN şi M. BOURCEANU, Determinarea unor caracteristici ale uleiului de tall brut (franc., rez. rom.) 79
AL. CAŞCAVAL, 2-Hidroxicetone (XVIII) (engl., rez. rom.) 85
V. BULACOVSCHI şi M. GROVU-IVĂNOIU, Policondensarea directă a acizilor cicloalcandicarboxilici cu diaminele aromatice în prezenţa de trifenilfosfit (engl., rez. rom.) 89
I. MAZILU, L. TĂTARU, I. COCÎRLĂ, C. PETRESCU şi T. LIXANDRU, Contribuţii la sinteza, polimerizarea şi copolimerizarea unor monomeri vinilici *p*-substituiţi (engl., rez..rom.) 95

BULETINUL INSTITUTULUI POLITEHNIC DIN IAŞI
BULLETIN OF THE POLYTECHNIC INSTITUTE OF JASSY
ИЗВЕСТИЯ ЯССКОГО ПОЛИТЕХНИЧЕСКОГО ИНСТИТУТА
Tome XXXV (XXXIX), Fasc. 1–2 1989

Section II

CHEMISTRY AND CHEMICAL ENGINEERING

CONTENTS

Pp.

N. CALU, M. BANGOURA et I. BERDAN, Étude du système de réaction Al(III) — hemateïne (French, Romanian summary) 1
D. BÎLBĂ, N. BÎLBĂ, A. BOLD et I. BERDAN, Séparation des ions Al(III), Ga(III), In(III) et Tl(III) sur des celluloses phosphate par chromatographie sur colonne (French, Romanian summary) 7
A. BOLD, A. POPA, M. GĂBURICI, E. POPOVICI and M. CRUCEANU, Molecular Sieves NaX as Stationary Phases for Thin Layer Chromatography (III), (English, Romanian summary) 13
T. ONOFREI, Sr(II) and Ba(II) Sorption and Separation on 4(4'-Azobenzylcellulose) 1-hydroxy-2-carboxybenzene (English, Romanian summary) . . . 19
A. TARHON and GH. IONESCU, Catalytic Removal of Oxygen from the Nitrogen — Hydrogen — Oxygen Mixture Used in the Ammonia Synthesis (English, Romanian summary) 23
T. ONOFREI, V. DULMAN, L. ODOCHIAN and V. ŞUNEL, Gravimetric Determination of Triethylenetetramine (English, Romanian summary), ... 29
I. CURIEVICI, V. NICU, ŞT. UNGUREANU, C. PETRILĂ, R. DIACONESCU, M. NICU, E. IONESCU et S. MATACHE, Le modèle mathématique de l'installation de fabrication de l'acide adipique (I) (French, Romanian summary) 35
I. CURIEVICI, V. NICU, C. PETRILĂ, ŞT. UNGUREANU, R. DIACONESCU, M. NICU, E. IONESCU et S. MATACHE, Le modèle mathématique de l'installation de fabrication de l'acide adipique (II) (French, Romanian summary) 43
F. MUSTAŢĂ, R. TUDOSE and E. COSTEA, Experimental Study on Meat Transfer in Thin Films of Non-newtonian Liquids (English, Romanian summary) 53
I. SIMINICEANU, Selection and Design of the Compressors for Ammonia Industry (English, Romanian summary) 59
C. HAGIU, Urea-Ammonium Phosphates Fertilisers (English, Romanian summary) 65
ST. PETRESCU, C. CALISTRU and AL. SZÉP Kinetics of KCl Dissolving in Ammoniun Suphate Solution (English, Romanian summary) 71
S. IFRIM, C. LUCHIAN et M. BOURCEANU, Détermination de quelques caractéristiques du talloïl brut (French, Romanian summary) 79
AL. CAŞCAVAL, 2-Hydroxyketones (XVIII) (English, Romanian summary) . 85
V. BULACOVSCHI and M. GROVU-IVĂNOIU, Direct Polycondensation of Cycloaliphatic Dicarboxylic Acids with Diamines Catalysed by Triphenyl Phosphite (English, Romanian summary) 89
I. MAZILU, L. TĂTARU, I. COCÎRLĂ, C. PETRESCU and T. LIXANDRU, Contributions to the Synthesis, Polymerization and Copolymerization of some *p*-Substituted Vinylic Monomers (English, Romanian summary) 95

BULETINUL INSTITUTULUI POLITEHNIC DIN IAŞI
BULLETIN OF THE POLYTECHNIC INSTITUTE OF JASSY
ИЗВЕСТИЯ ЯССКОГО ПОЛИТЕХНИЧЕСКОГО ИНСТИТУТА
Том XXXV (XXXIX), вып. 1—2 1989

Секция II

ХИМИЯ И ХИМИЧЕСКАЯ ПРОМЫШЛЕНОСТЬ

СОДЕРЖАНИЕ

Стр.

Н. КАЛУ, М. БАНГУРА и И. БЕРДАН, Изучение реакционного система Al (III)—гематоин (франц., рез. рум.) 1

Д. БЫЛБЭ, Н. БЫЛБЭ, А. БОЛД и И. БЕРДАН, Сепарация ионов Al (III), Ga (III), In (III) и Tl (III) на фосфатных целлюлоз в холонновой хромотографии (франц., рез. рум.) 7

А. БОЛД, А. ПОПА, М. ГЭБУРИЧ, Е. ПОПОВИЧ и М. КРУЧЯНУ, Молекулярные сита для тонкослойной хроматографии. Расделение органических красителей (англ., рез. рум.) 13

Т. ОНОФРЕЙ, Сорбция и отделения Sr (II) и Ba (II) на 4 (4′-азобензилцеллюлозе) 1-гидрокси-2- карбоксибензене (англ., рез. рум.) 19

А. ТАРХОН и Г. ИОНЕСКУ, Каталитическое устранение кислорода из N_2-H_2 смеси употребляющий в синтезе аммиака (англ., рез. рум.) 23

Т. ОНОФРЕЙ, В. ДУЛМАН, Л. ОДОКЯН и В. ШУНЕЛ, Гравиметрическое определение триэтилентетраамина (англ., рез. рум.) 29

И. КУРЬЕВИЧ, В. НИКУ, ШТ. УНГУРЯНУ, К. ПЕТРИЛЭ, Р. ДИАКОНЕСКУ, М. НИКУ, Е. ИОНЕСКУ и С. МАТАКЕ, Математический модель для установки для фабрикации адипинного кислота (I) (франц., рез.рум.) 35

И. КУРЬЕВИЧ, В. НИКУ, С. ПЕТРИЛЭ, ШТ. УНГУРЯНУ, Р. ДИАКОНЕСКУ, М.НИКУ, Е. ИОНЕСКУ и С. МАТАКЕ, Математический модель установки для фабрикауии адипинного кислота (II) (франц., рез. рум.) 43

О. МУСТАЦЭ, Р. ТУДОСЕ и Е. КОСТЯ, Экспериментальное изучение переноса теплоты в тонких пленок (англ., рез. рум.) 53

И. СИМИНИЧЯНУ, Выборка и проэктирование компрессоров для производства аммиака (англ., рез. рум.) 59

К. ХАДХИУ. Карбоамофос (англ., рез. рум.) 65

С. ПЕТРЕСКУ, К. КАЛИСТРУ и А. СЕП, Растворение KCl в растворе сульфата аммония (англ., рез. рум.) 71

С. ИФРИМ, К. ЛУКЯН и М. БОУРЧЯНУ, Определение некоторых характеристик таллового масла (франц., рез. рум.) 79

АЛ. КАШКАВАЛ, 2-гидроксикетоны (XVIII) (англ., рез. рум.) 85

В. БУЛАКОВСКИЙ и М. ГРОВУ-ИВЭНОЮ, Прямая поликонденсация циклоалифатических дикарбоновых кислот с диаминами в присутствии трифенилфосфита (англ., рез. рум.) 89

И. МАЗИЛУ, Л. ТЭТАРУ, И. КОКЫРЛЭ, К. ПЕТРЕСКУ и Т. ЛИСКАНДРУ, Вклад в синтезе, полимеризации и сополимеризации некоторых виниловых *p*-замещенных мономеров (англ., рез. рум.) . 95

BULETINUL INSTITUTULUI POLITEHNIC DIN IAŞI
Tomul XXXV (XXXIX), fasc. 1—2, 1989
Secţia II
CHIMIE ŞI INGINERIE CHIMICĂ

C.D. 661.862 ; 541.4

ÉTUDE DU SYSTÈME DE RÉACTION Al(III)—HEMATÉINE

PAR

N. CALU, M. BANGOURA et I. BERDAN

1. Introduction

Dans la réaction entre l'ion Al(III) et l'hématéine se forment, successivement, des complexes solubles. En général, l'évolution de ce système de réaction s'accorde avec le principe de la compatibilité des acides L e w i s avec les bases L e w i s, à savoir, les acides de classe *a* (Al^{3+}, Ti^{4+}, etc.) préfèrent à la coordination les ligands contenant des atomes fortement électronégatifs tel que l'atome d'oxygène de la molécule d'hématéine [1]...[3].

Bien que la formation des complexes dans le système mentionné ci-dessus est utilisée dans des buts analytiques [4], on ne trouve pas dans la littérature des recherches complètes, approfondies, sur la stabilité et la structure des espèces formées. En ce sens, le présent travail apporte de nouvelles informations concernant le processus de coordination de l'hématéine à l'ion Al(III).

2. Partie expérimentale

Les processus de formation des complexes entre l'ion Al(III) et l'hématéine ont été étudiés en milieu d'eau — alcool éthylique, dans des rapports qui varient entre 4 : 1 et 1 : 1,5. Les conditions de réaction ont été les suivantes :

$AlCl_3$: $c = 1 \cdot 10^{-4} ... 2 \cdot 10^{-3}$ moles/l ;

Hématéine : $c = 1 \cdot 10^{-4} ... 2 \cdot 10^{-3}$ moles/l ;

Solution tampon : CH_3COOH—$NaCH_3COO$, ayant des valeurs du pH différentes.

Les processus de formation des complexes ont été suivis par voie spectroscopique, les mesures d'absorbance étant effectuées à l'aide d'un spectrophotomètre de type SPEKORD UV—VIS, Carl Zeiss—Jena. Pour les mesures de pH on a utilisé un pH-mètre PHM—Radiometer Copenhague.

3. Résultats et discussions

3.1. Le caractère acido-basique de l'hematéine

Le caractère acido-basique de l'hématéine a été investigué par titrages pH-métriques avec une solution de KOH, dans des systèmes de concentrations différentes (Fig. 1 et 2) :

Sur les courbes de titrage pH-métrique de l'hématéine on met en évidence la neutralisation de celle-ci, qui correspond à l'ionisation successive de deux protons.

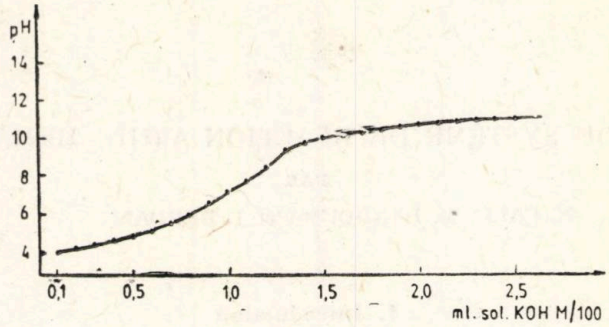

Fig. 1. — Titrage pH-métrique de l'hématéine avec KOH, en milieu eau—alcool éthylique, 4 : 1. Hématéine — 5 ml de concentration $2 \cdot 10^{-3}$ moles/l ; KOH—$2 \cdot 10^{-2}$ moles/l ; $t = 18°C$.

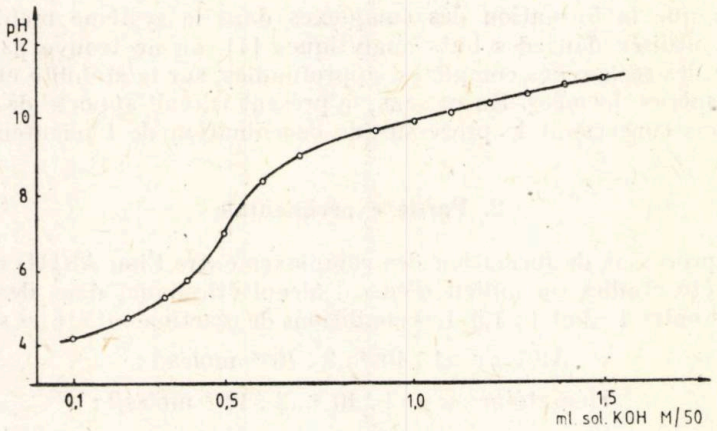

Fig. 2. — Titrage pH-métrique de l'hématéine avec KOH, en milieu eau—alcool éthylique, 4 : 1. Hématéine — 5 ml de concentration $1 \cdot 10^{-3}$ moles/l ; KOH — $1 \cdot 10^{-2}$ moles/l ; $t = 18°C$.

Les constantes d'acidité de l'hématéine, calculées à partir des déterminations pH-métriques, ont les valeurs :

$$pK_{a1} = 4{,}99 \text{ et } pK_{a2} = 5{,}31.$$

3.2 La formation de complexes dans le système Al(III) — hématéine

La formation de complexes dans le système Al (III)—hématéine a été étudiée par voie spectrophotométrique.

L'hématéine libre présente, dans le domaine visible du spectre électronique, une bande d'absorption avec $\lambda_{max} = 22\,300\ cm^{-1}$. À la suite de sa coor-

dination avec l'ion Al(III), dans le spectre apparait un effet batochrôme dont la grandeur dépend de la composition du milieu de réaction. La bande à transfert de charge, caractéristique du complexe formé, située à $\lambda_{max} = 19\,680\ cm^{-1}$, est proportionnelle à la concentration du complexe (Fig. 3).

a) *La composition des complexes du système Al(III)—hématéine*

Dans la réaction entre l'ion Al^{3+}_{aq}. (M) et l'hématéine (L), les complexes se forment successivement. Pour la détermination de leur composition on a utilisé des méthodes spectrophotométriques, en effectuant les mesures d'absorbance sur des solutions stabilisées dans le temps. Les solutions de réactants ont été préparées avec et sans système tampon.

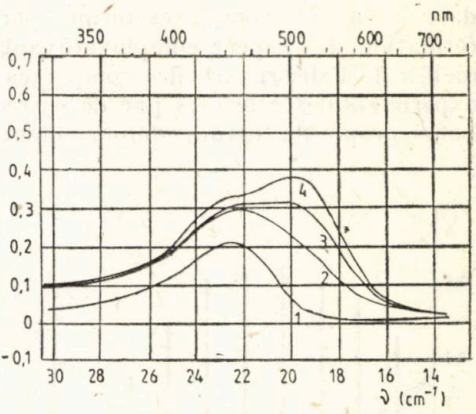

Fig. 3. — Spectres d'absorption enregistrés sur les solutions d'hématéine et de ses complexes avec Al(III), en milieu eau—alcool éthylique 2,33 : 1. Temps de réaction — 24 heures, cuve—0,2 cm ; *1* — Hématéine— 3.10^{-4} moles/l ; *2* — $1 \cdot 10^{-4}$ moles/l $AlCl_3$ — $3 \cdot 10^{-4}$ moles/l hématéine (1 M : 3 L) ; *3* — $2 \cdot 10^{-4}$ moles/l $AlCl_3$ — $3 \cdot 10^{-4}$ moles/l hématéine (1 M : 1,5 L) ; *4* — $3 \cdot 10^{-4}$ moles/l $AlCl_3$ — $3 \cdot 10^{-4}$ moles/l hématéine (1 M : 1 L).

Dans le cadre de la méthode des rapports molaires [5] on a effectué les déterminations expérimentales d'absorbance (A) tant pour $[M] = \text{const.}$ que pour $[L] = \text{const.}$ Les représentations graphiques des fonctions $A = f(L/M)$ et $A = f(M/L)$ sont données dans les Fig. 4 et 5. Les données ainsi obtenues mettent en évidence les étapes suivantes de réaction :

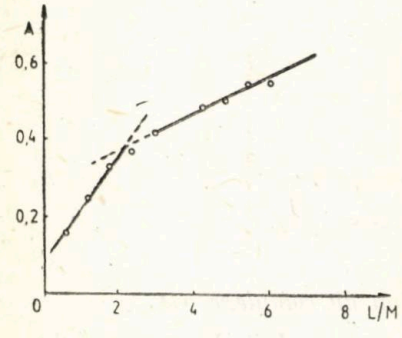

Fig. 4. — Représentation graphique de la fonction $A = f(L/M)$, pour le système Al(III) — hématéine, en milieu eau — alcool éthylique ; $[M] = 2 \cdot 10^{-4}$ moles/l; $\lambda = 19\,000\ cm^{-1}$; cuve—0,1 cm.

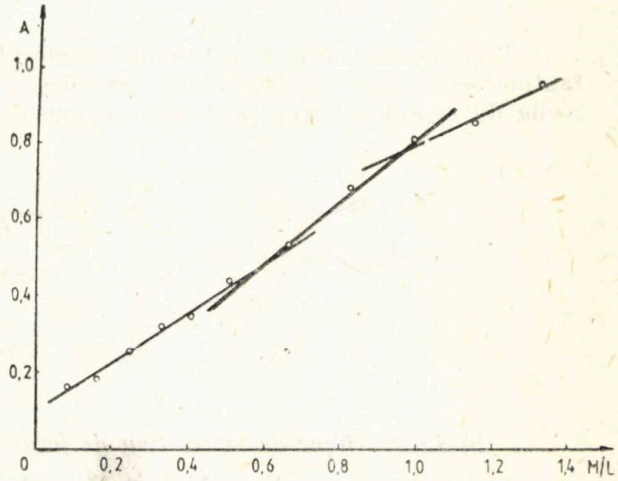

Fig. 5.—Représentation graphique de la fonction $A = f(M/L)$, pour le système Al(III) — hématéine, en milieu eau — alcool éthylique, 4,55 : 1 : $[L] = 3{,}6 \cdot 10^{-4}$ moles/l. Tampon : CH_3COOH — $NaCH_3COO$ (pH=4) ; temps de réaction — 2 heures ; $\lambda = 19\,350\ cm^{-1}$; cuve — 0,2 cm.

$$M+L \rightleftharpoons ML\,;\quad ML+L \rightleftharpoons ML_2.$$

Dans le cadre de la méthode des variations continues [6], peu utilisée dans le cas des complexes formés par étapes, on observe, en particulier, la formation de l'espèce complexe ayant un rapport molaire 1 : 1. Les valeurs réelles de l'absorbance des complexes ont été obtenues à partir des valeurs expérimentales affectées par de corrections qui tiennent compte de l'absorbance propre du ligand, conformément au procédé de la Fig. 6 *a* et 6 *b*.

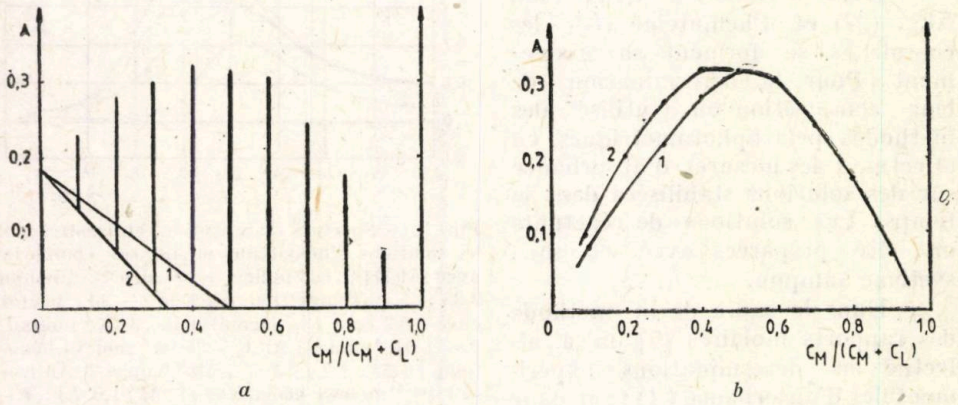

Fig. 6. — Représentation graphique de la fonction $A=f[C_M/(C_M+C_L)]$, pour le système Al(III) — hématéine : $C_M/(C_M+C_L)=1$; $AlCl_3$ — $4\cdot10^{-4}$ moles/l ; $C_M/(C_M+C_L)=0$; Hématéine — $4\cdot10^{-4}$ moles/l. Temps de réaction — 100 min. ; $\lambda = 19\,350$ cm^{-1} ; cuve — 0,2 cm ; *a* — élimination de l'absorbance du ligand des valeurs expérimentales, suivant les droites *1* (ML) et *2* (ML_2) ; *b* — la fonction $A = f[C_M/(C_M+C_L)]$ avec les valeurs correctées.

En se basant sur la structure de la molécule d'hématéine, avec ses formes tautomères et les représentations par des structures limites, la structure réelle du complexe ML_2 peut être conçue de la forme :

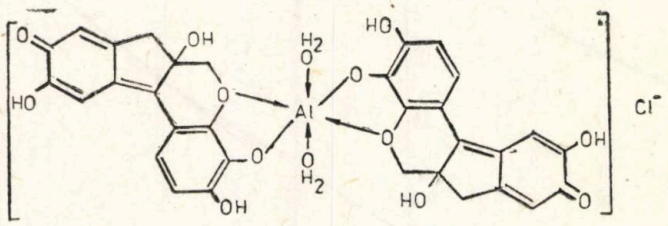

b) *La cinétique de la réaction de formation du complexe* ML_2

La réaction entre l'ion Al^{3+}_{aq} et l'hématéine se produit dans un certain intervalle de temps et est influencée par le pH du milieu de réaction.

Les calculs effectués à partir des mesures spectrophotométriques montrent que la réaction de formation des complexes commence suivant une ciné-

tique d'ordre 1, par rapport au métal, qui change dans le temps, avec une constante de vitesse qui dépend du pH de la solution (Tableau 1).

Tableau 1

Variation de la constante de vitesse en fonction du pH de la solution au cours de la formation des complexes dans le système Al(III) — hématéine

No.	pH	Constante de vitesse $k \cdot 10^2$ min.$^{-1}$
1	3,8	5,7
2	4,0	5,2
3	4,5	5,0
4	5,0	4,6
5	5,5	5,2
6	6,0	5,5

La diminution de la vitesse de réaction dans l'intervalle de pH =3,8...5,0 peut être corrélée avec l'état dissout du générateur de complexe qui passe dans des formes partiellement basiques, moins réactives, alors que son augmentation, à des pH plus élevés, est liée au processus prépondérent de déprotonation du ligand.

c) *La stabilité du complexe* ML_2

La stabilité du complexe ML_2 est appréciée à l'aide de la constante globale de stabilité, β_2, déterminée par mesures spectrophotométriques, propre à l'équation d'équilibre :

$$pM+qL \rightleftharpoons M_pL_q.$$

Ainsi, par application de la méthode Bent—French [7], en se basant sur la relation :

$$\log \beta_n = \log [M_pL_q] - p \log [M] - q \log [L],$$

on a obtenu la valeur

$$\beta_2 = 3{,}18 \cdot 10^8 \text{ l}^2 \cdot \text{moles}^{-2}.$$

En utilisant la méthode Edmonds—Birnbaum [8], partant de la relation :

$$\beta_n = (C_L^n \cdot A'' - C_{L''}^n A')/[C_L^n C_{L''}^n (A' - A'')]$$

on a obtenu les données indiquées dans le Tableau 2.

La valeur de la constante globale de stabilité, calculée par cette voie, est $\beta_2 = 0{,}47 \cdot 10^8$ l^2 . moles^{-2}. La constante globale moyenne, $\overline{\beta}_2 = 1{,}82 \cdot 10^8$ l^2 . moles^{-2}, indique une bonne stabilité pour le complexe ML_2 du système Al(III)—hématéine.

Tableau 2

Données concernant la stabilité du complexe ML_2 du système Al(III)—hématéine obtenues par la méthode Edmonds—Birnbaum

Paire de solutions	C_M moles/l	C_L moles/l	Absorbance A	β_n $l^n \cdot moles^{-n}$		
				$n=1$	$n=2$	$n=3$
1 2	$0{,}2 \cdot 10^{-3}$	$1{,}6 \cdot 10^{-4}$ $2{,}4 \cdot 10^{-4}$	0,35 0,47	$0{,}19 \cdot 10^{4}$	$0{,}45 \cdot 10^{8}$	$0{,}42 \cdot 10^{12}$
1 3	$0{,}2 \cdot 10^{-3}$	$1{,}6 \cdot 10^{-4}$ $3{,}2 \cdot 10^{-4}$	0,35 0,53	$0{,}29 \cdot 10^{4}$	$0{,}47 \cdot 10^{8}$	$0{,}38 \cdot 10^{12}$
2 3	$0{,}2 \cdot 10^{-3}$	$2{,}4 \cdot 10^{-4}$ $3{,}2 \cdot 10^{-4}$	0,47 0,53	$0{,}50 \cdot 10^{4}$	$0{,}49 \cdot 10^{8}$	$0{,}29 \cdot 10^{12}$

4. Conclusions

L'ion Al^{3+}_{aq} forme, successivement, avec l'hématéine, des complexes de type ML et ML_2. Le processus de formation des complexes a lieu suivant une cinétique d'ordre 1, par rapport au métal, qui change dans le temps, avec une constante de vitesse qui dépend du pH de la solution.

Les deux premières constantes d'acidité de l'hématéine sont : $pK_{a1} = 4{,}99$ et $pK_{a2} = 5{,}31$.

Dans la structure des complexes ML et ML_2 se trouvent des cycles spécifiques aux complexes internes.

La constante globale de stabilité du complexe ML_2, calculée à partir des données spectrophotométriques, est $\beta_2 = 1{,}82 \cdot 10^8\ l^2 \cdot moles^{-2}$.

Reçue le 13 février 1987

Institut Polytechnique, Jassy,
Chaire de Chimie Anorganique
Analytique
et Faculté d'Agronomie,
et
Jolo-Mamou, Guinée

BIBLIOGRAPHIE

1. Ahrland S., *Structure and Bonding*. Vol. **1**, Springer-Verlag, Berlin, Heidelberg, New-York, 1966.
2. Ahrland S., Chatt J., Davies N. R., Quart. Rev., **12**, 265 (1958).
3. Pearson R., J. Amer. Chem. Soc., **85**, 3533 (1963).
4. Singhal G. K., Taudon K. H., Talanta, **15**, 7, 707 (1968).
5. Yoe G., Jones A., Ind. Eng. Chem. Analyt. Ed., **16**, 11 (1944).
6. Job P., Ann. Chim. (France), *9*, 113 (1928) ; Ibid., *6*, 97 (1936).
7. Bent H. E., French C. L., J. Amer. Chem. Soc., **63**, 568 (1941).
8. Edmonds S. M., Birnbaum N., J. Amer. Chem. Soc., **63**, 1471 (1941).

STUDIUL SISTEMULUI DE REACȚIE Al(III) – HEMATEINĂ

(Rezumat)

Ionul Al^{3+}_{aq} formează cu hemateina combinații complexe solubile. Reacția de complexare se desfășoară în timp, corespunzător unei cinetici de ordinul 1, cu constanta de viteză depinzînd de mediul de reacție ; la pH = 5, valoarea constantei de viteză este $k = 4{,}6 \cdot 10^{-2}$ min.$^{-1}$

Compoziția complecșilor, determinată prin metode spectrofotometrice, corespunde formulelor generale ML și ML_2 (M=Al și L = hemateină). În structura moleculară a complecșilor se formează cicluri specifice complecșilor interni. Constanta globală de formare a complexului ML_2 este $\beta_2 = 1{,}82 \cdot 10^8\ l^2 \cdot mol.^{-2}$. Primele două constante de aciditate ale hemateinei sînt : $pK_{a1} = 4{,}99$ și $pK_{a2} = 5{,}31$.

BULETINUL INSTITUTULUI POLITEHNIC DIN IAŞI
Tomul XXXV (XXXIX), fasc. 1—2, 1989
Secţia II
CHIMIE ŞI INGINERIE CHIMICĂ

C.D. 66.067 85 ; 661.862 ; 564.681 : 547.256.82 ; 546.683

SÉPARATION DES IONS Al(III), GA(III), In(III) ET Tl(III) SUR DES CELLULOSES PHOSPHATE PAR CHROMATOGRAPHIE SUR COLONNE

PAR

DOINA BÎLBĂ, N. BÎLBĂ, ANIŞOARA BOLD et I. BERDAN

1. Introduction

La séparation de l'aluminium, du gallium, de l'indium et du thallium présente une grande importance tant au point de vue pratique — grâce à leur utilisation assez fréquente dans la technique moderne, qu'analytique — compte tenu que leurs propriétés physico-chimiques et de leurs combinaisons sont semblables.

La séparation complète des ions Al(III), Ga(III), In(III) et Tl(III) par échange ionique sur colonne a été éffectuée pour la première fois par K r a µ s et collaborateurs, en utilisant de la résine anionique Dowex-1 (Cl^-), en réalisant l'élution des éléments avec des solutions aqueuses d'acide chlorhydrique en fonction de la stabilité des chlorocomplexes formés [1].

Par voie expérimentale on constate que l'addition des solvants organiques à la solution chlorhydrique modifie le mécanisme de formation des chlorocomplexes et par conséquant les facteurs de séparation [2] ... [5]. Ainsi, en utilisant comme éluants les mélanges : acide chlorhydrique — alcools aliphatiques inférieurs, acide chlorhydrique — acétone, on a réalisé la séparation quantitative de l'aluminium, du gallium, de l'indium et du thallium sur des résines anioniques [6] et cationiques [7]...[9].

On mentionne toutefois que la séparation de ces éléments a été effectuée aussi bien et par chromatographie en couche mince sur des celluloses non-modifiées, en réalisant l'élution avec des mélanges acides halogénés — alcools [10] ou acides halogénés — acétone [11].

Dans ce qui suit on présente les résultats obtenus concernant la séparation de l'aluminium, du gallium, de l'indium et du thallium sur des celluloses phosphate, par chromatographie sur colonne.

2. Partie expérimentale

On a opéré avec des solutions de chlorures d'aluminium, de gallium, d'indium et de thallium (produits p.a.) standardisées, en utilisant des méthodes gravimétriques. Comme échangeurs d'ions on a utilisé deux sortes de cellulose phosphate dont les caractéristiques sont présentées dans le Tableau 1.

Les déterminations ont été effectuées tant dans des conditions statiques que dynamiques.

En conditions statiques, des échantillons pesant environ 0,5 g cellulose phosphate sont mis en contact avec 25 ml solution qui contient l'ion à échanger

(~1 mg) et des quantités variables d'acide chlorhydrique et de solvant organique. Après 24 heures, sous agitation intermitente, on sépare les phases et on détermine le contenu en ions de la solution par des méthodes spectrophotométriques appropriées.

Tableau 1

Propriétés caractéristiques des celluloses — échangeurs d'ions

Cellulose ionitique	Groupement échangeur d'ions	pK_a	Capacité d'échange m.éq./g	Valeur du pH pour la capacité maximum	
P_w-Serva	$-O-PO_3H_2$	6,6	0,74	1H	1,5
P_{11}-Whatman	$-O-PO_3H_2$	6,5 9,5	2,60 4,20	1H 2H	1,5 7,5

On exprime quantitativement la distribution d'ions à l'équilibre par l'intermédiaire du coefficient de distribution K_d.

La séparation est effectuée en faisant passer des mélanges qui contienent ~1 mg de chaque élément, par la colonne de cellulose ionitique imprégnée, préalablement, avec un éluant adéquat. L'éluant est ramassé à l'aide d'un collecteur automatique de fractions sous une vitesse d'écoulement de 0,5...1 ml/min. Après l'enlèvement du solvant par évaporation, chaque essai est soumis à l'analyse qualitative et quantitative.

3. Résultats et discussions

Les déterminations effectuées dans des conditions statiques ont mis en évidence l'influence de l'acidité du milieu et des solvants organiques (nature, concentration) sur la sorption des ions Al(III), Ga(III), In(III) et Tl(III) sur des celluloses phosphate [12], [13].

Les données expérimentales montrent que l'augmentation de la concentration de HCl dans la solution aqueuse, à l'équilibre, produit un diminution considérable de la sorption des ions et, par suite, les valeurs des coefficients de distribution peuvent être corrélées avec la capacité des ions de former des chlorocomplexes.

L'influence des solvants organiques sur la sorption des ions est dûe à la nature de ceux-ci (structure, constante diélectrique) et à leur concentration dans la solution initiale.

D'une manière générale, pour des fortes concentrations en HCl et solvant organique, les coefficients de distribution s'écartent sensiblement par rapport aux valeurs qui correspondent aux systèmes aqueuses.

Les résultats obtenus nous a permis de sélecter les meilleures conditions, pour séparer les éléments mentionnés ci-dessus.

3.1. Séparation des ions Al(III), Ga(III), In(III) et Tl(III) sur la cellulose P_w-Serva

Pour séparer les éléments sur la cellulose phosphate P_w-Serva on a utilisé comme éluants les mélanges suivants : HCl 0,01 M (20%) — méthanole (80%) et HCl 0,5 M (40%) — éthanole (60%).

Les valeurs des coefficients de distribution des ions Al(III), Ga(III), In(III) et Tl(III) sur la cellulose P_w dans le mélange HCl 0,01 M — méthanole (80%) sont présentées dans la Fig. 1. On observe que les différences entre les coefficients de distribution augmentent, les facteurs de séparation sont plus élevés et, par conséquent, le séparation s'améliore.

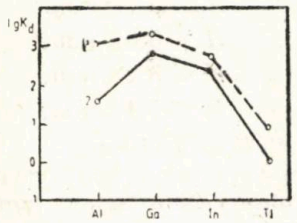

Fig. 1. — Distribution des ions Al(III), Ga(III), In(III), Tl(III) sur cellulose phosphate P_w-Serva: *1* — solution aqueuse HCl 0,01 M; *2* — mélange 20% HCl 0,01 M — 80% alcool méthylique.

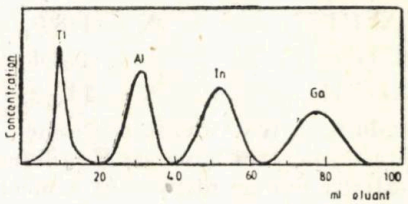

Fig. 2. — Séparation des ions Al(III), Ga(III), In(III), Tl(III) sur cellulose phosphate P_w-Serva avec l'éluant : 20% HCl 0,01 *M* — 80% alcool méthylique.

La séparation suggérée a été pratiquement vérifiée en passant un mélange synthétique qui contient ~1 mg de chacun des éléments sur une colonne avec $\varnothing = 10$ mm remplie avec 9 g cellulose P_w-Serva, la longueur du lit de sorbent étant égale à 750 mm.

Le mélange à séparer a été élué avec un volume total de 90 ml de mélange HCl 0,01 M — méthanole (80%). Les ions sont desorbés suivant l'ordre :

$$\text{Tl(III)} > \text{Al(III)} > \text{In(III)} > \text{Ga(III)}.$$

La courbe expérimentale d'élution est représentée dans la Fig 2.

Pour apprécier l'efficacité de séparation de la colonne chromatografique on a calculé le nombre de plateaux théoriques, N, ainsi que l'hauteur équivalente du plateau théorique, H.

Conformément à la théorie des plateaux, le nombre de passages effectives sorption — desorption ou le nombre de plateaux théoriques, N, on peut le calculer à l'aide de la relation :

$$N = 16\left(\frac{V_{max}}{w}\right)^2 = 8\left(\frac{V_{max}}{\beta}\right)^2 = \left(\frac{V_{max}}{\sigma}\right)^2,$$

où: V_{max} représente le volume de retention, [ml], (volume d'éluant qui correspond à la concentration maximum de l'ion désorbé) ; w — largeur de la bande d'élution, à la base de la curve G a u s s, mesurée entre les tangentes au points d'inflexion, [ml] ; σ — écartement standard en tant que mesure de la

dispersion de la zone ($w = 4\sigma$) ; β — largeur du pic chromatographique (de la bande d'élution) mesurée à l'hauteur de l'ordonné :

$$C = \frac{C_{max}}{e} = 0{,}368 C_{max}, \quad \beta = 2\sqrt{2}\,\sigma.$$

L'efficacité de la colonne chromatographique dépend de la hauteur du plateau théorique, $H = L/N$, où : L — longueur du lit de sorbent de la colonne, [mm] ; N — nombre de plateaux théoriques.

En appliquant ces relations pour la courbe expérimentale d'élution on obtient les valeurs ci-dessous :

Tl(III),	$N = 145{,}0$,	$H = 5{,}17$ mm,
Al(III),	$N = 148{,}0$,	$H = 5{,}07$ mm,
In(III),	$N = 143{,}4$,	$H = 5{,}2$ mm,
Ga(III),	$N = 147{,}2$,	$H = 5{,}1$ mm,

qui conduisent aux valeurs moyennes, $N = 145{,}9$ et $H = 5{,}14$ mm.

La valeur très basse de H indique une efficacité supérieure de la colonne chromatographique utilisée et concorde avec l'observation selon laquelle la grandeur H dépend du rayon des granules de l'échangeur.

Les valeurs des coefficients de distribution des ions Al(III), Ga(III), In(III) et Tl(III) lors de la sorption sur la cellulose phosphate P_w-Serva avec le mélange HCl 0,5 M — éthanole (60%) (Fig. 3) prouve la possibilité d'utiliser ce mélange comme éluant des ions ci-dessus.

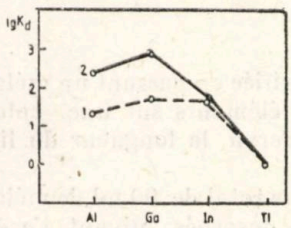

Fig. 3. — Distribution des ions Al(III), Ga(III), In(III), Tl(III) sur cellulose phosphate P_w-Serva: *1* — solution aqueuse HCl 0,5 M ; *2* — mélange 40% HCl 0,5 M — 60% alcool éthylique.

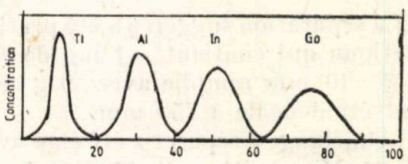

Fig. 4. — Séparation des ions Al(III), Ga(III), In(III) et Tl(III) sur cellulose phosphate P_w-Serva avec l'éluant 40% HCl 0,5 M — 60% alcool éthylique.

La séparation des ions a été réalisée à l'aide d'une colonne semblable à celle utilisée dans le cas précédent. l'ordre d'élution étant la suivante :

$$Tl(III) > In(III) > Al(III) > Ga(III).$$

La courbe expérimentale d'élution est représentée dans la Fig. 4.

3.2. Séparation des ions Al(III), Ga(III), In(III) et Tl(III) sur la cellulose phosphate P_{11}-Whatman

La séparation des ions sur la cellulose phosphate P_{11}-Whatman a été étudiée en utilisant les mélanges eau — solvant organique avec une acidité 1 M en HCl, qui contient 60% acétone, 40% tétrahydrofourane, respectivement 20% dioxane [13].

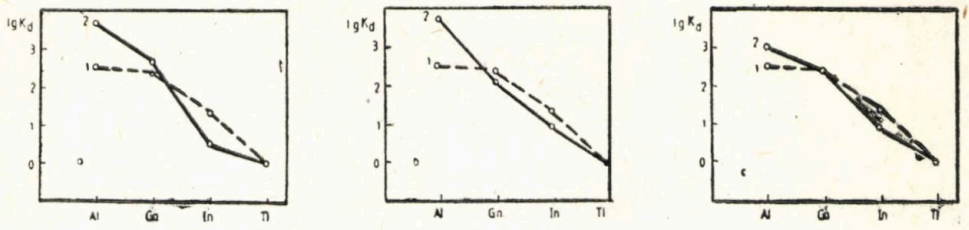

Fig. 5. — Distribution des ions Al(III), Ga(III), In(III), Tl(III) sur cellulose phosphate P_{11}-Whatman : *1* — solution aqueuse HCl 1 M ; *2* — solution HCl 1 M avec 60% acétone (*a*), 40% tétrahydrofuran (*b*) et 20% dioxane (*c*).

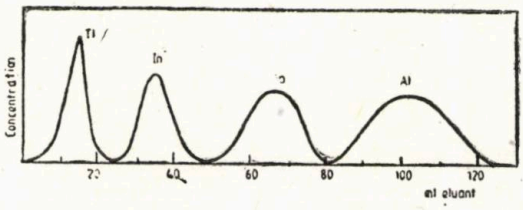

Fig. 6. — Séparation des ions Al(III), Ga(III), In(III) et Tl(III) sur colonne avec cellulose P_{11}-Whatman en utilisant comme éluant le mélange HCl 1 M — 60% acétone.

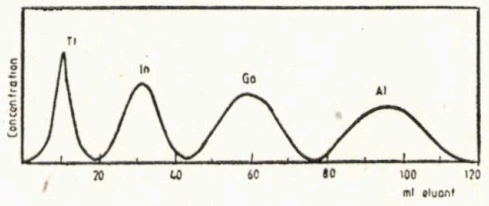

Fig. 7. — Séparation des ions Al(III), Ga(III), In(III) et Tl(III) sur cellulose P_{11}-Whatman avec l'éluant 60% HCl 1 M — 40% tétrahydrofurane.

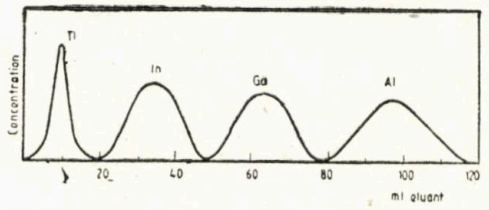

Fig. 8. — Séparation des ions Al(III), Ga(III), In(III) et Tl(III) sur cellulose P_{11}-Whatman avec l'éluant 80% HCl 1 M — 20% dioxane.

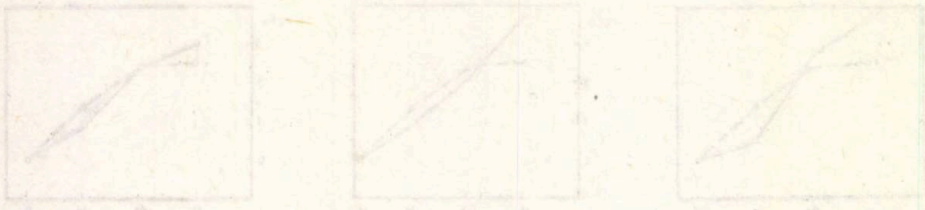

Les valeurs des coefficients de distribution lors de la sorption sur la cellulose P_{11} de la solution aqueuse 1 M d'acide chlorhydrique et respectivement des mélanges avec des solvants organiques sont présentées dans la Fig. 5.

La représentation graphique exige l'utilisation des systèmes à base de solvants organiques comme éluants pour la séparation quantitative des éléments étudiés.

Les séparations ont été effectuées sur une colonne avec la longueur $l = 500$ mm et le diamètre $\varnothing = 10$ mm, qui contient 7,5 g cellulose phosphate P_{11}-Whatman. Les courbes d'élution pour les trois (systèmes) mélanges sont symétriques, l'ordre d'élution étant le même à savoir :

$$Tl(III) > In(III) > Ga(III) > Al(III)$$

(v. Figs. 6...8).

Pour déterminer l'efficacité de la colonne chromatographique dans le cas de l'utilisation du mélange 40% HCl 1 M — acétone 60%, on a calculé les valeurs N et H :

Tl(III),	$N = 118{,}4$,	$H = 4{,}22$ mm,
In(III),	$N = 113{,}12$,	$H = 4{,}42$ mm,
Ga(III),	$N = 116{,}8$,	$H = 4{,}28$ mm,
Al(III),	$N = 121{,}6$,	$H = 4{,}11$ mm,

avec les valeurs moyennes $N = 117{,}5$ et $H = 4{,}26$ mm.

L'accroissement des facteurs de séparation des ions dans des mélanges eau — solvant organique par rapport aux systèmes aqueux est dû à la modification de la distribution des ions à échanger.

Les constituants organiques à basse polarité produisent, d'une part, la diminution, même la destruction de l'enveloppement de hydratation des ions, et d'autre part, l'imhibition préférentielle de la cellulose ionitique.

L'influence différente de la présence des solvants organiques exercée sur la séparation des ions étudiés dépend aussi de l'acidité du milieu.

4. Conclusions

1. L'étude du comportement à la sorption des ions Al(III), Ga(III), In(III) et Tl(III) sur des celluloses phosphate indique la possibilité de les séparer.

2. Les possibilités de séparation des éléments étudiés, sur des celluloses ionitiques, s'élargissent considérablement lorsqu'on utilise des mélanges eau—solvants organiques.

3. On a suggéré et vérifié par voie expérimentale les séparations suivantes : a) séparation des ions Al(III), Ga(III), In(III) et Tl(III) sur la cellulose phosphate P_w-Serva avec l'éluant 20% HCl 0,01 M — 80% alcool méthylique ou 40% HCl 0,5 M — 60% alcool éthylique ; b) séparation des ions Al(III), Ga(III), In(III) et Tl(III) sur la cellulose phosphate P_{11}-Whatman

avec HCl 1 M — solvant organique (60% acétone, 40% tétrahydrofurane ou 20% dioxane).

4. On a estimé l'efficacité des colonnes chromatographiques par le calcul des grandeurs N et H.

Reçue le 18 septembre 1987

Institut Polytechnique, Jassy,
Chaire de Chimie Anorganique
et Analytique

BIBLIOGRAPHIE

1. Kraus K. A., Nelson F., Smith G. W., J. Phys. Chem., **58**, 11 (1954).
2. Горокова А. Н., Алимарин И. П., Тинтевич Е. П., ЖНХ, **11**, 191 (1966).
3. Шишкова Л. Г., Докл. Болг. АН, **24**, *10*, 1 369; (1971); Ibid., **25**, *10*, 1371 (1972).
4. Казанцев Е. И., Плюснин А. В., Изв. ВУЗ, Хим. Технол., **12**, *2*, 300 (1974).
5. Тинтевич Е. П., Алимарин И. П., Горокова А. П., Вестник МГУ, серия Химия, **24**, *1*, 91 (1969).
6. Korkisch J., Hazan I., Analyt. Chem., **36**, *12*, 2308 (1964); Ibid., **27**, 707 (1965).
7. Strelow F.W.E., Van Zyl C.R., Bothma C.J.C., Analyt. Chim. Acta, **45**, *1*, 81 (1969).
8. Strelow F.W.E., Victor A. H., Talanta, **19**, *9*, 1019 (1972).
9. Strelow F.W.E., Talanta, **27**, *3*, 231 (1980).
10. Gagliardi E., Brodar B., Chromatographye, **2**, *6*, 267 (1969).
11. Soljic Z., Turina S., Z. analyt. Chem., **257**, *5*, 348 (1971).
12. Bîlbă D., Fişel S., Mikrochim. Acta, 985 (1974).
13. Фишел С., Былбэ Д., ЖАХ, **30**, *7*, 1 317 (1975)

SEPARAREA IONILOR DE Al(III), Ga(III), In(III) ŞI Tl(III) PE CELULOZE FOSFAT PRIN CROMATOGRAFIE PE COLOANĂ

(Rezumat)

Factorii de separare ai aluminiului (III), galiului (III), indiului (III), taliului (III) cresc considerabil în amestecuri apă—solvenţi organici.

Cu ajutorul unor coloane conţinînd celuloze fosfat (P_w şi P_{11}) şi eluanţi convenabili (amestecuri apă—solvenţi organici) s-au realizat separări cantitative ale celor patru elemente aflate în amestec.

BULETINUL INSTITUTULUI POLITEHNIC DIN IAŞI
Tomul XXXV (XXXIX), fasc. 1—2, 1989
Secţia II
CHIMIE ŞI INGINERIE CHIMICĂ

D.C. 544.84 ; 668.8

MOLECULAR SIEVES NaX AS STATIONARY PHASES FOR THIN LAYER CHROMATOGRAPHY

III. SEPARATION OF SOME ORGANIC DYES

BY

ANIŞOARA BOLD, ANGELA POPA, MARIA GĂBURICI, EVELINE POPOVICI and M. CRUCEANU

1. Introduction

Some results regarding the possibility and technique of preparation of a molecular sieves adhesive layer on glass plates for thin layer chromatography (S.L.C.) as well as the experimental data referring to the separation of certain inorganic cations and organic compounds have been reported in a previous paper [1].

Also the separation of some strong acid inorganic cations from mixture, having their diameter much larger than that of the access window in molecular sieve, has been investigated and some assumptions concerning the separation mechanism of them have been formulated. On the basis of some correlations between the R_f values and thermodynamic quantities of the ion-exchange in a solvent system as mobil phase it was found that in the case of the investigated cations, their migration and separation takes places by ion-exchange process [2].

The present paper deals with some theoretical and experimental aspects in connection with the separation on NaX zeolite of some weak ionic components with large geometrical size such as some acid or basic organic dyes.

2. Experimental

The molecular sieve, employed as stationary phase, was of the NaX type, supplied by Natrium Products Works, Govora, and preparation of plates as well as their developing was made as previously described [1].

The experiments were performed with 0.5% aqueous solutions of the following acid dyes : Red acid, Yellow *R* acid, Blue 5 *R* acid and basic dyes : Red melacryl *BL*, Yellow melacryl and Blue melacryl *BLK*.

The developing solvents were selected from M a c e k and P r o c h a z k a 's eluotropic series [3] and, localization and identification of the chromatographic spots was carried out visually.

3. Results and Discussion

In order to evaluate the separation ability of the selected solvents, first was made some tests according to microcircular technique developed by S t a h l [4] and R a n d e r a t h [5]. The results of the tests are sum-

marized in Table 1. As it can be seen in Table 1, in the selected solvents the two types of dyes do not exhibit large dissimilarities and in both cases the solvents with little polarity hinder the migration, while those with high polarity favour excessively it carrying the dye with their front. Consequently, the developings were carried out with binary or ternary mixtures of solvents, chosen in such a manner that the compensation of the two behaviours to be realized, using orientatively the calculated value of dielectric constant.

Table 1

Migration Behaviour of the Investigated Dyes in certain Solvents

Run	Solvent	Dielectric constant	Acid dyes			Basic dyes		
			*R**)	*G*	*A*	*R***)	*G*	*A*
1	Nitrobenzene	36.4	+	+	+	+	+	+
2	Methanol	31.2	∞	∞	∞	∞	∞	∞
3	Isopropanol	26.0	+	∞	∞	∞	+	∞
4	Ethanol	25.8	∞	∞	∞	∞	∞	∞
5	Acetone	21.5	∞	∞	∞	∞	∞	∞
6	Methyl ethyl ketone	18.0	+	+	+	+	+	+
7	Amyl alcohol	16.0	+	+	+	∞	∞	∞
8	Benzyl alcohol	13.0	+	∞	∞	∞	∞	∞
9	Chloroform	5.1	0	0	0	∞	0	∞
10	Toluene	2.3	0	0	0	+	0	+
11	Benzene	2.24	0	0	0	0	0	0
12	Heptane	1.97	0	0	0	0	0	0

*) *R* — Red acid ; *G* — Yellow acid ; *A* — Blue 5*R* acid.
**) *R* — Melacryl Red *BL* ; *G* — Melacryl yellow ; *A* — Melacryl blue *BLK*.
∞ — the spots migrate with the developant front ;
\+ — the spots migrate with different rates ;
0 — the spots do not migrate.

A part of the solvents systems and R_f values obtained experimentally are summarized in Tables 2 and 3.

On the basis of the data from Table 2, in some measure the qualitative observation referring to correlation with dielectric constant of the system is verified and at the same time we get informations that evidence the fact that the separation of dyes mixtures is possible only with solvents systems which have large dielectric constant. The systems which the dielectric constant less than 10, although according with the data in Tables 2 and 3, they allow a certain separation, however they cannot be employed practically because the differences between the R_f values for acid dyes are very low and, for basic dyes the resolution is not satisfactory enough.

In the systems with high dielectric constant the mixtures of acid dyes should be separated much better, for dielectric constants ranging from 13 to 26 and, the mixtures of the basic dyes in the systems with dielectric constant of 19...21.

Also, the result evidences the fact that from all investigated dyes only Yellow acid *R* is pure, all the other giving several chromatographic spots are impure.

Table 2

Solvents Systems and the R_f Values for Acid Dyes

Run	System of solvents	Ratio of solvents V/V	Dielectric constant ε	R_f		
				Red acid	Yellow acid *R*	Blue acid 5*R*
S_1	Nitrobenzene—Ethanol	3 : 1	33.7	0.95	0.92	0.95
S_2	Ethanol—Isopropanol	1 : 1	25.9	0.81 0.70	0.58	0.37 0.07
S_3	Nitrobenzene—Benzene—Heptane	4 : 2 : 1	21.7	0.28	0.11	0.46 0.41
S_4	Benzyl alcohol—Nitrobenzene	2 : 1	20.3	0.86 0.79	0.75	0.62 0.36
S_5	Methyl ethyl ketone—Acetone	1 : 1	19.7	0.73 0.68	0.68	0.64 0.47
S_6	Nitrobenzene—Toluene	1 : 1	19.4	0.20	0.10	0.36 0.30
S_7	Benzyl alcohol—Ethanol—Chloroform	2 : 1 : 1	14.2	0.71 0.60	0.65	
S_8	Benzyl alcohol—Amyl alcohol	2 : 1	13.9	0.74 0.70	0.66	0.52 0.46
S_9	Toluene—Methyl ethyl ketone — Acetone	1 : 1 : 1	13.8	0.41 0.30	0.21	0.46 0.18
S_{10}	Benzene—Methyl ethyl ketone —Acetone	4 : 2 : 1	9.5	0.11	0.08	0.12

Table 3

Solvents Systems and the R_f Values for Basic Dyes

Run	System of solvents	Ratio of solvents V/V	Dielectric constant ε	R_f		
				Melacryl red *BL*	Melacryl yellow	Melacryl blue *BLK*
S_1	Ethanol—Isopropanol	1 : 1	25.9	0.95 0.95 0.98	0.75	0.73
S_2	Nitrobenzene—Benzene—Heptane	4 : 2 : 1	21.7	0.64 0.45	0.42 0.31 0.16	0.80 0.52
S_3	Nitrobenzene—Toluene	1 : 1	19.4	0.62 0.52 0.41	0.39 0.33 0.15	0.79 0.56
S_4	Toluene—Methyl ethyl ketone — Acetone	1 : 1 : 1	13.8	0.82 0.55	0	0.47
S_5	Benzene—Methyl ethyl ketone — Acetone	4 : 2 : 1	9.5	0 0.87	0	0.79

The shape of the chromatographic spots (Fig. 1) and resolution obtained make possible utilization for analysis and separation of the mixture of acid dyes the systems with alcohols (S_2, S_8 — Table 2) and for basic dyes the systems of solvents with nitrobenzene and hydrocarbons (S_3 and S_5 — Table 3).

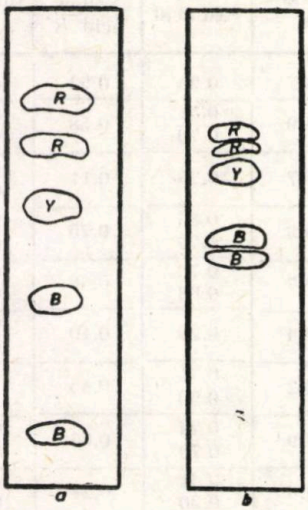

Fig. 1. — Separation of some mixtures of acid dyes on zeolite NaX : *a* — mobile phase: ethanol — isopropanol (1 : 1 V/V) ; *b* — mobile phase : benzyl alcohol — amyl alcohol (2 : 1 V/V).

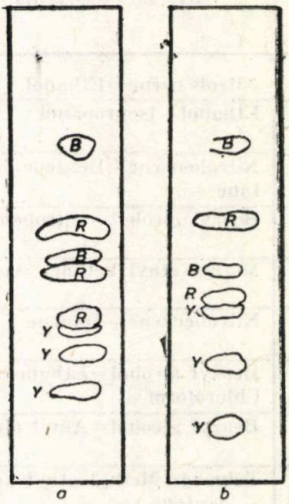

Fig. 2. — Separation of some mixtures of basic dyes on zeolite NaX : *a* — mobile phase : nitrobenzene — toluene (1 : 1 V/V) ; *b* — mobile phase : nitrobenzene — benzene — heptane (4:2:1, V/V).

Because in each class of dyes the migration rate and R_f value are dependent on the polarity of solvent system, it is clear that in this case the separation by S.L.C. on the molecular sieves NaX takes place according with an adsorption mechanism by interactions of multipolar type. Although, the investigated dyes, by their structure, has not a permanent dipole, e.g. Yellow acid *R*:

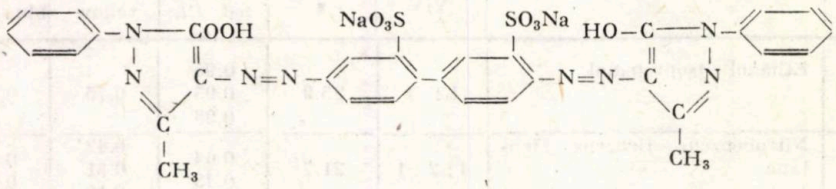

Yellow acid R

However, according to G o r e l [6], the molecules provided with polar groups can be adsorbed on the polar surface of stationary phase and, according to C h e s s i k *et al.* [7] statement, the value of adsorption energies of different polar groups in molecule is proportional to their dipolar moment. These general remarks, valid for stationary phases of different nature, in the case

of molecular sieves become more particulary, first, due to the strong polar character of the zeolite surface, caused by the OH groups bonded at silicon atoms in their structure and on the other hand due to the particular porosity structure of these adsorbants.

For example while in silicagel the porous structure has a large pores size distribution from any tens to any hundred of Angstroms, the value of mean diameter being almost 30...100 Å, at the molecular sieves this distribution includes only one pore size. In this case, the curve of Gaussian's distribution becomes a single line, which in the case, e.g. for the molecular sieve NaX, is situated at the value of 13 Å. Due to this fact, at inner adsorption surfaces are accessible only the molecules of geometrical size less than „zeolite windows". However, for investigated dyes the values regarding the molecule dimensions are not available due to their state in solution of different polarities , these data should have only an orientative value, but taking into account some known values, e.g. critical diameter of benzene (5.60 Å), as well as mobility of the molecular components around the chain axis, let us consider that on zeolite NaX with 13 Å windows, separation of the investigated dyes took place by an adsorption process of them in both inner and outer crystalline structure.

To verify these hypotheses, the separation attempts were carried out, under the same conditions, but with stationary phases made up of the molecular sieve NaA. These molecular sieves, having the window of 4 Å is sure that any access possibility of dye molecules inside the zeolite is excluded.

Table 4

Comparative Separations of Red Acid R and Blue Acid 5R on the Molecular Sieves NaX and NaA

System of solvents	Ratio of solvents V/V	Dielectric constant ε	R_f/NaX		R_f/NaA	
			Red acid *R*	Blue acid *R*	Red acid *R*	Blue acid *R*
Ethanol—isopropanol	1:1	25.9	0.81	0.37	∞	∞
Methyl ethyl ketone—acetone	1:1	19.7	0.73	0.64	∞	∞
Benzyl alcohol—amyl alcohol	2:1	13.8	0.74	0.52	∞	∞

The data of Table 4 show that independently from the dielectric constant of the employed solvents system, the tested dyes migrate with the solvent, fact that shows that in the case of zeolite NaA no adsorption phenomenon takes places, while on zeolite NaX the separation is due to this phenomenon.

At the same time, however the surface is equal polar, but separation takes place only on zeolite NaX, then we can make the remark that in the case of weak ionic components, their separation is carried out only by adsorption.

4. Conclusions

Investigation of the possibility of some acid and basic dyes to be analysed by S.L.C. on zeolite NaX has shown that separation can be realized with high resolution and that the R_f values depend on both dielectrical constant of mobil phase and the nature of the employed solvents. The separation of some weak ionic character organic components on zeolite NaX takes place according with a separation mechanism of adsorption, proving our initial hypothesis.

The developed method can be employed successfully for the purity determination of some dyes as well as for analysis of their mixtures.

Received, July 7, 1987

Polytechnic Institute, Jassy,
Department of Inorganic
and Analytical Chemistry
and
Department of General
Chemistry and Technology

REFERENCES

1. Bold A., Popa A., Cruceanu M., Popovici E., Rev. Chimie, **35**, *12*, 1123 (1984).
2. Bold A., Popa A., Cruceanu M., Găburici M., Popovici E., Rev. Roum. Chim. (sous presse),
3. Hais I. M., Macek K., *Cromatografia pe hîrtie*, (transl. from Czech.). Ed. Tehn., Bucureşti, 1960, 112.
4. Stahl E., *Dünnschicht-Chromatographie, ein Laboratoriumshandbuch*. II. Ed., Springer Verlag, Berlin, 1967, 125.
5. Randerath K., *Thin-Layer Chromatography*. Ed. II, Academic Press, New York, 1966, 53, 67.
6. Corel J. P., Bull. Soc. Chim. France, 653 (1964).
7. Chessik J. J., Canad. J. Chem., **33**, 251 (1965).

SITE MOLECULARE NaX FAZE STAŢIONARE ÎN CROMATOGRAFIA PE STRAT SUBŢIRE

III. Separarea unor coloranţi organici

(Rezumat)

S-a studiat posibilitatea de separare a unor coloranţi acizi şi bazici prin cromatografia pe strat subţire cu sită moleculară NaX.

S-au folosit mai multe sisteme de developare.

S-au calculat valorile R_f şi s-a stabilit că acestea depind atît de valoarea constantei dielectrice a sistemului de developare cît şi de natura solvenţilor componenţi ai acestuia.

Referitor la mecanismul de separare s-a formulat ipoteza că acesta se desfăşoară numai pe baza unui fenomen de adsorbţie moleculară.

BULETINUL INSTITUTULUI POLITEHNIC DIN IAŞI
Tomul XXXV (XXXIX), fasc. 1—2, 1989
Secţia II
CHIMIE ŞI INGINERIE CHIMICĂ

D.C. 621.928 ; 546.42 ; 546.431

Sr(II) AND Ba(II) SORPTION AND SEPARATION ON 4(4'-AZOBENZYLCELLULOSE)1-HYDROXY-2-CARBOXYBENZENE

BY

TINCA ONOFREI

1. Introduction

In several previous papers [1]...[3] we have published data referring to Be(II), Mg(II), Ca(II), Zn(II), Cd(II) and Hg(II) sorption and separation on 4(4'-azobenzylcellulose)1-hydroxy-2-carboxybenzene used as a chelating sorbent.

We carried these researches further, investigating Sr(II) and Ba(II) sorption on the same sorbent as well as the possibility of separating chromatographically these two elements.

2. Experimental

4(4'-azobenzylcellulose)1-hydroxy-2-carboxybenzene was obtained by diazotation of PAB-cellulose and coupling it with salicylic acid in a slightly alkaline medium.

In order to assess the mechanism of Sr(II) and Ba(II) sorption on 4(4'-azobenzylcellulose)1-hydroxy-2-carboxybenzene the following determinations have been made :

a) Dependence of distribution coefficients (K_d) vs. pH, at 25°C.

b) Sorption isotherms at 25°C.

c) Sorption isobars between 0° and 100°C.

d) Determination of apparent free enthalpy.

e) Reflectance electronic spectra.

f) IR spectra of the sorbent before and after sorption, between 400 and 4 000 cm^{-1}.

The distribution coefficients were determined by an equilibrium method that was reached by stirring 0.5 g sorbent with 20 cm^3 standard solution of $Sr(ClO_4)_2$ (70.4 μg Sr (II)/cm^3) and $Ba(ClO_4)_2$ (81.9 μg Ba(II)/cm^3) with a specified pH, at a constant temperature, for an hour. The solid phase was separated by filtering. The equilibrium pH (pH_e) was measured in the aqueous phase. Sr(II) and Ba(II) excess was spectrophotometrically determined by

the *o*-cresolphtaleincomplexone method [4]. For isotherms, standard solutions with concentrations ranging from 1.10^{-3} to 1.10^{-2} M were used.

3. Results and Discussions

From the study of the dependence of the distribution coefficients vs. pH, there follows that Sr(II) sorption increases gradually from $pH_e = 2.2$ (K_d=2.00) to $pH_e = 4.3$ ($K_d = 4.78$), while Ba(II) sorption increases from $pH_e = 2.8$ ($K_d = 2.17$) to $pH_e = 4.7$ ($K_d = 41.70$). For all the determinations the equilibrium pH was experimentally found to be lower than the pH of the solution that comes in touch with the sorbent.

The sorption isotherms for Sr(II) and Ba(II) (Fig. 1) assume different shapes. The sorption isotherm for Sr(II) shows an overlapping of the chemical sorption over the physical sorption, the latter being prevalent. The sorption isotherm for Ba(II) assumes a shape that pleads in favour of a combined process of physical and chemical sorption, chemosorption being prevalent.

The study of the sorption isobars for Sr(II) and Ba(II) (Fig. 2) lead to the same conclusions as in the previous case. The decrease of the distrib-

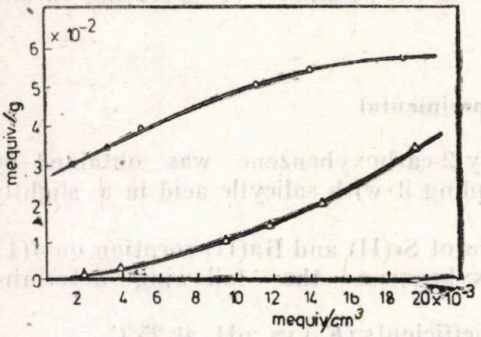

Fig. 1. — The sorption isotherms at $pH_e = 4.3$ and 25°C : Δ — Sr(II) ; o — Ba(II).

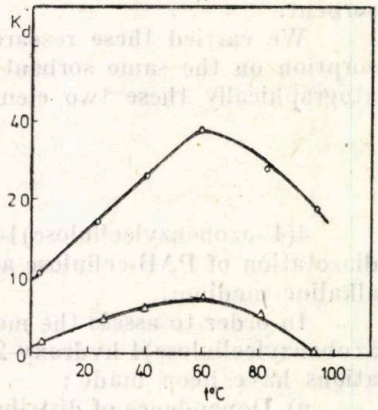

Fig. 2. — The sorption isobars between 0°...100°C : Δ — Sr(II) ; o — Ba(II).

ution coefficients above 62°C is attributed to the partial degradation of the sorbent.

The apparent free enthalpy, calculated with the help of the relation

$$\Delta G = -RT \ln K,$$

has the value — 670 cal/mol for Ba(II), which shows an overlapping of the chemical sorption over the physical one. For Sr(II) this value cannot be calculated since the obtained data for its isotherm do not meet the conditions required by Nikolski's relation [5], [6].

The sorbent is yellow and displays an absorption maximum at 440 nm (Fig. 3, curve *1*), which shifts to 455 nm after complexing (Fig. 3, curve *2*).

From the study of IR spectra there follows that modifications arise only with the —COOH groups of the salicylic acid, the complexes behaving as carboxylates in which the vibration frequencies assume intermediary values between $\nu_{C=O}$ and ν_{C-O}. The —OH group is screened by the hydroxylic groups of cellulose. The frequencies of valency vibration of the azo group are not modified after the sorption process occurs, which lead to the conclusion that the formation of chelates occurs with the carboxyl and hydroxyl groups:

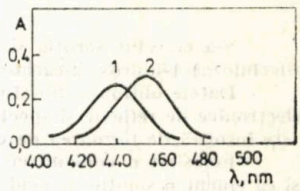

Fig. 3. — The reflectance electronic spectrum: before (curve *1*) and after sorption (curve *2*).

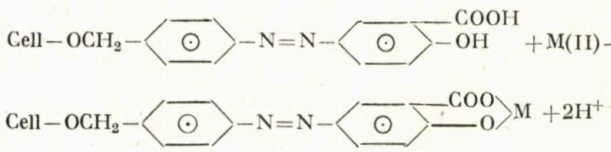

The decrease of pH during the sorption process as well as the data yelded by IR spectra and the electronic reflectance spectra lead to the conclusion that the physical sorption of Sr(II) and Ba(II) is accompanied by an ionic exchange and by a reaction with formation of chelates whose scheme was given above.

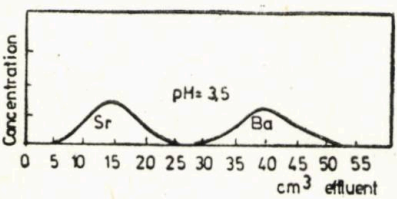

Fig. 4. — Separation of Sr(II) from Ba(II).

The satisfactory separation of the two elements was carried out on a column (250 mm long and 10 mm in diameter), filled with 4 g sorbent, using as eluent a solution of 0.1 M perchloric acid — sodium perchlorate with pH = 3.5 (Fig. 4). The obtained results represented in the figure hold true in the domain of a ratio of 1/10 between the components.

Received, May 8, 1987

Polytechnic Institute, Jassy,
Department of Inorganic and
Analytical Chemistry

REFERENCES

1. Ungurenașu-Onofrei T., Fișel S., Proc. 3rd Nat. Anal. Chem. Conf., Brașov Romania, **4**, 61 (1971).
2. Ungurenașu-Onofrei T., Fișel S., Rev. Chim., **24**, 926 (1973).
3. Ungurenașu-Onofrei T., Fișel S., Chem. Analyt. (Warszawa), **19**, 257 (1974).
4. Pollard F.H., Martin J. V., Analyst, **81**, 348 (1956).
5. Никольский Б. П. К.т.н. дисс., Ленинград, 1939.
6. Никольский Б. П., ЖПХ, **8**, 1935 (1939).

SORBȚIA ȘI SEPARAREA Sr(II) ȘI Ba(II) PE 4(4'-AZOBENZILCELULOZA) 1-HIDROXI-2-CARBOXIBENZEN

(Rezumat)

S-a cercetat sorbția și separarea Sr(II) și Ba(II) pe polimerul chelatizant 4(4'-azobenzilceluloza) 1-hidroxi-2-carboxibenzen.

Datele obținute din studiul dependenței sorbției față de pH, izoterme, izobare, spectre electronice de reflexie și spectre IR au condus la concluzia că sorbția fizică a Sr(II) și Ba(II) este însoțită de formarea de chelați.

Folosind o coloană cu umplutură de 4(4'-azobenzilceluloza) 1-hidroxi-2-carboxibenzen și ca eluent o soluție de acid percloric—perclorat de sodiu 0,1 M cu pH = 3,5, cele două elemente au fost separate în mod satisfăcător.

BULETINUL INSTITUTULUI POLITEHNIC DIN IAŞI
Tomul XXXV (XXXIX), fasc. 1—2, 1989
Secţia II
CHIMIE ŞI INGINERIE CHIMICĂ

D.C. 66.097 ; 661.53

CATALYTIC REMOVAL OF OXYGEN FROM THE NITROGEN—HYDROGEN—OXYGEN MIXTURE USED IN THE AMMONIA SYNTHESIS

BY

ANA TARHON and GH. IONESCU

1. Introduction

The main industrial procedures for obtaining nitrogen and hydrogen lead to their impurification with other gases, among which oxygen. These impurities are, in the reaction of ammonia synthesis, the so called „inert gases".

The influence of the inert gas on the degree of conversion of a chemical reaction is analysed by means of the thermodynamic equation of the form [1] :

$$\left(\frac{\partial \xi}{\partial n_{0j}}\right)_{p,T,n_{0i\neq j}} = \frac{x_j \sum \nu_i - \nu_j}{n_j[\sum \nu_i^2/n_i - (\sum \nu_i)^2/\sum n_i]}, \tag{1}$$

where : ξ — the degree of conversion (advancement) of the reaction ; n_{0j} — initial number of moles of the inert gas j ; ν_j, x_j, n_j — the stoichiometric coefficient of the inert gas, the mole fraction and the number of moles of the mixture with nitrogen and hydrogen, respectively ; $\sum n_i$, $\sum \nu_i$ and $\sum \nu_i^2/n_i$ are quantities reffering to the reaction of ammonia synthesis.

From the thermodynamic point of view an inert gas with respect to a certain reaction is defined by the condition :

$$\nu_j = 0. \tag{2}$$

Mathematically it can be demonstrated that the expression in the square brackets, (Eq. (1)), is a positive one. Since x_j and n_j are, by their meaning, positive quantities, the sign of the derivative of this equation will be given only by the sign of the $\sum \nu_i$ quantity.

By considering, for the ammonia synthesis, the stoichiometric equation :

$$N_2 + 3H_2 = 2NH_3, \tag{3}$$

the quantity $\sum \nu_i$ has the value equal to -2, hence is negative. It follows that the derivative $(\partial \xi/\partial n_{0j})$, in conditions of preassure, temperature and constant number of moles of the other gases (excepting for the inert gas j), will be negative. Hence, the increase of oxygen concentration in the nitrogen—hydrogen mixture will result in decreasing the ammonia yield. Starting from a certain concentration of oxygen (inert gas) in the nitrogen—hydrogen mixture the lowering of the ammonia yield becomes significant and the oxygen removal from the reacting gases becomes necessary.

In the modern industrial procedures the oxygen removal from the nitrogen—hydrogen mixture can be accomplished by passing the nitrogen—hydrogen—oxygen mixture over a suitable catalyst, for the combustion reaction,

$$2H_2 + O_2 = 2H_2O, \tag{4}$$

to take place at the ambient temperature and the heat evolved in this highly exothermic reaction (-571.9 Kj/mol O_2) [2] to be taken off by introducing in the catalytic reactor some heat

recovery devices (economizers) and used in various technological purposes, which contributes to the energetic optimization of the whole industrial process of ammonia synthesis.

The present paper is aimed to test the catalyst H-14-19 with 0.25% Pd, supplied by the firm „Katalysatoren-Werke Houdry-Hüls GMBH-D 4 370, Marl", in the reaction of oxygen removal from the nitrogen—hydrogen—oxygen mixture, by combustion reaction (4). The catalyst characteristics are find in the firm catalogue [3].

2. Experimental, Results and Discussion

For investigating the above discussed problems a technological process was sketched and an appropriate equipment, at a laboratory scale, has been accomplished (Fig. 1).

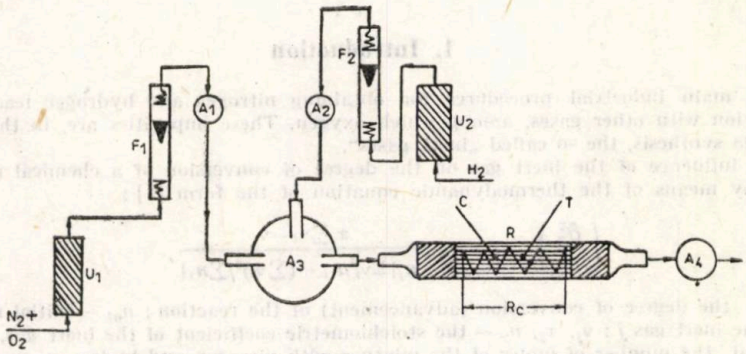

Fig. 1. — Technological flux and principle diagram of installation for catalytic elimination of oxygen from mixture nitrogen—hydrogen—oxygen : R — reactor ; C — catalyst ; R —heat recuperator ; T — thermometer ; U_1, U_2 — dryer vessel with silicagel ; F_1, F_2 — flawmeters ; A_3 — reagent gas-mixer ; A_1, A_2, A_3, A_4 — analysis points.

The reaction development has been followed by the gas-chromatography on a „molecular-sieve" column using argon as gas carrier. The molecular sieves exhibit the advantages of retaining quickly and totally the water vapours from the initial reagent mixture and from the reaction products. The chromatograph used was of Pye 104 type, with Orion KTS recorder ; the catharometer temperature 50°C ; the oxygen flow-rate, measured by the put out of level of sulphuric acid ($\rho = 1.4$) with a differential manometer has $\Delta h = 25$ mm col. H_2SO_4 ; the bridge current was 50 mV ; different gas volumes injected and various sensitivities.

To illustrate the accuracy of analysis as regards the possibility of component separation (N_2, O_2, H_2) in Fig. 2 a chromatogram of the initial mixture of these gases (mixer A_3) and one of the reaction product at the outlet of the catalytic reactor (A_4 node) are showed. It can be noticed that in our conditions the retention times sensibly differ, so that distinct, well individualized peaks for each gas in mixture are obtained.

The experimental data indicated a particularly high activity of the catalyst used wich respect to the reaction (4). Thus, if a H_2/O_2 volume ratio equal at least with the stoichiometric ratio (2/1) is used, the oxygen will be absent in the reaction products even at the ambient temperature.

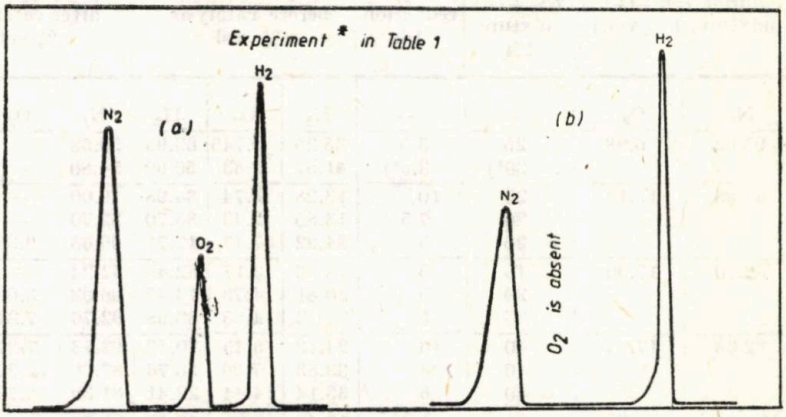

Fig. 2. — Chromatogram regarding the accuracy of the used analysis : *a* — chromatogram before the catalysis : $V = 1$ mL, $S = 50$ for N_2 and O_2 and $S=500$ for H_2, v (paper) $= 76.2$ cm/h, $h=25$ mm column H_2SO_4, $t=50°C$, argon—mobile phase, molecular sieves—stationary phase ; *b* — chromatogram after catalysis, $S = 500$ for both gases ; other conditions are given to point *a*.

In case of the reactor used (diameter $\varnothing=20$ mm), containing 125 g catalyst, 750 mm lengthwise, the temperature was maintained at 20°C by means of a cooling coil over the whole length of the catalyst layer. As cooling liquid water has been used, the water flow rate being correlated with the flow rate of the reaction mixture (nitrogen—hydrogen—oxygen) and with the H_2/O_2 ratio.

The efficient cooling of the reactor is required, on one hand, for the energetic optimization of the overall process of ammonia synthesis and on the other hand for avoiding the attaining of ignition temperature (explosion in closed space) of the hydrogen—oxygen mixture due to of combustion reaction (580°...590°C) [4].

To modify the initial composition of the nitrogen—hydrogen—oxygen mixture, in the mixer (A_3) a mixture of nitrogen and oxygen of constant composition and a hydrogen flux are separately introduced. By varying the ratio of flow rates of the two gas fluxes which penetrate in the mixing chamber, nitrogen—hydrogen—oxygen mixtures of various concentrations have been obtained. The analysis of the composition of these mixtures prior to and after passing through the reactor with catalyst (in the nodes A_3 and A_4 respectively), evidenced the change of concentrations of hydrogen and oxygen, as a result of the equation (4), which becomes a reaction of cold combustion [5].

In Table 1 the experimental data for nine run groups are listed. Each group is characterized by a constant concentration of the nitrogen, oxygen mixture, and variable composition of the nitrogen—hydrogen—oxygen mixture in the mixing chamber (A_3).

Table 1

Experimental Data

Nr.	Composition of initial (N_2+O_2) mixture, [% vol.]		Flow rate of (N_2+O_2) mixture l/h	Flow rate of H_2 for reduction l/h	Composition of ($N_2+O_2+H_2$), before catalysis % vol			Composition of ($N_2+O_2+H_2$), after catalysis % vol.		
	N_2	O_2	—	—	N_2	O_2	H_2	N_2	O_2	H_2
1	93.02	6.98	25	3.5	35,25	0.745	63.99	50.58	—	49.42
			30*)	3.5*)	41.57	1.53	56.90	54.80	—	45.20
2	84.88	15.12	20	10	13.28	1.74	84.98	19.00	—	81.00
			20	7.5	13.85	2.43	83.70	32.70	—	67.30
			20	5	24.82	57.47	17.71	90.66	9.33	—
3	82.70	17.30	15	5	14.38	3.17	82.45	62.24	—	37.76
			20	5	20.81	4.73	74.45	96.92	3.08	—
			25	5	26.12	4.85	68.98	92.76	7.24	—
4	82.06	17.94	40	10	24.13	5.45	70.42	92.73	7.27	—
			40	8	33.83	7.96	58.76	87.78	12.22	—
			40	6	63.14	14.44	22.41	81.30	18.70	—
5	79.10	20.90	20	5.5	17.40	2.91	79.69	95.70	—	4.30
			20	4	25.55	4.95	69.50	90.53	—	9.47
			30	10	14.13	12.50	73.37	30.10	—	69.90
6	77.68	22.32	30	4	32.39	4.45	63.16	90.50	—	9.50
7	69.00	31.00	40	10	36.58	12.27	51.15	77.15	22.40	0.45
			40	5	46.18	15.86	37.95	77.76	22.23	—
8	63.52	36.48	30	12.5	8.41	2.61	88.98	45.29	—	54.71
			30	10	44.27	19.10	36.63	94.10	5.90	—
9	61.70	38.30	20	7.5	7.77	2.50	89.73	88.75	—	11.25
			20	3.5	16.70	8.69	74.60	69.50	30.50	—

3. Conclusions

1. The main conclusion that can be drawn is that at the ambient temperature the activity of the catalyst used is particularly high so that the reaction (4) becomes a „cold combustion reaction".

2. The reaction (4) is highly exothermic and its development at the specified temperature requires the use of an efficient cooling system in the reactor. Such a system can function as an economizer, thus contributing to the increase of efficiency of the whole synthesis process of ammonia.

3. By using a minimum H_2 to O_2 volume ratio of 2/1 the total consumption of the oxygen from the nitrogen—hydrogen—oxygen mixture is assured, since the rate of equation (4) is very high.

4. The high reaction rate favours short contact times between reagents and catalyst which positively influence the increase of gas rates in passing through the catalyst layer and thus the reactor productivity and size ; a smaller reactor will require simpler cooling devices.

Received, January 23, 1987

Polytechnic Institute, Jassy,
Department of Physical Chemistry

REFERENCES

1. Şchiopu M., unpublished data.
2. Landolt-Börnstein, *Eigenschaften der Materie in ihren Aggregatzuständen.* II. Bd., 4. Teil, *Kalorische Zustandsgrössen.* Springer-Verlag, Berlin-Göttingen-Heidelberg, 1961, 181.
3. *** Katalog *Katalysatoren Houdry-Hüls, Marl,* 1975.
4. *** *Manualul Inginerului Chimist.* Ed. Tehn., Buc., 1952, 1991.
5. Pancenkov G. M., Lebedev V. P., *Chemical Kinetics and Catalysis.* Mir Publishers, Moscow, 1976, 169.

ELIMINAREA CATALITICĂ A OXIGENULUI DIN AMESTECUL AZOT–HIDROGEN UTILIZAT ÎN SINTEZA AMONIACULUI

(Rezumat)

S-a testat activitatea catalizatorului solid H-14-19 cu 0,25% Pd, în reacţia de ardere H_2/O_2, în scopul purificării de oxigen a amestecului azot–hidrogen, utilizat în sinteza amoniacului. Catalizatorul testat, livrat de Firma „Katalysatoren-Werke Houdry-Hüls GMBH-D 4 370, Marl", s-a dovedit a fi deosebit de activ, încît reacţia are loc cu viteză mare chiar la temperatura mediului ambiant. Pentru menţinerea unei astfel de temperaturi este necesară răcirea intensă a reactorului, deoarece reacţia fiind puternic exotermă ar putea conduce, în sistem închis, la realizarea temperaturii de aprindere şi la explozia sistemului. Recuperarea căldurii de reacţie poate contribui la optimizarea energetică a procesului global de sinteză a amoniacului iar eliminarea oxigenului (care constituie un gaz inert în raport cu această reacţie de sinteză) conduce la realizarea unui randament practic, în amoniac, cît mai apropiat de randamentul termodinamic posibil.

BULETINUL INSTITUTULUI POLITEHNIC DIN IAŞI
Tomul XXXV (XXXIX), fasc. 1—2, 1989
Secţia II
CHIMIE ŞI INGINERIE CHIMICĂ

D.C. 547.553

GRAVIMETRIC DETERMINATION OF TRIETHYLENETETRAMINE

BY

TINCA ONOFREI, VIORICA DULMAN, LUCIA ODOCHIAN and VALERIU ŞUNEL

1. Introduction

Triethylenetetramine (TRIEN), used in syntheses in chemical industry, can be determined by titrimetric [1] ... [3], colorimetric and nephelometric methods [4] ... [7] and gravimetrically with salicylic aldehyde [8].

In order to analyse the technical products and the solutions in which TRIEN is to be found in a high concentration we have investigated the possibility of extending the gravimetric methods. Three methods of gravimetric analysis have been worked out using as precipitating agents derivatives of salicylic aldehyde. In contrast with the method previously described [8] we have obtained crystalline precipitates that could easily be filtered and that do not adhere to the walls of the beaker.

2. Experimental, Results and Discussions

The methods of gravimetric determination we have worked out are based on the precipitating reaction between TRIEN and 3-nitro-, 5-nitro- and 5-chlorinesalicylaldehyde with the formation of Schiff bases :

$$H_2N-(CH_2)_2-NH-(CH_2)_2-NH-(CH_2)_2-NH_2+2\ R-CHO \rightarrow$$

$$\underset{\displaystyle R}{\overset{|}{CH}}=N-(CH_2)_2-NH-(CH_2)_2-NH-(CH_2)_2-N=\underset{\displaystyle R}{\overset{|}{CH}}$$

where

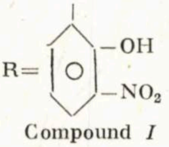

Compound *I*

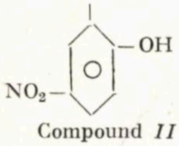

Compound *II*

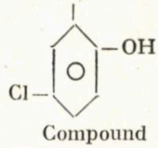

Compound *III*

The precipitating forms have been characterized by elementary, thermogravimetric analysis and by IR spectra.

The structure of precipitates *I*, *II* and *III* has been determined on the basis of elementary analyses (Table 1) and of IR spectra.

From the analysis of IR spectra there results the appearance of an absorption maximum at 1 620 cm^{-1} attributed to C=N group, a band at 1 135...1 140 cm^{-1} for C—N and the absence of the signal corresponding to the vibration

Table 1

Analytic Data of Precipitating Forms

Compound	Formula	C, [%]		H, [%]		Cl, [%]		N, [%]	
		Calc.	Found	Calc.	Found	Calc.	Found	Calc.	Found
I	$C_{20}H_{24}N_6O_6$	54.05	54.58	5.40	5.82	—	—	14.41	14.79
II	$C_{20}H_{24}N_6O_6$	54.05	54.63	5.40	5.95	—	—	14.41	14.90
III	$C_{20}H_{24}Cl_2N_4O_2$	56.73	57.60	5.67	6.65	16.78	17.52	13.23	14.15

of the C=O group from the initial molecules of salicylaldehydes, which confirms their condensation with TRIEN.

The thermograms have been registered in the air under nonisothermic conditions at a heating rate of 12°C/min using a MOM—Budapest derivatograph.

From the thermogram of compound *I* (Fig. 1) there follows that the degradation occurrs in three well separated stages up to 300°C, the second stage, the most important one, being accompanied by a strong exothermic effect.

The thermograms of compounds *II* and *III* (Fig. 2) point out three

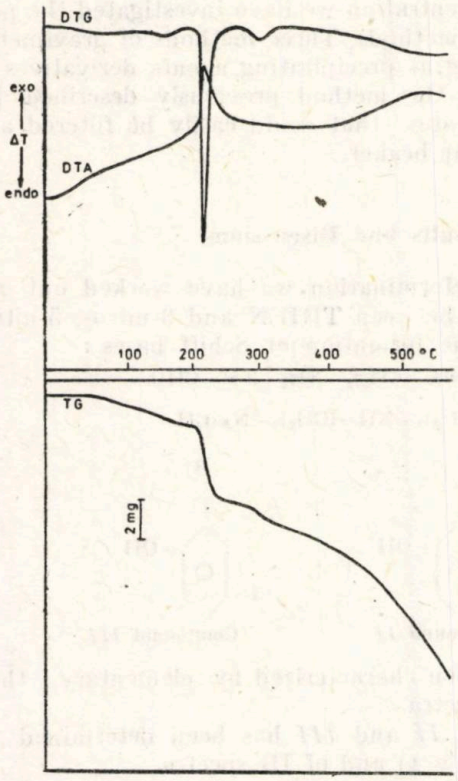

Fig. 1. — DTG, DTA and TG curves of compound *I*.

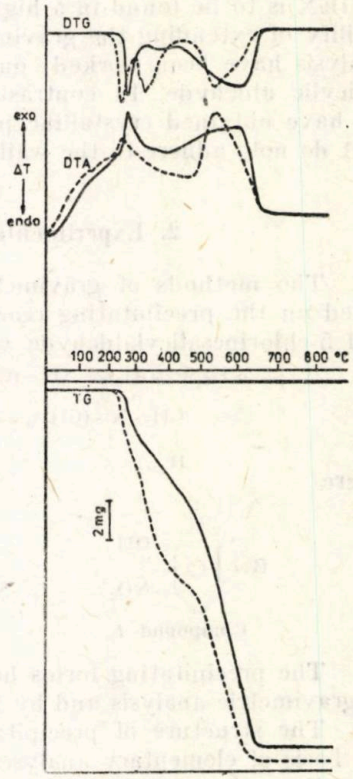

Fig. 2. — DTG, DTA and TG curves : — compound *II* ; — — — compound *III*.

stages of decomposition up to 660°C, the lest one being significant (exothermic effect).

The thermostability of the precipitating forms was determined on the basis of the initial decomposing temperatures (Table 2), of the temperatures

Table 2

The Characteristic Temperatures for the First Stage

Compound	T_i, [°C]	T_m, [°C]	T_f, [°C]
I	45	154	195
II	227	263	321
III	177	258	296

at low transformation degrees (Fig. 3) and of the activating energies calculated by Freeman-Carroll method [9] for first stage (Table 3). The

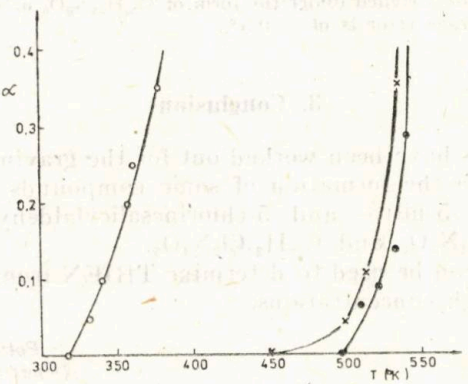

Fig. 3.— The transformation degree dependence on temperature: o—compound *I*; ●—compound *II*; x—compound *III*.

Table 3

The Kinetic Parameters

Compound	Stage I		Stage II		Stage III	
	n	E_a, [Kj/mol]	n	E_a, [Kj/mol]	n	E_a, [Kj/mol]
I	—	—	0	432.32	1.4	339.68
II	5	459.5	—	—	—	252.4
					—	110.1
III	0.5	199.4	2	333.3	—	287.2
					—	120.9

results we have obtained lead to the conclusion that the thermic stability follows the order :

compound *II* > compound *III* > compound *I*.

Compound *I* is stable up to 45°C, compound *II* up to 227°C and compound *III* up to 177°C. Having in view the low thermostability of compound *I*, in contrast with compounds *II* and *III*, it cannot be brought to a constant mass in gravimetric determination by heating.

2.1. Procedure

The solution containing 0.1...0.15 g TRIEN is diluted with 70...75 cm^3 distilled water and is treated with a solution of 3-nitro-, 5-nitro- or 5-chlorinesalicylaldehyde (0.4...0.5 g aldehyde, 10 cm^3 distilled water and 0.25 g NaOH) under constant stirring. It is let to rest for 30 min. and pH is corrected at 8.3 with H_2SO_4 27% and 0.1 N in the presence of phenolphtaleine (alcoholic solution 0.1%) and with universal indicator paper, after which it is let to rest for an hour. An equal volume of ethylic alcohol (100 cm^3) is added. The precipitate remains in contact with the solution for 5...24 hours and then it is filtered through a G_4 crucible. The washing is done with a $C_2H_5-OH-H_2O$ solution (1 : 1 v/v).

Compound *I* is orange in colour. It is dried for about two hours in vacuum desiccator and is weight as $C_{20}H_{24}N_6O_6$.

Compounds *II* and *III* are dried for about two hours at 100°C. The precipitates are yellow in colour. They are weighed under the form of $C_{20}H_{24}N_6O_6$ or $C_{20}H_{24}Cl_2N_4O_2$.

The relative average error is of $\pm$ 0.5%.

3. Conclusions

Three methods have been worked out for the gravimetric determination of TRIEN based on the formation of some compounds of the Schiff bases type with 3-nitro-, 5-nitro- and 5-chlorinesalicylaldehyde. The forms of weighing are $C_{20}H_{24}N_6O_6$ and $C_{20}H_{24}Cl_2N_4O_2$.

The methods can be used to determine TRIEN from technical products and solutions of high concentrations.

Received, July 30, 1987

Polytechnic Institute, Jassy,
Department of Inorganic and Analytical Chemistry
and
Department of Organic and Macromolecular Chemistry and Technology

REFERENCES

1. Bellen Z., Chem. Analit. (Warszawa), **11**, 57 (1966).
2. Bellen Z., Chem. Analit. (Warszawa), **11**, 1011 (1966).
3. Fişel S., Ungurenaşu-Onofrei T., Dulman V., Rev. Chim. (Bucureşti), **32**, 483 (1981).
4. Zaleski I., Chojnicka B., Roczn. panst. Zakl. Hig., **16**, 171 (1965).
5. Chojnicka B., Roczn. panst. Zakl. Hig., **16**, 477 (1965).
6. Chojnicka B., Roczn. panst. Zakl. Hig., **16**, 545 (1965).
7. Омелянец Н. И., Лаб. Дело, 483 (1966).
8. Fişel S., Ungurenaşu-Onofrei T., Dulman V., Rev. Chim. (Bucureşti), **31**, 585 (1980).
9. Freeman E. S., Carroll B., J. Phys. Chem., **62**, 394 (1958).

DETERMINAREA GRAVIMETRICĂ A TRIETILENTETRAAMINEI

(Rezumat)

S-au elaborat trei metode de determinare gravimetrică a trietilentetraaminei (TRIEN) bazate pe formarea unor compuși de tip baze Schiff cu 3-nitro-, 5-nitro- și 5-clorsalicilaldehida.

Precipitatele obținute au fost caracterizate prin analiză elementară, termogravimetrică și spectre IR.

Formele de cîntărire sînt $C_{20}H_{24}N_6O_6$ și $C_{20}H_{24}Cl_2N_4O_2$. Eroarea medie relativă este de $\pm 0,5\%$.

Metodele se pot folosi pentru determinarea TRIEN din produse tehnice și soluții cu concentrații mari.

BULETINUL INSTITUTULUI POLITEHNIC DIN IAȘI
Tomul XXXV (XXXIX), fasc. 1—2, 1989
Secția II
CHIMIE ȘI INGINERIE CHIMICĂ

C.D. 547.476.7 ; 66.013.5

LE MODÈLE MATHÉMATIQUE DE L'INSTALLATION DE FABRICATION DE L'ACIDE ADIPIQUE (I)

PAR

I. CURIEVICI, VIORICA NICU, ȘT. UNGUREANU, CORNELIU PETRILĂ, RODICA DIACONESCU, M. NICU, ELENA IONESCU et SAVEL MATACHE

1. Présentation de l'installation modélée

Dans le travail ci-présent on élabore le modèle mathématique d'une installation industrielle pour la fabrication de l'acide adipique à partir du cyclohexanol dont l'oxydation catalytique (métavanadate d'ammonium et sels de cuivre) se produit en deux étapes, avec acide azotique, conformément aux réactions :

$$(1)\qquad 10\,C_6H_{11}-OH+20\,HNO_3 \rightleftharpoons 10\,HOOC-(CH_2)_4-C\begin{matrix}NOH\\ \diagup\!\!\diagdown\\ NO_2\end{matrix}+20\,H_2O,$$

$$(2)\qquad 10\,HOOC-(CH_2)_4-C\begin{matrix}NOH\\ \diagup\!\!\diagdown\\ NO_2\end{matrix}+7\,H_2O \rightleftharpoons 10\,HOOC-(CH_2)_4-COOH+$$
$$+2\,HNO_3+4\,N_2+6\,H_2O+5\,N_2O.$$

La réaction globale est donc :

$$(3)\qquad 10\,C_6H_{11}-OH+18\,HNO_3 \rightleftharpoons 10\,HOOC-(CH_2)_4-COOH+5\,N_2O+4\,N_2+$$
$$+19\,H_2O.$$

Le schéma de principe d'une telle installation est présenté dans la Fig. 1. Comme on peut y voir, l'installation présente deux cycles successifs : pendant le premier on réalise la transformation la plus poussée possible du cyclohexanol en acide nitrolique et la transformation partielle de celui-ci en acide adipique ; pendant le deuxième cycle a lieu la transformation complète du cyclohexanol en acide nitrolique et puis la transformation de ce dernier en acide adipique.

Le premier cycle est justifié par la nécessité de maintenir la température du réacteur à un niveau relativement réduit (la réaction globale est largement exothermique), ce qu'on peut réaliser en recyclant intensivement la masse réactionnelle refroidie après sa sortie du réacteur. Ce refroidissement est précédé par la séparation et l'envoi vers le deuxième cycle d'une fraction

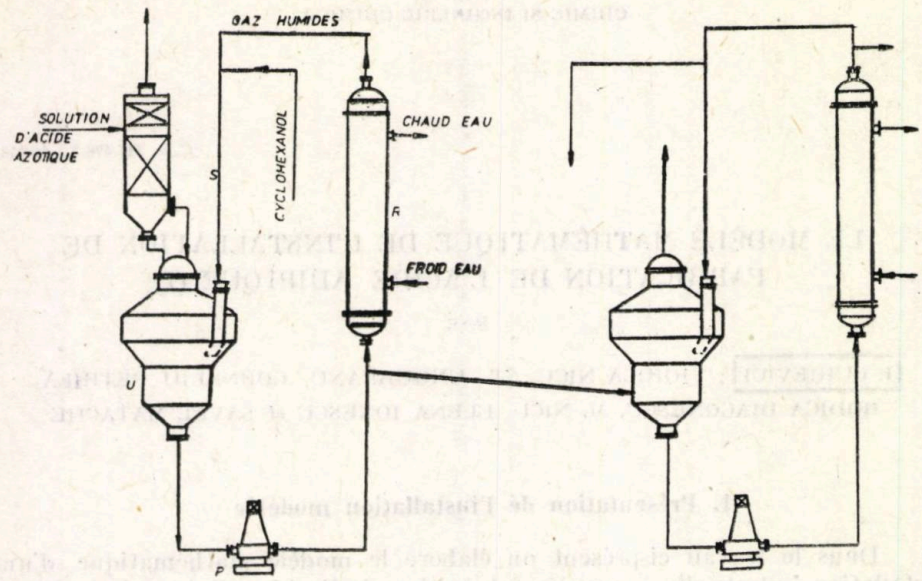

Fig. 1. — Schéma de principe de l'installation de fabrication de l'acide adipique.

qui correspond aux réactants frais introduits dans le système. La masse recyclée est refroidie dans un réfrigérant R jusqu'à un certain niveau qui évite la séparation de l'acide adipique de la solution. Le recyclage est effectué à l'aide de la pompe P. Pour oxyder le cyclohexanol on utilise une solution d'acide azotique. Le catalyseur est introduit en même temps que la solution d'acide azotique. Du réacteur se dégagent des gaz humides. C'est ainsi que la solution d'acide azotique avec catalyseur est utilisée dans le laveur de gaz W pour retenir partiellement ces gaz.

2. Cinétique et thermodynamique du processus

Ce sont des problèmes que la littérature de spécialité [1]...[5] et le Centre de recherches pour fibres synthétiques de Săvinești [6] ont bien approfondi.

Du point de vue cinétique le processus de formation de l'acide adipique, par oxydation avec acide azotique, en présence des catalyseurs ci-dessus mentionnés, à une température ne dépassant pas 60°C environ, est une réaction consécutive ayant la forme :

$$\text{Cyclohexanol} \xrightarrow{k_1} \text{acide nitrolique} \xrightarrow{k_2} \text{acide adipique.} \tag{4}$$

En notant par C_{A_0} la concentration molaire totale de substance organique dans la masse réactionnelle à un certain moment τ et par X, Y, Z les fractions molaires du cyclohexanol et respectivement de l'acide nitrolique et adipique en phase organique, il résulte que :

$$C_{A_0} = C_{A_0}X + C_{A_0}Y + C_{A_0}Z. \tag{5}$$

Dans les travaux [1]...[4] on met en évidence que la réaction de formation de l'acide nitrolique est de premier ordre par rapport au cyclohexanol et donc :

$$r_A = -\frac{dC_{A_0}X}{d\tau} = -k_1 C_{A_0}X. \tag{6}$$

En intégrant l'équation (6), dont la condition initiale est $X=1$ pour $\tau=0$, on obtient, pour la fonction du variation en temps de la concentration du cyclohexanol, l'expression :

$$X=e^{-k_1\tau}. \tag{7}$$

La réaction selon laquelle l'acide nitrolique passe en acide adipique est également de I-er ordre et par conséquent :

$$r_B = \frac{dC_{A_0}Y}{d\tau} = C_{A_0}(k_1X - k_2Y). \tag{8}$$

En intégrant l'équation (8), dont la condition initiale est $Y=0$ pour $\tau=0$, on obtient, pour la variation de la concentration de l'acide nitrolique :

$$Y=\frac{k_1}{k_2-k_1}(e^{-k_1\tau}-e^{-k_2\tau}) \tag{9}$$

et

$$\frac{dZ}{d\tau}=k_2Y. \tag{10}$$

Si la condition initiale est $Z=0$ pour $\tau=0$, la concentration de l'acide adipique est :

$$Z=1-\frac{k_2}{k_2-k_1}e^{-k_1\tau}+\frac{k_1}{k_2-k_1}e^{-k_2\tau}. \tag{11}$$

La variation des constantes de vitesse k_1 et k_2 en fonction de la température est du type Arrhenius et a la forme [6] :

$$k_1^T=2{,}9245\cdot 10^9 e^{-\frac{7976{,}84}{T}} \tag{12}$$

et respectivement

$$k_2^T=1{,}0145.10^{10}e^{-\frac{9562{,}15}{T}}. \tag{13}$$

Les deux réactions sont exothermiques [6], à savoir :

$$\Delta H_{R_1}^{298}=-195{,}22 \text{ Kcal/mol}, \tag{14}$$

$$\Delta H_{R_2}^{298}=-3{,}775 \text{ Kcal/mol}. \tag{15}$$

On ne dispose pas d'informations concernant la variation de l'effet thermique fonction de température, c'est pourquoi (comme hypothèse simplificatrice) on va la négliger.

3. Hypothèses de travail

Le processus situé à la base du modèle mathématique a comme point de départ quelques hypothèses fondamentales auxquelles, au long des calculs, viennent s'ajouter d'autres, d'une moindre importance.

Les hypothèses fondamentales adoptées dans l'étude effectueé sont les suivantes :

a) Le système fonctionne en régime stationnaire. Il en résulte que le débit de masse, sur la chaîne dirigée vers le cycle de l'hydrolise de l'acide adipique, doit être égal au débit total de masse au moment de l'alimentation sans le débit de masse de gaz et vapeurs, qui quittent le premier cycle par le laveur.

b) En principe, la concentration du cyclohexanol en phase organique, au point de la ramification vers le deuxième cycle, pourrait avoir n'importe quelle valeur, selon les dimensions du système de réaction du premier cycle et selon les conditions de travail. On va accorder une attention particulière à la situation où le cyclohexanol est complètement consommé au point de ramification.

c) Si l'on considère le chiffre de recyclage comme le rapport entre la masse de réaction recyclée pendant le premier cycle et la masse qu'on envoie vers le cycle d'hydrolise de l'acide nitrolique, on pourra déduire ce chiffre à condition que la température dans le réacteur U ne dépasse pas une limite préalablement fixée du point de vue technologique.

4. Géométrie du système et caractéristiques de la batterie de travail

Les deux systèmes cycliques sont identiques du point de vue constitutif. On va considérer que chacun est formé de quatre réacteurs : a) réacteur U — réacteur principal ; b) réacteur V — représenté par le système de tuyaux reliant le réacteur U et l'échangeur de chaleur y compris l'espace offert par la pompe de recirculation P ; c) réacteur R, qui est en même temps un échangeur de chaleur ; d) réacteur S — les tuyaux qui relient l'échangeur de chaleur R et le réacteur U.

Vu que dans le réacteur U a lieu un moussage et implicitement une forte agitation naturelle, on peut le considérer soit comme un réacteur continu où le mélange est parfaitement réalisé, soit comme un réacteur où le mélange n'est réalisé que dans une certaine mesure. On va considérer les trois autres réacteurs du type au déplacement total.

5. Alimentation du système

Pour calculer l'alimentation du système on part de la production annuelle d'acide adipique P, [t/an], et de son utilisation pendant 330 jours de l'année.

En négligeant, dans une première approximation, les pertes de masse dues aux gaz qui s'échappent du réacteur quittant le système et les pertes de rendement provoquées par les transformations incomplètes de l'acide adipique, on détermine la quantité de cyclohexanol fonction de la production, à l'aide de la relation :

$$F_{A_0} = \frac{P \cdot 10^3}{7\,920 \cdot 146 \cdot 3\,600}, \quad [\text{Kmol s}^{-1}]. \tag{16}$$

On va corriger cette valeur, comme on le verra ci-dessous, en évaluant les pertes de gaz humides et le rendement de la transformation du cyclohexanol en acide adipique.

L'acide azotique est introduit en rapport volumétrique b, [m³ solution d'acide azotique ayant une teneur C_0/m³ en cyclohexanol]. Le rapport molaire correspondant, b' [mol HNO_3/mol cyclohexanol], est :

$$b' = b \frac{\rho_{HNO_3,c_0} C_0 M_{01}}{\rho_{01} M_{HNO_3} 100} . \tag{17}$$

Les débits de masse d'alimentation seront :

$$G_{01} = F_{A_0} M_{01}, \text{ [Kg/s cyclohexanol]}, \tag{18 a}$$

$$G_{HNO_3} = b' F_{A_0} M_{HNO_3}, \text{ [Kg/s acide azotique]}, \tag{18 b}$$

$$G_{eau} = b' F_{A_0} M_{HNO_3} (100 - C_0)/C_0, \text{ [Kg/s eau]}. \tag{18 c}$$

Le débit total de masse d'alimentation de la première étape du processus G_0, sera:

$$G_0 = F_{A_0} \left(M_{01} + b' M_{HNO_3} + b' M_{HNO_3} \frac{100 - C_0}{C_0} \right), \text{ [Kg/s]}. \tag{19}$$

On considère que les matières premières présentent une pureté de 100% et que la température d'alimentation est de 50°C.

6. Calcul du chiffre de recyclage

Conformément à la définition qu'on donne dans le §3 c, le chiffre de recyclage est donné par :

$$n_R = \frac{G_R}{G_p} = \frac{G_R}{G_{01} + G_{HNO_3}} . \tag{20}$$

La voie principale pour calculer le chiffre de recyclage est basée sur la température maximum admissible T_{max} dans le réacteur. Du bilan de masse du réacteur U (en négligeant les gaz qui le quittent) il résulte :

$$G_R = G_U - (G_{01} + G_{HNO_3}) \tag{21}$$

et par conséquent :

$$n_R = \frac{G_U}{G_{01} + G_{HNO_3}} - 1, \tag{22}$$

où : G_U représente le débit de masse total de substance qui passe par le réacteur U qui est calculé à l'aide la relation :

$$G_U = \frac{\Delta Q_U}{C_{p,am} \Delta T_U} . \tag{23}$$

L'augmentation de la température admissible dans le réacteur est

$$\Delta T_U = T_{max} - T_{am,i} . \tag{24}$$

On peut calculer la température du mélange au moment de l'entrée dans le réacteur, $T_{am,i}$, en fonction des débits d'alimentation en cyclohexanol et

en acide azotique, du débit du mélange recyclé, des températures et des chaleurs spécifiques qui leur correspondaient avant d'avoir réalisé le mélange. Comme à ce moment n_R est inconnu, il sera évalué par itérations spécifiques, en imposant, au point de la ramification, une certaine valeur à la température du matériel recyclé ainsi qu'à d'autres grandeurs qu'on va préciser au moment opportun.

La variation de l'enthalpie de la masse réactionnelle dans le réacteur est donnée par la relation :

$$\Delta Q_U = Q_{U,i} - Q_{U,p}, \tag{25}$$

où :

$$Q_{U,i} = Q_{01} + Q_{HNO_3} + Q_{r,U} + Q_R, \tag{26}$$

$$Q_{01} = G_{01} C_{p,01} t_a, \tag{27}$$

(G_{01} est donné par la relation (18 a)) et :

$$Q_{HNO_3} = (G_{HNO_3} + G_{eau}) C_{p,HNO_3} t_a. \tag{28}$$

En considérant que, dans le réacteur, le cyclohexanol ne se transforme que partiellement (dans une proportion m) la chaleur après la réaction sera :

$$Q_{rU} = \frac{mQ_r}{100}, \tag{29}$$

où :

$$Q_r = F_{01} \Delta H_{R_1}. \tag{29 a}$$

La quantité de chaleur qui entre en même temps que le matériel recyclé est calculée à l'aide de la relation :

$$Q_R = G_R C_{p,mr} T_R. \tag{30}$$

La quantité de chaleur perdue dans le réacteur est :

$$Q_{Up} = Q_{pa} + Q_g. \tag{31}$$

Une certaine quantité de chaleur, Q_{pa}, qui est perdue par la surface extérieure du réacteur, on peut la calculer avec la relation :

$$Q_{pa} = \alpha_{pa} S_{pa} (T_p - T_m). \tag{32}$$

Le coefficient total de transfert de chaleur par convection et rayonnement, à partir des parois du réacteur vers le milieu environnant, est donné par la relation [7] :

$$\alpha_{pa} = [9{,}74 + 0{,}07\,(T_p - T_m)] \cdot 10^{-3}, \ [\text{KJ/m}^2.\ \text{grd}]. \tag{33}$$

Pour évaluer l'enthalpie des gaz quittant le système on peut apprécier le débit et les compositions en les considérant comme saturés en vapeurs d'eau à la température d'évacuation. Cette évaluation doit satisfaire tant le bilan thermique que celui des matériaux du système.

Notations

b — rapport volumétrique acide azotique : cyclohexanol, dans l'alimentation, [m^3/m^3] ;
b' — rapport molaire acide azotique : cyclohexanol ;
C_{A_0} — concentration molaire totale de phase organique, [Kmol/m^3] ;
C_0 — concentration de la solution d'acide azotique utilisée pour alimenter l'installation, [%],
C_p — chaleur spécifique pour pression constante, [KJ/Kg. grd] ;
$C_{p,am}$ — chaleur spécifique du mélange réactionnel du réacteur U, [KJ/Kg. grd] ;
$C_{p,01}$ — chaleur spécifique du cyclohexanol au moment de l'alimentation, [KJ/Kg. grd];
$C_{p,mr}$ — chaleur spécifique de la masse réactionnelle recirculée, [KJ/Kg. grd] ;
F_A^0 — débit molaire d'alimentation en cyclohexanol, [Kmol/s] ;
G_0 — débit de masse total d'alimentation, [Kg/s] ;
G_{01} — débit de masse d'alimentation de l'installation en cyclohexanol, [kg/s];
G_{HNO_3} — débit de masse d'alimentation en acide azotique, [Kg/s] ;
G_{eau} — débit de masse d'alimentation en eau, [Kg/s] ;
G_R — débit de masse recirculée, [Kg/s] ;
G_p — débit de masse du produit quittant la première étape, [Kg/s] ;
G_U — débit total de masse du mélange réactionnel qui passe par le réacteur U, [Kg/s] ;
$\Delta H_{R_1}, \Delta H_{R_2}$ — effet thermique de la réaction pendant la première et respectivement la seconde étape, [KJ/Kmol] ;
k_1, k_2 — constantes des vitesses de réaction pendant la première et la seconde étape de la réaction ;
m — quantité de cyclohexanol transformé, [%],
M_{01}, M_{HNO_3} — masses moléculaires du cyclohexanol et respectivement de l'acide azotique, [Kg/Kmol] ;
n_R — chiffre de recyclage,
p — production annuelle d'acide adipique, [t/an] ;
Q — quantité de chaleur, [KW] ;
Q_g — quantité de chaleur contenue par les gaz quittant le système, [KW] ;
Q_{HNO_3} — quantité de chaleur de la solution d'acide azotique de l'alimentation, [KW] ;
Q_{01} — quantité de chaleur du cyclohexanol introduit par l'alimentation de l'installation, [KW] ;
Q_{pa} — quantité de chaleur perdue par la surface extérieure du réacteur, [KW] ;
Q_r — quantité de chaleur obtenue après la réaction par transformation complète du cyclohexanol, [KW] ;
Q_R — quantité de chaleur entrée en même temps que le matériel recirculé, [KW] ;
$Q_{r,n}$ — quantité de chaleur obtenue après la réaction par transformation d'une fraction m de cyclohexanol, [KW] ;
$Q_{U,p}$ — quantité de chaleur perdue dans le réacteur U, [KW] ;
ΔQ_U — variation de l'enthalpie du mélange réactionnel dans le réacteur U, [KW] ;
r_A — vitesse de réaction par rapport au cyclohexanol, [Kmol/m^3 . s] ;
r_B — vitesse de réaction par rapport à l'acide nitrolique, [Kmol/m^3 . s] ;
S_U — surface extérieure du reacteur U, [m^2] ;
t_a — température des composants au moment de l'alimentation de l'installation, [°C] ;
T — température, [°C] ;
T_{max} — température maximum admissible dans le réacteur U, [°C] ;
$T_{am,i}$ — température de la masse réactionnelle au moment de l'entrée dans le réacteur, [°C];
T_m — température moyenne annuelle de l'air environnant, [°C] ;
T_p — température des parois de l'installation, [°C] ;
T_R — température du mélange recirculé, [°C] ;
ΔT_U — augmentation admissible de la température dans le réacteur U, [°C] ;
X — fraction molaire du cyclohexanol en phase organique ;
Y — fraction molaire de l'acide nitrolique en phase organique ;
Z — fraction molaire de l'acide adipique en phase organique ;
α_{pa} — coefficient de transfert de chaleur entre les parois des tuyaux et le milieu environnant, [KJ/m^2. grd] ;

ρ_{HNO_3,C_0} — densité de la solution d'acide azotique de concentration C_0 ;
τ — durée, [s].

Reçue le 11 mai 1987

Institut Polytechnique, Jassy,
Chaire de Génie Chimique

BIBLIOGRAPHIE

1. Van Asselt W. J., Van Krevelan D. W., Rec. trav. chim., **82**, *1*, 51 (1963).
2. Van Asselt W. J., Van Krevelan D. W., Rec. trav. chim., **82**, *5*, 429 (1963).
3. Van Asselt W. J., Van Krevelan D. W., Chem. Eng. Sci., **18**, *8*, 471 (1963).
4. Лубяницкий И. и сотр.. Хим. Пром., 7, 529 (1960).
5. Лубяницкий И. и сотр., ЖФХ, **36**, *3*, 567 (1962).
6. Matache S. et al., *Fabricarea acidului adipic*, Săvineşti, 1971.
7. Pavlov K. F. et al., *Procese şi aparate în ingineria chimică*, (traduit du russe). Ed. Tehn., Bucureşti, 1981.

MODELUL MATEMATIC AL INSTALAŢIEI DE FABRICARE A ACIDULUI ADIPIC (I)

(Rezumat)

În vederea modelării matematice a instalaţiei de fabricare a acidului adipic prin oxidarea ciclohexanolului cu acid azotic — proces continuu şi ciclic — se consideră că fiecare din cele două sisteme ciclice este constituit din patru reactoare în serie. Prima parte a lucrării prezintă ipotezele de lucru în stabilirea modelului precum şi datele necesare modelării : cinetica şi termodinamica procesului, geometria sistemului, date asupra alimentării sistemului şi calculul cifrei de reciclare.

BULETINUL INSTITUTULUI POLITEHNIC DIN IAŞI
Tomul XXXV (XXXIX), fasc. 1—2, 1989
Secţia II
CHIMIE ŞI INGINERIE CHIMICĂ

C.D. 549.476.7 ; 66.013.5

LE MODÈLE MATHÉMATIQUE DE L'INSTALLATION DE FABRICATION DE L'ACIDE ADIPIQUE (II)

PAR

I. CURIEVICI, VIORICA NICU, CORNELIU PETRILĂ, ŞT. UNGUREANU, RODICA DIACONESCU, M. NICU, ELENA IONESCU et SAVEL MATACHE

1. Élaboration du modèle mathématique pour le premier cycle

Le système d'équations décrivant la première étape de réaction part du point de ramification vers la deuxième étape, respectivement de la ramification de la masse recyclée vers l'échangeur de chaleur R [1].

Vu que le débit de masse sur le tuyau se dirigeant vers la deuxième étape doit être égal à celui d'alimentation du système sans tenir compte du débit des gaz saturés en vapeurs d'eau, le débit peut être immédiatement calculé sur cette ramification. Compte tenu du chiffre de recirculation, il résulte qu'on peut également calculer le débit de masse sur l'échangeur de chaleur. Quant aux compositions de ces deux courants, elles sont évidemment identiques au point de la ramification, mais elles sont établies selon la structure dimensionnelle et les conditions de travail de la première étape. En considérant pour l'instant tant la structure dimensionnelle que les conditions de travail comme des variables disponibles, on peut analyser la composition au point de ramification, dans deux hypothèses :

a) Au point de ramification, la quantité de cyclohexanol est entièrement transformée en acide nitrolique.

b) Ce n'est qu'une fraction quelconque de cyclohexanol qui se transforme en acide nitrolique.

On vérifie ensuite, par des essais successifs, si les régimes réalisés dans les hypothèses ci-dessus peuvent conduire au régime stationnaire supposé au début du processus.

1.1. Calcul de la composition, au point de ramification, dans l'hypothèse de la transformation complète du cyclohexanol

En considérant les fuites de gaz comme une fraction $\varepsilon(\ll 1)$ du débit d'alimentation du système en cyclohexanol, à l'aide du bilan de masse globale du système on obtient :

$$P = G_{01}(1-\varepsilon)\frac{M_{\text{ac. adipique}}}{M_{01}}. \tag{1}$$

Ayant également en vue le rendement du processus, la production d'acide adipique sera :

$$P=\eta\, G_{01}(1-\varepsilon)\frac{M_{\text{ac. adipique}}}{M_{01}}. \tag{2}$$

Avec la valeur du débit de masse du cyclohexanol obtenue par cette voie et à partir des relations (18), (19) [1] on peut calculer le débit total de masse d'alimentation G_0 de la première étape du processus. En utilisant la relation (20) [1] il résulte que le débit de masse du mélange réactionnel à recycler sera :

$$G_R=n_R G_0. \tag{3}$$

Compte tenu que G_0 este donné par la relation (19) [1] il résulte que :

$$F_{AR}=n_R F_{A_0}. \tag{4}$$

En considérant que ρ_{am} représente la densité de la masse réactionnelle du système, le débit volumétrique de masse réactionnelle sera G_R/ρ_{am} et par conséquant la concentration de la masse réactionnelle en phase organique, dans le circuit de recyclage, sera :

$$C_{A_0}=\frac{F_{AR}\rho_{am}}{G_R}=\frac{F_{A_0}}{G_0}\rho_{am}. \tag{5}$$

Dans l'hypothèse de la consommation complète du cyclohexanol au point de la ramification :

$$Y+Z=1. \tag{6}$$

La fraction molaire de l'acide nitrolique en phase organique au point de la ramification découle de la cinétique de réaction. De l'équation (8) [1] il résulte que la fraction molaire de l'acide nitrolique atteint sa valeur maxima à :

$$\tau_{max}=\frac{\ln(k_1/k_2)}{k_1-k_2} \quad \text{et} \quad (8) \qquad Y_{max}=\left(\frac{k_2}{k_1}\right)^{k_2/(k_1-k_2)}. \tag{7}$$

Les constantes de vitesse fonction de température sont données par les expressions (12) et (13) [1].

Les fractions molaires d'acide nitrolique et adipique en phase organique, ainsi que la concentration de ce dernier étant connues, on peut déterminer la concentration de ces deux composants. À l'aide de la consommation complète du cyclohexanol on peut calculer, du point de vue stoechiométrique, la consommation d'acide azotique et donc la teneur de la masse réactionnelle en acide azotique.

1.2. Calcul de la composition au point de ramification dans l'hypothèse de la transformation partielle du cyclohexanol

Soit $1>x>0$ la fraction molaire du cyclohexanol en phase organique au point de ramification. De la vitesse de réaction de la première étape (équation (6) [1]) on peut déterminer la durée de réaction. À l'aide de l'équation (11)

[1] on détermine ensuite la fraction molaire de l'acide adipique. X et Z étant déterminés, on peut calculer la fraction molaire de l'acide nitrolique à partir de l'équation (9) [1]. Les autres grandeurs qui décrivent la composition sont calculées tout comme dans le § **1**. .

2. Équations de bilan sur l'échangeur de chaleur

Soit T_{R_0} la température de la masse réactionnelle recyclée au moment où elle entre dans l'échangeur de chaleur et soit ΔT_R la chute maximum admissible de la température de la masse réactionnelle le long (des tubes) de l'échangeur de chaleur.

C'est l'acide nitrolique qui est le composant dont on suit l'évolution. En poursuivant la variation de sa concentration en phase organique on suit implicitement la variation de la concentration du cyclohexanol et de l'acide nitrolique.

Le calcul sera dirigé d'une manière générale, respectivement pour une concentration quelconque de l'acide nitrolique C_A, $Y_R(l)$, où l représente la distance entre les orifices d'entrée des tubes de l'échangeur et le point considéré. Le bilan différentiel de masse est :

$$\frac{dY_R(l)}{dl} = \frac{N\pi D_R^2}{4n_R F_{A_0}} [r_A(l) + r_B(l)] . \tag{9}$$

On calcule la vitesse de réaction $r_B(l)$ conformément à la relation (8) [1]. La condition initiale pour intégrer l'équation (9) est soit la valeur Y_{max}, donnée par la relation (8) dans le cas de la première hypothèse, soit la valeur qui résulte en imposant à X une certaine valeur tout comme dans le § **1.2.**

La température, en tant que fonction de l, par l'intermédiaire de la constante de la vitesse de réaction, intervient comme une inconnue. C'est pourquoi il s'avère nécessaire encore une équation différentielle qu'on peut obtenir du bilan thermique.

Pour simplifier on va supposer que la température est une fonction linéaire de l, du type :

$$T_R(l) = T_{R_0} - \frac{\Delta T_R l}{L_R} . \tag{10}$$

En tenant compte de l'effet thermique des deux réactions, ΔH_{R_1} et ΔH_{R_2} et de l'échange de chaleur avec l'extérieur et en acceptant pour K une valeur constante le long des tubes de l'échangeur de chaleur, l'équation de bilan thermique intégral se présente sur la forme :

$$n_R G_0 C_{p,am} T_{R_0} - n_R G_0 C_{pm} \Delta T_R - K S_R \Delta T_{R_m} +$$

$$+ N \frac{\pi D_R^2}{4} \Delta H_{R_1} \int_0^{L_R} dr_B(l) + N \frac{\pi D_R^2}{4} \Delta H_{R_2} \int_0^{L_R} dr_A(l) = 0, \tag{11}$$

où ΔT_{R_m} représente la différence moyenne logarithmique de température le long des tubes de l'échangeur de chaleur et S_R—la surface totale d'échange de chaleur à l'intérieur de l'échangeur. La chaleur spécifique de la masse réactionnelle est calculée fonction de sa composition moyenne aux moments où celle-ci entre et sort de l'échangeur.

La solution simultanée des équations (9) et (11), avec les conditions à la limite correspondantes, aboutit au profil de la fraction molaire de l'acide nitrolique en phase organique et de la température le long des tubes de l'échangeur de chaleur.

3. Équations de bilan sur les tuyaux supérieurs

Soient, pour un cas quelconque, $X_{R,f}$, $Y_{R,f}$ et $Z_{R,f}$ les fractions molaires respectives du cyclohexanol, de l'acide nitrolique et de l'acide adipique, au moment où elles sortent de l'échangeur. Soient encore D_S et L_S le diamètre et respectivement la longueur des tuyaux supérieurs arrivant jusqu'au réacteur.

Ayant en vue la transformation du cyclohexanol en acide nitrolique et la transformation partielle de ce dernier en acide adipique, on obtient pour le bilan différentiel de masse de l'acide nitrolique, l'équation :

$$F_{AR}\frac{dY_S(l)}{dl}=\frac{\pi D_S^2}{4}[r_A(l)+r_B(l)]. \tag{12}$$

Le bilan thermique est nécessaire tout comme dans le cas de l'échangeur. Dans l'équation du bilan thermique interviennent l'effet thermique de réaction et la chaleur échangée avec l'environnement. La forme différentielle de cette équation est :

$$G_R C_{p,\,am}\frac{dT_S(l)}{dl}+\pi\alpha_{pa}D_S[T_S(l)-T_m]= \tag{13}$$
$$=\frac{\pi D_S^2}{4}[r_A(l)\,\Delta H_{R_1}+r_B(l)\,\Delta H_{R_2}],$$

avec la condition initiale :

$$T_{S_0}=T_{Rf}. \tag{14}$$

Dans l'équation ci-dessus, pour calculer la transmission de chaleur vers l'environnement on n'a pas eu en vue que la résistance thermique principale représentée par la couche d'air extérieure. Pour le coefficient α_{pa} on utilise des valeurs usuelles.

L'intégration simultanée des équations (12) et (13), avec les conditions à la limite correspondantes, aboutit au profil des fractions molaires des composants en phase organique et de la température de la masse réactionnelle au long des tubes supérieurs.

4. Équations de bilan sur le réacteur

Ayant en vue les conditions à l'intérieur du réacteur (dégagement puissant de gaz, température élevée) on peut, en principe, accepter qu'il s'agit d'un réacteur au mélange parfait.

On peut caractériser l'éventuel écart du mélange parfait par un coefficient empirique $0<\beta<1$ appliqué aux vitesses de réaction. Vu cette possibilité, la composition à la sortie du réacteur sera calculée séparément pour le mélange parfait et respectivement pour le mélange imparfait.

Le calcul de la composition de la masse réactionnelle au moment où elle sort du réacteur sera effectué d'une manière générale et il sera ensuite particularisé pour $\beta = 1$.

Dans le réacteur entrent le débit de masse à recycler, G_R, dont la composition est calculée dans le § 1, ainsi que du cyclohexanol et de l'acide azotique dilué, calculées dans le § 5.

Pour la densité ρ_{am} du mélange réactionnel recyclé, les débits volumétriques des deux courants seront :

a) pour les matières premières fraîches :

$$Q_{V_1}=\frac{F_{A_0}100}{\rho_{01}}+\frac{G_0-F_{A_0}100}{\rho_{HNO_3,\,C_0}},\ [m^3/s], \tag{15}$$

b) pour le mélange recyclé :

$$Q_{V_2}=\frac{n_R G_R}{\rho_{am}},\ [m^3/s], \tag{16}$$

le débit total en résultant :

$$Q_{VT}=Q_{V_1}+Q_{V_2}. \tag{17}$$

Le courant global d'alimentation contient comme phase organique :

$$F_{A_0}+n_R F_{A_0} X_{Sf},\ [\text{Kmol/s cyclohexanol}], \tag{18 a}$$

$$n_R F_{A_0} Y_{Sf},\ [\text{Kmol/s acide nitrolique}], \tag{18 b}$$

$$n_R F_{A_0}(1-X_{Sf}-Y_{Sf}),\ [\text{Kmol/s acide adipique}]. \tag{18 c}$$

La teneur totale en phase organique de l'alimentation du réacteur est donc $F_{A_0}(n_R+1)$.

Les fractions molaires des trois composants en phase organique, au moment où elles entrent dans le réacteur, seront :

$$X_{U,0}=\frac{1}{n_R+1},\ \text{pour le cyclohexanol;} \tag{19 a}$$

$$Y_{U,0}=\frac{n_R Y_{Sf}}{n_R+1},\ \text{pour l'acide nitrolique;} \tag{19 b}$$

$$Z_{U,0}=\frac{n_R(1-Y_{Sf})}{n_R+1},\ \text{pour l'acide adipique.} \tag{19 c}$$

La concentration molaire totale en phase organique à l'entrée dans le réacteur est :

$$C_{A_0.U}=\frac{F_{A_0}(n_R+1)}{Q_{VT}},\ [\text{Kmol/m}^3]. \tag{20}$$

En considérant la concentration des composants à leur sortie du réacteur, ainsi que la température, comme identiques à celles qu'on trouve a l'intérieur du réacteur, même si le mélange n'est pas parfait, pour un volum V_U du réacteur le bilan intégral de masse du cyclohexanol est de la forme :

$$F_{A_0}(1+n_R X_{Sf})-F_{A_0}(n_R+1)\ X_{U,f}-V_U r_A\beta=0, \tag{21}$$

la vitesse de réaction en résultant de l'équation :

$$r_A=k_1\ X_{U,f}\frac{F_{A_0}\ (n_R+1)}{Q_{VT}}. \tag{22}$$

Dans les mêmes hypothèses, le bilan intégral de masse de l'acide nitrolique est :

$$F_{A_0}n_R Y_{S,f}-F_{A_0}(n_R+1)\ Y_{U,f}+V_U\beta\ r_B=0 \tag{23}$$

et la vitesse de réaction :

$$r_B=\frac{F_{A_0}(n_R+1)}{Q_{VT}}(k_1X_{U,f}-k_2Y_{U,f}). \tag{24}$$

En négligeant les pertes de chaleur qui accompagnent les gaz s'échappant du réacteur, pour une surface d'échange de chaleur avec l'extérieur S_U, le bilan énergétique intégral du réacteur est :

$$\begin{aligned}&G_0(n_R+1)\ C_{p,am}(T_{U,0}-T_{U,f})+F_{A_0}\ (n_R+1)(X_{U,0}-X_{U,f})\ \Delta_{R_1}+\\&+F_{A_0}(n_R+1)(Z_{u,f}-Z_{u,i})\Delta H_{R_2}-\alpha_{p,a}S_U(T_{f,U}-T_m)=0.\end{aligned} \tag{25}$$

La solution simultanée des équations (21), (23) et (25) conduit aux valeurs des fractions molaires des composants de la masse réactionnelle du réacteur et de la température du réacteur.

5. Équations de bilan sur les tuyaux inférieurs

Le débit molaire de phase organique le long du trajet des tuyaux inférieurs qui relient le réacteur et l'échangeur de chaleur est $F_{A_0}(n_R+1)$. Les fractions molaires des trois composants — cyclohexanol, acide nitrolique et acide adipique — sont respectivement $X_v(l)$, $Y_v(l)$ et $Z_v(l)$.

Le débit de masse totale le long des tuyaux est $G_0(n_R+1)$, [Kg/s] et le débit volumétrique, pour une densité ρ_{am} de la masse réactionnelle, est :

$$Q_{VT}=\frac{G_0(n_R+1)}{\rho_{am}}. \tag{26}$$

Pour l'acide nitrolique l'équation différentielle de bilan de masse, le long du trajet des tuyaux, sera :

$$F_{A_0}(n_R+1)\frac{dY_V(l)}{dl} - \frac{\pi D_V^2}{4}\cdot\frac{F_{A_0}(n_R+1)}{Q_{VT}}[k_1X_V(l)-k_2Y_V(l)]=0 \tag{27}$$

et pour le cyclohexanol :

$$F_{A_0}(n_R+1)\frac{dX_V(l)}{dl} + \frac{\pi D_V^2}{4}\cdot\frac{F_{A_0}(n_R+1)}{Q_{VT}}k_1X_V(l)=0. \tag{28}$$

Les conditions initiales de la solution du système antérieur sont constituées par les fractions molaires des composants en phase organique et par la température de la masse réactionnelle au moment où elle sort du réacteur. L'intégration est effectuée sur la longueur L_v des tuyaux inférieurs.

6. Modèle mathématique de la première étape du processus

C'est l'ensemble d'équations de bilan de masse et énergétique pour les quatre parties du système considéré qui constitue son modèle mathématique à savoir : a) équations (9) et (11) ; b) équations (12) et (13) ; c) équations (21), (23), (25) ; d) équations (27), (28) et

$$G_0(n_R+1)C_{pm}\frac{dT_V(l)}{dl} - \frac{\pi D_V^2}{4}\cdot\frac{F_{A_0}(n_R+1)}{Q_{VT}}[k_1X_V(l)- \tag{29}$$

$$-k_2Y_V(l)]\Delta H_{R_2} - \frac{\pi D_V^2}{4}\cdot\frac{F_{A_0}(n_R+1)}{Q_{VT}}k_1X_V(l)\Delta H_{R_1}+$$

$$+\alpha_{pa}\pi D_V[T_V(l)-T_m]=0.$$

Les conditions initiales pour chaque réacteur sont constituées par les valeurs finales de la température et des fractions molaires du réacteur précédent.

Les intéractions commencent à l'entrée dans l'échangeur de chaleur en imposant une certaine valeur à $T_{R,0}$ et en calculant la composition selon le procéde indiqué dans le § **1**.

7. Paramètres disponibles du modèle

Il en résulte qu'on peut considérer comme paramètres disponibles : la température à l'entrée dans l'échangeur de chaleur, la composition de la masse réactionelle au moment où elle entre dans l'échangeur, le rapport acide azotique : cyclohexanol, le volume du contour de la réaction qui peut être particularisé pour ses différents composants et β — le degré qui caractérise le mélange dans le réacteur proprement-dit du système.

Par une variation adéquate des paramètres mentionnés ci-dessus il faudra aboutir, après avoir calculé le cycle entier, à une composition de

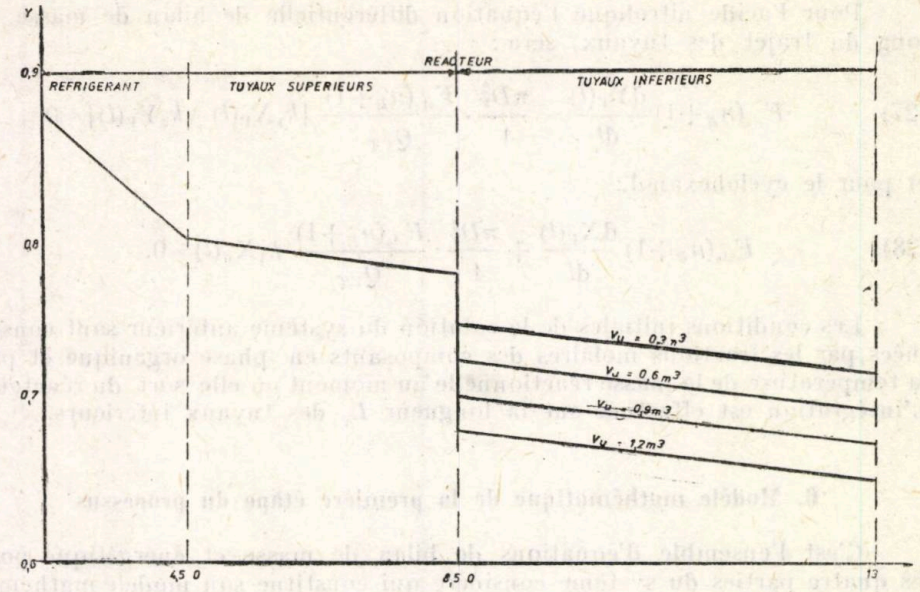

Fig. 1. — Profils des fractions molaires de l'acide nitrolique pendant le premier cycle pour différents volumes du réacteur U.

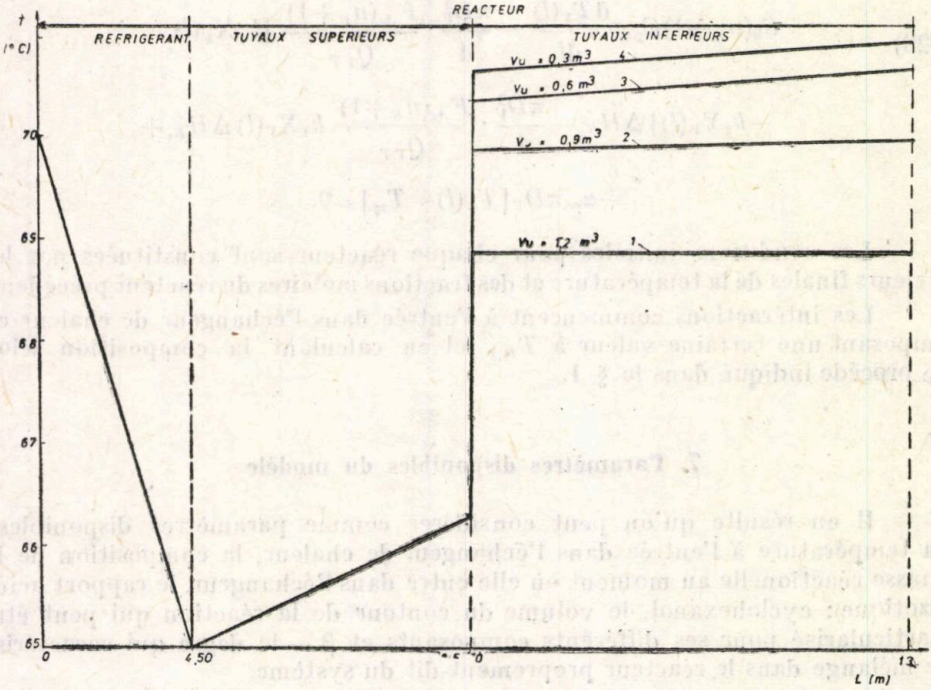

Fig. 2. — Profils de la température pendant le premier cycle pour différents volumes du réacteur U.

la masse réactionelle et à une température d'entrée dans le réfrigérant qui soient identiques à celles qu'on avait choisies au début du calcul.

Selon ce qu'on a déjà mentionné, le calcul du cycle en entier implique des itérations successives.

Après avoir calculé le premier cycle on calcule le deuxième de la même manière pour les deux variantes, c'est-à-dire en introduisant ou non le cyclohexanol dans le cycle.

Les Fig. 1 et 2 exemplifient l'intégration du modèle mathématique avec les conditions à la limite specifiées. L'équation de la vitesse de réaction qui se produit dans le réacteur est donnée par l'équation (6) [1].

Notations

C_{A^0} — concentration molaire totale de phase organique, [Kmol/m^3] ;
D — diamètre, [m] ;
D_R — diamètre des tubes de l'échangeur de chaleur R, [m] ;
D_S — diamètre des tuyaux supérieurs, [m] ;
D_V — diamètre des tuyaux inférieurs, [m] ;
F — débit molaire, [Kmol/s] ;
F_{A_0} — débit molaire d'alimentation de l'installation en cyclohexanol, [Kmol/s] ;
F_{A_R} — débit molaire de phase organique récirculée dans le système, [Kmol/s] ;
G — débit de masse, [Kg/s] ;
G_{01} — débit de masse du cyclohexanol d'alimentation, [Kg/s] ;
G_R — débit de masse réactionnelle récirculée, [Kg/s] ;
G_0 — débit de masse total d'alimentation, [Kg/s] ;
k_1, k_2 — constantes des vitesses de réaction pour la première et respectivement la seconde étape dela réaction ;
K — coefficient total de transfert de chaleur entre l'agent refroidisseur (l'eau) et la masse réactionnelle, [KJ/m^2·s·grd] ;
l — distance courante, [m] ;
L — longueur, [m] ;
L_R — longueur des tubes de l'échangeur de chaleur, [m] ;
L_V — longueur des tuyaux inférieurs, [m] ;
M — masse moleculaire;
$M_{\text{ac. adipique}}$ — masse de l'acide adipique ;
M_{01} — masse du cyclohexanol ;
N — nombre des tubes de l'échangeur de chaleur ;
n_R — chiffre de recirculation ;
P — production annuelle d'acide adipique, [t/an] ;
Q_V — débit volumétrique, [m^3/s] ;
Q_{V1} — débit volumétrique pour le courant d'alimentation de l'installation, [m^3/s] ;
Q_{V2} — débit volumétrique pour le mélange recyclé, [m^3/s] ;
Q_{VT} — débit volumétrique total, [m^3/s] ;
r_A — vitesse de réaction par rapport au cyclohexanol, [Kmol/m^3·s] ;
r_B — vitesse de réaction par rapport à l'acide nitrolique, [Kmol/m^3·s] ;
S — surface, [m^2] ;
S_R — surface totale de transfert dans l'échangeur de chaleur R, [m^2];
S_U — surface d'échange de chaleur avec l'extérieur du réacteur U, [m^2] ;
T — température, [°K] ;
T_m — température de l'environnement, [°K] ;
ΔT_R — chute maximum de température admissible le long des tubes de l'échangeur de chaleur R, [°K] ;
$\Delta T_{R,m}$ — différence moyenne logarithmique de température le long des tubes de l'échangeur de chaleur, [°K] ;
V_U — volume du réacteur, [m^3] ;
X — fraction molaire du cyclohexanol eu phase organique ;
Y — fraction molaire de l'acide nitrolique en phase organique ;
Z — fraction molaire de l'acide adipique en phase organique ;

α_{pa} — coefficient de transfert de chaleur entre les parois des tubes et l'environnement, [KJ/m^2·s·grd] ;
β — coefficient d'écart par rapport au mélange parfait ;
ΔH_{R_1}, ΔH_{R_2} — effet thermique de la réaction pendant la première et respectivement la deuxième étape de la réaction, [KJ/kmol] ;
ε — fraction de la fuite des gaz ;
ρ — densité, [Kg/m^3] ;
ρ_{am} — densité de la masse réactionnelle du système, [Kg/m^3] ;
ρ_{01} — densité du cyclohexanol, [Kg/m^3] ;
ρ_{HNO_3} — densité de la solution d'acide azotique de concentration C_0, [Kg/m^3].

Indices

R — échangeur de chaleur ;
S — tuyaux supérieurs ;
U — réacteur proprement-dit ;
V — tuyaux inférieurs ;
0 — à l'entrée dans le réacteur correspondant ;
f — à la sortie du réacteur correspondant.

Reçue le 11 mai 1987

Institut Polytechnique, Jassy,
Chaire de Génè Chimique

BIBLIOGRAPHIE

1. Curievici I. et collab., *Le modèle mathématique de l'installation de fabrication de l'acide adipique (I)*. Bul. Inst. polit. Iaşi, **XXX (XXXIX)**, *1—2*, s. II, 35—42 (1989).
2. Curievici I., *Bazele tehnologiei chimice*. Vol. **I**, Inst. polit., 1981.
3. Rase H. F., *Chemical Reactor Design for Process Plants*. Vol. **I, II**, John Wiley & Sons, New York, 1977.
4. Mihail R., *Modelarea reactoarelor chimice*. Ed. Tehn., Bucureşti, 1976.
5. Crowe C. M., *Chemical Plant Simulation*. Prentice Hall Intersc., NY, 1971.

MODELUL MATEMATIC AL INSTALAŢIEI DE FABRICARE A ACIDULUI ADIPIC (II)

(Rezumat)

Elaborarea modelului matematic pentru primul ciclu al procesului de obţinere a acidului adipic prin oxidarea ciclohexanolului începe de la punctul de ramificaţie spre al doilea ciclu prin calcularea compoziţiei pe baza datelor din prima parte a lucrării. În continuare se aplică bilanţul de masă şi termic pe fiecare din cele patru zone ale sistemului. Calculul ciclului implică iteraţii succesive.

BULETINUL INSTITUTULUI POLITEHNIC DIN IAȘI
Tomul XXXV (XXXIX), fasc. 1—2, 1989
Secția II
CHIMIE ȘI INGINERIE CHIMICĂ

D.C. 536.2 ; 66.069

EXPERIMENTAL STUDY ON HEAT TRANSFER IN THIN FILMS OF NON-NEWTONIAN LIQUIDS

BY

FĂNICĂ MUSTAȚĂ, RADU TUDOSE and ELENA COSTEA

1. Introduction

The heat transfer in thin film flow has numerous applications in the industrial operations such as heating, cooling, evaporation, condensation, absorption, desorbtion, demonomerization.

The liquid film can be formed mechanically (agitated film), gravitationally (falling film) or under the action of a gaseous phase (vapours or air) by envolving. In spite of the large number of papers in the field, approaching the heat transfer in thin film flow of Newtonian fluids [1], [2], [4],...,[13], there are few papers concerning the heat transfer in non-Newtonian liquid film.

J. T. Davies [3] has investigated the heat transfer in the flow of an aqueous polyacrylamide (Separan MG 200) solution, with non-Newtonian behaviour, and found a partial heat transfer coefficient lower than that of water.

The aim of this paper is to derive a correlation for partial heat transfer coefficient in thin film flow of non-Newtonian liquids.

2. Experimental Equipment

The main part of the experimental equipment, depicted in Fig. 1, is formed of a heat exchange tube and a circuit of thermostated hot water. The non-Newtonian liquid is set in motion by the pump (*2*) through the heat exchanger (*3*) and the flowmeter (*4*) and distributed by the device (*5*) over the external surface of the heat exchange tube (*1*) ($\varnothing = 44$ mm, $L = 2\,000$ mm). The heated non-Newtonian liquid is collected in the tank (*6*) and recycled through the heat exchanger (*3*) to the distribution device (*5*) and back to the tank (*6*) for regulating the flow rate and temperature.

The heating water, from the tank (*7*), is passed through the heater (*9*) by pump (*8*), and redistributed for regulating the flow rate and temperature at the tank (*7*) and then at the lower part of the heat exchange tube (*1*) through the flowmeter (*10*). The temperature of the heating water is higher than that of the non-Newtonian liquid, the heat transfer taking place in counter current, from the hot water to the liquid film.

Since the vibrations can increase the partial heat transfer coefficient up to 300% [12] the heat exchange tube was fed with the two liquids by

means of rubber tubes and the pumps have been mounted in such a way as to avoid the vibration generation.

On the external surface of the heat exchange tube, nine Copper—Constantan thermocouples have been mounted helically (Fig. 2).

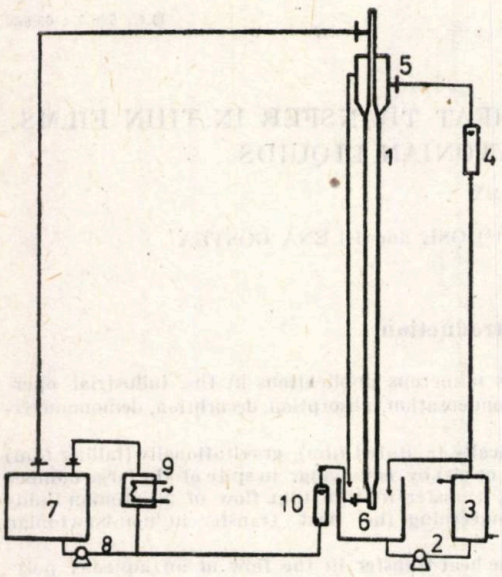

Fig. 1. — Experimental equipment : *1* — heat exchange tube ; *2* — pump ; *3* — heat exchanger ; *4* — flowmeter ; *5* — distribution device ; *6* — tank ; *7* — tank ; *8* — pump ; *9* — electric heater ; *10* — flowmeter.

Though according to literature informations [12] the heat losses up to 70°C can be considered negligible and do not significantly influence the heat transfer coefficient, the heat exchange tube was protected with transparent plexiglass.

The inlet and outlet temperatures of the two fluids in the working section have been measured by means of Copper—Constantan thermocouples and Hg thermometer with an accuracy of ± 0.1°C. The temperatures at the tube and at the film surfaces have also been measured by thermocouples. To avoid some errors in measuring the temperature, the thermocouples have been made with no additional weldings.

A Dewar vessel filled with water and ice was used as zero point; the opposing electromotive force was measured by means of a Kipp a. Zonen milivoltmeter on the scales 1 ; 2 ; 5 mV.

3. Experimental

For determining the partial heat transfer coefficient, the temperature and flow rate of the two fluids at the input and at the output of the working zone as well as the temperatures at the external tube surface and the film surface have been measured.

Two solution of polyethyleneoxide 4 000 (provided by G.I.P. Brazi) of 46% and 56% concentration, respectively, have been used as non-Newtonian fluids. The rheological measurements have been accomplished on a Rheotest RV_2 — G.D.R. apparatus.

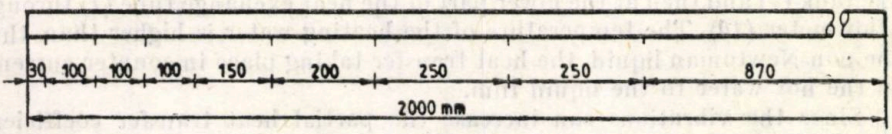

Fig. 2. — Distribution of thermocouples over the tube length.

Table 1

Variation of the Solution Densities with Temperature for the Solutions of Polyethylene Oxide 4 000

T, [°C]	30	31	32	33	34	35	36	37	38	39	40	41	42	43	44	45
ρ, [kg/m^3] $c = 56\%$	1 091	1 090	1 089	1 087	1 085	1 084	1 083.5	1 083	1 082.5	1 082	1 081.5	1 081	1 081	1 080	1 079.5	1 079
ρ, [kg/m^3] $c = 46\%$	1 070	1 069	1 068	1 067	1 065	1 064	1 063	1 062	1 061	1 060	1 059	1 058	1 057,5	1 057	1 057	1 056

Table 2

Variation of the Consistency (acording of the O s t w a l d de W a e l e law) *with Temperature for Solutions of Polyethylene Oxide 4 000*

T, [°C]	25	28	30	32	34	36	38	40	42	44	46	Flow index
K, [g/cm^2.s^n] $c = 46\%$	0.110	0.106	0.106	0.096	0.094	0.090	0.085	0.072	0.067	0.063	0.060	0.98
K, [g/cm^2.s^n] $c=56\%$	0.236	0.204	0.201	0.168	0.155	0.194	0.122	0.108	0.105	0.1035	0.103	0.99

The variations with temperature of the densities of the two fluids and of the indices of consistency (according to the Ostwald–de Waele law) are showed in Tables 1 and 2, respectively.

The runs were carried out for volume flow rates between 400 and 900 l/h which correspond to $\mathcal{R}e$ numbers between 400 and 1 720 at temperatures of the heating fluids of 45°, 50° and 60°C. The $\mathcal{R}e$ number was calculated by Silvester's relationship [14].

4. Results and Discussion

In the flow of thin films of solutions of polyethylene oxide 4 000 the following flow zones can be noticed :

a) A smooth flow zone occuring at the upper part of the heat exchange tube which exhibit a swell immediately after the liquid leaves the distribution gap.

b) A zone of flow with periodic waves where unstable waves occur at the same points which degenerates and accumulates as drops shifting on the surface of a liquid sublayer [15], [16].

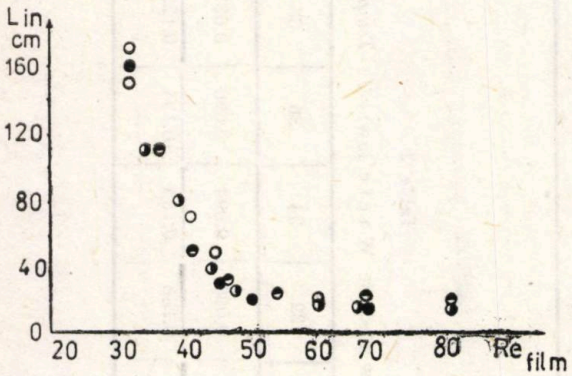

Fig. 3. — Variation of the input length vs. the $\mathcal{R}_e$ number of the film at T_{inlet}=26°C (○); T_{inlet}= 40°C (●); T_{inlet}=50°C (◒); T_{inlet}=55°C (◑).

c) The transition zone where the drops have different sizes and shift at different rates which results in their coalescence and breakdown.

d) The zone of flow with stabilized waves, characterized by a narrow distribution of the drop sizes and rates, their amplitude remaining constant along the flow surface.

These zones can coexist all or only partially, function of $\mathcal{R}e$ value.

The length of the smooth zone decreases with increasing temperatures and $\mathcal{R}e$ values (Fig. 3).

The partial heat transfer coefficient in the film was calculated by the relationship :

$$\alpha_F = K \frac{\Delta t_m}{\Delta t_M} . \tag{1}$$

If the obtained data are worked statistically the dependence of the partial heat transfer coefficient in the film vs. the $\mathcal{R}e$ number values of the two fluids and the temperature of heating agent was obtained :

$$\alpha_F = 147.1\, \mathcal{R}e_{film}^{0.708}\, \mathcal{R}e_{int}^{0.407}\, \mathcal{G}a_{film}^{-0.312}. \tag{2}$$

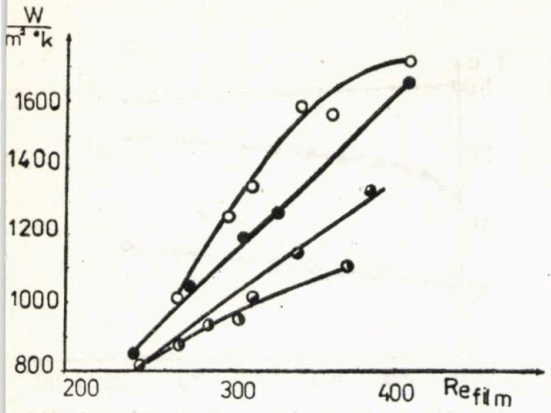

g. 4. — Variation of the partial heat transfer coefficient . the $\mathcal{R}_e$ number of the film at T_{inlet}=40°C (C=56) % and $_{inlet}$=7 800 (○); $\mathcal{R}_{e_{inlet}}$=11 000 (●); $\mathcal{R}_{e_{inlet}}$=15 400 (◒); $\mathcal{R}_{e_{inlet}}$=18 000 (◑).

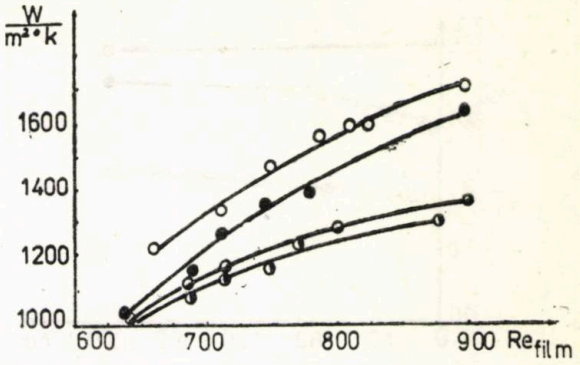

Fig. 5. — Variation of the partial heat transfer coefficient vs. the $\mathcal{R}_e$ number of the film at T_{inlet}= 50°C (C=56 %) and R_{inlet}= 7 700 (○); $\mathcal{R}_{e_{inlet}}$ = 11 000 (●); $\mathcal{R}_{e_{inlet}}$= =13 800 (◒); $\mathcal{R}_{e_{inlet}}$ =19 000 (◑).

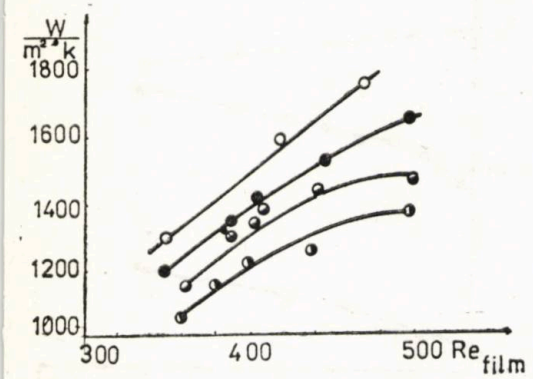

Fig. 6. — Variation of the partial heat transfer coefficient vs. the $\mathcal{R}_e$ number of the film at T_{inlet}= =60°C (C = 56 %) and $\mathcal{R}_{e_{inlet}}$ =7 800 (○); $\mathcal{R}_{e_{inlet}}$= =10 800 (●); $\mathcal{R}_{e_{inlet}}$=15 000 (◒); $\mathcal{R}_{e_{inlet}}$=19 000 (◑).

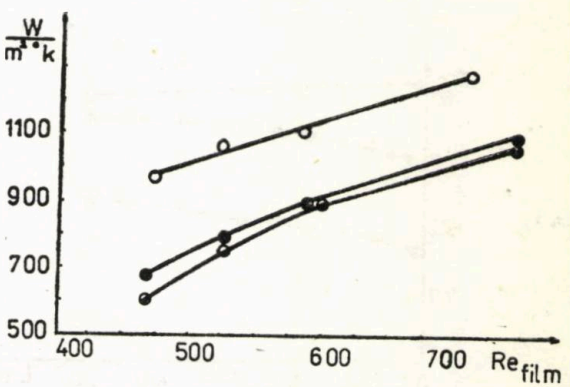

Fig. 7. — Variation of the partial heat transfer coefficient vs. the $\mathcal{R}_e$ number of the film at T_{inlet}= 37.5°C (C =46 %) and $\mathcal{R}_{e_{inlet}}$ = 8 000 (○); $\mathcal{R}_{e_{inlet}}$ = 12 200 (●); $\mathcal{R}_{e_{inlet}}$= =17 500 (◒).

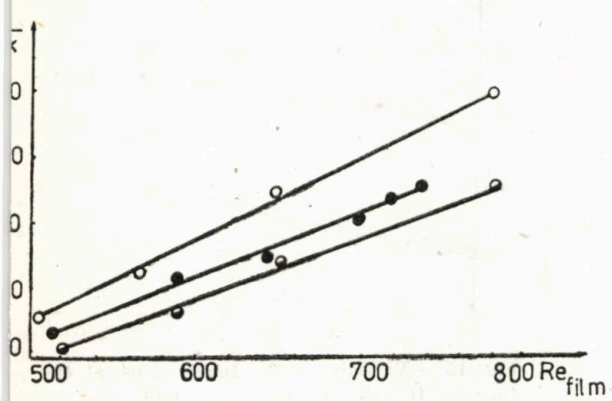

8. — Variation of the partial heat transfer coefficient vs. $\mathcal{R}_{e_{inlet}}$ number of the film at T_{inlet} = 45°C (C = 46 %) and $_{inlet}$ = 7 800 (○); $\mathcal{R}_{e_{inlet}}$ = 12 600 (●); $\mathcal{R}_{e_{inlet}}$ = 15 600 (◒).

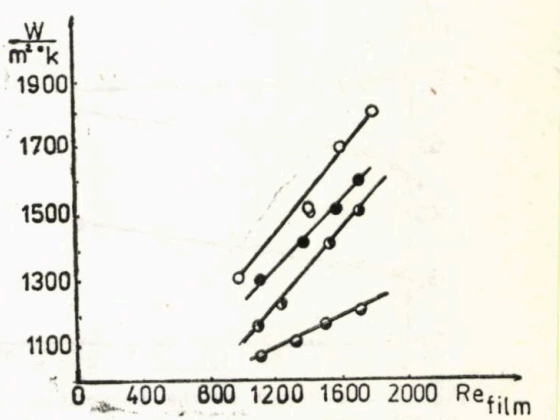

Fig. 9.—Variation of the partial heat transfer coefficient vs. the $\mathcal{R}_e$ number of the film at T_{inlet}= 60°C (C=46 %) and $\mathcal{R}_{e_{inlet}}$=7 700 (○); $\mathcal{R}_{e_{inlet}}$=11 000(●); $\mathcal{R}_{e_{inlet}}$ = 13 800 (◑); $\mathcal{R}_{e_{inlet}}$=19 000 (◒).

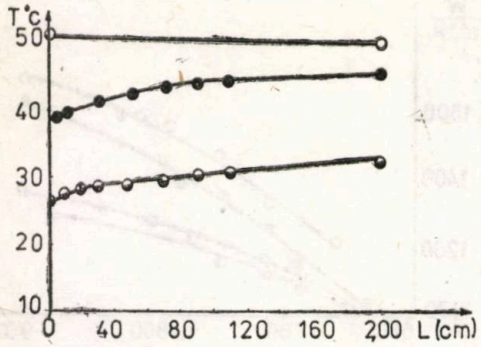

Fig. 10. — Variation of the temperature at the tube and film surfaces at $T_{inlet} = 50°C$ ($C = 56\,\%$), $\mathcal{R}e_{inlet} = 15\,000$, $\mathcal{R}e_{film} = 540$; hot water (○), wall (●), film (◒).

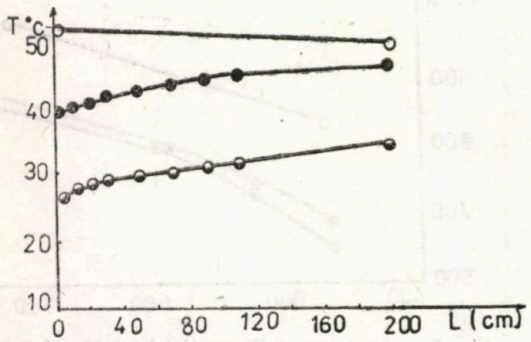

Fig. 12. — Variation of the temperature at the tube and film surface at $T_{inlet} = 50°C$ ($C = 56\,\%$), $\mathcal{R}e_{film} = 800$, $\mathcal{R}e_{inlet} = 15\,000$; hot water (○), wall (●), film (◒).

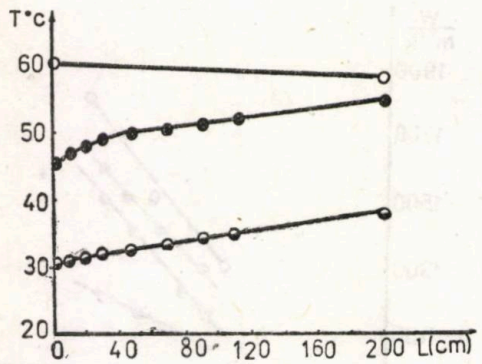

Fig. 14. — Variation of the temperature at the tube and film surface at $T_{inlet} = 60°C$ ($C = 56\,\%$), $\mathcal{R}e_{film} = 890$, $\mathcal{R}e_{inlet} = 18\,000$; hot water (○), wall (●), film (◒).

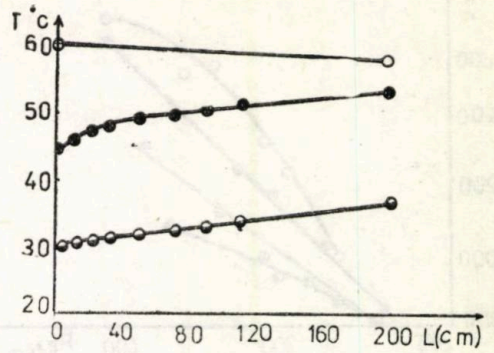

Fig. 11. — Variation of the temperature at the tube and film surfaces at $T_{inlet} = 60°C$ ($C = 56\,\%$), $\mathcal{R}e_{film} = 920$, $\mathcal{R}e_{inlet} = 18\,000$; hot water (○); wall (●); film (◒).

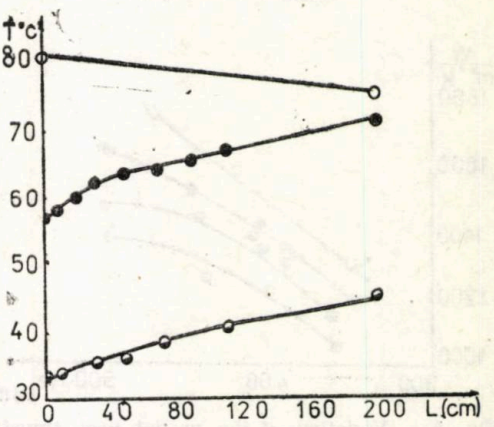

Fig. 13. — Variation of the temperature at the tube and film surfaces at $T_{inlet} = 80°C$ ($C = 56\,\%$), $\mathcal{R}e_{film} = 1\,040$, $\mathcal{R}e_{inlet} = 15\,000$; hot water (○), wall (●), film (◒).

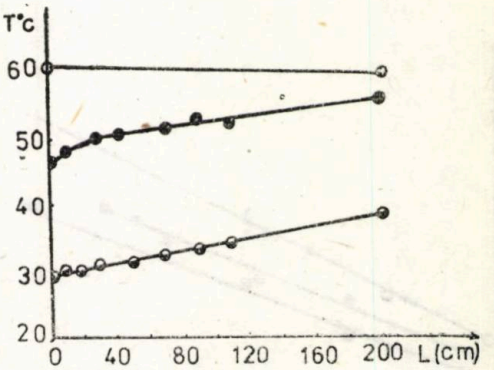

Fig. 15.— Variation of the temperature at the tube and film surface at $T_{inlet} = 60°C$, $\mathcal{R}e_{film} = 890$ ($C = 56\,\%$), $\mathcal{R}e_{inlet} = 24\,000$; hot water (○), wall (●), film (◒).

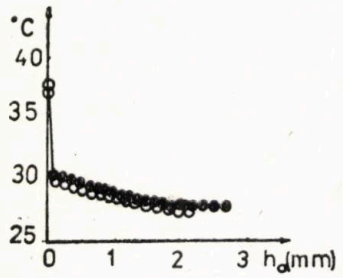

Fig. 16. — Variation of temperature vs. thickness at $\mathcal{R}e_{film} = 580$, $\mathcal{R}e_{inlet} = 18\,000$, $T_{film} = 25°C$, $T_{inlet} = 45°C$; length 30 mm (○), 130 mm (●); $C = 56\,\%$.

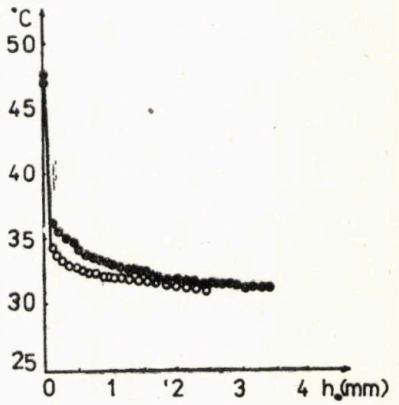

Fig. 17. — Variation of temperature vs. thickness at $\mathcal{R}e_{film} = 490$, $\mathcal{R}e_{inlet} = 18\,250$, $T_{film} = 30°C$, $T_{inlet} = 60°C$; length 30 mm (○), 130 mm (●); $C = 56\,\%$.

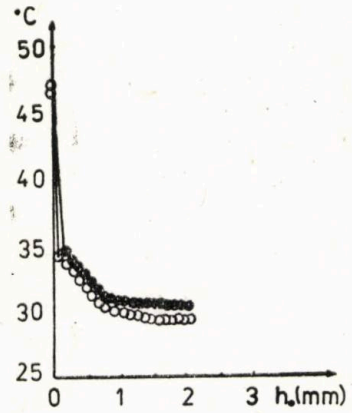

Fig. 18. — Variation of temperature vs. thickness at $\mathcal{R}e_{film} = 650$, $\mathcal{R}e_{inlet} = 18\,250$, $T_{film} = 30°C$, $T_{inlet} = 60°C$; length 30 mm (○), 130 mm (●); $C = 56\,\%$.

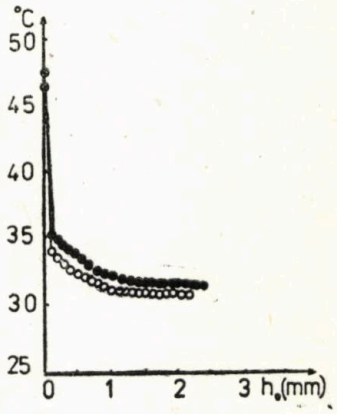

Fig. 19. — Variation of temperature vs. thickness at $\mathcal{R}e_{film} = 920$, $\mathcal{R}e_{inlet} = 18\,250$, $T_{film} = 30°C$, $T_{inlet} = 60°C$; length 30 mm (○); 130 mm (●); $C = 56\,\%$.

In Figs 4...9 the variations of the partial heat transfer coefficient vs. the $\mathcal{R}e$ number values, at various temperatures and concentrations, as well for some $\mathcal{R}e$ number values of the heating fluids are plotted.

The variation of the temperature of the tube surface and of the film w.r.t. the distance to the input zone, at various $\mathcal{R}e$ numbers of the fluids and at various temperatures of the heating fluid, are depicted in Figs. 10...15.

The dependence of the film temperature vs. the distance from the input zone, for various temperatures and $\mathcal{R}e$ numbers of the film, is represented in Figs. 16...19.

The flow regime and the temperature of the heating agent have a significant influence on the values of the partial heat transfer coefficient in the thin film. At the same $\mathcal{R}e$ number and the same temperature of the heating fluid the partial heat transfer coefficient significantly increases with increasing $\mathcal{R}e$ number of the film.

The increase of solution concentration, which leads to the consistency increase, determines the diminution of the film transfer coefficient.

5. Conclusions

In the thin film flow of the polyethylene oxide solutions the partial heat transfer coefficient at the film side is strongly affected by the $\mathcal{R}e$ number and temperature of the heating fluid.

The main resistance to the heat transfer is located near the solid surface in a layer of about 10 μm at all distances from the input zone, in the zone of smooth flow.

Notations

d — diameter, [m] ;
g — gravity acceleration, [m/s^2] ;
H — height of the surface the flow takes place on, [m];
k — index of consistency, [kg/m sec^{2-n}];
K — overall heat transfer coefficient, [W/m^2 gr] ;
n — index of flow (flow index) ;
t_{1f} — inlet temperature of the film, [°C] ;
t_{2f} — outlet temperature of the film, [°C] ;
t_{1AC} — inlet temperature of the heating fluid, [°C] ;
t_{2AC} — outlet temperature of the heating fluid, [°C],
t_{mp} — wall average temperature, [°C] ;
t_{mf} — film average temperature, [°C] ;
Dt_1 — $t_{mp}-t_{mf}$ — temperature difference, [°C] ;
Dt_m — minimum temperature difference at the ends of the heat exchanger, [°C] ;
Dt_M — maximum temperature difference at the ends of the heat exchanger, [°C] ;
$Dt_{m\ \log}$ — mean temperature difference ;
w — rate of the heating fluid, [m/s] ;

$\mathcal{R}e_{\text{int}} = \dfrac{Wd\,\rho_{AC}}{\eta_{AC}}$ — Reynolds number for the heating fluid ;

$\mathcal{R}e_F = \dfrac{12n}{2n+1} \cdot \dfrac{\Gamma}{\delta g} \left(\dfrac{\delta g \rho_F}{k} \right)^{1/n}$ — Reynolds number of the film ;

$\mathcal{G}a_F = H^3 g \left(\dfrac{\rho_F}{k} \right)^{2/n}$ — Galileu number of the film ;

α_F — partial heat transfer coefficient at the film, [W/m^2] ;

h_0 — mean thickness of the film in the smooth zone, [mm];
η_{AC} — viscosity of the heating fluid, [Pa.s];
ρ_F — density of the fluid flowing in thin film, [Kg/m^3];
ρ_{AC} — density of the heating fluid, [Kg/m^3];
Γ — volume flow rate per unit width, [m^2/s].

Received, June 19, 1986

Institute for Macromolecular Chemistry
„Petru Poni", Jassy, Romania
and
Polytechnic Institute, Jassy,
Department of Chemical Engineering

REFERENCES

1. Adams M.C., Drew T. B., Bays C.S., Trans. ASME, **62**, 627 (1940).
2. Davies E. I., Ind. Eng. Chem. Fund., **8**, 153 (1969).
3. Davies J. T., Shawki A.N., Chem. Eng. Sci., **29**, 1081–1088 (1974).
4. Ishigai S., Nakanisi S., Takehara M., Oyabu Z., Bul. of the ISME, **17**, *103*, 106–114 (1974).
5. Leonard W. K., Estrin J., AIChE J. **18**, *2*, 439–442 (1972).
6. Mukerje D., Davis E. J., AIChE J., **18**, *1*, 94–101 (1972).
7. Nuselt W., Ver. Deut. Ing., **67**, 206 (1923).
8. Norman W. S., Mc. Intrye V., Trans. Inst. Chem. Eng., **38**, 301 (1960).
9. Ponter A. B., Alamir A. A., Mangers R. I., Tenside Detergents, **17**, 306–313 (1980).
10. Ponter A. B., Davies G. A., AIChE J., **12**, 1029 (1966).
11. Ponter A. B., Davies G. A., Chem. Eng. Sci., **23**, *6*, 664 (1968).
12. Yih S. M., Liu J. L., AIChE J., **29**, *6*, 903–909 (1983).
13. Wilke W., Ver. Deut. Ing. Forsch., 490 (1962).
14. Silvester N. D., Tyler J. S., Skelland A.U.P., The Canadian J. of Chem., Eng., **51** (1973).
15. Tudose R. Z., Naforniţă C., Revue Roumaine de Chimie, **25**, *1*, 155–163 (1980).
16. Vitan F., *Studiul curgerii lichidelor în filme subţiri*. Ph. D. Diss., Polyt. Inst., Jassy, 1985.

STUDIUL EXPERIMENTAL AL TRANSFERULUI TERMIC LA CURGEREA ÎN FILME SUBŢIRI DE LICHIDE NENEWTONIENE

(Rezumat)

Se stabileşte o corelaţie pentru coeficientul parţial de transfer termic la curgerea în filme su bţiri a unor lichide nenewtoniene.

Cu creşterea numărului $\mathcal{R}_e$ al filmului şi al lichidului încălzitor creşte coeficientul parţial de transfer termic de partea filmului, iar cu creşterea viscozităţii are loc o scădere a acestuia.

BULETINUL INSTITUTULUI POLITEHNIC DIN IAŞI
Tomul XXXV (XXXIX), fasc. 1—2, 1989
Secţia II
CHIMIE ŞI INGINERIE CHIMICĂ

D.C. 621.51 ; 661.518

SELECTION AND DESIGN OF THE COMPRESSORS FOR AMMONIA INDUSTRY

BY

ILIE SIMINICEANU

1. Introduction

Nowadays the industrial output of ammonia amounts to roughly 100 million t/year and approximately 100 million of crude oil or its equivalent in other energy sources are consumed. This enormous energy consumption is the predominant area of concern in the nitrogen industry today [1]. The majority of large plants, exporting ammonia at — 33°C, based on hydrocarbon reforming, have a compression system that uses about 8×10^6 J/kg NH_3, equal to 20% of the total energy for ammonia production. This compression system includes : compression of natural gas and air before reforming, synthesis gas compression, recycle gas compression plus compression of ammonia vapour to supply refrigeration in the synthesis loop, as shown in Fig. 1.

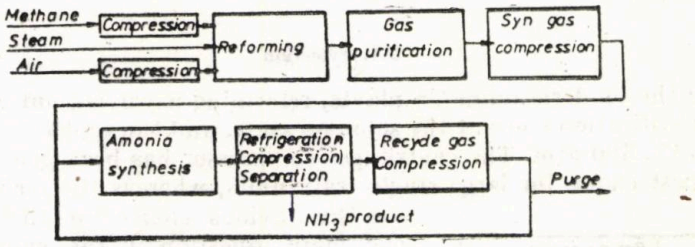

Fig. 1. — Simplified process flowsheat of an ammonia plant.

The syngas, makeup and recycle compressors account for 50 to 60% of the total compression power, depending on the synthesis loop pressure, the air and methane compressors account for 24%. The refrigeration compressor accounts for 20% [2].

Designers have reduced the compression energy requirement in some plants by substituting the mechanical refrigeration with the absorption one, which utilizes low level waste heat from the process or a flue gas stream. In a few ammonia plants, the condensing turbine drive for the air compressor has been replaced by a gas turbine drive. Further improvements of the compression systems for ammonia plants are however possible by a proper selection of the compressor types and their accurate design.

The criteria of selection of the compressor type and the basic equations for simplifying calculations, from a chemical engineer's point of view, are given in this paper.

2. Compressor Types and Selection

The principal types of compressor used in the chemical industry are : reciprocating, centrifugal, axial-flow and rotary compressors.

a) *The Reciprocating Compressors* are suitable for high pressure and low flow processes. They are generally considered for applications where the inlet gas rate is about 5,000 m^3/h or less. The maximum discharge pressure ranges from more than 4,000 atm for small machines to about 200 atm for larger units. The maximum compression ratio per stage is usually about 3 to 4. The outlet temperature and the mechanical stress usually limit the compression ratio. The mechanical design limit is usually 175°...200°C but lower temperatures may be required, depending on the gas properties: corrosiveness, tendancy to form polymer or gum, or undergo other chemical reactions, reactivity withs the compressor lubricating oil, oxidation or explosion possibilities, etc.

b) *The Centrifugal, or Radial Turbo-Compressors* are used for process applications from about 850 to 340,000 m^3/h. The performance of the centrifugal compressors can usually be approximated by the „fan laws". The volumetric flow rate varies approximately with rotating speed, the head with the square of speed and the power input with the cubic of speed. The maximum compression ration per stage is limited by the outlet temperature. The usual limit is 260°...280°C because they have diaphragms between impellers which tend to expand radially, due to the temperature rise. Sometimes, the compression ratio is set by maximum number of impellers that manufacturer can provide within a single casing (up to about 6...8).

The operating range for a centrifugal running at fixed speed is typically from 100% to about 50% of the design flow. The low end of this range is set by the surge point, where operation becomes unstable due to flow oscillation and vibration.

c) *The Axial Turbo-Compressors* are generally used for clean, non-corrosive gases, since these machines are more susceptibles to deposits corrosion and erosion than the centrifugals ones. They are suitable for high flow rates (125,000...1,000,000 m^3/h), and low pressures (9...10 atm). The operating range for an axial, running at fixed speed is much norrower than that of the centrifugals since the surge point is usually 85...95% of design capacity. The outlet temperature limit is about 315°C.

d) The common types of *Rotary Compressors* are : helical screw, spiral axial, straight lobe, sliding vane, liquid ring. Their maximum flow ranges from 10,000 m^3/h (sliding vane) to 50,000 m^3/h (straight lobe). The overall efficiences range from 50% (liquid ring) to 75% (helical screw).

2.1. Selection

In the modern ammonia plants, reforming is carried out at 30...40 atm, all the purification steps at the some pressure, and the synthesis loop is carried out at 135...300 atm. The centrifugal compressor has been generally accepted as the best choise for large single train units, whereas the reciprocating type was the obvious choice for the small plants. The main question is the capacity level at which the balance swings from one to other. For several years, the consensus was about 600 t NH_3/day as the dividing point. It is difficult to generalize, however, because so many factors are involved, namely : flow rate, maximum pressure developed, reliability, turndown, control, type of drive, investment and operating costs, type of operation.

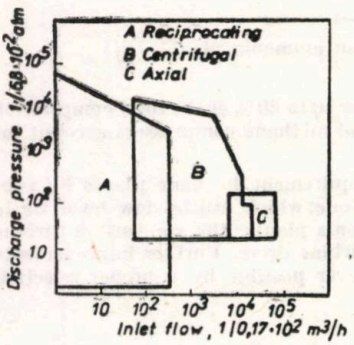

Fig. 2. — Approximate ranges of application for the main types of compressors [3].

Fig. 2 shows the approximate ranges of application for the main types of compressors taking into account only the first two factors : the discharge pressure and the inlet flow rate.

3. Compressor Design

A given compressor can be analysed by using one of the folowing calculation models : isothermal, adiabatic and polytropic.

a) *The Isothermal Calculation Model* has the advantage of supplying the minimum theoretical power requirement, assuming the heat of compression is fully removed by cooling. The basic assumption is that the temperature of the compressed gas never increases above the inlet temperature. Generally, this is not achieved or even approached in a industrial-scale compressor.

The theoretical power, W_{is}, for a reversible isothermal compression is :

$$W_{is} = P_s V_s \ln \frac{P_d}{P_s}, \tag{1}$$

where P_s and P_d are the gas pressures at suction and discharge, respectively. The heat of compression makes the gas temperature to rise, increasing the power requirement over the isothermal value computed by Eq. (1). The power delivered to the gas in a real compressor, W_g, and the brake power delivered by the driver, W_b, can be related to a reversible isothermal compressor by using, respectively, the following equations :

$$W_g = \frac{W_{is}}{\eta_{is}}, \tag{2}$$

$$W_b = \frac{W_{is}}{\eta_{is}\eta_m} = \frac{W_{is}}{\eta_{is0}}, \tag{3}$$

where : η_{is} is the isothermal efficiency, η_m — the mechanical efficiency and η_{is0} — the overall isothermal efficiency.

b) *The Adiabatic Calculation Model* is widely used for reciprocating and rotary compressors. The theoretical power requirement, W_{ad}, is given by

$$W_{ad} = \frac{P_s V_s}{m}\left[\left(\frac{P_d}{P_s}\right)^m - 1\right], \tag{4}$$

where : $m = (k-1)/k$ — adiabatic exponent ; $k = C_p/C_v$ — molar specific heat ratio. Although the Eq. (4) is established for an ideal gas with a constant specific heat, it gives fairly acc urateresults for real gases. It can be applied to real compressors using appropriate efficiency correlations :

$$\eta_{ad} = \frac{W_{ad}}{W_g}, \tag{5}$$

$$\eta_m = \frac{W_g}{W_b}. \tag{6}$$

The overall adiabatic efficiency (η_{ad0}) will be

$$\eta_{ad0} = \frac{W_{ad}}{W_b} = \eta_m \eta_{ad}. \tag{7}$$

When the polytropic efficiency is known the adiabatic efficiency can be estimated by the equation:

$$\eta_{ad} = \frac{(P_d/P_s)^m - 1}{(P_d/P_s)^{m'} - 1}. \tag{8}$$

The discharge temperature for an adiabatic stage of compression (T_d) is given by

$$T_d = T_s \left(\frac{P_d}{P_s}\right)^m . \tag{9}$$

This relation is plotted in Fig. 3.

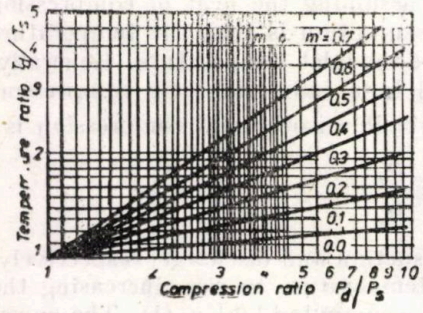

Fig. 3. — Temperature ratio T_d/T_s vs. compression ratio P_d/P_s.

c) *The Polytropic Compression Model* considers the compressor as a heat transfer device. This model is especially useful for radial and axial turbo-compressors. The polytropic compression follows the equation $PV^n = \text{const}$. The basic equation for one-stage of polytropic compression are analogous to those for an adiabatic one:

$$W_{pol} = \frac{P_s V_s}{m'} \left[\left(\frac{P_d}{P_s}\right)^{m'} - 1 \right], \tag{10}$$

where: $m' = (n-1)/n$ — polytropic exponent and n — exponent of the basic polytropic relation.

The polytropic exponent can be computed from the specific heat ratio (k) and the polytropic efficiency :

$$m' = \frac{1}{\eta_{pol}} \left(\frac{k-1}{k}\right) = \frac{m}{\eta_{pol}} , \tag{11}$$

$$\eta_{pol} = \frac{m}{m'} = \frac{(k-1)/k}{(n-1)/n} . \tag{12}$$

The polytropic efficiency is usually estimated from the empirical correlations. The Fig. 4 gives approximate polytropic efficiencies for radial and axial turbo-compressors.

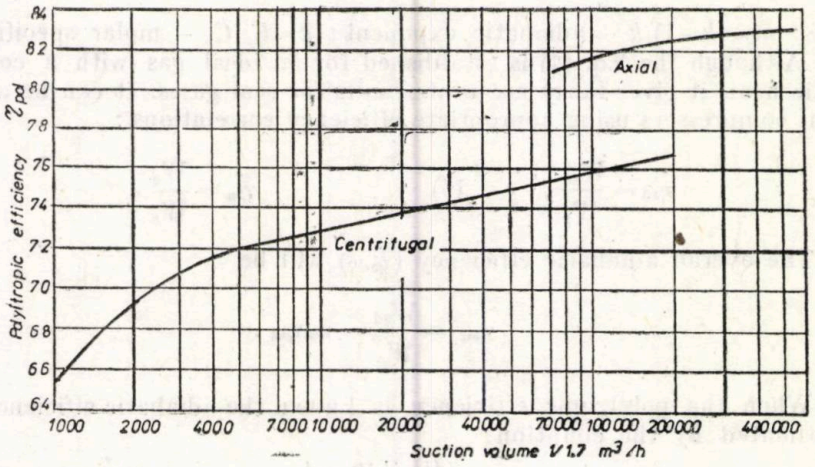

Fig. 4. — Approximate polytropic efficiency for radial and axial turbo-compressors [3].

The outlet temperature is computed by a relation analogous to the isentropic Eq. (9), plotted in Fig. 3.

In a multistage system, the polytropic formulas must be applied separately to each stage as in the adiabatic compression. A stage of compression may be defined as one or more units in series with no intercoolers between units. A radial or axial turbo-compressor casing with multiple impellers and no intermediate coolers is thus a single stage of compression.

Eq. (13) correlates the overall compression ratio of a multiple stage unit (z_0) and the N stages of compression with the same compression ratio for each stage (z):

$$N = \log \frac{z_0}{z} . \tag{13}$$

This equation neglects the pressure drop across the intercoolers, separators, interstage piping, etc. The number of stages is often set by the maximum discharge temperature limit. The outlet temperature in a multiple stage system should be computed by energy balance.

4. Conclusions

A chemical engineer can select the types of compressor used in ammonia industry employing the equations and charts presented here above, but the complex design and construction of these machines is not possible without the decisive contribution of the mechanical engineer.

Received, February 11, 1985

Polytechnic Institute, Jassy,
Department of Chemical
Inorganic Technology

REFERENCES

1. Calistru C., Leonte C., Siminiceanu I., Hagiu C., *Technologia îngrășămintelor minerale*. Vol. I, Ed. Tehn., Buc., 1984.
2. Stokes K. J., Chem. Eng. Process, **7**, 88 (1979).
3. Dimoplan W., Hydrocarbon Processing, **5**, 221 (1978).

SELECTAREA ȘI PROIECTAREA COMPRESOARELOR PENTRU INDUSTRIA AMONIACULUI

(Rezumat)

Procesele din industria amoniacului se desfășoară la presiuni ridicate. O fabrică contemporană de mare capacitate include un sistem de comprimare care consumă circa 8.10^6 J/kg NH_3, ceea ce reprezintă 20% din consumul total de energie al instalației de producere a amoniacului.

Se prezintă, din punctul de vedere al inginerului chimist, criteriile de selectare și o metodă de proiectare rapidă a compresoarelor pentru industria amoniacului.

BULETINUL INSTITUTULUI POLITEHNIC DIN IAŞI
Tomul XXXV (XXXIX), fasc. 1—2, 1989
Secţia II
CHIMIE ŞI INGINERIE CHIMICĂ

D.C. 631.859 ; 531.841.7

UREA-AMMONIUM PHOSPHATES FERTILISERS

BY

CAROLINA HAGIU

1. Introduction

The procedures of obtaining complex urea-ammonium phosphates fertilizers by combining the urea flowsheets with those of phosphoric acid can be accomplished in various technological variants, as a function of the peculiarities of technological procedures of urea obtaining. The analysis of the technological versions proposed by authors on the basis of mathematical models of mass and thermal balances [1] leads to the conclusion that using the urea solutions from stripping and first stage expansion, suspensions of urea-ammonium phosphates fertilizers with a N: P_2O_5 ratio varying between 1: 0.6 and 1 : 1.2, with a moisture content of 20...30% are obtained, which can be sent to granulation with or without previous concentration. In case of using the solutions resulted from the second stage of expansion, with a low NH_3 content fertilizer suspensions, with $N : P_2O_5 = 1 : 0.067$ are obtained, unsuitable for the common fertilizers ; this variant implies the correction of N : P ratio by introducing in the technological sheet a new preneutralizing process of the phosphoric acid and by changing the $m^0_{urea} : m^0_{acid}$ ratio.

In these paper the experimental results concerning the investigation of the possibilities of converting the urea solutions of various compositions into urea-ammonium phosphates fertilizers, by using two technological versions with and without preneutralization of the phosphoric acid are reported. The influence of the composition of reagent phases, the phase ratio and duration of the process achievement on the quality of the obtained fertilizers is investigated.

2. Experimental Results and Discussion

Urea solutions and suspensions of various compositions have been used, as follows : solutions taken from stripping Stamicarbon equipments after expansion at 3.5 and 1 ata (the solutions *1* and *2*), Stamicarbon with working the liquid phase by expansion in two stages (solution *3* — after expansion, the second stage) and the synthetic solution in the urea—NH_4OH—H_2O system (solution *4*). The composition of urea solution is given in Table 1.

Table 1

Composition of Urea Solution

Solution	Composition, [%]				
	$(NH_2)_2CO$	$(CO_2)_{carbamate}$	$NH_2-CO-NH_4$	NH_3	H_2O
1	61.2	3.09	5.47	4.28	29.05
2	71.5	0.21	0.37	0.58	27.55
3	64.91	0.26	0.47	0.30	34.22
4	39.50	—	—	5.89	44.61

The laboratory equipment consisted of a discontinuous reactor, with mechanical stirring, thermally insulated, provided with feed and outlet connections and test cock, control thermometer and gas removal connection. The process has been accomplished in an adiabatic thermal regime, the evolved heat determining the increase of the reaction mass temperature and water evaporation so that a fertilizer paste be finally obtained.

For accomplishing the variant with ammonia preneutralization a reactor for ammonia bubbling has also been included. The sketch of the experimental equipment is depicted in Fig. 1.

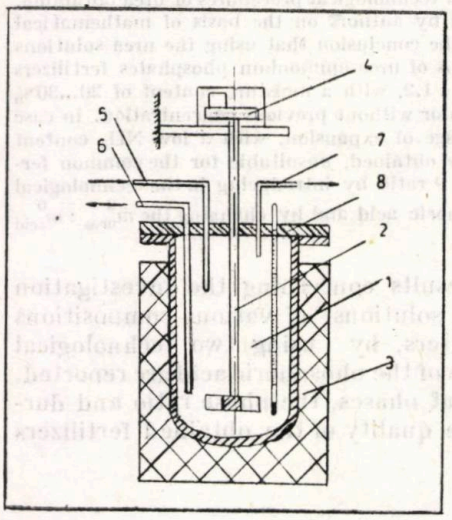

Fig. 1. — Diagram of the experimental equipment : *1* — Reactor ; *2* — Stirrer ; *3* — Thermal insulation ; *4* — Motor-reduction gear ; *5*, *6* — Feed connection and sampling device ; *7* — Gas removal connection ; *8* — Control thermometer.

To settle the optimum conditions for obtaining various sorts of fertilizers the influence of the chemical composition of reagent phases, of the phase ratio and of the residence time on the quality of the obtained fertilizers has been investigated, according to two versions of the technological process : with and without acid preneutralization.

The quality of the urea-ammonium phosphates fertilizer has been determined by means of the $N : P_2O_5$ ratio. For determination of the

P_2O_5 content, the gravimetric method of precipitating with quinoleine phosphate [2] has been used, the overall nitrogen being determined by K j e l d a h l method [3].

2.1. Influence of the Residence Time

Using the synthetic solution *4*, phosphoric acid with a content of $x_{P_2O_5} = 0.3209$, and carrying the process in thermal adiabatic regime for residence times varying between 5 and 30 min. the results listed in Table 2 have been obtained.

Table 2

Influence of Residence Time

No.	Time min.	Temperature °C	Suspension composition, $\bar{x}_{N_{overal}} \cdot 100$ %	$\bar{x}_{P_2O_5} \cdot 100$ %	$\frac{\bar{x}_N}{\bar{x}_{P_2O_5}}$	Fertilizer type
1	5	58	16.56	10.51	1.57 : 1	1 : 0.636
2	10	59	16.73	10.54	1.58 : 1	1 : 0.633
3	20	58	16.45	10.54	1.56 : 1	1 : 0.641
4	30	58	16.64	10.53	1.58 : 1	1 : 0.633

The process is found to proceed at high rates, after five minutes the suspension composition remaining practically constant the heat of reaction determines the increase of reaction mass temperature up to 58°...59°C and water evaporation, fertilizer suspensions with $N : P_2O_5$ ratio of 1.56...1.58 to 1 being obtained.

2.2. Influence of the Chemical Composition and of the Reagent Phase Ratio

The ratio of reagent phase is thus calculated as to assure the neutralization of free ammonia and of that found as carbamate in the urea solution up to an ammonization degree $\eta_A = 1.5$ [4].

Based on the mass balance equations [1] and assuming that the decomposition of ammonia carbamate and CO_2 desorption proceed completely, the following equation for calculating the phase ratio, has been derived:

$$\frac{m^0_{urea}}{m^0_{acid}} = \frac{0.434\bar{x}^0_{H_3PO_4}}{\bar{x}^0_{NH_3\ free} + 0.434\,\bar{x}^0_{cm}}. \quad (1)$$

The influence of chemical composition of the solutions and of the mass ratio of the latter is pointed out in Table 3.

Using synthetic urea solutions of various compositions and phosphoric acid with $x^0_{H_3PO_4} = 0.685$ at a phase ratio comprised between 1.11 and 2.32, fertilizer suspensions with an overall active substance varying between 25.94%

Table 3

Influence of the Chemical Composition and of the Reagent Phase Ratio

No.	Urea solution			Suspension composition			Fertilizer type
	$\bar{x}^0_u \cdot 100$ %	$\bar{x}^0_{NH_3T} \cdot 100$ %	$\frac{m^0_{urea}}{m^0_{acid}}$	$\bar{x}^0_N \cdot 100$ %	$\bar{x}_{P_2O_5} \cdot 100$ %	$\frac{\bar{x}_N}{\bar{x}_{P_2O_5}}$	
1	33.78	8.12	2.09 : 1	14.55	11.39	1.27 : 1	1 : 0.78
2	39.36	8.94	2.32 : 1	17.68	14.82	1.19 : 1	1 : 0.83
3	40.80	15.40	1.11 : 1	14.84	23.90	0.62 : 1	1 : 1.61

and 38.74% are obtained, the ratio between the essential nutrient element being comprised between (0.62...1.27) : 1.

2.3. Versions of Technological Process

The diversification of urea-phosphatic fertilizer sorts and the correction of N : P_2O_5 ratio is possible by introducing in the technological sheet of a pre-neutralizing process of phosphoric acid. The experimental results obtained with urea solution taken from the industrial equipment with the composition given in Table 1 (solutions *1*...*3*), using two variants of technological process, are listed in Tables 4 and 5.

Table 4

Composition of the Suspension of Urea Ammonium Phosphates Fertilizers
(Variant without Preneutralization)

No.	Urea solution	$\bar{x}^0_{H_3PO_4} \cdot 100$ %	$\frac{m^0_{urea\ sol.}}{m^0_{acid}}$	Suspension composition,		Fertilizer type
				$\bar{x}_N \cdot 100$ %	$\bar{x}_{P_2O_5} \cdot 100$ %	
1	Solution *1*	67.63	3.9	16.50	10.22	1 : 0.62
2		67.63	4.0	16.86	9.97	1 : 0.59
3		51.07	2.9	15.54	9.51	1 : 0.61
4		51.07	3.3	18.58	8.80	1 : 0.48
5	Solution *2*	67.63	7.5	19.38	5.76	1 : 0.29
6		67.63	7.5	19.82	5.94	1 : 0.29
7		51.07	5.6	18.63	5.50	1 : 0.29
8		51.07	5.5	18.10	5.89	1 : 0.32
9	Solution *3*	67.63	54	30.05	0.88	1 : 0.026
10		67.63	55	31.20	0.83	1 : 0.026
11		51.07	44	29.80	0.82	1 : 0.027
12		51.07	45	30.10	0.818	1 : 0.027

As can be seen in Table 4 the use of urea solutions with low ammonia content (free and in carbamate form) results in fertilizer suspensions with low P_2O_5 content and respective N : P_2O_5 ratio unusable in common fertilizers. The solutions from stripping (*1*) containing 4.28% free NH_3 and 5.47% carbamate lead to the obtaining of suspensions with N: P_2O_5=1: (0.48...0.62).

To correct the $N : P_2O_5$ ratio a process of phosphoric acid preneutralization has been included in the process.

Table 5

Composition of the Suspensions of Urea-Ammonium Phosphates Fertilizers
(Variant with Preneutralization)

No.	Urea solution	$\frac{m^0_{urea}}{m^0_{acid}}$	Suspension composition, [%]		Fertilizer type
			$\bar{x}_N \cdot 100$	$\bar{x}_{P_2O_5} \cdot 100$	
1	Solution *1*	1	16.38	25.02	1 : 1.50
2		1.66	16.42	18.65	1 : 1.13
3		2	16.75	16.77	1 : 1
4		3	17.15	12.60	1 : 0.73
5	Solution *2*	1.5	18.12	20.50	1 : 1.12
6		1.66	18.55	18.69	1 : 1
7		2	18.50	16.46	1 : 0.89
8		3	19.13	12.45	1 : 0.65
9	Solution *3*	0.66	21.53	29.40	1 : 1.36
10		1.00	21.87	23.84	1 : 1.09
11		1.33	22.94	20.56	1 : 1.89
12		1.66	23.68	17.76	1 : 0.75

The experimental results obtained in the case of variant with acid preneutralization (Table 5) indicated that the suspensions have $N : P_2O_5 = 1 : (0.65...1.5)$ which corresponds to the common fertilizers.

By changing the parameters of the technological process a large variety of urea-ammonium phosphates fertilizers of different compositions specific to various soils and cultures can be obtained.

3. Conclusions

The process of neutralization of the ammonia contained in the various urea solutions proceeds at a high rate with the removal of a significant water amount which leads to the obtaining of fertilizer suspensions which can be submitted to granulation with or without recirculation of the solid material.

The urea solutions with low ammonia content, resulting from the industrial equipment after expansion, lead to the obtaining of fertilizers with low P_2O_5 content, unsuitable for common fertilizers. The correction of the $N : P_2O_5$ ratio is accomplished by preneutralization of the acid with gases containing ammonia, coming also from the urea equipments.

The change of composition of urea solutions, of phase ratio and the introduction of a preneutralization process allow the obtaining of a wide game of urea-ammonium phosphates fertilizers.

Received, July 9, 1987

Polytechnic Institute, Jassy,
Department of Chemical
Inorganic Technology

REFERENCES

1. Hagiu C., Calistru C., III rd Symp. on Chemical Process Eng., P. Neamţ, 345 (1983).
2. * * * STAS 8623/3 (1970).
3. Liteanu C., Hopârţan E., *Chimie analitică cantitativă. Volumetrie.* EDP, Bucureşti, 1972.
4. Hagiu C., *Cercetarea procesului de amonizare a soluţiilor de acid fosforic* Ph. D. Diss., Polyt. Inst., Jassy, 1980.

ÎNGRĂŞĂMINTE UREO-FOSFATICE

(Rezumat)

Se expun rezultatele cercetărilor experimentale privind obţinerea îngrăşămintelor ureo-fosfatice prin integrarea liniilor de uree, acid fosforic şi / sau ortofosfaţi de amoniu. Modificarea parametrilor de realizare a procesului permite obţinerea unei game variate de sortimente de îngrăşăminte ureo-fosfatice, necesare diferitelor tipuri de soluri şi culturi.

BULETINUL INSTITUTULUI POLITEHNIC DIN IAȘI
Tomul XXXV (XXXIX), fasc. 1—2, 1989
Secția II
CHIMIE ȘI INGINERIE CHIMICĂ

D.C. 661.832.31 ; 66.061.6

KINETICS OF KCl DISSOLVING IN AMMONIUM FULPHATE SOLUTION

BY

STELIAN PETRESCU, C. CALISTRU and AL. SZÉP

1. Introduction

The study of the dissolving kinetics processes of a salt in an aqueous solution of another salt which contains different ionic species is less found in literature [1]...[3]. Literature presents many works dealing with the kinetics of dissolving of inorganic salts in water or in their aqueous solutions [4]...[10].

In the above quoted works [1]...[3] there is presented the macrokinetics and mathematical modelling of the dissolving process of KCl in ammonium sulphate solution based on the grain pattern.

Using the disk pattern, in what follows there in established a mathematical model which allows the determination of the dissolving rate and, respectively, of the mass transfer individual coefficient during solids dissolving.

The rate of potassium chloride dissolving in ammonium sulphate aqueous solution and the mass transfer individual coefficient are experimentally determined by using the disk pattern ; on this basis the influence of kinetic parameters over the rate of global dissolving process is studied.

2. Determination of the Mathematical Pattern

With the aim to determine the mathematical pattern of the dissolving of a disk form grain in an aqueous solution there was begun from the definition relation of component A dissolving rate [11] :

$$V_D = -\frac{dn_A}{S d\tau}, \tag{1}$$

where : n_A is the number of solute moles of disk grain at one time ; S — the disk surface in contact with solution ; τ — the duration of the process.

The variation of the number of moles of component A in an infinitesimal period of time is :

$$dn_A = \frac{dm_A}{M_A} = \rho \frac{\bar{x}_A}{M_A} dV_{[l]_s} = \rho^* dV_{[l]_s}. \tag{2}$$

According to Fig. 1, the correspondent variation of the grain volume is :

$$(3) \qquad dV_{[\,]_s} = \pi R^2\, dh$$

and consequently :

$$(4) \qquad dn_A = \pi R^2 \rho^*\, dh.$$

The disk surface in contact with liquid phase is unchanged in time and it is given by the relation :

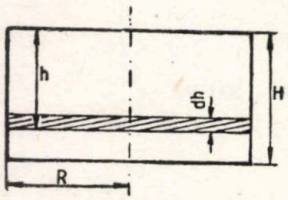

Fig. 1.—Disk grain pattern.

$$(5) \qquad S = \pi R^2.$$

Replacing relations (4) and (5) in Eq. (1) it results the following equation for dissolving rate :

$$(6) \qquad V_D = -\rho^* \frac{dh}{d\tau}.$$

As known, the degree of solute transformation is defined by the relation [11] :

$$(7) \qquad \eta_A = \frac{n_A^0 - n_A}{n_A^0},$$

where : n_A^0 is the number of solute moles from the initial grain ; n_A — the number of solute moles out of the grain at one time.

If the number of A moles is expressed by mass and there is passing to volume, is results :

$$(8) \qquad \eta_A = 1 - \frac{m_{[\,]_s}}{m^0_{[\,]_S}} = 1 - \frac{h}{H}.$$

The height of disk at one time is given by the following relation :

$$(9) \qquad h = H(1 - \eta_A).$$

Replacing relation (9) in (6) and taking into account that :

$$n_A^0 = \pi R^2 \rho^* H,$$

another form of the mathematical pattern of the solids dissolving occurs :

$$(10) \qquad V_D = \frac{n_A^0}{\pi R^2} \cdot \frac{d\eta_A}{d\tau}.$$

In conditions when the elementary transfer process have a leading part in the dissolving rate, there is possible to write :

$$(11) \qquad V_D = K_l (C_A^s - C_A).$$

Since the intinitesimal variation of solute moles number leads to an infinitesimal variation of the solution concentration, it results :

(12) $$-dC_A = \frac{\pi R^2 \rho^*}{V^0_{[]_l}} dh.$$

By integrations of Eq. (12) between the limits $h=H$, $C_A=0$ and $h=h$, $C_A=C_A$ we obtain :

(13) $$C_A = \frac{\pi R^2 \rho^*}{V^0_{[]_l}} (H-h).$$

Inserting relation (13) in Eq. (11) and using the following notation :

$$a = \left(\frac{C^e_A V^0_{[]_l}}{\pi R^2 \rho^*} - H \right)^{-1}$$

it results :

(14) $$V_D = K_l \left(C^e_A - \frac{\pi R^2 \rho^* H}{V^0_{[]_l}} \right) (1+ah),$$

whence :

(15) $$K_l = \frac{\rho^*}{(\pi R^2 \rho^* H / V^0_{[]_D} - C^e_A)(1+ah)} \cdot \frac{dh}{d\tau}.$$

Replacing Eq. (9) in (14) and (15), V_D and K_l become :

(16) $$V_D = \frac{n^0_A K_l}{V^0_{[]_l}} [1+a_1(1-\eta_A)],$$ (17) $$K_l = \frac{V^0_{[]_l}}{\pi R^2 [1+a_1(1-\eta_A)]} \cdot \frac{d\eta_A}{d\tau},$$

where :

$$a_1 = \left(\frac{C^e_A V^0_{[]_l}}{n^0_A} - 1 \right)^{-1}.$$

Eqs. (14)...(17) represent different forms of the mathematical pattern of solids dissolving in case when the elementary transfer process of potassium chloride through liquid phase is rate determinant.

In case when solute concentration in liquid phase is very small, ($C_A \simeq 0$), it may be neglected and the equations for the mass transfer individual coefficient become :

(18) $$K_l = -\frac{\rho^*}{C^e_A} \cdot \frac{dh}{d\tau},$$ (19) $$K_l = -\frac{n^0_A}{\pi R^2 C^e_A} \cdot \frac{d\eta_A}{d\tau}.$$

3. Experimental Technique

Experimental determinations were made using a laboratory installation depicted in Fig. 2. The installation consists of a laboratory thermostat (*1*), a stirring flask (*2*) supplied with an agitator with blades (*3*).

In the flask there is immersed a support cylinder (*4*) (20 mm depth from the blade and 10 mm distance from the flask wall), with a potassium chloride disk inside (*5*). To check the temperature of the mass of the reaction the reactor is equipped with a contact thermometer (*6*).

The installation is supplied with a belt-drive system (7) connected to an electric engine (8), which is fixed to a support.

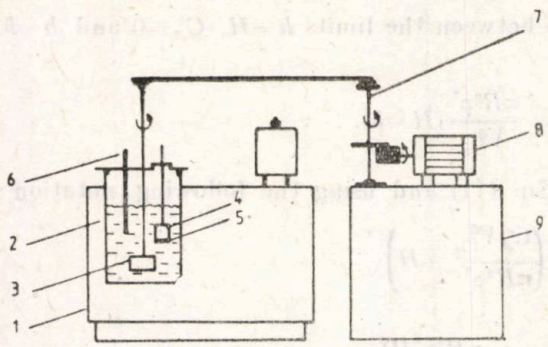

Fig 2. — Experimental installation.

Experimentally has been worked using chemically pure potassium chloride and an ammonium suphate solution prepared from technical ammonium sulphate resulted by caprolactam synthesis. The potassium chloride disk was made by moulding grains with granulosity $d_p < 0.045$ mm in the seat of the support cylinder.

For every kinetic curve, in reactor were introduced 500 ml of ammonium sulphate solution of a certain concentration, the stirrer being switched on afterwards.

Reaching the prescribed value of temperature, in the stirring flask there were immersed successively six support cylinders with potassium chloride disks, which were beforehand weighed with an analytical balance. For every cylinder it was mesured the contact time of the disk with ammonium sulphate solution. The contact time disk — solution was established as function of temperature, number of rotations and initial concentration of the ammonium sulphate solution.

At the end of the contact period of every cylinder, they were pulled out of reactor and put into an ethanol bath in order to remove the solution traces from the surface of the disk.

This operation take place in a very short time (approx. 10 sec.). The cleaning of the disk was followed by drying at 100°...105° C in a drying chamber. The dried disks together with the cylindrical support were weighed again.

By difference there was found the mass of potassium chloride passed into solution, respectively the amount of dissolved potassium chloride.

The variable parameters during the experiments were: temperature of the solution (T =25° ; 40° ; 60°C), initial concentration of ammonium sulphate solution ($\bar{X}^0_{(NH_4)_2SO_4} = 0{,}25$; 0,35), number of rotations of the stirrer (n =230 ; 540 r.p.m.).

4. Results and Discussions

The obtained experimental data were used for the tracing of the kinetic curves η_{KCl} vs. τ. In order to calculate the degree of potassium chloride transformation there was used the relation :

$$\eta_{KCl} = \frac{\sum_{i=1}^{n-1} m_i}{\sum_{i=1}^{n} m_i}, \tag{20}$$

where : m_i is the potassium chloride dissolved of the disk ; n — the total number of disks used for a single kinetic curve ;

The η_{KCl} vs. τ diagrams are represented in Figs. 3 and 4. The correlations found in these diagrams show that, for small amounts of dissolved potassium chloride, the transformation degree of KCl varies linearly during dissolution time. This observation point out that the dissolution rate of potassium chloride in ammonium sulphat solution is constant in time, in experiment conditions specified before.

Having in view the correlations from Figs. 3 and 4 were calculated the dissolution rate and the mass transfer individual coefficient of potassium chloride in ammonium sulphate solution.

Since the amount of dissolving KCl is small, $C_{KCl} \approx 0$, and to calculate the dissolving rate and the coefficient K_l were used Eqs. (10) and (19).

The mass transfer individual coefficient was calculated for the temperature of 25°C because, for the system K^+, NH_4^+ // Cl^-, SO_4^{2-}, H_2O exist equilibrium data only for this temperature.

The obtained results are shown in Fig. 5 and in Table 1.

Table 1

Variation of Dissolving Rate V_D and K_l Coefficient with Concentration and Number of Stirrer Rotations

	n r.p.m.	C^0, [mass %]	
		25	35
$10^5 \times V_D$ Kmol/m². s	230	3.0855	2.2978
	540	—	3.2225
$10^5 \times K_l$ m/s	230	2.3767	2.1152
	540	—	2.9667

From Fig. 5 it may be observed that the dissolving rate of KCl in ammonium sulphate solution increases with the growth of temperature.

Further on, using experimental data there was determined the apparent activating energy of dissolving process, appling with that end in view the graphic method.

Representing the dependence lg $1/\tau$ vs. $-1/T$ (Fig. 6), according to Arrhenius equation, the activation energy is given by the slope of the resulting stright lines. The diagram from Fig. 6 indicates, for dissolving KCl in ammonium sulphate solution of 35% mass concentration, the apparent activation energy of 6 398 cal/mol, in the temperature range 25°...60°C, for any values of transformation degree of potassium chloride. In connection with facts bellow there is obviously that in temperature range 25°...60°C, the elementary transfer process of KCl is rate determinant.

As shown in Table 1, the dissolving rate of potassium chloride in ammonium sulphate solution is increased by the number of rotations and decreased by the concentration of ammonium sulphate initial solution.

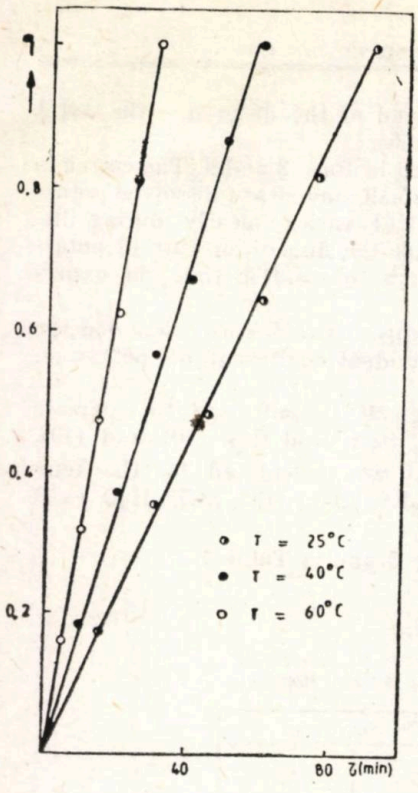

Fig. 3. — Dependence η_{KCl} vs. τ; n = = 230 r.p.m., $\bar{x}^0_{(NH_4)_2SO_4} = 0.35$.

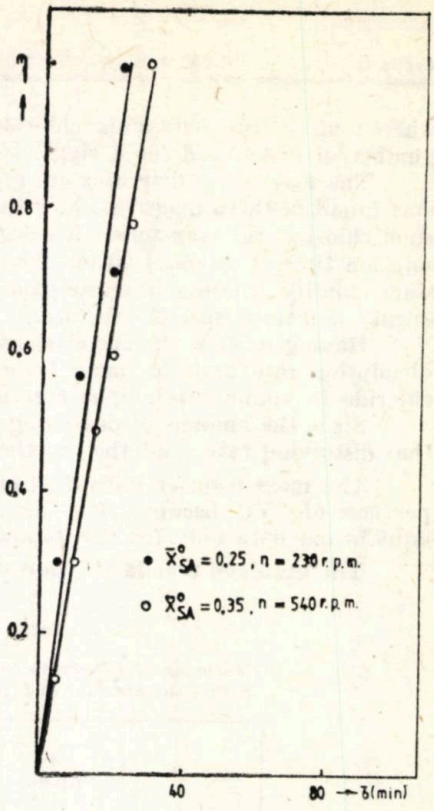

Fig. 4. — Dependence η_{KCl} vs. τ; T = 25°C.

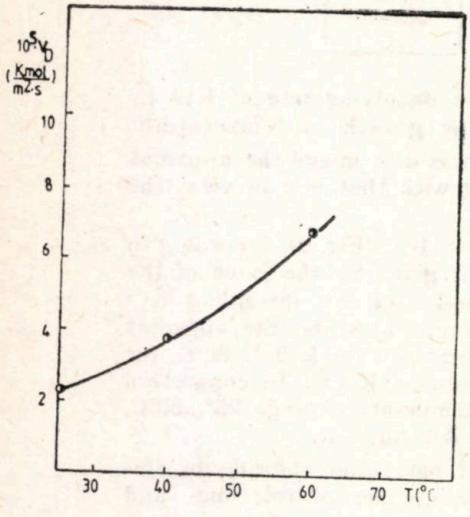

Fig. 5. — Dependence V_D vs. T; n=230 r.p.m., $\bar{x}^0_{(NH_4)_2SO_4} = 0.35$.

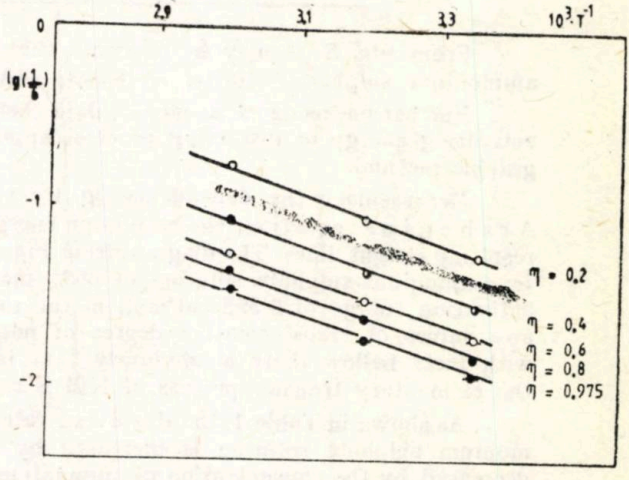

Fig. 6. — Dependence lg $1/\tau$ vs. $1/T$; n = 230 r.p.m., $\bar{x}^0_{(NH_4)_2SO_4} = 0.35$.

At regards the mass transfer individual coefficiert it increases with the number of rotations and decreases with growing concentration of ammonium sulphate initial solution.

These data point out too the fact that at low temperatures, the elementary transfer process of potassium chloride through liquid phase is speed determinant of the global process.

5. Conclusions

It was established a mathematical pattern for dissolving the disk form grains which allows experimental determination of the dissolving rate and of the mass transfer individual coefficient.

Using this pattern, the experimental values of the dissolution rate and of the mass transfer individual coefficient were determined by potassium chloride disk — form grains dissolving in an aqueous solution of ammonium sulphate at different concentrations, temperatures and number of rotations of the stirrer.

There was studied the influence of kinetic parameters upon the global dissolving process rate and established the rate determinant elementary process in certain experimental conditions.

Notations

C_A^e — equilibrium solute concentration, [Kmol/m^3];
C_A — solute concentration at one time, [Kmol/m^3];
ρ^* — molar density of the solute, [Kmol/m^3];
H — initial height of the disk, [m];
h — height of the disk at one time, [m];
R — radius of the disk, [m];
l, s — liquid, solide;
[ ] — phase.

Received, February 25, 1988

Polytechnic Institute, Jassy,
Department of Analytical and Inorganic Chemistry and Chemical Inorganic Technology

REFERENCES

1. Calistru C., Leonte C., Petrescu St., The Third Symp. on Chemical Processes Engineering, P. Neamţ, 1983, 57.
2. Calistru C., Petrescu St., Tordai E., Bul. şt. stud., Inst. polit. Iaşi, **IX**, 30 (1984).
3. Petrescu St., *Cercetarea de inginerie chimică a procesului de obţinere a sulfatului de potasiu prin valorificarea soluţiei de sulfat de amoniu rezultată la fabricarea caporolactamei*. Ph. D. Diss., Polyt. Inst., Jassy, 1987.
4. Ruckenstein E., St. cerc. chim., **15**, *1*, 1 (1967).
5. Sherwood T. R., Pigford R. L., Wilke C. R., *Mass Transfer*. McGraw-Hill, New York, 1975.
6. Mullin J. W., Nienow A. W., J. Chem. Eng., **9**, *4*, 526 (1964).
7. Bovington C. H., Jones A. L., Trans. Farad. Soc., **55**, *8*, 2088 (1970).
8. Boon Long S., Laguerie C., Coudere J. P., Chem. Eng. Sci., **33**, *7*, 813 (1978).

9. Inoue A., Tsujino T., Ind. Eng. Chem. Process Des. Dev., **23**, *1*, 122 (1984).
10. Trambouze P., Van Landeghem H., Wauquier J. P., *Les réacteurs chimiques*. Ed. Technip, Paris, 1984.
11. Calistru C., Leonte C., *Tehnologia substanțelor anorganice*. EDP, București, 1972.

CINETICA DIZOLVĂRII KCl ÎN SOLUȚIE DE SULFAT DE AMONIU

(Rezumat)

Se stabilește un model matematic al dizolvării solidelor pe baza căruia se poate calcula viteza de dizolvare și coeficientul individual de transfer de masă.

Rezultatele obținute pun în evidență influența parametrilor cinetici asupra vitezei procesului de dizolvare a clorurii de potasiu sub formă de discuri, în soluție apoasă de sulfat de amoniu, precum și procesul elementar, determinant, de viteză.

BULETINUL INSTITUTULUI POLITEHNIC DIN IAŞI
Tomul XXXV (XXXIX), fasc. 1—2, 1989
Secţia II
CHIMIE ŞI INGINERIE CHIMICĂ

C.D. 668.473

DÉTERMINATION DE QUELQUES CARACTÉRISTIQUES DU TALLOÏL BRUT

PAR

SAVEL IFRIM, CRISTINA LUCHIAN et MILITINA BOURCEANU

1. Introduction

Le talloïl brut est un mélange homogène de substances organiques ayant une grande valeur par ses multiples possibilités d'utilisation. Pratiquement c'est un sous-produit de la fabrication de la cellulose par le procédé „sulfate".

On connait que dans la composition du talloïl il y a un grand nombre de produits chimiques, appartenant surtout aux catégories des acides résiniques, des acides gras saturés et non-saturés, des produits insaponifiables, tels que des alcools, des stérols et des hydrocarbures [1]. Il peut également contenir un très petit pourcentage de substances volatiles, ainsi que traces d'eau (environ 2% ou plus).

La composition chimique du talloïl varie en larges limites et elle dépend de plusieurs facteurs à savoir : l'espèce ligneuse utilisée dans le processus d'ébullition, la qualité du bois, la région géographique de croissance du celui-ci, l'âge du bois, etc.

À partir du talloïl, par usinage [2], [3], on peut séparer des acides gras, des acides résiniques, du colophane et également d'autres produits organiques importants, qu'on peut utiliser, à leur tour, dans l'industrie des savons, des laques et des vernis, des résines synthétiques et des onguents, à l'encollage du papier. On peut utiliser ainsi le talloïl dans le processus de flottation ou bien dans des buts analytiques [4]...[6].

Compte tenu de l'importance particulière du ce produit organique, dans le présent travail on détermine quelques caractéristiques plus importantes du talloïl brut, séparé au Combinat de Fibres, Cellulose et Papier, Dej.

2. Partie expérimentale

Le talloïl utilisé pour analyse se présente comme un liquide homogène, consistant et huileux, ayant une couleur brune et une odeur moins agréable, proche à celle des conifères. Le produit a une viscosité relative grande à la température ambiante, pourtant il coule d'une façon continue sous l'influence de la gravitaton. Par chauffage vers 80°...100°C sa viscosité diminue et il devient plus fluide. Le talloïl est légèrement soluble en White-spirit, en méthanol et partiellement soluble en éthanol.

En solution diluée d'hydroxyde de sodium (10%) et également de carbonate de sodium concentrée, par chauffage, il se saponifie ; par dilution à l'eau et agitation mécanique on obtient des dispersions colloïdales ou même des solutions. En solution concentrée d'hydroxyde de sodium il se solidifie.

Pour caractériser le talloïl brut on a effectué les suivantes déterminations : l'humidité, l'indice d'acidité, le contenu des acides résiniques et des acides gras, l'indice de saponificaton, le contenu des substances insaponifiables et le pourcentage de cendre.

Afin de constater si ces caractéristiques changent dans un certain laps de temps, on a soumis à l'analyse des échantillons de talloïl séparés en 1981, 1983 et 1985.

Pour déterminer l'humidité et le pourcentage de cendre on a utilisé les méthodes classiques, connues.

La détermination de *l'indice d'acidité* est fondé sur le titrage d'une quantité de produit dissous en méthanol, avec une solution d'hydroxyde de potassium 0,5 n (en méthanol), en présence de bleu de bromothymol ; l'apparition de la couleur bleu indique l'équivalence. On utilise la relation :

$$\text{indice d'acidité} = \frac{56{,}1\ AN}{B}, \text{ [mg KOH/g produit]},$$

où : A — la solution de KOH, ayant le titre connu, [ml], N — la normalité de la solution alcaline, B — le poids de l'échantillon, [g].

Le dosage des *acides résiniques* a été effectué comme suit : dans un ballon de 250 ml on pèse par voie analytique le produit à analyser, on introduit 100 ml méthanol et 50 ml solution d'acide sulfurique en méthanol (400 ml méthanol et 5,43 ml acide sulfurique concentré, d=1,831). On reflue au bain-marie 30 min. Après refroidissement on y ajoute 1 ml de bromothymol (0,1 g pour 100 ml éthanol) et on titre avec une solution d'hydroxyde de potassium 0,5 n en méthanol, jusqu'à l'apparition d'une teinte marron-jaunâtre. En même temps on a suivi la valeur du pH, qui doit être égale à 4. On note avec a le nombre de ml de solution méthanolique de KOH utilisée. On continue le titrage jusqu'au virage de la solution vers vert-bleuâtre, en suivant toujours le pH, qui doit croître à 10,5. On note avec b, [ml], le volume de solution de KOH utilisée. Le contenu des acides résiniques est donné par la relation:

$$\%\ \text{acides résiniques} = 30{,}2\ \frac{AN}{B},$$

où : $A = b - a$ — la solution méthanolique de KOH, [ml] ; N — la normalité de la solution de KOH ; B — le poids de l'échantillon, [g].

Le contenu en acides gras résulte par la différence : % acides gras = = 100 — (acides résiniques + substances insaponifiables).

Pour déterminer *l'indice de saponifcation* on pèse l'échantillon dans un ballon de 250 ml et on ajoute 50 ml solution méthanolique de KOH 0,5 n. On reflue au bain-marie 30 min. On refroidit le ballon et sans laver le refrigérant on titre la solution avec H_2SO_4 0,5 n. Parallèlement on réalise une épreuve de contrôle, en titrant 50 ml de solution KOH 0,5 n avec la solution H_2SO_4 0,5 n. L'indice de saponification est donné par la relation :

$$\text{I.S.} = \frac{56{,}1\ (B - A)\ N}{C},$$

où : A — la solution de H_2SO_4 0,5 n utilisée pour le titrage, [ml] ; B — la solution de H_2SO_4 0,5 n utilisée pour le titrage de l'épreuve de contrôle, [ml] ; C — le poids de l'épreuve, [g] ; N — la normalité de la solution de H_2SO_4.

On réalise le dosage des *substances insaponifiables* de la manière suivante : dans un ballon à fond plat on pèse 5 g de talloïl, on y ajoute 15 ml solution alcoolique de KOH (132 g KOH en 150 ml de l'eau distillée et de l'éthanol jusqu'à 1 000 ml). On reflue 90 min. On ajoute 50 ml de l'eau distillée et on passe le contenu du ballon dans un entonnoir de séparation. On lave le ballon avec 40 ml éther, qui est introduit aussi dans l'entonnoir de séparation. On agite l'entonnoir et après la séparation des deux couches on passe la couche aqueuse dans un autre entonnoir de séparation. On effectue quatre extractions successives de 40 ml éther chacune, de la couche aqueuse.

On passe les extraits étheriques ensemble dans un ballon préalablement pesé. On distile l'éther et on sèche le residu pendant 10...15 min. à 100...105°C, en étuve. Après refroidissement on pèse le ballon, on dissout le contenu en 50 ml isopropanol neutre et on titre avec une solution alcoolique d'hydroxyde de potassium 0,1 n, en présence du bleu de bromothymol. Pour calculer le contenu en substances insaponifiables on utilise la relation :

$$\text{S.I.} = \frac{A - 0{,}302\ CN\ 100}{B},$$

où : A — le poids du résidu seché, [g] ; B — le poids de l'épreuve utilisée, [g] ; C — la solution de KOH 0,1 n utilisée au titrage, [ml] ; N — la normalité de la solution alcaline.

Tous les résultats des analyses sont présentés dans le Tableau 1.

Tableau 1

Humidité %	Indice d'acidité mg KOH/g	Acides résiniques %	Acides gras %	Indice de saponification	Substances insaponifiables %	Cendre %
Talloïl brut 1981						
1,0	112,21	70,60	12,80	98,11	20,65	2,10
1,2	111,80	68,60	14,20	99,26	20,81	2,90
1,4	109,70	66,50	16,20	100,30	18,66	3,00
Moyenne : 1,2	111,27	68,56	14,40	99,22	20,04	2,66
Talloïl brut 1983						
2,95	83,08	61,45	20,26	109,39	18,30	5,02
3,04	82,46	61,62	20,12	104,19	18,78	5,09
2,86	84,06	62,12	21,00	103,00	16,22	4,66
Moyenne : 2,95	83,20	61,73	20,46	105,33	17,76	4,92
Talloïl brut 1985						
2,99	112,83	66,61	14,91	111,02	18,48	4,08
2,50	109,49	66,68	15,10	110,96	18,22	4,20
2,40	112,22	66,83	14,64	110,04	18,53	4,21
Moyenne : 2,63	111,51	66,71	14,88	110,67	18,41	4,16

3. Interprétation des résultats

Par l'analyse des résultats enregistrés dans le Tableau 1 on observe qu'il n'y a pas de grandes différences concernant les caractéristiques du talloïl brut. Pourtant on peut mentionner une diminution de l'indice d'acidité pour l'épreuve de 1983 et une augmentation du pourcentage en acides gras. On observe également, pour l'épreuve de 1981, un indice de saponification moindre que pour les deux dernières, résultat qui peut être expliqué par l'existence d'un pourcentage plus élevé en substances insaponifiables.

Les caractéristiques physiques du talloïl, ainsi que le contenu réduit d'eau et de cendre, prouvent que ce produit est assez bien séparé au combinat de Dej, ayant une bonne pureté.

Dans tous les cas le contenu des acides résiniques est assez élevé et les données analytiques présentent une petite dispersion. Le pourcentage élevé des acides résiniques constitue un argument pour utiliser le talloïl comme matière première pour la séparation de la colophane ou comme agent de l'encollage du papier, compte tenu que les acides résiniques sont les composants fondamentaux de la colophane, agent classique de l'encollage.

La présence d'une proportion importante d'acides gras recommande le talloïl comme matière première pour obtenir ces produits, nécessaires pour la production des savons, des détergents, des laques, des teintures, etc. Même le talloïl brut, sans autres usinages, peut servir à l'obtention des savons. Les acides carboxiliques favorisent l'utilisation du talloïl pour obtenir des esters ; ce sont les esters de tall utilisés à la préparation des laques.

Puisque le talloïl contient des substances insaponifiables on peut l'utiliser pour isoler de tels produits parmi lesquels les plus connus sont les produits stéroliques.

Les observations présentées ci-dessus prouvent que le talloïl séparé au combinat de Dej est un produit de grande valeur, en représentant une source de substances organiques et sa récupération s'avère nécessaire dans toutes les fabriques de cellulose où ça c'est possible.

4. Conclusions

On détermine les principales caractéristiques physico-chimiques du talloïl brut, séparé au combinat de fibres, cellulose et papier — Dej. Ces caractéristiques sont déterminées pour le talloïl séparé en différentes périodes, en résultant qu'il n'y a pas de différences importantes entre elles. Compte tenu de sa composition chimique, on indique les principales directions de mise en valeur de ce mélange de produits organiques. On recommande d'isoler le talloïl dans toutes les fabriques de spécialité.

Reçue le 17 décembre 1986

Institut Polytechnique, Jassy,
Chaire de Chimie générale
et Technologie

BIBLIOGRAPHIE

1. Lorens C., Peintures – Pigments – Vernis, **47**, *7*, 388 (1971).
2. Трофимов А. Н., Бочарников Е. В., Узлов Г. А., Тобурдановская Л. А., Коган В. Б., Гидрол. и лесохим. пром., *1*, 10 (1974).
3. Узлов Г. А., Жукова И. П., Гидрол. и лесохим. пром., *2*, 12 (1973).
4. Ciobanu D., Cecal Al., Rev. de chimie, **35**, *1*, 68 (1984).
5. Ciobanu D., Cecal Al., Rev. de chimie, **35**, *3*, 267 (1984).
6. Ciobanu D., Cecal Al., Rev. de chimie, **35**, *5*, 420 (1984).

DETERMINAREA UNOR CARACTERISTICI ALE ULEIULUI DE TALL BRUT

(Rezumat)

Se determină cele mai importante caracteristici fizico-chimice ale uleiului de tall brut separat la combinatul de fibre, celuloză și hîrtie din orașul Dej. S-au supus la analiză probe din anii 1981, 1983 și 1985, constatîndu-se că nu apar diferențe importante privitoare la caracteristicile determinate, ele fiind invariabile în raport cu timpul de recoltare. Deoarece uleiul de tall are o compoziție chimică complexă, se propun cîteva direcții de valorificare a acestui subprodus, care apare la fabricile de obținere a celulozei prin procedeul „sulfat". Se recomandă separarea acestui produs la toate întreprinderile de specialitate.

BULETINUL INSTITUTULUI POLITEHNIC DIN IAŞI
Tomul XXXV (XXXIX), fasc. 1—2, 1989
Secţia II
CHIMIE ŞI INGINERIE CHIMICĂ

D.C. 547.572.1

2-HYDROXYKETONES

XVIII[1]). SYNTHESIS OF SOME NEW 3, 3, 6, 7, 8-PENTASUBSTITUTED 4-CHROMANONES

BY

ALEXANDRU CAŞCAVAL

1. Introduction

The well-known Mannich reaction applied to some *ortho*-hydroxyphenylketonea has been the subject of extensive synthetic effort in the last twenty years [2]...[5]. Ths most recent interesting result is reported by Werner [6] which converted 2'-hydroxyacetophenone in 3-dimethylaminomethyl-4-chromanone as a result from both a cyclocondensation and Mannich reaction in a „one-pot" reaction (we have given the name Werner—Mannich reaction for this synthesis).

Our interest in the synthesis of various oxygen-containing heterocyclic compounds exhibiting physiological activities, led us to apply the Werner—Mannich reaction to some halogenated alkyl 2-hydroxyphenyl ketones and so we have developed a facile one-step synthesis of some new bis-Mannich bases as 3, 3, 6, 8-tetrasubstituted 4-chromanones [7]. More recent we have reported a new versatile (possible to be generalized) synthesis of some mono-Mannich bases of 2, 3, 3, 6, 8-pentasubstituted 4-chromanones in a Werner—Mannich reaction applied to a substituted 2'-hydroxychalcone [8].

Kallay et al. [9] reported that some alkyl substituted 4-chromanones from natural sources exhibit physiological activity and more recent Ninagawa et al. [10] have found that two 2, 2, 5, 7, 8-pentasubstituted 4-chromanones are very useful as UV-absorbers.

2. Theoretical Considerations

Our recent results concerning the pharmacological screenings of some 3, 3, 6, 8-tetrasubstituted 4-chromanones[11] encouraged us to publish a very simple, one-step synthesis of some new 3, 3, 6, 7, 8-pentasubstituted 4-chromanones as bis-Mannich bases by both cyclocondensation and Mannich reaction : 3'-bromo-2'-hydroxy-4', 5'-dimethyl acetophenone (1) reacts with aqueous formaldehyde and cyclic secondary amines (2) to afford 3,3-/cyclo-amino-methyl/-8-bromo-6,7-dimethyl-4-chromanones (3) :

[1]) s. [1].

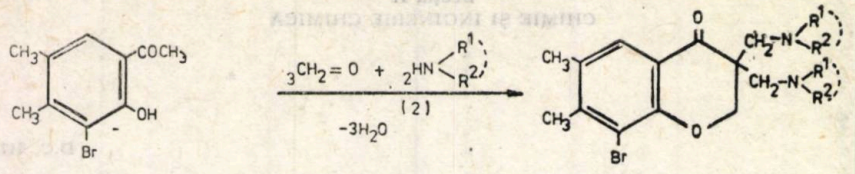

(1) (3)

2 3	R^1 R^2
a	$-(CH_2)_4-$
b	$-CH_2)_5-$
c	$-CH_2-CH_2-O-CH_2-CH_2-$

The most probable mechanism of this W e r n e r - M a n n i c h reaction is given by the reactions :

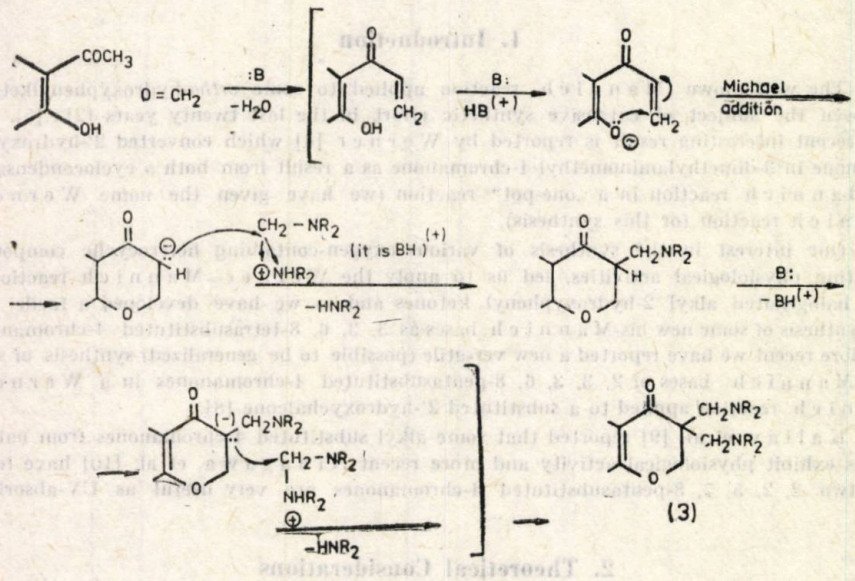

In summary we have developed a simple one-step synthesis of some new bis-M a n n i c h bases of 4-chromanones starting from *ortho*-hydroxyketones, formaldehyde and cyclic secondary amines with a great possibility of generalization of *this type of M a n n i c h reaction in basic medium*; basic medium is given by methylene-bis-amine ($CH_2(NR_2)_2$) which can be obtained by the reaction between formaldehyde and secondary amines.

Preliminary screening tests showed that the compounds (3) as dihydrochloride exhibit remarcable bactericidal and fungicidal activities [12].

The structures of compounds (1) and (3) were proven by microanalytical, I.R.-, and ^1H—N.M.R. - spectral data.

3. Experimental Part

3.1. 3′-Bromo-2′-hydroxy-4′,5′-dimethyl Acetophenone (1)

To a solution of 2′-hydroxy-4′, 5′-dimethylacetophenone [13] (16.5 g, 0.1 mol) in chloroform (100 ml) is added slow drop by drop bromine (16 g, 0.1 mol) at room temperature. The solution is allowed to stand at room temperature for 24 hours. The crude precipitate is recrystallized from ethanol ; yield 76% ; m.p. 105°...106°C.

		C%	H%	Br%
$C_{10}H_{11}BrO_2$ (243)	calculated	49.38	4.53	32.92
	found	49.50	4.62	33.11

I.R. (KBr) : ν 2 900 (CH) ; 1 630 (CO) cm^{-1}.

$^1H-N.M.R.$ ($CDCl_3/TMS_{int}$) : δ=2.2 (*s*, 3H, CH_3-5′) ; 2.3 (*s*, 3H, CH_3-4′) ; 2.5 (*s*, 3H, CH_3-CO) ; 12.1(*s*, 1H, OH — deuterable) ppm.

3.1. 3.3-Bis/cycl-Aminomethyl/-8-bromo-6.7-dimethyl-4-chromanones (3) ; General Procedure

To a solution of acetophenone (1) (243 mg, 1 mmol) and the cyclic secondary amine (2) (technical grade, 2.5 mmol) in ethanol (25 ml) is added aqueous 30% formaldehyde (0.5 ml, 4 mmol) and the mixture is refluxed for 3 h. Cold water (100 ml) is then added and the product (3) is extracted with ether (2×25 ml). The extract is dried with sodium sulfate and evaporated to give crude product. For purification, products (3) are recrystallized from ethanol (Table 1).

Table 1

Substituted 4-Chromanones (3) Prepared

Product	Yield %	m.p. °C	Molecular Formula[a)]	I.R.(KBr) ν, [cm^{-1}]	$^1H-N.M.R.$ ($CDCl_3/TMS_{int.}$)[b)] δ, [p.p.m.]
3 *a*	83	111...112	$C_{21}H_{29}BrN_2O_2$ (421)	2 900 (CH) 1 680 (CO) 1 240 (C−O−C)	7.5(*s*, 1H, H-5) ; 4.48(*s*, 2H, CH_2) ; 2.4−3.0 (*m*, 18H, $2CH_3+6CH_2N$) ; 1.5−1.8 (*m*, 8H, $4CH_2C$).
3 *b*	77	114...115	$C_{23}H_{33}BrN_2O_2$ (449)	2 900 (CH) 1 685 (CO) 1 250 (C−O−C)	7.5 (*s*, 1H, H-5) ; 4.5 (*s*, 2H, CH_2) ; 2.5−3.0 (*m*, 18H, $2CH_3+6CH_2N$) ; 1.5−2.0 (*m*, 12H, $6CH_2C$).
3 *c*	60	123...124	$C_{21}H_{29}BrN_2O_4$ (453)	2 900 (CH) 1 675 (CO) 1 230 (C−O−C)	7.45 (*s*, 1H, H-5) ; 4.5 (*s*, 2H, CH_2-2) ; 3.35−3.55 (*t*, 8H, $4CH_2O$) 2.2−2.9 (*m*, 18H, $2CH_3+6CH_2N$).

a) The microanalysis were in satisfactory agreement with the calculated values : C, ±0.25 ; H, ±0,20 ; N, ±0.25 ; Br, ±0.25.

b) Recorded on a JEOL instrument at 50°C and 60 MHz.

* * *

The author is thankful to „Alexander von Humboldt-Stiftung", Bonn, for providing a fellowship at the University of Freiburg i.Br., also Prof. Dr. Hans-Joachim Cantow and Prof. Dr. Gerhard Wegner for encouragements and generosity, BASF/Ludwigshafen (West-Germany) also Petrochemical Works, Borzești, Romania, for the gift of several compounds.

Received, December 28, 1984

Polytechnic Institute, Jassy, Department of Organic and Macromolecular Chemistry and Technology

REFERENCES

1. Caşcaval Al., *1.2-Hydroxyketones.* XVII, (private communication).
2. Котон М. М., Андреева И. В., Турбина А. И., Синявский В. Г., ДАН СССР, **159**, 602 (1964).
3. Турбина А. И., Синявский В. Т., Романкевич И., УХЖ, **31**, 85 (1965).
4. Tramontini M., Synthesis, 703 (1973).
5. Kabbe H. J., Synthesis, 886 (1978).
6. Werner W., Arch. Pharm. (Weinheim Ger.), *309*, 1011 (1976).
7. Caşcaval A., Synthesis, 579 (1983).
8. Caşcaval Al., Synthesis, 277 (1984).
9. Kállay F., Janzsó G., Egyed I., Baitz-Gács E., in *Flavonoids and Bioflavonoids Current Research Trends*, edited by Farkas L., Gabor M., Kállay F., Akademiai Kiadó, Budapest, 1977, 235.
10. Ninagawa A., Iseki T., Matsuda H., Makromol. Chem., *184*, 71(1983).
11. Caşcaval Al., Mişcovici E., Chiorean V., Romanian Patent (RSRP) *79907* (1982).
12. Caşcaval Al., Radu C., private communication.
13. v. Auwers K., Bundesmann H., Wieners F., Liebigs Ann. Chem., *447*, 162 (1926).

2-HIDROXICETONE

XVIII. Sinteza cîtorva noi 4-cromanone 3, 3, 6, 7, 8-pentasubstituite

(Rezumat)

Se studiază extinderea reacției Mannich—Werner descrisă de noi în 1983 [7] constînd în folosirea în calitate de *orto*-hidroxicetonă a produsului (1)-3′-brom-2′-hidroxi-4′, 5′-dimetilacetofenona, care în reacție cu formaldehida (soluție apoasă) și aminele ciclice secundare (2) conduce cu randamente bune (între 60 și 83%) la bis-bazele Mannich—Werner (3 *a*...*c*). Se propune un mecanism al acestei reacții iar substanțele sintetizate sînt caracterizate din punct de vedere analitic și spectral (I.R., R.M.N.).

BULETINUL INSTITUTULUI POLITEHNIC DIN IAŞI
Tomul XXXV (XXXIX), fasc. 1—2, 1989
Secţia II
CHIMIE ŞI INGINERIE CHIMICĂ

D.C. 678.675.462

DIRECT POLYCONDENSATION OF CYCLOALIPHATIC DICARBOXYLIC ACIDS WITH DIAMINES CATALYSED BY TRIPHENYL PHOSPHITE

BY

V. BULACOVSCHI and MARIA GROVU—IVĂNOIU

1. Introduction

It is allready known that phosphites, especially diphenyl and triaryl phosphites, react non-oxidatively with carboxylic acids in presence of pyridine to give acyl-oxy-N-phosphonium salt of pyridine accompanied by dephenoxylation, which produces the corresponding amides and esters on aminolysis and alcoholysis [1], [2]. The reaction promoted by triphenyl phosphite (TPP) and pyridine has been succesfully applied to the direct polycondensation of *p*-aminobenzoic acid and isophthalic acid and diamines. High yields and high molecular weight polymers were obtained except when terephthalic acid was the monomer [3].

To overcome this difficulty it was suggested to realise these reactions in a mixed solvent of pyridine and N-methylpyrrolidone (NMP) or N,N-dimethylacetamide (DMAA) containing LiCl and $CaCl_2$ (separately or mixed) to increase the dissolution capacity of solvents [4]. Some considerations were also published concerning condition and order of introducing reactants and catalyst. More favourable results were obtained when inorganic salts were dissolved in presence of pyridine prior to use and the TPP in NMP was prewarmed.

In this paper we examine conditions for the synthesis of aromatic — cycloaliphatic polyamides by direct polycondensation of 1,2-cyclopropane- and 1-methyl-1,2-cyclopropanedicarboxylic acids (CPDA and MCPDA) with various aromatic diamines in presence of pyridine (Py) and TPP. The obtained polymers were characterised by spectral and thermal way.

2. Experimental Part

The cycloaliphatic dicarboxylic acids were prepared by the method mentioned in [5], [6]. Anhidrous $CaCl_2$ and LiCl were dried at 180°C for 8 h and 130°C for 4 h, respectively. The employed solvents were dried on CaH_2 and purified by vacuum distillation. Pyridine was dried on KOH and distilled over molecular sieves.

The polycondensation was carried out with magnetical stirring in a three neck flask, equipped with a reflux condenser, N_2 inlet tub and dropping funnel. The whole system was heated at 100°C for 2 h. The resulting polymer was ground in methanol, separated by filtration, washed with water and methanol and then dried in vacuum at 40°C. The viscosity of polymer sol-

utions was measured on an Ubbelohde viscometer, in H_2SO_4 (0.5 g/dL) at 30°C. The melting range was established on a hot-stage microscope in polarized light. Thermal analysis was run on a Paulik–Paulik–Erdey MOM, Budapest, apparatus, in a dynamical heating regime (7°C/min). The IR spectra (KBr pellets) were registered on a SPECORD – IR apparatus.

3. Results and Discussion

As a typical experiment of this investigation, a mixture of 0.65 g (5 mmol) CPDA, 0.541 g (5 mmol) *p*-phenylendiamine (*p*-PDA) and 2.1 g LiCl (or the preestablished quantities of $CaCl_2$ and LiCl) is dissolved in 30 mL NMP and 10 mL pyridine on warming (50°...60°C). From the dropping funnel, a solution of TPP (3.1 g; 10 mmol) in 20 mL NMP preheated at approx. 60°C is added, then the temperature is rised at 100°C and maintained for 2 h. The catalytic presence of TPP favours, practically, a quantitative conversion of reactants; in equivalent amounts it brings also an important increase of the polymer viscosity.

The direct polycondensation of dicarboxylic acids with diamines promoted by phosphites, can be described by the following sequence of reactions [7]:

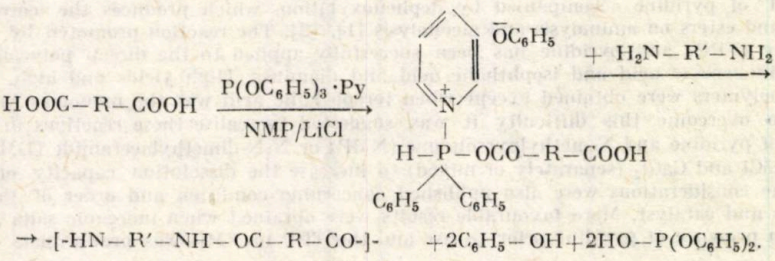

An important role is played by pyridine which improves the solubility of the salt, and solutions of higher concentration can be obtained. The better solubility might be due to the formation of a complex such as $CaCl_2 \cdot n$Py which may be readly soluble in NMP or DMAA. Pyridine enables also formation of the acyl-oxy-N-phosphonium intermediate, on what finally depend conversion and viscosity of the synthesised polymers.

The direct polycondensation of CPDA and *p*-PDA was carried out at 100°C for 2 h in a solution containing LiCl (2.1 g) initially dissolved in 50 mL NMP in the presence of various amounts of pyridine (Table 1). The viscosity of the resulting polymer increases with the amount of pyridine, showing better results for NMP/Py = 50/10 [mL/mL] and Py/LiCl = 2.5 ratioes.

The polycondensation of CPDA and *p*-PDA was carried out also in various solvents containing LiCl in presence of pyridine. Among the solvents tested, NMP and DMAA proved to be more effective (Table 2). They readly dissolve the inorganic salt and resulted polymer, and possible, they influence the reactivity of the acyl-oxy-N-phosphonium intermediate. All reactions were carried out at constant monomer concentration and solvent/pyridine ratio.

Table 1

Polycondensation of CPDA and p-PDA in NMP/Py Solution Containing LiCl (time = 2 h ; T = 100°C)

Pyridine mL	Py/LiCl mol/mol	Conversion %	η_{inh}
0	0	96.1	0.015
4.1	1	94.0	0.14
6.1	1.5	100.0	0.2
10.2	2.5	100.0	0.35

CPDA = *p*-PDA = 5 mmol ; NMP = 50 mL ; $P(OC_6H_5)_3$ = 10 mmol ; LiCl = 2.1 g.

Table 2

Effect of Solvent Nature on Polycondensation of CPDA and MCPDA with p-PDA

Dicarboxylic Acid	Solvent	Conversion %	η_{inh}	Softening range °C
CPDA	DMAA	100	0.33	300
MCPDA	DMAA	97.3	0.23	291...300
CPDA	NMP	100	0.35	300
MCPDA	NMP	100	0.19	251...260
CPDA	DMF	31.8	0.11	—
CPDA	DMSO	30.8	0.09	—

Dicarboxylic acid = Diamine = 5 mmol ; Solvent = 50 mL ; $P(OC_6H_5)_3$ = 10 mmol ; Py = 10 mL ; T = 100°C ; time = 2 h ; LiCl = 2.1 g.

Nearly good yields were obtained in DMF and DMSO. Although LiCl was soluble in these solvents at the used concentration the obtained results are poor due, probable, to the lower solubility of the synthesised polyamides.

Table 3 retains some data concerning the influence of inorganic salts in the polycondensation process. Despite use of the same solvent composition and amount of metal salts, the reaction with the mixture of $CaCl_2$ and LiCl dissolved in NMP/Py gave better results (η_{inh} = 0.42). This phenomenon can be attributed to the increased solubility of the polymer and to an initial double salt complex $CaCl_2$.LiCl.*n*Py which favors the polycondensation reaction [4].

Several aromatic — cycloaliphatic polyamides from CPDA, MCPDA and aromatic diamines were prepared by carrying out the reaction under the most favorable conditions for the reaction of CPDA and *p*-PDA (Table 4). Changing the diamine no significant effects were observed. However, it appears that substituted monomers give some higher molecular weight polyamides, and that polymers of MCPDA are of lower viscosity. Former aspects can be attributed to the increased solubility of the obtained polymer.

Table 3

The Influence of the Nature and Salts Quantity upon the Polycondensation of CPDA and MCPDA with p-PDA in NMP/Py Solution

Dicarboxylic acid	Inorganic salt	Conversion %	η_{inh}	Softening range °C
CPDA	LiCl	100	0.35	300
CPDA	$CaCl_2$	98.5	0.12	295...300
MCPDA	$CaCl_2$	98.9	0.11	282...290
CPDA	$CaCl_2$/LiCl	100	0.42	300
MCPDA	$CaCl_2$/LiCl	100	0.39	296...300

Dicarboxylic acid = Diamine = 5 mmol ; NMP = 50 mL ; Py/($CaCl_2$+LiCl) = 2.5 mol/mol; $CaCl_2$/LiCl = 3 : 1 g/g ; Salt concentration = 4% ; $P(OC_6H_5)_3$ = 10 mmol ; T = 100°C ; time = 2 h.

Table 4

Polyamides from CPDA, MCPDA and Several Diamines Prepared by Direct Polycondensation Technique in NMP/Py Solution Containing 4% w ($CaCl_2$+LiCl)

Dicarboxylic acid	Diamine	η_{inh}	State of the system
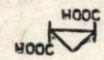	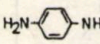	0.42	Very viscous solution
	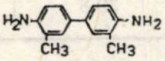	0.48	Very viscous solution
	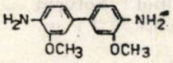	0.57	Gel
	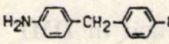	0.23	Gel
	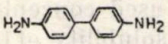	0.30	Fluid gel
	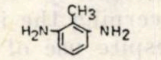	0.29	Consistent gel
	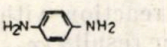	0.25	Viscous solution
	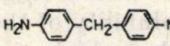	0.226	Viscous solution
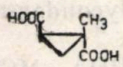	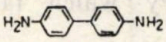	0.25	Fluid gel
	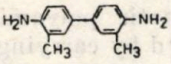	0.28	Viscous solution
	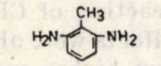	0.18	Gel

Dicarboxylic acid = Diamine = 5 mmol; $P(OC_6H_5)_3$ = 10 mmol; NMP/Py = 50/10 mL/mL ; $CaCl_2$/LiCl = 3/1 g/g ; T = 100°C ; time = 2h.

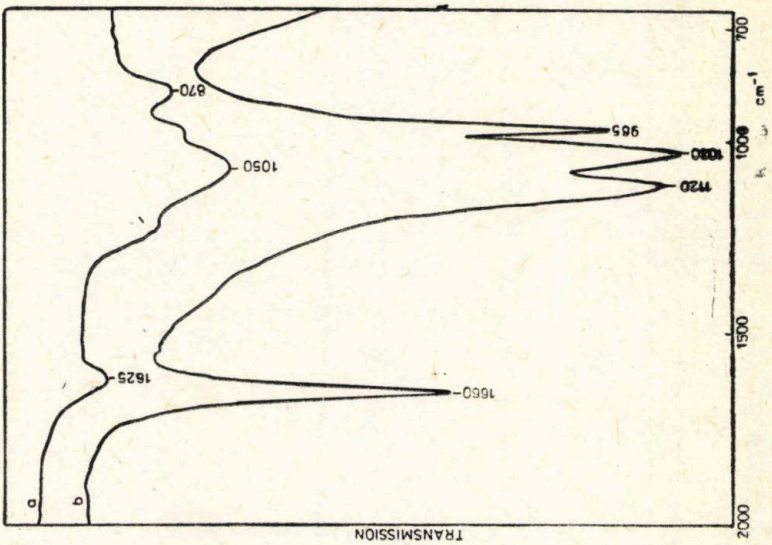
700
1000
1500
2000
cm⁻¹
870
965
1050
1080
1120
1625
1660
a
b
TRANSMISSION

Fig. 2

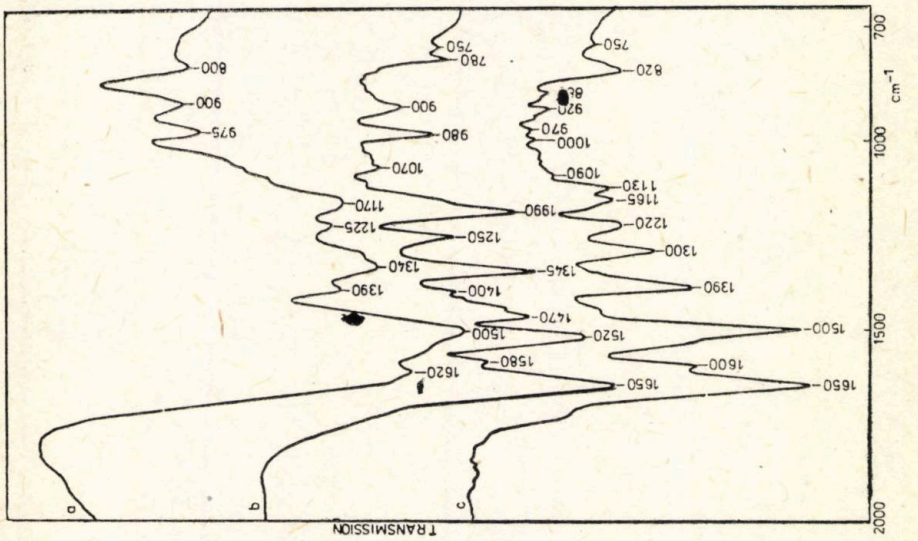
700
1000
1500
2000
cm⁻¹
750
780
800
820
900
920
975
980
1000
1070
1090
1130
1165
1170
1190
1220
1225
1250
1300
1340
1345
1390
1400
1470
1500
1520
1580
1600
1620
1650
a
b
c
TRANSMISSION

Fig. 1

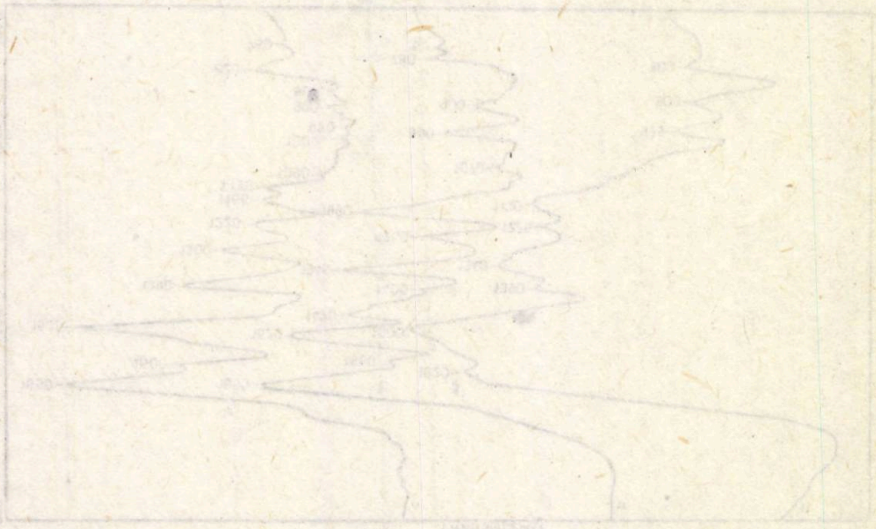

In a similar manner we have prepared copolyamides of the *p*-aminobenzoic acid (*p*-ABA), CPDA and *p*-PDA (Table 5). Reaction proceeds almost quantitatively to products of high inherent viscosities and high melting points (over 300°C). These copolymers proved themself to be also of remarcable thermostability. They loose less than 10% of their weight on heating at 375°...450°C.

Table 5

Aromatic—Cycloaliphatic Copolyamides Prepared in NMP/Py Solution Containing 4% w ($CaCl_2$+LiCl)

Comonomers, [mmol]			Conversion %	η_{inh}
p-ABA	CPDA	*p*-PDA		
20	—	—	100	0.67
17	1.5	1.5	99.1	1.02
14	3.0	3.0	98.4	1.08
10	5.0	5.0	98.8	1.10
5	7.5	7.5	99.3	1.12

NMP = 130 mL ; Pyridine = 20 mL ; $CaCl_2$/LiCl = 3/1 g/g ; $P(OC_6H_5)_3$ = 20 mmol.

Table 6

Thermal Behaviour of Polyamides with Cycloaliphatic Units in the Chain

No.	Polymer structure	Reaction order	E_a, [Kcal/mol]			Decomposition domain, °C
			I	*II*	*III*	
1	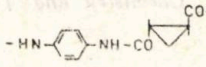	1	—	67.06	—	430...620
2	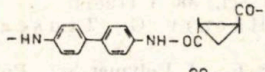	2.4	—	127.67	—	480...630
3	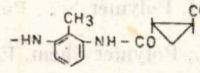	2.5	—	49.63	—	420...610
4	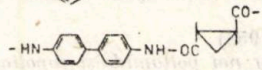	0.08	21.02	—	—	300...480
		1.7	—	29.08	—	550...750
5	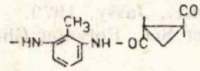	0.0	27.51	—	—	130...210
		1.1	—	62.67	—	550...670
6	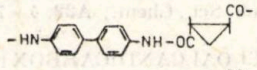	1.6	—	63.72	—	510...660
		1.5	—	—	91.86	790...880
7	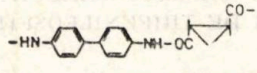	2.5	46.33	—	—	120...200
		0.0	—	36.27	—	530...650
		1.8	—	—	21.78	780...870

Polymers 1...4 were obtained by interfacial polycondensation ; polymers 5...7 were obtained by direct polycondensation.

Spectral registrations of the synthesised polymers outline some characteristic IR-absorbtions like those at 1 600...1 650 cm^{-1} for amide *I* or 1 500...1 520 cm^{-1}, for amide *II* structures (Fig. 1). For these polymers they are better revealed than in the products of the same structure but prepared by interfacial polycondensation [8].

The structural characteristics of the copolyamides are in good agreement with their composition. Cyclopropane unit in the macromolecular chain is outlined by 965 cm^{-1} stretching vibration and amide *I* structure by 1 625...1 660 cm^{-1} absorbtion (Fig. 2 *b*). There are no absorbtions for amide *II* structure and, as a matter of fact, these spectra appear to be more simple.

To further understand the relationship of chemical structure to thermal stability, a thermogravimetric analysis of the synthesised products was undertaken. The results summarized in Table 6 show that the thermodegradative processes proceed in two or three steps. Also, the behaviour of cycloaliphatic—aromatic polyamides stands apart from other products having increased thermostability (400°...450°C). High activation energies, especially for the symmetrical polymers, were calculated. For comparation, Table 6 includes also data concerning thermal behaviour of polyamides obtained by interfacial polycondensation technique.

4. Conclusions

The obtained results indicate that direct polycondensation technique may be succesfully used in the synthesis of aromatic—cycloaliphatic polyamides. Reaction proceeds with almost quantitative yields and to high molecular products, which show good thermal and chemical stability. By their properties the aromatic—cycloaliphatic polyamides are very close to the common aramides.

Received, April 23, 1987

Polytechnic Institute, Jassy,
Department of
Organic and Macromolecular
Chemistry and Technology

REFERENCES

1. Yamazaki N., Higashi F., Adv. in Polymer Sci., **38**, 1 (1981).
2. Chiriac C., Grăescu D., Chiriac F., Răcaru G., Truscan I., Mat. plastice, **22**, 147 (1985).
3. Yamazaki N., Matsumoto M., Higashi F., J. Polymer Sci., Polymer Chem. Ed., **13**, 1378 (1975).
4. Higashi F., Ogata S. I., Aoki Y., J. Polymer Sci., Polymer Chem. Ed., **20**, 2081 (1982).
5. Mc. Coy E. L., J. Amer. Chem. Soc., **80**, 6568 (1958).
6. Bouchi E. Al., *Cercetări în domeniul sintezei unor noi poliamide și copoliamide cu secvențe cicloalifatice în lanț.* Ph. D. Diss., Polyt. Inst., Jassy, 1979.
7. Higashi F., Goto M., Kakinoki H., J. Polymer Sci., Polymer Chem. Ed., **18**, 1711 (1980).
8. Bulacovschi V., Simionescu C., J. Macromol. Sci., Chem., **A22**, 5—7, 561 (1985).

POLICONDENSAREA DIRECTĂ A ACIZILOR CICLOALCANDICARBOXILICI CU DIAMINELE AROMATICE ÎN PREZENȚA DE TRIFENILFOSFIT

(Rezumat)

Se studiază posibilitatea sintezei de poli- și copoliamide aromatic—cicloalifatice prin tehnica policondensării directe a acizilor dicarboxilici cu diaminele în prezență de trifenil fosfit. Reacția decurge cu randament cantitativ în soluție mixtă de N-metil pirolidonă și piridină în care s-a dizolvat în prealabil o sare anorganică (LiCl și/sau $CaCl_2$).

BULETINUL INSTITUTULUI POLITEHNIC DIN IAŞI
Tomul XXXV (XXXIX), fasc. 1—2, 1989
Secţia II
CHIMIE ŞI INGINERIE CHIMICĂ

D.C. 66.095.2

CONTRIBUTIONS TO THE SYNTHESIS, POLYMERIZATION AND COPOLYMERIZATION OF SOME *p* - SUBSTITUTED VINYLIC MONOMERS

BY

I. MAZILU, LUCIA TĂTARU, I. COCÎRLĂ, CAMELIA PETRESCU and TATIANA LIXANDRU

1. Introduction

Polymers carrying reactive groups on the macromolecular chain have aroused a special interest, both from the theoretical and practical point of view. They may be used in analogous polymer reactions, on one side soluble, while on the other one, they may form tridimensional structures.

Literature data make mention of a series chloroformylated vinylic derivatives and of their polymerization [1]...[5].

The present paper studies the synthesis and characterization of some *p*-substituted chloroformylated compounds, their thermal polymerization and copolymerization, as whel as the properties of the obtained compounds. Experimental data, correlated with LCAO—MO H ü c k e l calculations, permitted certain considerations regarding the influence of the *p*-positioned substituents of the first and second order on the monomer reactivity, in the polymerization reaction.

2. Experimental Part

Monomers of the type

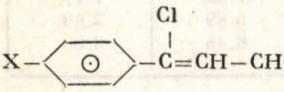

X=Cl, Br, I, CH_3, C_2H_5, i-C_3H_7, OCH_3, OC_2H_5, NO_2

have been synthesized according to the method described in literature for similar compounds [3], [6]...[8], by the reaction of the acetylated derivatives with the Vilsmeier complex.

The reaction of thermal polymerization and copolymerization was performed in inert medium, in closed glass vials. Fractions soluble and unsoluble in usual organic solvents have been obtained. Purification of the soluble fractions was achieved by their solving in benzene and by precipitation with acidified methanol, while the purification of the unsoluble ones by repeated solvent washings, for the removal of monomers.

The IR spectra, in KBr tablets, have been registered with an UR-20 spectrophotometer, while the RMN spectra, with a Jeoltype equipment, by using $CDCl_3$ as solvent and TMS as a standard.

The thermal stability of the monomers and polymers has been estimated through the thermograms registered with a derivatograph of the type MOM Budapest, J. Paulik – F. Paulik–L. Erdey.

The monomer reactivity has been estimated by LCAO–MO calculations, on an Iris-50 computer.

3. Results and Discussions

3.1. Structure and Reactivity of Monomers

Chloroformylated vinylic derivatives have been characterized by elemental, spectral (IR and RMN) and thermodifferential analysis.

a) *The IR Spectra* of all monomers evidence characteristics bands of the $\rangle C=O$ groups, at 1 650 cm^{-1} (X=Br, I, OCH_3, OC_2H_5); 1 675 cm^{-1} (X=Cl, CH_3); 1 680 cm^{-1} (X=i-C_3H_7); 1 690 cm^{-1} (X=NO_2) as well as of the *p*-substituted aromatic ring (700...900 cm^{-1}). Absorptions caused by the ethylenic double bond and by the halogene fixed to the unsaturated carbon atom are superposed on the aromatic ring. The *p*-positioned substituents appear in the IR spectra at specific frequencies, namelly: $\nu_{CH_3\,sym.}$=2 880 cm^{-1}, $\nu_{CH_3\,asym.}$=2 913 cm^{-1}, $\nu_{NO_2\,sym.}$=1 355 cm^{-1}, $\nu_{NO_2\,asym.}$=1 525 cm^{-1}; the ether link C–O–C, 1 025 cm^{-1}.

The monomer structure is also confirmed by the values of the chemical shifts in RMN spectra:

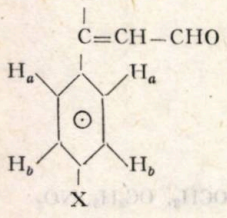

δ, [ppm]

X	CHO	=CH	H_a	H_b
Cl	10.29	6.63	7.68	7.50
Br	10.28	6.62	7.56	7.80
I	10.41	6.55	7.32	7.70
CH_3	10.15	6.58	7.62	7.17
OCH_3	10.33	6.58	6.89	7.69
NO_2	10.45	6.75	8.45	8.00

b) *The Thermodifferential Analysis* shows a good thermal stability of the monomers up to 100°C, above which a two or three step degradation occurs.

At high temperatures (700°, 800°C) the monomer decomposition is almost total.

For estimating the influence of the *p*-positioned substituent on the monomer reactivity in the polymerization reaction, the LCAO–MO Hückel method was applied. By performing the HMO calculations, the parameters listed in Fig. 1 have been used [9]...[11].

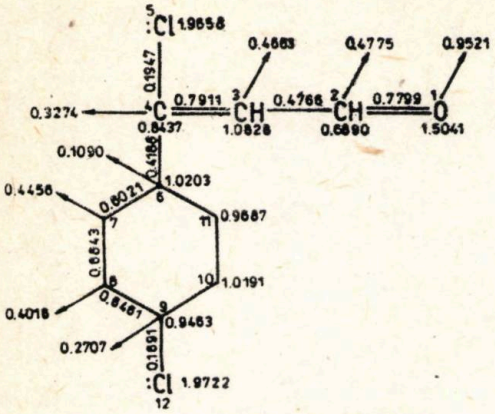

Fig. 2. — Molecular diagram of α-chloro-β-formyl-*p*-chlorostyrene.

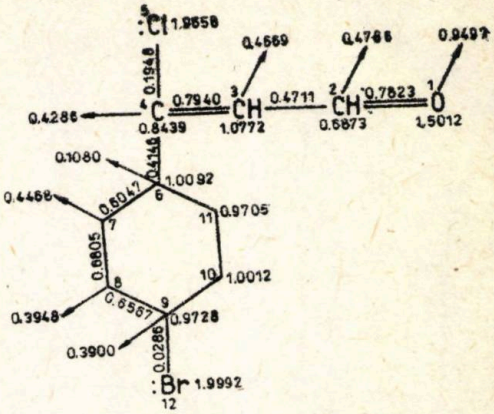

Fig. 3. — Molecular diagram of α-chloro-β-formyl-*p*-bromostyrene.

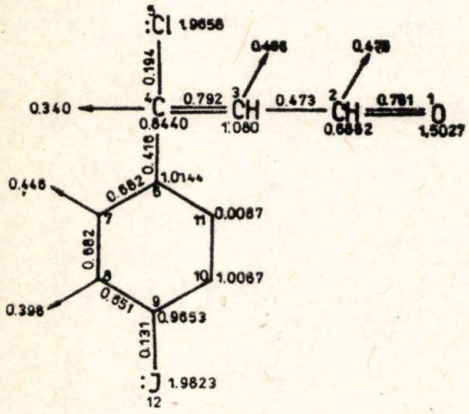

Fig. 4. — Molecular diagram of α-chloro-β-formyl-*p*-iodostyrene.

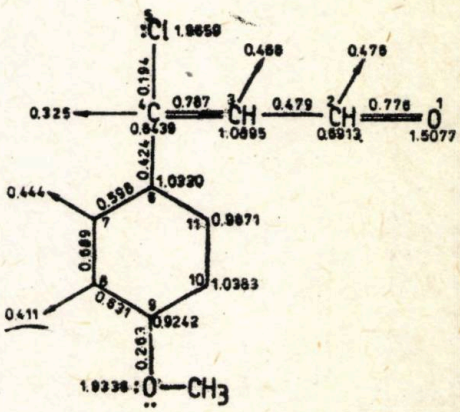

Fig. 5. — Molecular diagram of α-chloro-β-formyl-*p*-metoxystyrene.

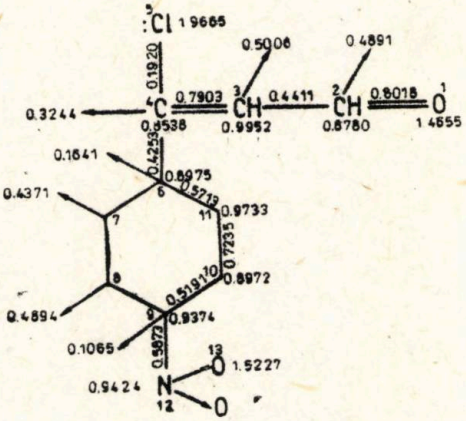

Fig. 6. — Molecular diagram of α-chloro-β-formyl-*p*-nitrostyrene.

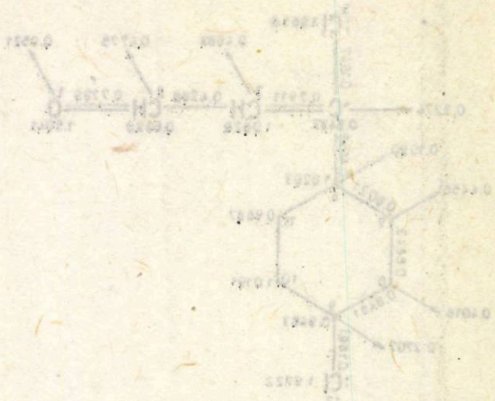

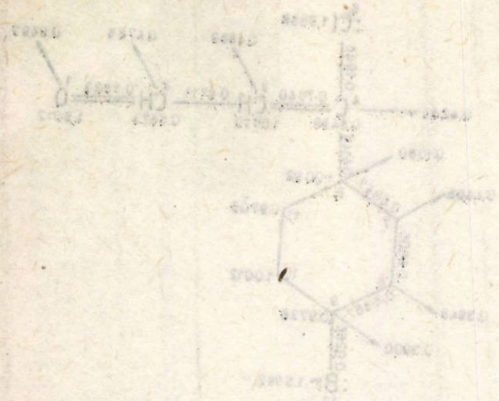

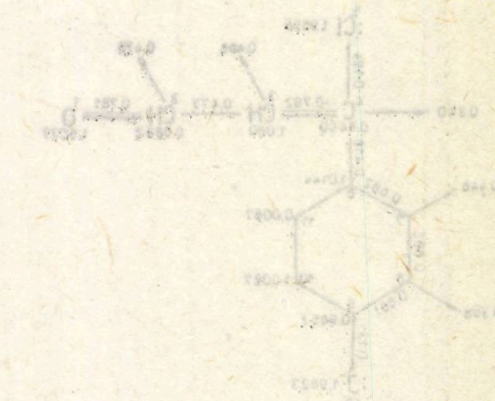

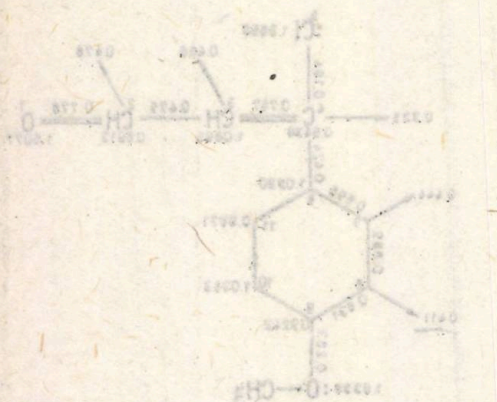

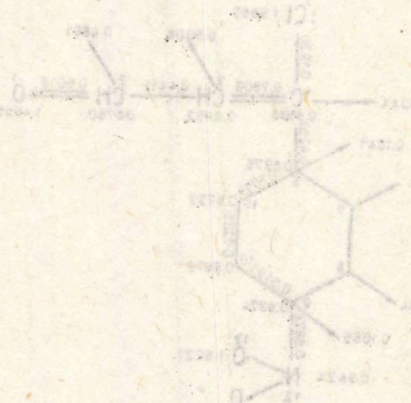

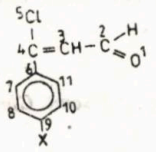

$\alpha_O = \alpha + \beta$ $\beta_{C-Cl} = 0.6\beta$
$\alpha_{\ddot{O}} = \alpha + 2\beta$ $\beta_{C-Br} = 0.4\beta$
$\alpha_{Cl} = \alpha + 2.5\beta$ $\beta_{C-J} = 0.3\beta$
$\alpha_{Br} = \alpha + 2.4\beta$ $\beta_{C-O} = 0.8\beta$
$\alpha_J = \alpha + 1.2\beta$ $\beta_{C-NO_2} = \beta$
$\alpha_{C_6H_5} = \alpha + 2\beta$ $\beta_{NO(NO_2)} = \beta$
$\alpha_{N(NO_2)} = \alpha + \beta$ $\beta_{C-C_6H_5} = 0.7\beta$
$\alpha_{O(NO_2)} = \alpha + 1.5\beta$ $\beta_{1,2} = \beta_{3,4} = 1.1\beta$
$\beta_{2,3} = 0.9\beta$

Fig. 1. — Values of the α (the Coulomb integral) and β (the resonance integral) parameters.

The obtained values are indicated in the molecular diagrams from Figs. 2 ... 6 and Table 1.

Table 1

Molecular Characteristics of α-Chloro-β-Formyl-p-Substituted Derivatives

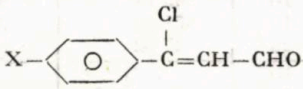

X	Total energy E_π, [β]	Resonance energy E_R, [β]	n_π	E_R/n_π
H	19.5634	2.963	12	0.247
Cl	24.6642	3.064	14	0.218
Br	24.3663	2.966	14	0.212
I	22.0030	3.403	14	0.243
CH_3	23.5436	2.943	12	0.210
OCH_3	23.7720	3.172	14	0.226
NO_2	24.7919	3.692	14	0.263

n — number of π electrons.

The E_R value represents the thermodynamic stability, while E_R/n — the chemical stability of the molecules [12].

By taking into account the values of the resonance energies and the chemical stability, one can estimate the influence of the substituents on the monomer reactivity, which increases in the order:

$$NO_2 < H \leqslant I < OCH_3 < Cl \leqslant Br \leqslant CH_3.$$

In the case of a radicalic process, present in thermal polymerization, the information from molecular diagrams evidence that, for all compounds, the radicalic attack (possibly, oxygen traces) begins at the C_3 atom ($F_3 > F_4$; Figs. 2 ... 6).

3.2. Thermal Polymerization of α-Chloro-β-Formyl-*p*-X-Styrene

The influence of temperature and of the reaction time on the conversion and degree of polymerization has been studied; the data obtained are listed in Table 2.

As shown in Table 2, for the same reaction time, conversion increases with temperature. At the same temperature and reaction time, conversion

Table 2

Experimental Data concerning the Thermal Polymerization and some Characteristics of the Obtained Products

X	Reaction temperature, [°C]	Time h	Conversion %	$\bar{P}$	M.p. °C	Reference
Cl	180	10	6.98	6	204	[13]
	200	10	8.03	8	218	[13]
	230	10	18.10	12	195	[13]
	300	10	35.82	4	249	[13]
	300	20	22.91	3	202	[13]
Br	180	10	35.08	7	230	[13]
	200	10	43.79	6	250	[13]
	230	10	43.98	9	266	[13]
	300	10	51.72	3	294	[13]
	300	20	47.52	3	284	[13]
I	150	10	—*)			[15]
	180	10	—*)		—	
			25.5		256	[15]
	200	10	—*)		—	
			47.7		256	[15]
CH_3	180	10	18.5	6	256	[14]
	200	10	27.8	7	210	[14]
	230	10	31.8	14	256	[14]
	230	20	33.8			[14]
	300	10	44.5		300	[14]
C_2H_5	200	10	10		195	
	230	10	24			
	300	10	54		300	
	300	20	37		200	
$i\text{-}C_3H_7$	200	10	17		190	
	230	10	19.5			
	300	10	32.6		280	
	300	20	29		300	
OCH_3	150	10	10.5*)		162	[15]
			7		210	
	180	10	9*)		165	
			17		220	[15]
	200	10	—*)		—	
			36.7		220	[15]
OC_2H_5	150	10	—		—	[15]
	180	10	15*)		176	
			18.5		235	[15]
	200	10	—*)		—	[15]
			34		235	[15]
NO_2	180	10	68.3		185	[14]
	200	10	79		185	[14]
	230	10	76.4			[14]
	230	20	77.62			[14]
	300	10	59.6			[14]

*) soluble fraction.

increases in the series Cl<Br<I for X = halogene while for X = alkyl, it decreases with the size of the alkyl residue ($CH_3 > C_2H_5 > i \cdot C_3H_7$). The conversion variation for OCH_3 and OC_2H_3 is insignificant. The highest conversion has been registered for $X = NO_2$, which is in good agreement with the fact that the less reactive monomer (by LCAO—MO calculations) allows the formation of some tridimensional structures.

The average degree of polymerization, for soluble fractions, increases with the reaction temperature up to 230°C, gradually decreasing afterwards; at 300°C trimers or tetramers are being formed.

Doubling the time for the same reaction temperature leads to the decrease of the conversion and of the average degree of polymerization. Thus, the conclusion that may be drawn is that, for a longer reaction time, scission of the macromolecular chains occur.

In the case of X = Cl, Br, CH_3, C_2H_5, $i.C_3H_7$ fractions soluble in most organic solvents have been only obtained, while unsoluble products resulted with $X = NO_2$. In the case of X, = I, OCH_3, OC_2H_5 mixtures of soluble and unsoluble fractions have resulted; the soluble fraction decreases with the increase of the unsoluble one in the case of rising the reaction temperature.

a) *The Kinetics of the Polymerization Process* has been studied by the gravimetric method, for X = CH_3, $i.C_3H_7$, Cl, Br. Data obtained are listed in Table 3.

The graphical representation of the variation with time led to stright lines passing through the origin (Figs. 7, 8), which indicates a first order reaction [16].

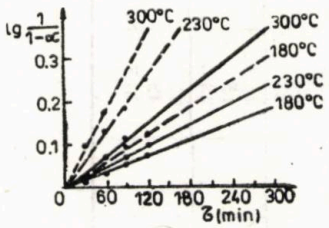

Fig. 7 *a*. — Variation of — log [1/(1 — α)] vs. time, in the polymerization process of α-chloro-β-formyl-*p*-X-styrene (X=Cl —; X=Br - - -).

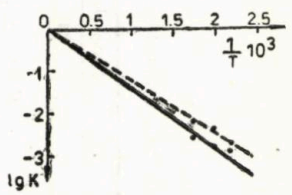

Fig. 7 *b*. — Variation of — log *K* vs. $1/T \times 10^3$ in polymerization process of α-chloro-β-formyl-*p*-X-styrene (X=Cl —; X= =Br - - -).

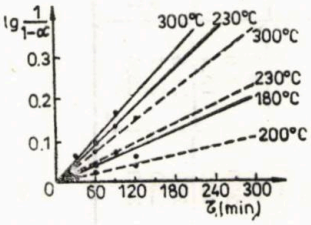

Fig. 8 *a*. — Variation of — log [1/(1 — α)] vs. time in the polymerization of α-chloro-β-formyl-*p*-X-styrene (X=CH_3 —; X=$i \cdot C_3H_7$ - -).

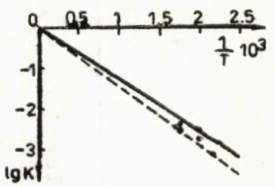

Fig. 8 *b*. — Variation of — log *K* vs. $1/T \times 10^3$ in polymerization process of α-chloro-β-formyl-*p*-X-styrene (X = CH_3 —; X=$i \cdot C_3H_7$ - -).

Table 3

Kinetic Data concerning the Thermal Polymerization of α-Chloro-β-Formyl-p-X-Styrene

X	Temperature °C	Time, [min.] 30 Conv. %	30 M	60 Conv. %	60 M	90 Conv. %	90 M	120 Conv. %	120 M	300 Conv. %	300 M	Rate constant k, [s^{-1}]	Energy activation E_a Kcal/mol
CH_3	180	17		8.2		24		14	620	27	382	1.52×10^{-3}	
	230	21		15		32		30	1 510	42	900	3.45×10^{-3}	5.796
	300	14		22		56	935	52	841	53	835	4.61×10^{-3}	
i. C_3H_7	180	3				3.3		8.6	1 018			7.67×10^{-4}	
	230			4		20		45	1 242	32	680	1.82×10^{-3}	6.524
	300	7.4		5.8		53		48	1 379	54	790	2.88×10^{-3}	
Cl	180	4.6		15.6		13.1		17	1 380	19	1 300	1.47×10^{-3}	
	230	3.9		8.1		15		21.4	611	33	523	1.85×10^{-3}	6.020
	300	15.4		24		23.6		24.3	1 380	33	1 910	3.06×10^{-3}	
Br	180	21.5	682	28.3		21		26.5	1 550	47	1 150	2.42×10^{-3}	
	230	33.7	4 300	29		42		43	2 860	47.6	1 020	5.37×10^{-3}	5.460
	300	39.6	1 120	46		30.8		44.5	1 542	49	1 090	7.30×10^{-3}	

In all situations considered, the rate constant varies unsignificantly with temperature, except for X = i . C_3H_7; in this case it increases with an order of magnitude, when temperature rises from 200° to 230°C. The activation energy decreases in the order:

$$i\,.\,C_3H_7 > Cl > CH_3 > Br.$$

3.3. Molecular Structure of Polymers

The structure of the products obtained by the polymerization of α-chloro-β-formyl-*p*-X-styrene has been explained by IR spectra and elemental analysis.

Generally, IR spectra show absorption bands characteristic to monomers, yet of lower intensity: $\delta_{p\text{-disubstituted aromatic CH ring}} = 700...900\ cm^{-1}$, $\nu_{C-C\ aromatic} = 2\,970...3\,100\ cm^{-1}$. The absorptions caused by the olephinic link and by halogene superpose themselves on those of the aromatic ring.

The IR spectra of all synthesized products, at different temperatures and reaction times, are identical, which leads us to the conclusion that these factors do not influence the polymer structure. The soluble fractions proved to be oligomers with linear structure and degrees of polymerization ranging from 3 to 14. If a comparative analyze of the spectroscopic data and of the average degree of polymerization ($\bar{p}$) is effectuated, there can be stated that at temperatures above 230°C, a competitive reaction of polymerization also occurs, yet, without affecting the products structure, the IR spectra being identical. Prolongation of the reaction time stimulates too the depolymerization process.

Results of elemental analysis and of spectral data evidence a dehydrohalogenation [17]...[19] or dehaloformylation occurring during the polymerization process. In the situation in which the dehydrohalogenation or dehaloformylation of the monomer [6], [8] proceeds at a higher ratio than the polymerization reaction, the acetylenic monomer, which may copolymerize with the vinylic monomer, is being formed.

Thus, in the process of thermal polymerization there take place several concurrent reactions which lead to a copolymer possessing diene or polyenic units on the macromolecular chain, for which we suggest the structure:

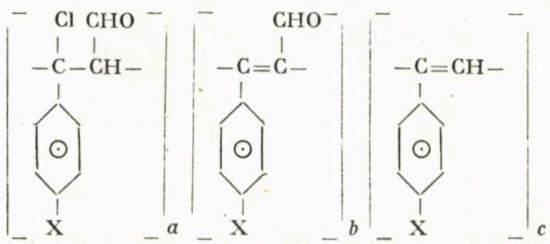

The presence of a system of double bonds conjugated on the macromolecular chain is confirmed too by the values of the electric conductivities, varying between 10^{-14} and 10^{-12} $ohm^{-1}\,.\,cm^{-1}$; these values attest semiconducting properties of the synthesized products.

The thermodifferential analysis evidences that the thermal decomposition takes place in several steps, the products being stable up to approx. 250°C.

3.4. Copolymerization of α-Chloro-β-Formyl-*p*-X-Styrene

The copolymerization of α-chloro-β-formyl-*p*-X-styrene has been studied for X=Cl, Br, CH_3, C_2H_5, *i*.C_3H_7. Styrene and phenylacetylene were used as comonomers.

In all cases, copolymers soluble in usual solvents have been used. Special mentions must be made of the fact that, while the thermal polymerizzation of the chloroformylated monomers does not occur at 150°C, the copolymerization with styrene and phenylacetylene does. The influence of time and the reaction temperature is manifested on the conversion, as it is the case of the polymerization reaction [16].

3.5. The Molecular Structure of Copolymers

The copolymer molecular structure has been analyzed on the basis of the spectral data and the constants of copolymerization [16].

IR spectra show absorption bands characteristic to monomers : $\nu_{C=O}$ = =1 670...1 680 cm^{-1}, $\nu_{C-C\ aromatic}$ =1 400...1 610 cm, $\nu_{CH\ aromatic}$ =2 930...3 100 cm^{-1}, *para*-disubstituted aromatic ring, 700...900 cm^{-1}.

The copolymerization constants have been determined by LCAO—MO calculations, applying the relation :

$$-RT \ln r = (\Delta E_{rs})^1 - (\Delta E_{rs})^2 ,$$

where $(\Delta E_{rs})^1$, $(\Delta E_{rs})^2$ represent resonance energies for stabilizing the transition state between the radical and its monomer and, respectively, between the same radical and comonomer [19]. The ΔE_{rs} values have been computed according to literature data [20], being expressed in $-(\Delta\beta^2/\beta)$ units. The *r* and *s* indices in ΔE_{rs} refer to the monomer atom and, respectively, to the radical one, participating in the transition state. The *I*...*IV* monomers take part in the transition state with atom 3, the electronic density on the marginal orbitals being maximum for these positions. In all these cases, atom 4 is radicalic :

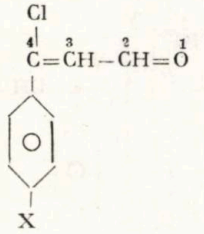

I X = Br
II X = Cl
III X = NO_2
IV X = CH_3

The copolymerization constants, *r*, calculated for 60°C (333° K) are indicated in Table 4. The molar ratio of the two monomers is not significant.

In the situations A_1...D_1 the copolymer contains more styrene (more reactive), the monomers *I*...*IV* polymerizing themselves in the end. Phenylacetylene being less reactive than the monomers had in view, in cases A_2, B_2

Table 4

Copolymerization Constants [16]

	Radical	Monomer	$\Delta E_{rs}=\Delta\beta^2/\beta$	Difference $\Delta E_{rs}-\Delta\beta^2/\beta$	$r_{computed}$	r_1r_2
A_1	*I*	*I*	0.7188	0.1718	0.53	1.11
	I	S	0.8906			
	S	S	0.9323	−0.2035	2.11	
	S	*I*	0.7288			
A_2	*I*	*I*	0.7188			1.01
	I	FA	0.6506	−0.0682	1.28	
	FA	FA	0.6650			
	FA	*I*	0.7288	0.0638	0.79	
B_1	*II*	*II*	0.7148			1.08
	II	S	0.8935	0.1787	0.51	
	S	S	0.9323			
	S	*II*	0.7272	−0.2051	2.13	
B_2	*II*	*II*	0.7148			1.001
	II	FA	0.6515	−0.0633	1.26	
	FA	FA	0.6650			
	FA	*II*	0.7272	0.0622	0.795	
C_1	*III*	*III*	0.7116			3.99
	III	S	0.8497	0.1381	0.60	
	S	S	0.9323			
	S	*III*	0.4183	−0.5140	6.66	
C_2	*III*	*III*	0.7116			2.82
	III	FA	0.6752	−0.0364	1.14	
	FA	FA	0.6650			
	FA	*III*	0.4183	−0.2467	2.48	
D_1	*IV*	*IV*	0.7092			1.005
	IV	S	0.9100	0.2008	0.47	
	S	S	0.9323			
	S	*IV*	0.7258	−0.2065	2.14	
D_2	*IV*	*IV*	0.7092			0.966
	IV	FA	0.6578	−0.0514	1.21	
	FA	FA	0.6650			
	FA	*IV*	0.7258	0.0608	0.799	

S — styrene ; FA — phenylacetylene.

and D_2 the copolymer has a higher content of the monomers *I*...*IV*. In the case C_2, both copolymerization constants being higher than the unity, the homopolymerization tendency is stronger, the blockcopolymer being formed here of a mixture of the two homopolymers.

In most cases, copolymers show a statistical structure. On the macromolecular chain there exist systems of conjugated double bonds, as in the case of homopolymers, too, as a consequence of the dehydrohalogenation or dehaloformylation of the copolymer or of the chloroformylated vinylic mer:

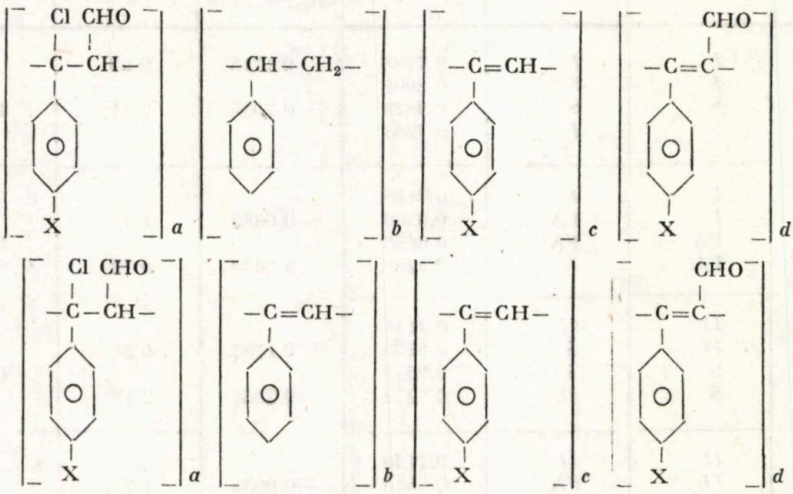

Copolymers do not evidence semiconducting properties, which is probably due to the prevention of coplanarity of the units possessing conjugated double bonds.

4. Conclusions

From the effectuated study the following conclusions regarding the synthesis, thermal polymerization and copolymerization with styrene and phenylacetylene of some *p*-disubstituted chloroformylated vinylic derivatives are established:

1. Monomers may be characterized by chemical, spectral (IR, RMN) and thermodifferential analyses.

2. Radical initiated thermal polymerization led to soluble ($X = Cl$, Br, CH_3, C_2H_5, $i.C_3H_7$) and unsoluble ($X = NO_2$) fractions, or to a mixture of soluble and unsoluble products ($X = I$, OCH_3, OC_2H_5).

3. Conversion increases with temperature, up to 230°C, this limit exceeded, both conversion and the average degree of polymerization of the soluble compounds decreases, due to a depolymerization process. Prolongation of the reaction time over 10 hours promotes, too, the depolymerization process.

4. Kinetic data on the thermal polymerization show a first order reaction.

5. LCAO–MO calculations were undertaken, from which some conclusions on the monomer reactivity in the polymerization reaction have been drawn.

6. Soluble products are oligomers, possessing an average degree of polymerization (ranging from 3 to 14), a linear structure and conjugated units

on the macromolecular chain. Unsoluble compounds have branched structures.

7. Correlation of analytical and spectral data indicated that the obtained products are copolymers, as a consequence of the dehydrohalogenation and dehydroformylation reaction of the polymer or of the monomer, which subsequently polymerizes with the vinylic mer.

8. Copolymerization of α-chloro-β-formyl-*p*-X-styrene with styrene and phenylacetylene has been studied, being established that over a certain temperature and reaction time, conversion decreases as a consequence of the concurrent reaction of depolymerization.

9. Calculation of the copolymerization constants, by the LCAO—MO method, permitted the estimation of the mers reactivity and, possibly, their sequence on the macromolecular chain.

10 Correlation of elemental analyses with spectral data and the values of the copolymerization constants attest that the synthesized products are copolymers having a linear structure and units with conjugated double bonds on the chain, possessing fragments with statistical and fragments with block structures.

Received, October 13, 1986

Polytechnic Institut, Jassy,
Department of Organic and
Macromolecular Chemistry
and Technology

REFERENCES

1. Юргова Г. А., Чюмаков У. В., Ежова Т. М., Джасин Л. Д., Сосин С. Л., Коршак В. В., Высокомол соед., **13**, 2 761 (1971).
2. Воронина М. А., Вишнякова Т. П., Таушкин Я. М., Божилова М. А., Альев Л. Н., Высокомои соед., **11**, 882 (1969).
3. Rosenblum M., Brown N., Popenmeier J., Applebaum M., J. Organometal. Chem., **6**, *2*, 173 (1966).
4. Schlögl K., Steyer W., Monats., **96**, 1520 (1965).
5. Ликсандру Т., ЖОХ, **42**, 1991 (1972).
6. Bodendorf K., Mayer R., B., **98**, 3554 (1965).
7. Simionescu Cr., Dumitrescu Sv., Lixandru T., Dăringă M., Simionescu B., Vâţă M., European Polymer J., **8**, 719 (1972).
8. Weissenfels M., Schurig H., Huhsam G., Z. Chem., **6**, 471 (1966).
9. Purcell W. P., Singer J. A., J. Chem. and Data., **12**, 235 (1967).
10. Стейтвизер Е., *Теория молекулярных орбит* (пер. с. англ.). Изд. Мир., М., 1965, 126.
11. Хигаси К., Баба Н., Рембаум А., *Квантовая органическая химия* (пер. с англ.). Изд. Мир., М., 1967
12. Pullman B., Pullman A., *Quantum Biochemistry*. J. Wiley & Sons, New York, London, 1963.
13. Lixandru T., Tătaru L., Mazilu I., Cocîrlă I., Rev. Roum. Chim., **20**, 129 (1975).
14. Lixandru T., Tătaru L., Mazilu I., Cocîrlă I., Bul. Inst. polit., Iaşi, **XXI (XXV)**, *3—4*, s. II, 69 (1975).
15. Mazilu I., Tătaru L., Cocîrlă I., Petrescu C., Lixandru T., Bul. Inst. polit., Iaşi, **XXXIV (XXXVIII)**, *1—4*, s. II (1988).
16. Lixandru T., Tătaru L., Mazilu I., Cocîrlă I., Bul. Inst. polit., Iaşi, **XXII (XXVI)**, *1—2*, s. II, 55 (1976).

17. Geddes W. C., European Polymer J., **3**, 733 (1967).
18. Hayashi K., Yonezawa T., Nagata C., Okamura S., Fukui K., J. Polymer. Sci., **20**, 537 (1956).
29. Stromberg R., Straus S., Achhammer B., J. Polymer Sci., **35**, 355 (1959).
20. Yonezawa S., Hayashi K., Nagata C., Okamura S., Fukui K., J. Polymer. Sci., **14**, 312 (1954).

CONTRIBUŢII LA SINTEZA, POLIMERIZAREA ŞI COPOLIMERIZAREA UNOR MONOMERI VINILICI *p*-SUBSTITUIŢI

(Rezumat)

Se prezintă sinteza, polimerizarea termică şi copolimerizarea cu stirenul şi fenilacetilena a unor monomeri vinilici cloroformilaţi *p*-substituiţi.

Influenţa substituentului asupra reactivităţii monomerilor a fost apreciată pe baza calculelor LCAO—MO şi a datelor experimentale.

S-au obţinut oligomeri solubili cu structură liniară şi produşi insolubili cu structură ramificată, avînd unităţi conjugate şi grupe reactive pe catenă, cu proprietăţi semiconductoare.

Studiul cinetic al polimerizării termice pune în evidenţă o reacţie de ordinul întîi.

Datele analitice şi spectrale ca şi valorile constantelor de copolimerizare atestă pentru copolimerii cu stirenul şi fenilacetilena o structură liniară cu unităţi conjugate pe catenă, prezentînd fragmente cu structură bloc şi fragmente cu structură statistică.

PETROCHEMICAL WORKS BRAZI

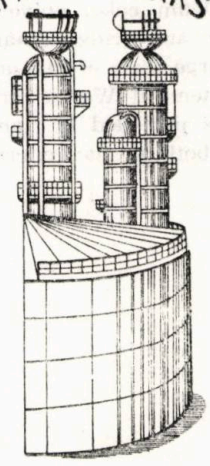

PRODUCES AND DELIVERS

- Comburents
- Aromatic hydrocarbons
- Polyisoprenic rubber
- Polybutadienic rubber
- Phenol
- Nonylphenol
- Ortosecundarbuthylphenol
- Acetone
- Low density polyethylene
- Phthalic and maleic anhydrides
- Choline chloride
- Dimethylterephtalate
- Ethanolamine
- Polyglicols 200 - 4000
- Monoethylene glicole

MINISTRY OF CHEMICAL AND PETROCHEMICAL INDUSTRY
INDUSTRIAL CENTRAL OF OIL DISTILERYES AND PETROCHEMISTRY, BRAZI

Phone : 43121 ; Telex : 19343

PETROCHEMICAL WORKS — BRAZI

The Petrochemical Works, Brazi, is a complex and modern unit of advanced technology for the oil processing and advanced chimization of the petroleum fractions, rendering profitable the base raw material.

The works produces a wide variety of petrochemical and oil products: comburents, fuels aromatic hidrocarbons, petroleum coke, polyethylene, ethylene oxide, dimethylterephthalate, maleic and phtholic anhydrides, ethanolamine, modifiers, synthetic rubbers, products which cover a large scale of utilizations.

The products manufactured by the Petrochemical Works, Brazi, are of high quality level according to the quality conditions provided in standards and common on the world market. They are destined both to the external and internal customers.

SYNTHETIC FIBRE WORKS, IAȘI, a modern unit of advanced technology, much ahead in Romania chemical industry, produces and deliveries a wide range of polyester fibers, yarns and sheets as well as equipments and spare parts for chemical and textile industry as it follows :

1. Polyester synthetic fibers :

- polyester fiber cotton type ;
- polyester fiber wool type (staple, top and tow) ;
- polyester fiber flax type ;
- polyester fiber high shrinkage.

2. Polyester synthetic textile yarns :

- polyester continuous filament textile twisted yarns for courtains and tissues ;
- polyester continuous filament drawn yarns for sewing thread ;
- polyester continuous filament textured yarn (semi-dull or bright, round or profiles, raw white or dyed) for knittings, tissues of cloths.

Colour card for dyed yarns includes about 100 shades classified in : light, medium and heavy shades.

3. Polyester industrial yarns (drawn, twisted, plyed) for different technical end-uses.

4. Polyester sheets (transparent or light dull) for electrochemical industry.

Besides its textile and chemical profile SYNTHETIC FIBERS WORKS, IAȘI, is also a manufacturer of equipments used in chemical and textile industries such as :

- equipments used for synthetic fiber production (technological lines) ;
- machinery for the chemical industry ;
- refrigeration plants ;
- precision conning machines according to the SCHWEITER licence ;
- inside rectification spindles ;
- yarn guides from sintered alumine ;
- metal structures ;
- different spare parts.

The SYNTHETIC FIBRE WORKS, IAȘI, exports its products by :
— I.C.E. DANUBIANA, BUCHAREST, service E. 9, telex 11184 for fibre and yarn.
— I.C.E. MASINIEXPORTIMPORT, BUCHAREST, telex 11206, for equipments and spare parts.
— I.C.E. ELECTROEXPORTIMPORT, BUCHAREST, service 44, telex 11388, for polyester sheets.
For any additional details please write directly to :

COMBINATUL DE FIBRE SINTETICE, IAȘI
29 Țuțora str., code 6600
Telex 022251

ENTERPRISE FOR PROCESSING OF PLASTIC MATERIALS, IAȘI

In the past few years, the enterprise for processing plastic materials from Iași, has assimilate and processed new types of products from plastic materials, extending the scale of goods produced and processed polymers.

The traditional products are presented in the catalogue „Products Processed from Plastic Materials" edited by the Ministry of Chemical and Petrochemical Industry in 1988 which can be obtained from the sale office of the enterprise.

Besides the mentioned goods in 1988 have been assimilated new products processed from poly(vinylchloride) :

a) Protective sheets for constructions.

b) Fireproof thermocontractible profiles.

c) Polyethylene products :

- Polyethylene aprons ;
- Protecting sheets with valves ;
- Flower pots ;
- Cloth covers ;
- High pressure tubings.

d) Polyurethane products :

- Valves ;
- Guiding rings ;
- Tighting cuffs ;
- Couplings.

e) Products from polypropilene :

- Cords and cables.

f) Products from PPAS :

- Profiles.

g) Products from ABS and polystirene :

- Thermoformings from plates.

SYNTHETIC FIBERS WORKS, SĂVINEȘTI
produces and delivers :

- *Synthetic Fibers and Yarns*

  — Acrylic fibers Melana (R) ;
  — Polyamidic fibers Relon (R) ;
  — Polyamidic synthetic Yarns Relon (R) ;
  — Polyamidic yarns carpet Relontex (R) ;
  — Polyamidic technical and card yarns Relon (R) ;
  — Brasnes cards.

- *Chemical Products*

  — Caprolactam ;
  — Adipic acid ;
  — Tetrachlorethane ;
  — Cyanuril chloride — Savicid (R) ;
  — Dibenzyldiizocianate DBDI ;
  — Polyethyleneglycole adipate PEGA ;
  — Polyamidic grains for plastics Relon (R) ;
  — Polyamidic plates and bars Relon (R).

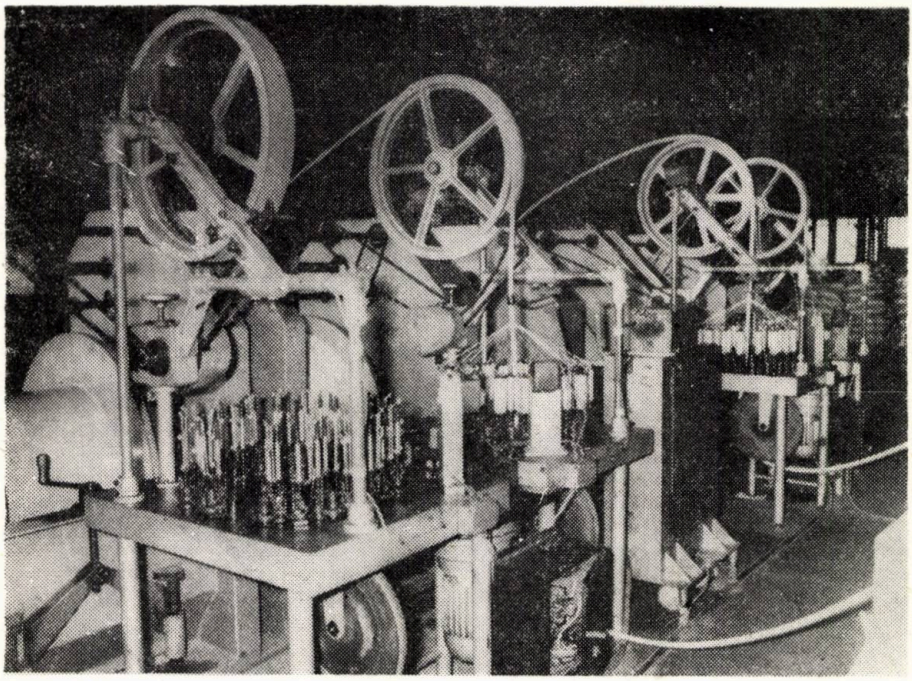

- *Equipement and Spare Parts for Synthetic Fibers Industry*

  — Complete lines for synthetic fiber drawing ;
  — Spinning pumps for synthetic fibers ;
  — Spinning nozzles for melt spinning ;
  — Pressure pumps for cleanning vessels in chemical industry ;
  — Yarns winding machines ;

— Sprindles for textile industry machines ;
— Cutting rolls for fibers ;
— Various spare parts used in chemical fibers industry.

Producer : SYNTHETIC FIBERS SĂVINEȘTI, PIATRA NEAMȚ
TELEX 025221 — 222
TELEGRAPH CFS, SĂVINEȘTI

EXPORTERS :

— Synthetic fibers and yarns :

ICE DANUBIANA, BUCHAREST,
Bd. Republicii Nr. 10—12
Sector 4, BUCHAREST
TELEX 11184 danaz

— Equipments and spare parts

ICE INDUSTRIALEXPORTIMPORT, BUCHAREST

Str. Scaune 1—3
Telex 10052—10930
POB 764

OORSZÁGOS MŰSZAKI INFORMÁCIÓS KÖZPONTI KÖNYVTÁR 1983

1969 AUG 15

40822

F 1503/2

BULETINUL INSTITUTULUI POLITEHNIC DIN IAȘI

Tomul XXXV (XXXIX)

Fasc. 3–4

Secția II

CHIMIE ȘI INGINERIE CHIMICĂ

1989

BULETINUL INSTITUTULUI POLITEHNIC DIN IAŞI

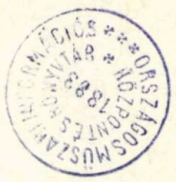

Tomul XXXV (XXXIX)

Fasc. 3–4

L. 041641

Secţia II

CHIMIE ŞI INGINERIE CHIMICĂ

1989

COLEGIUL DE REDACȚIE

Prof. dr. chim. **CAMELUȚA BELDIE** (președinte)
Prof. dr. ing. **ADRIAN RADU**
Prof. dr. ing. **M. GAFIȚANU**
Conf. dr. ing. **D. LIUȚE**
Prof. dr. doc. **D. MANGERON**
Prof. dr. ing. **GH. MAXIM**
Acad. prof. dr. doc. **CRISTOFOR SIMIONESCU**
Prof. dr. doc. **GH. CHIRIȚĂ**
Prof. dr. doc. **VALERIU BLIDARU**

Această fascicolă a apărut și cu sprijinul material al comitetului sindical și consiliului U.A.S.C.R. al Institutului politehnic din Iași

COMITETUL DE READCȚIE AL SECȚIEI

II. **CHIMIE ȘI INGINERIE CHIMICĂ**

Prof. dr. doc. **RADU TUDOSE**
Prof. dr. **ANGELA POPA**
Prof. dr. ing. **I. ROȘCA**
Conf. dr. ing. **SPIRIDON OPREA**

REDACȚIA

Prof. dr. doc. **D. MANGERON**
(redactor responsabil)

Prof. dr. ing. **HUGO ROSMAN**
(secretar)

Conf. dr. ing. **VICTOR BULACOVȘCHI**
(redactor)

ECATERINA IRIMIEA
(tehnoredactor)

BULETINUL INSTITUTULUI POLITEHNIC DIN IAŞI
BULLETIN OF THE POLYTECHNIC INSTITUTE OF JASSY
ИЗВЕСТИЯ ЯССКОГО ПОЛИТЕХНИЧЕСКОГО ИНСТИТУТА
Tomul XXXV (XXXIX), Fasc. 3–4 1989

Secţia II

CHIMIE ŞI INGINERIE CHIMICĂ

SUMAR

Pag.

I. ROŞCA, Sinteza şi studiul polimerilor de coordinaţie ai Th (IV) şi acidului difenilfosfinic (rusă, rez. rom.) 1
A. BOLD, D. BEJAN, D. BÎLBĂ şi L. TOFAN, Sorbţia şi separarea unor ioni metalici pe răşini schimbătoare de ioni modificate cu agenţi sulfonaţi de chelatizare (engl., rez. rom.) 7
V. DULMAN, AL. CECAL, T. ONOFREI şi C. BURCOVEANU, Concentrarea toriului cu colectori microbiologici (engl., rez. rom.) 15
AL. CECAL, Utilizarea diluţiei izotopice interne pentru determinarea solubilităţii unor sulfuri greu solubile (engl., rez. rom.) 21
I. M. POPA, D. HRIŢCU şi GH. IONESCU, Aplicarea cromatografiei în faza lichidă de înaltă presiune la separarea produselor farmaceutice (engl., rez. rom.) 27
ŞT. IVĂŞCAN, F. BANDRABUR şi M. APOSTOLESCU, Unele posibilităţi de reducere a consumurilor specifice de materiale şi de energie în procesul de cromare electrolitică (engl., rez. rom.) 31
C. HAGIU şi M. MICU, Noi sortimente de îngrăşăminte din fosfoghips (engl., rez. rom.) 37
S. PETRESCU şi C. CALISTRU, Cercetarea cineticii procesului de obţinere a sulfatului de potasiu prin dublu schimb din KCl şi $(NH_4)_2SO_4$ (engl., rez. rom.) 41
M. MACOVEANU şi P. TALPALARU, Algoritm de optimizare de tip mixt (engl., rez. rom.) 47
M. FOURAR şi A. ALIANE (Algeria), Studiul unei coloane cu pulsaţii pentru extracţie lichid–lichid (I) (franc., rez. rom.) 53
S. IFRIM, Cercetări privind comportarea liniei drept componentă de cuplare (franc., rez. rom.) 61
C. LEONTE, E. CARP, S. DUMITRESCU, ŞT. CILIANU şi R. BOZGA, Structuri amidice cu acţiune asupra sistemului nervos central (I) (franc., rez. rom.) 67
E. CARP, C. LEONTE, S. DUMITRESCU, ŞT. CILIANU şi R. BOZGA, Structuri amidice cu acţiune asupra sistemului nervos central (II) (franc., rez. rom.) 73
AL. CAŞCAVAL, T. NICOLAESCU, ŞT. BIBIAN-CILIANU şi C. V. ZĂNOAGĂ, Noi baze Mannich ale 3-*n*butil-4-metilumbeliferonei (engl., rez. rom.) . 77
V. ŞUNEL şi C. CIUGUREANU, Noi derivaţii ai acidului *L*-asparagic cu activitate antitumorală potenţială (engl., rez. rom.) 81
C. I. SIMIONESCU, V. BULACOVSCHI şi C. MIHĂILESCU, Polimerizarea acrilonitrilului iniţiată de sistemul redox peroxidisulfat–sare di Bunte (engl., rez. rom.) 87
M. RUSU, Amestecuri de policlorură de vinil (IV) (engl., rez. rom.) 93

BULETINUL INSTITUTULUI POLITEHNIC DIN IAŞI
BULLETIN OF THE POLYTECHNIC INSTITUTE OF JASSY
ИЗВЕСТИЯ ЯССКОГО ПОЛИТЕХНИЧЕСКОГО ИНСТИТУТА
Tome XXXV (XXXIX), Fasc. 3–4 1989

Section II

CHEMISTRY AND CHEMICAL ENGINEERING

CONTENTS

Pp.

I. ROŞCA, Synthesis and Characterization of Th(IV) Coordinative Polymers Based on Diphenylphosphine (Russian, Romanian summary) 1
A. BOLD, D. BEJAN, D. BÎLBĂ and L. TOFAN, Sorption and Separation of some Metal Ions by Chelating Sulfonated Agent-Loaded Ion Exchangers (English, Romanian summary) 7
V. DULMAN, AL. CECAL, T. ONOFREI and C. BURCOVEANU, The Concentration of Thorium by Means of Microbiological Collectors (English, Romanian summary) 15
AL. CECAL, The Use of Internal Isotopic Dilution for the Solubility Determination of certain Hard Soluble Sulphides (English, Romanian summary) . 21
I. M. POPA, D. HRIŢCU and GH. IONESCU, Application of Liquid High Pressure Chromatography in the Separation of Pharmaceutical Products (English, Romanian summary) 27
ŞT. IVĂŞCAN, F. BANDRABUR and M. APOSTOLESCU, Some Possibilities of Reducing the Material and Power Consumptions in the Process of Chrome Electrodeposition (English, Romanian summary) 31
C. HAGIU and M. MICU, New Sorts of Phosphogypsum Fertilizers (English, Romanian summary) 37
S. PETRESCU and C. CALISTRU, Investigations about the Kinetics of the Obtaining Process of Potassium Sulphate by Double Exchange from KCl and $(NH_4)_2SO_4$ (English, Romanian summary) 41
M. MACOVEANU and P. TALPALARU, Mixed-Type Optimizing Algorithm (English, Romanian summary) 47
M. FOURAR et A. ALIANE (Algérie), Étude d'une colonne à pulsations pour l'extraction liquide–liquide (I), (French, Romanian summary) 53
S. IFRIM, Investigations concernant le comportement de la laine comme composant de copulation (French, Romanian summary) 61
C. LEONTE, E. CARP, S. DUMITRESCU, ŞT. CILIANU et R. BOZGA, Structures amidiques avec action sur le système nerveux central (I) (French, Romanian summary) 67
E. CARP, C. LEONTE, S. DUMITRESCU, ŞT. CILIANU et R. BOZGA, Structures amidiques avec action sur le système nerveux central (II) (French, Romanian summary) 73
AL. CAŞCAVAL, T. NICOLAESCU, ŞT. BIBIAN-CILIANU and C. V. ZĂNOAGĂ, New Mannich Bases of 3-*n*Buthyl-4-methylumbelliferone (English, Romanian summary) 77
V. ŞUNEL and C. CIUGUREANU, New Derivatives of *L*-asparagic Acid with Potential Antitumoral Activity (English, Romanian summary) 81
C. I. SIMIONESCU, V. BULACOVSCHI and C. MIHĂILESCU, Polymerization of Acrylonitrile Initiated by the Peroxydisulfate–di Bunte Salt Redox Couple (English, Romanian summary) 87
M. RUSU, Poly(vinil chloride) blends (IV) (English, Romanian summary) . . 93

BULETINUL INSTITUTULUI POLITEHNIC DIN IAŞI
BULLETIN OF THE POLYTECHNIC INSTITUTE OF JASSY
ИЗВЕСТИЯ ЯССКОГО ПОЛИТЕХНИЧЕСКОГО ИНСТИТУТА
Том XXXV (XXXIX), вып. 3—4 1989

Секция II

ХИМИЯ И ХИМИЧЕСКАЯ ПРОМЫШЛЕНОСТЬ

СОДЕРЖАНИЕ

Стр.

И. РОШКА, Синтез и исследование координационных полимеров Th(IV) на основе дифенилфосфиновой кислоты (русск., рез. рум.) · · · 1

А. БОЛД, Д. БЕЖАН, Д. БЫЛБЭ и Л. ТОФАН, Сорбция и разделение металлических ионов модифицированным ионообменником с реагентами содержащих сульфогруппы (англ., рез. рум.) · · · · · · · 7

В. ДУЛМАН, АЛ. ЧЕКАЛ, Т. ОНОФРЕЙ и К. БУРКОВЯНУ, Концентрирование торя с помощью микробиологических коллекторами (англ., рез. рум.) · 15

АЛ. ЧЕКАЛ, Использование внутреннего изотопического распределения растворимости некоторых трудно-растворимых сульфидов (англ., рез. рум.) · 21

И. М. ПОПА, Д. ХРИЦКУ и Г. ИОНЕСКУ, Применение жидкостой хроматографии высокого давления для разделения фармацевтических продуктов (англ., рез. рум.) · · · · · · · · · · · · · · · · · · · 27

Ш. ИВЭШКАН, Ф. БАНДРАБУР и М. АПОСТОЛЕСКУ, Некоторые способности снижения удельных расходов материялов и энергии в процессе электролитической хромирования (англ., рез. рум.) . . 31

К. ХАДЖИУ и М. МИКУ, Новые удобрение из фосфогипс (англ., рез. рум.) · 37

С. ПЕТРЕСКУ и К. КАЛИСТРУ, Исследование кинетики процесса получения сульфата калия двойным обменом KCl и $(NH_4)_2SO_4$ (англ., рез. рум.) · 41

М. МАКОВЯНУ и П. ТАЛПАЛАРУ, Смещанным алгоритм оптимизации (англ., рез. рум.) · 47

М. ФУРАР и А. АЛИАНЕ (Алжыр), Изучение жидкостной пульсирующей экстракционной колонны (I) (франц., рез. рум.) · · · · · · · 53

С. ИФРИМ, Исследования относительно применения шерсти как азосочетания компонент (франц., рез. рум.) · · · · · · · · · · · · · · · 61

К. ЛЕОНТЕ, Э. КАРП, С. ДУМИТРЕСКУ, Ш. ЧЛИИАНУ и Р. БОЗГА, Амидные соединения с действием на центральную нервную систему (I) (франц., рез. рум.) · 67

Э. КАРП, К. ЛЕОНТЕ, С. ДУМИТРЕСКУ, Ш. ЧИЛИАНУ и Р. БОЗГА, Амидные соединения с действием на центральную нервную систему (II) (франц., рез. рум.) · 73

АЛ. КАШКАВАЛ, Т. НИКОЛАЕСКУ, Ш. БИБИАН-ЧИЛИАНУ и К. В. ЗЭНОАГЭ, Новые Манних основания от 3-*н*бутил-4-метилумбеллиферoны (англ., рез. рум.) · 77

В. ШУНЕЛ и К. ЧЮГУРЯНУ, Новые производные *L*-аспаражик кислоты с потенциальным противотуморальным действием (англ., рез. рум.) 81

К. И. СИМИОНЕСКУ, В. БУЛАКОВСКИЙ и К. МИХЭИЛЕСКУ, Редокс полимеризация акрилонитрила в присутствии системы персульфат—соль ди-Бунте (англ., рез. рум.) · · · · · · · · · · · · · · · · · · 87

М. РУСУ, Поливинилхлоридные композиции (IV) (англ., рез. рум.) 93

BULETINUL INSTITUTULUI POLITEHNIC DIN IAŞI
Tomul XXXV (XXXIX), Fasc. 3-4, 1989
Secţia II
CHIMIE ŞI INGINERIE CHIMICĂ

УДК 54-92; 546.843; 547.63

СИНТЕЗ И ИССЛЕДОВАНИЕ КООРДИНАЦОННЫХ ПОЛИМЕРОВ Th(IV) НА ОСНОВЕ ДИФЕНИЛФОСФИНОВОЙ КИСЛОТЫ

И. РОШКА

1. Введение

В последнее время с целью получения новых термостойких материалов проводятся широкие исследования различных координационных полимеров [1]...[10]. Так получены многочисленные координационные полимеры на основе диорганофосфиновых кислот и различных катионов переходных металлов [1]...[11].

Особенно интересными являются полимеры диорганофосфиновой кислоты с различными катионами, полученные К о р ш а к о м и сотр. [5], [6] ; эти полимеры разлагаются при температурах выше 350°Ц.

Недавно синтетизнрованы и исследованы новые координационные полимеры UO_2^{2+}, Co^{2+}, Ni^{2+}, Fe^{3+}, Ce^{3+} с дифенил- и диалкилфосфиновыми кислотами и с соответствующими тиокислотами [7]...[11].

В настоящей работе получены и исследованы некоторые координационные-полимеры Th^{4+} на основе дифенилфосфиновой кислоты.

2. Экспериментальная часть

Дифенилфосфиновую кислоту $(C_6H_5)_2PO_2H$, получали по описанным ранее методам [12], дважды перекристаллизировали из этанола т. пл. 192°,5 ...193,5°Ц (по [12] т. пл. 190°...192°Ц).

Ацетилацетонат Th(IV), $Th(C_5H_7O_2)_4$, получали по описанной ранее методике [9] из ацетилацетона и $Th(OH)_4$.

Общим методом получения гидроокисей $Th(OH)_4$ является взаимодействие раствора $ThCl_4$ с щелочами.

Синтез координационных полимеров производили поликонденсацией в расплаве, в органических растворителях, в обычной и инертной атмосферах.

Поликонденсация в расплаве 0,2 моля дифенилфосфиновой кислоты и 0,1 моля свеже синтетизированной гидроокиси Th(IV) тщательно измельчивали и помещали в колбу, снабжённую прямым холодильником с градуированным приёмником и трубкой для ввода азота. В течение часа температуру постепенно поднимали до 195°... 200°Ц и реакционную смесь выдерживали при этой температуре 2 ч. Затем смесь охлаждали, снова тщательно измельнивали и грели в течение двух часов, повышая температуру до 195°... 200°Ц. Полученные полимеры экстрагировали ацетоном и этанолом в аппарате Сокслета. Так синтетизирован полимер типа *I*.

Аналогично получали полимеры *II* из 0,2 моля дифенилфосфиновой кислоты и 0,1 моля ацетилацетоната Th(IV) и *III* из 0,1 моля ацетилацетоната Tn(IV) и 0,4 моля $(C_6H_5)_2PO_2H$.

Выход полимеров : 96...98% ; они частично растворимы в бензоле, хлороформе, спирте и др.

Поликонденсация в органических растворителях 0,1 моля ацетилацетоната Th(IV) и 250 мл бензола, толуола, этанола или бутанола, 0,2 моля дифенилфосфиновой кислоты, помещали в трехголую колбу, снабжённую прямым холодильником, мешалкой и капиляром для ввода азота. Длительность реакций — 4 ч. Реакцию заканчивали после прекращения выделения ацетилацетона. Осадок отфильтровывали, промывали этанолом и экстрагировали в аппарате Сокслета этанолом. Состав этого соединения соответствует составу полимера *II*.

Аналогично получали и дифенилфосфинат Th(IV) из 0,1 моля дифенилфосфиновой кислоты и 0,025 моля ацетилацетоната Th(IV), соответствующий составу полимера *III*.

Осадок нерастворимого полимера промывали несколько раз этанолом и сушили до постоянного веса при 105°Ц. Растворимую фракцию полимера выделяли испарением растворителей и сушили до постоянного веса. Выход полимеров 90...95%. Эти полимеры частично растворимы в бензоле, хлороформе, спирте и других растворителях и имеют те-же самые составы, что и соответствующие полимеры, полученные в расплаве. Все эти синтетизированные соединения — порошок белого цвета.

3. Полученные данны

Молекулярная масса растворимых фракций полимеров была определена эбуллиоскопическим методом в бензоле (табл. 1).

Найлучшие результаты были получены при взаймодействии дифенилфосфиновой кислоты и ацетилацетонатом Th(IV) или гидроокисью Th(IV). Элементный состав растворимых и нерастворимых идентичен (табл. 1).

Таблица 1

Элементный состав и молекулярная масса растворимых фракций полимеров

Полимер	Вычислено, [%]				Найдено [%]				M
	C	H	P	Th	C	H	P	Th	
I	41,14	3,14	8,85	33,14	42,02	3,81	9,01	33,4	5 020
II	47,22	4,16	7,17	26,85	48,11	4,72	7,12	29,0	9 080
III	52,36	3,63	11,27	21,28	52,88	3,96	11,76	21,6	1 200

Результаты гель - хроматографического фракционирования координнационных полимеров, осуществлённого на приборе типа „Watter" (наполнитель — стирекс, элюент — циклогестанон) показывают (рис. 1), что эти полимеры имеют различающееся ММР.

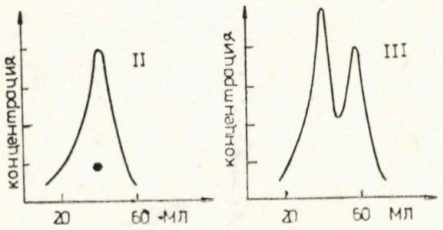

Рис. 1. — Кривые ГПХ полимеров *II* и *III*.

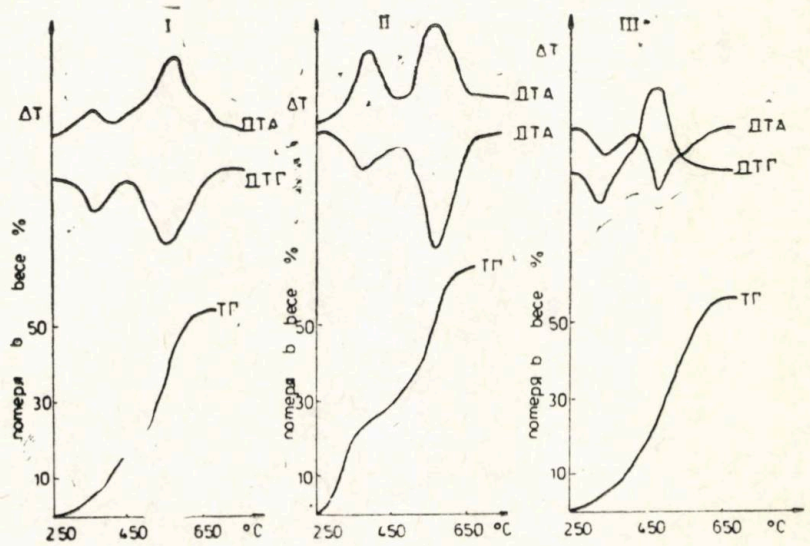

Рис. 2. — Кривые ДТА и ТГА полимеров *I*, *II* и *III*.

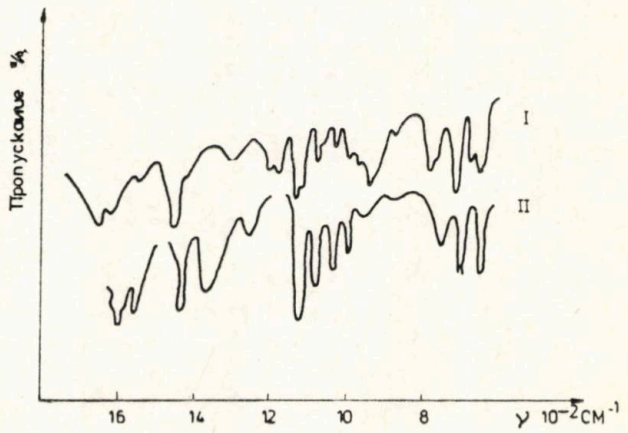

Рис. 3. — ИК - спектры полимеров *I* и *II*.

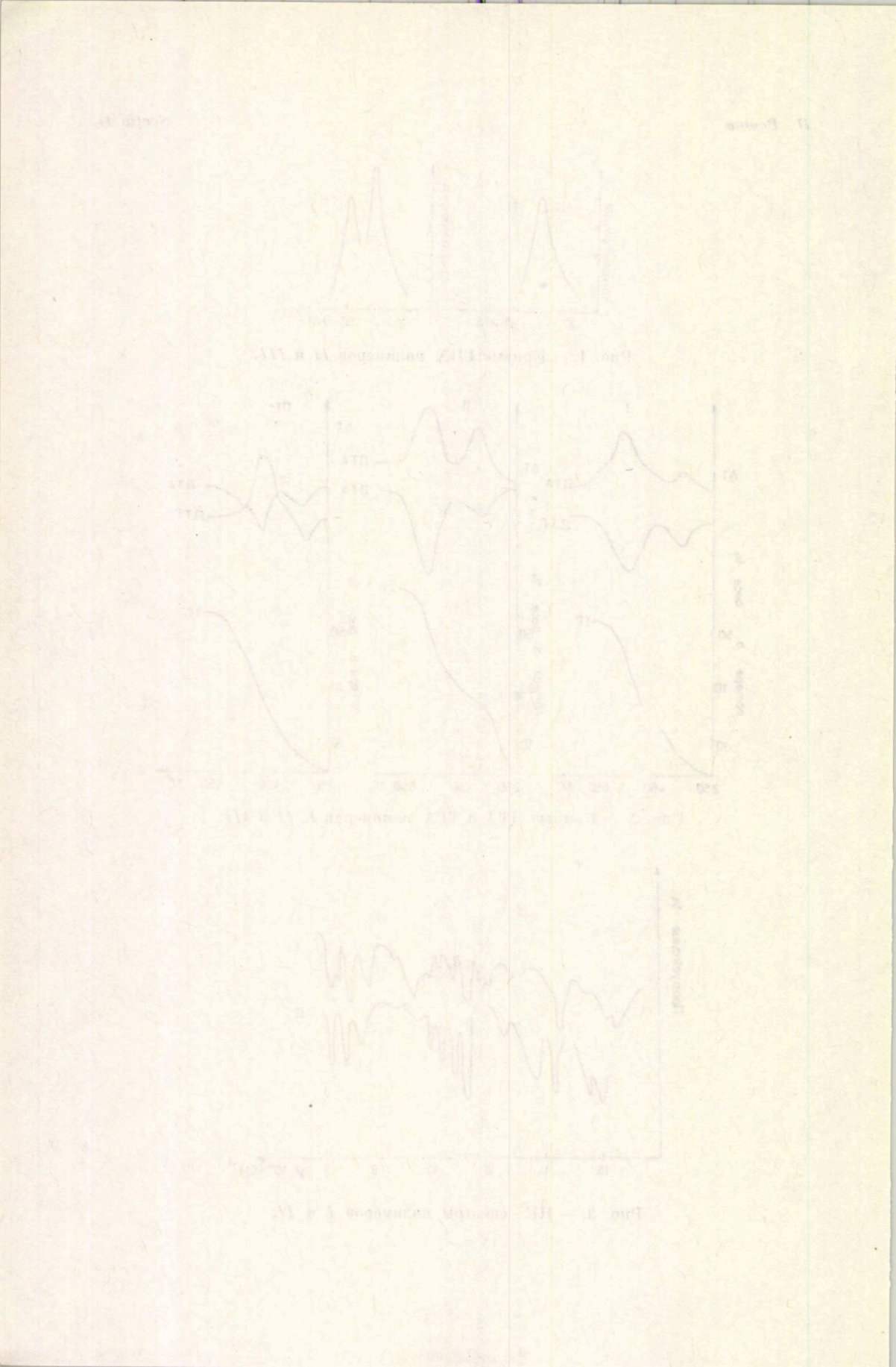

Термогравиметрический м дифференциальный термические анализы этих полимеров (скорость нагревания 10°Ц/мин.) показали (рис. 2) что начало разложения наблюдается при 250°... 405°Ц. Разложение полимеров сопровождается энергичным выделением тепла (острый экзотермический пик на кривой ДТА).

Анализируя полученные результаты, можно сказать что полимер *III* является несколько более термостойким, чем *I* и *II* (табл. 2).

Деструкция полимеров происходит о отщеплением органических радикалов : остаток отвечает формуле $ThO_2 \cdot P_2O_5$.

Таблица 2

Характерные температуры термического разложения координационных полимеров

Полимер	Температуты, [°Ц]			
	Начало разложения	Прекащения разложения	Соответсвующие потерям в весе	
			10%	25%
I	260	780	380	435
II	300	760	430	495
III	380	790	550	620

Исследованные координационные полимеры обладают более высокой термостойкостью, чем соединения из которых они получены и это подтверждает факт образования полимеров мостикового типа с более устойчивыми хелатными циклами. На всех стадиях порядок реакций и энергию активаций разложения определяли по методу из [14]. На всех этапах разложения порядок реакций близок к единице (табл. 3).

Таблица 3

Значения порядка реакции и эффективной энергии активации термического разложения полимеров I, II, III

Полимер	Порядок реакции		$E_{эф.}$, [кДж/мол]	
	Стадия I	Стадия II	Стадия I	Стадия II
I	0,78	0,86	75,9	88,8
II	0,8	0,9	78,8	89,8
III	0,86	0,93	80,1	90,7

Для более точной характеристики полученных продуктов были записаны их ИК-спектры. Наиболее удобной областью спектра для количественного определения содержания радикалов дифенилфосфиновой кислоты является область 700...900 и 1 100...1 200 $см^{-1}$. Полосы в области

700... 900 $см^{-1}$ обусловалены неплоскими колебаниями ароматических групп фенильного ядра : они узки и интенсивны.

Характерные полосы поглощения связи P—O не изменяются в полимерах по сравнению с соответствующими полосами дифенилфосфиновой кислоты, но изменяются полосы поглощения группировок PO_2 (рис.3).

При образований связей (из радикала кислот) и

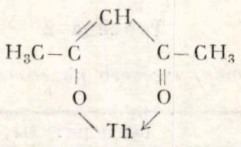

полосы поглощения, соотвествующие колебаниям группировок P=O и C=O (рис. 3) изменяются из-за удлинения связей P=O и C=O. Эти колебательные частоты у полимеров меньше частот для соответствующей свободной кислоты и ацетилацетона [16]. Группировка P=O для дифенилфосфиновой кислоты имеет характерные полосы поглощения в области 1 150... 1 180 $см^{-1}$.

Обозначая через ν частоту характерного колебания соответствующих группировок P=O в свободной кислоте а через ν' частоту техже самых группировок в полимерах, по уравнению $\Delta\nu=(\nu-\nu')/\nu\times 100$ можно найти изменение колебательной частоты группировок, которые определяют образование координационных связей, а именно : для полимера *I*, $\Delta\nu=2{,}4$; для *II*, $\Delta\nu=2{,}8$ и для *III*, $\Delta\nu=2{,}9\%$.

Координационный полимер *II* обладает полупроводниковыми свойствами в области температур 20°...200°Ц. Изменения удельной электропроводности этого полимера показали, что она существенно зависит от температуры, подчиняясь закону $\sigma = \exp(E/2kT)$. Полимер *II* имеет энергию активаций проводимости 0,68 эв и удельную электропроводность при 100°Ц равную $8.\ 10^{-12}\ \Omega\ см^{-1}$.

3. Дискусся результатов

Из экспериментальных результатов следует, что на каждый ион Th^{4+} в полимерах *I* приходятся две группы OH и два остатка дифенилфосфиновой кислоты. Так, как эти радикалы играют роль бидентатных лигандов, ионы Th^{4+} могут осуществлять устойчивое координационное число восемь, характерное для этого иона во многих комплексах [10], [11], [15], [16]. На каждый ион Th^{4+} в полимере *II* приходятся две ацетилацетонатные группы и два остатка дифенилфосфиновой кислоты, для *III* — на каждый ион Th^{4+} приходятся четыре остатка дифенилфосфиновой кислоты. Эти радикалы играют роль бидентатных лигандов через посредство атомов кислорода что доказывают ИК-спектры полимеров *II* и *III*. В ацетилацетонате Th(IV) и во многих комплексах Th^{4+} этот ион имеет координа-

ционное число восемь [10], [15], [16]. Из ИК-спектров полимеров *I*, *II* и *III* следует, что радикалы дифенилфосфиновой кислоты, OH и ацетилацетона, связаны с ионами Th^{4+} посредством координирования, как и в координационных соединениях, где центральный ион Th^{4+} имеет координационное число восемь.

В соответствий с теорией поля лигандов [15], [16] образование координационных полимеров происходит при формирований молекулярных орбителей (МО) между ионами Th^{4+} и радикалами дифенилфосфиновой кислоты, OH и ацетилацетона. При образований МО от ионов Th^{4+} участвуют орбитали $6d$, $7s$ и $7p$; от лигандов атомы кислорода — 16 электронов, которые располагаются на связывающих орбиталях.

Внешие орбитали 5 и $7p$ центрального иона Th^{4+} взаимодействуют и лигандами сильно, а экранированные и внутренние орбитали 4— слабо. На оснований этих заключений можно установить возможную схему образования МО исследованных координационных полимеров с додекаэдрической структурой :

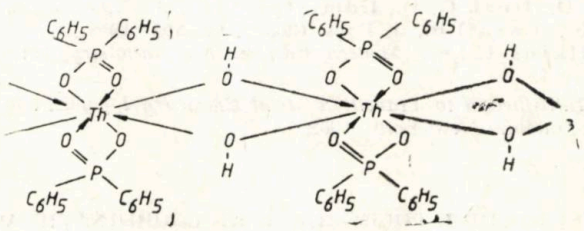

(I)

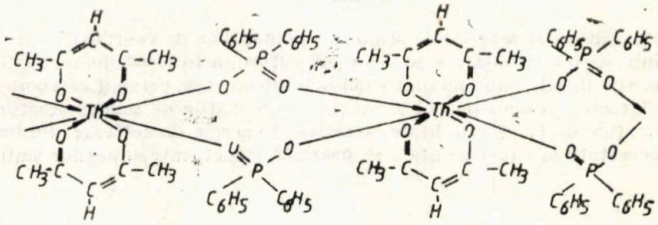

(II)

4. Выводы

В работах [10], [15], [16] доказана структура координационных полимеров Th^{4+} с координационным числом восемь (с додекаэдрической структурной единицей). На основе экспериментальных результатов и литературных данных, мы так же предлагаем структуру этих полимеров с додекаэдрической структурной единицей (с координационным числом восемь для центрального атома иона Th^{4+}).

Поступило с 15 февраля 1989 г.

Ясский политехнический институт,
Кафедра аноpганический и аналитический химии

ЛИТЕРАТУРА

1. Blok B. P., Simkin J., Ocane L. R., J. Amer. Chem. Soc. **84**, 1749 (1962).
2. Blok B. P., Rose L., Schuman C. W., Roth E., J. Amer Chem. Soc., **84**, 3200 (1962).
3. Crescenzi V., Giancotti V., Ripemoti A., J. Amer. Chem. Soc., **87**, 391 (1965).
4. * * * *Успехи в области синтеза элементоорганических полимеров.* Изд. Наука, Москва, 1966, 59.
5. К'оршак В. В., Круковский С. П., Жун-Хан Ван, Локшин Б. В., Высокомолек соедин., **Б 9**, 628 (1967).
6. Коршак В. В., Круковкий С. П., Жун-Хан Ван, Высокомолек. соедин., **Б 9**, 583 (1967).
7. Roşca I., Bul. Inst. polit. Iaşi, **16** (**20**), *3—4*, 15 (1970).
8. Roşca I., Bul. Inst. polit. Iaşi, **17** (**21**), *3—4*, 21 (1971).
9. Roşca I., *Compuşi termostabili ai acetilacetonaţilor de Cr(III), Mn(II), Fe (III), Cr (II), Ni (II), UO_2^{2+} cu acizi şi tioacizi dialchilfosfinici şi difenilfosfinic.* Докт. дисс., Полит. инст., г. Яссы, 1975.
10. Golgoţiu T., Roşca I., Macromoleck. Chem. **59**, 160 (1972).
11. Голгоцю Т., Рошка И., Высокомолек. соед., **А 9**, 2086 (1973).
12. Kosolopoff G. M., J. Amer Chem. Soc., **64**, 2982 (1942).
13. Freedman L. D., Doak G. D., Edmisten J. R., J. Organ. Chem., **26**, 284 (1961).
14. Freeman E. S., Caroll B., J. Phys. Chem., **62**, 394 (1958).
15. Lewis J., Wilkins C. R., *Modern Coordination Chemistry.* Intersci. Publ., New York, 1964.
16. Orgel L. *An Introduction to Transition Metal Chemistry Ligand Field Theory.* Intersci, Publ., London—New York, 1962.

SINTEZA ŞI STUDIUL POLIMERILOR DE COORDINAŢIE Al Th(IV) ŞI ACIDULUI DIFENILFOSFINIC

(Rezumat)

Se prezintă sinteza şi rezultatele studiului polimerilor de coordinaţie ai Th(IV) şi acidului difenilfosfinic ca o continuare a preocupării autorului în acest domeniu. S-au înregistrat spectrele de absorbţie în IR, s-au efectuat calcule termocinetice privind descompunerea termică a polimerilor sintetizaţi şi s-au pus în evidenţă proprietăţile de semiconductori prin determinările experimentale de conductibilitate electrică şi energie de activare. Pe baza datelor din literatura de specialitate şi experimentale se prezintă structura compuşilor sintetizaţi.

BULETINUL INSTITUTULUI POLITEHNIC DIN IAŞI
Tomul XXXV (XXXIX), Fasc. 3—4, 1989
Secţia II
CHIMIE ŞI INGINERIE CHIMICĂ

D. C. 661.183.123 ; 541.57

SORPTION AND SEPARATION OF SOME METAL IONS BY CHELATING SULFONATED AGENT-LOADED ION EXCHANGERS

BY

ANIŞOARA BOLD, DOINA BEJAN, DOINA BÎLBĂ and LAVINIA TOFAN

1. Introduction

One of the most important and modern method for separation and concentration of the element traces in order to be then analysed is the sorption by chelating resins. The rapid and efficient recovery of the microelements from large volumes of solution with complex saline composition is assured by the high selectivity of chelate sorbents, selectivity due to both nature of the chelating groups bonded on polymer matrix and the sorption conditions, namely acidity, temperature, masking compounds, etc.

The chelating group ion exchangers obtained synthetically, are well known and employed in the analytical practice [1], [2], but they have a series of disadvantages such as : special methods of synthesis, high cost, difficult regeneration and unsatisfactory kinetic characteristics.

A simple way, of great interest in the last time, for obtention of some modified ion exchangers with complexing properties and high selectivity, is sorption of some chelating organic reagents on usual ion exchangers [3].

Utilisation of the chelating agent-loaded ion exchangers for preconcentration, selective separation and determination of some metal ions involves that the mechanism and retention conditions of organic reagents and complexes of the elements as well, as kinetics of sorption—desorption to be known [4]...[13].

The purpose of the present work is to obtain some ion exchangers loaded with 5-sulphosalicylic acid (SSA), starting from the anion exchangers Dowex 2x4 and Vionit AT-14 and their utilization for concentration and separation of Fe(III), Cu(II) and Zn(II) from aqueous solutions.

Selection of the SSA as modifier agent was determined by the fact that it contains two groups able to interact with other compounds, namely the sulphonic groups ($-SO_3^-$) for bonding with the anion exchanger and the *o*-hydroxicarboxyl groups to react selectively with a series of elements ($pK_2(-COOH) = 2.67$; $pK_3(-OH) = 11,74$).

2. Experimental

For preparation of the chelating agent-loaded resins we used the chloride form of a strongly basic anion exchanger Dowex 2x4, gel, with the functional group $-CH_2\overset{+}{N}(CH_3)_2C_2H_4OH$ and batch exchange capacity of 3.0

mequiv/g and Vionit AT-14, macroporous, strongly basic, with functional group $-CH_2\overset{+}{N}-(CH_3)_3$ and batch exchange capacity of 3.0 mequiv/g.

The SSA employed as chelating agent was of reagent grade Merck, aqueous solution 0.125 M. Sorption of the SSA on the anion exchangers above mentioned under batch conditions, was studied using samples of about 0.1 g resin and 25 mL solution containing determined amounts of chelating agent. After 24 hours, with intermittent stirring, the phases was separated by filtration and in solution was determined the unretained amount of SSA, spectrophotometrically with $FeCl_3$ at pH=2...3. The amount of the Cl^- ions liberated from resin was determined by potentiometrical titration with $AgNO_3$, using $E_i = EM - Cl^-$ and $E_R = Ag/AgCl$.

The chelating agent-loaded ion exchangers preparated under conditions of maximum retention were employed for study the Fe(III), Cu(II) and Zn(II) ions sorption by batch method.

The solutions of Fe(III), Cu(II) and Zn(II) of 10^{-2} M, prepared by dissolution of their salts (chlorides and sulphates), have been standardized gravimetrically.

Concentrations of the metal ions in solutions at equilibrium have been determined by atomic absorbtion spectrometry (Cu(II) and Zn(II)) and by spectrophotometrical method (Fe(III) with SSA).

3. Results and Discussion

To establish the proper conditions for preparation of the chelating agent loaded resins, interaction of Dowex 2x4 and Vionit AT-14 with SSA against acidity and concentration of chelating agent has been studied. The results represented in Fig. 1 show that the sorption exhibits a maximum at pH = =2.5...3.5.

For the initial concentration of 3 mmol SSA/g resin, the maximum retention degree is of about 60 and 46% for Dowex 2x4 and Vionit AT-14 respectively.

The sorption isotherms of SSA on investigated resins in solutions with pH=2.5...3.0, represented in Fig. 2, points out the fact that the maximum value of exchange capacity of 2.2...2.3 mmol/g Dowex 2x4 and 1.6...1.7 mmol/g Vionit AT-14, namely about 90% and 60% from theoretical capacity of the two resins, respectively.

Table 1

The Ratio $[Cl^-]/[\overline{SSA}]$ from Dowex 2x4 and Vionit At-14

	Dowex 2×4				Vionit AT-14			
	SSA initial mmol/g	SSA retained mmol/g	Cl^- liberated mmol/g	$\frac{[Cl^-]}{[\overline{SSA}]}$	SSA initial mmol/g	SSA retained mmol/g	Cl^- liberated mmol/g	$\frac{[Cl^-]}{[\overline{SSA}]}$
1	0,75	0.7293	1.396	1.914	0.75	0.618	1.0719	1.734
2	1.50	1.430	2.405	1.688	1.50	1.136	1.844	1.623
3	2.25	1.842	2.677	1.4533	2.25	1.4218	2.236	1.5726
4	3.00	2.062	2.813	1.3609	3.00	1.576	2.2988	1.4586
5	3.75	2.255	2.868	1.272	3.75	1.686	2.3200	1.376
6	4.50	2.361	2.738	1.160	4.50	1.799	2.270	1.2615

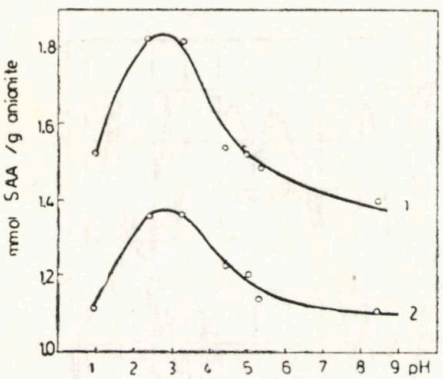

Fig. 1. — Effect of pH of the absorbtion of SSA on anionic resins: *1* — Dowex 2x4; *2* — Vionit AT-14.

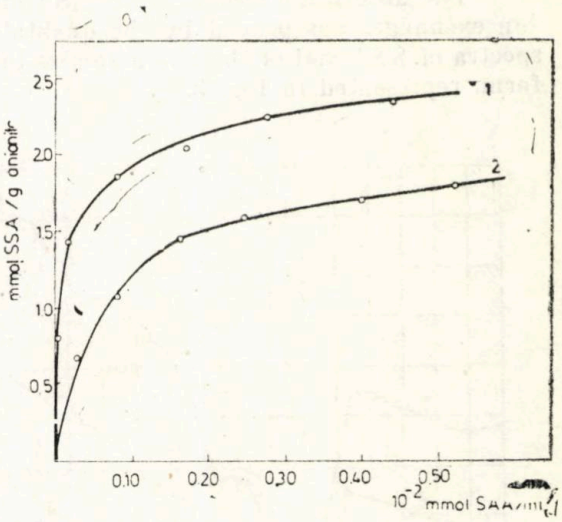

Fig. 2. — Sorption isotherms of SSA on the anionic resins: *1* — Dowex 2x4; *2* — Vionit AT-14.

If an excess of 50% SSA was employed, its retention was 52.5% on Dowex 2x4 and 40% on Vionit AT-14, while for dilute solution, e.g. 25% of stoichiometric necessary amount, retention becomes close to 100% (92.2% for Dowex 2x4 and 82.4% for Vionit AT-14).

The bonding mechanism of SSA and the ion exchange stoichiometry can be elucidated by the determination of the ratio between amount of liberated chlorine and amount of SSA bonded ($[Cl^-]/[\overline{SSA}]$) for different saturation degrees of resin with chelating agent (Table 1).

The data from Table 1 show that in all cases the ratio $[Cl^-]/[\overline{SSA}]$ is greather als the unity, but not higher as 2.0 and becomes lower when amount of absorpted SSA increases. These results lead to the conclusion that, at a low saturation degree of resin, SSA behaviours as a divalent anion, for the exchange reaction of the Cl^- ions in resin participating both sulphonic groups and carboxylic groups of the chelating agent:

$$RCl_m + {}^-O_3SC_6H_4(OH)COO^- = [RCl_{m-2}]^{2+}[O_3SC_6H_4(OH)COO]^{2-} + 2Cl^-.$$

At the same time, with SSA concentration increasing the sorption of chelating agent in resin is controlled more and more by the ion exchange between Cl^- and sulphonate anion of SSA:

$$RCl_m + {}^-O_3SC_6H_4(OH)COOH = [RCl_{m-1}]^+[O_3SC_6H_4(OH)COOH]^- + Cl^-.$$

Also, the interactions between resin matrix and chelating agent molecule, i.e. van der Waals forces, molecular adsorption, hydrogen bonds, cannot be neglected, even their effect is a minor one.

The absorbtion mechanism of SSA on the investigated resins, based on ion exchange, was proved by the qualitative information given by the IR spectra of SSA and of the two anionites in both Cl^- and modified with SSA form, represented in Fig. 3.

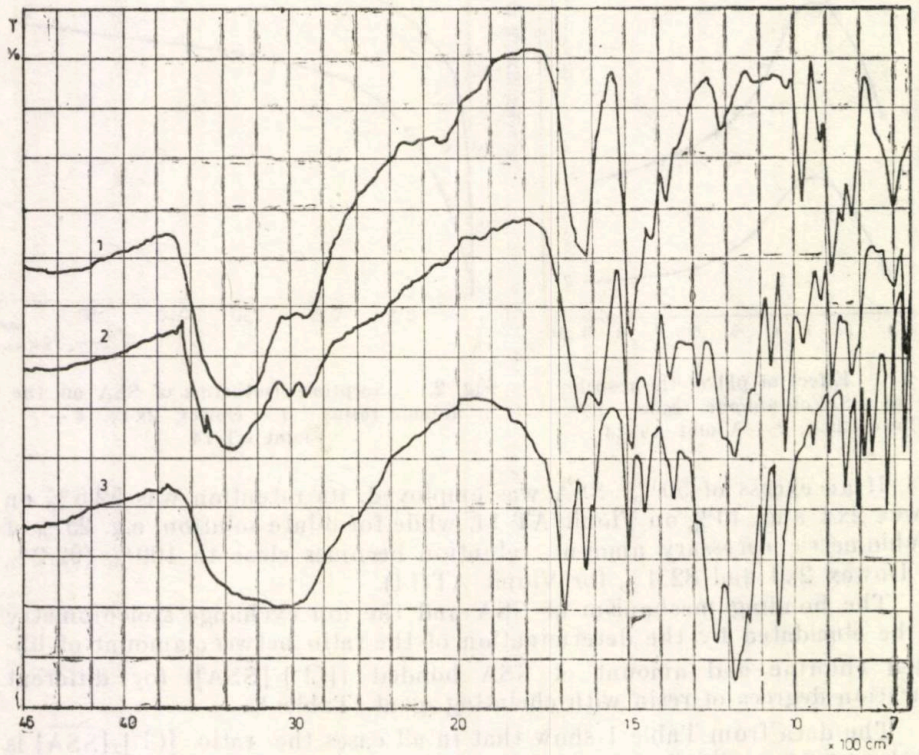

Fig. 3. — IR Spectra: *1* — Vionit AT-14; *2* — Vionit AT-14+SSA; *3* — SSA.

A comparison of the IR spectra, presented in Fig. 3, shows the absorbtion bends atributed to valence vibrations of the $-SO_3^-$ group in the spectre of loaded resin, what proves retention of SSA on anionite ($\nu_{SO_3 asym.}$ =1 180 cm^{-1}; $\nu_{SO_3 sym.}$ =1 070 cm^{-1}; 1 030 cm^{-1}; ν_{S-O} =670 cm^{-1}).

The absorbtion bends atributed to valence vibrations and deformation ones of the OH^- group (1 640 cm^{-1}, 1 210 cm^{-1}) being affected shows a modification of the hydrogen bonds system, caused by the SSA absorbtion on resin. Also, modification of the ratio between intensities of some absorbtion bends pleads for electrostatic character of the bond between amminic functional group and SSA.

The Dowex 2x4 and Vionit AT-14 loaded with SSA with medium saturation degree, were employed for sorption of the Fe(III), Cu(II) and Zn(II) ions. The experimental results, represented in Fig. 4, point out that the retention of metal ions depends on pH.

Absorbtion of Fe(III) is larger than that of the other ions, the pH range corresponding to the ratio Fe(III) : SSA = 1 : 1, complex formation being a little out-of-place towards high values against the same complex in aqueous solution.

Absorbtion of Cu(II) becomes higher as pH increases from 2 to about 5.5, the maximum sorption degree being only 20...25% w.r.t. the initial concentration.

In the case of Zn(II), there is no modification of absorption in the pH range 2...6, the retention degree being low, about 10%.

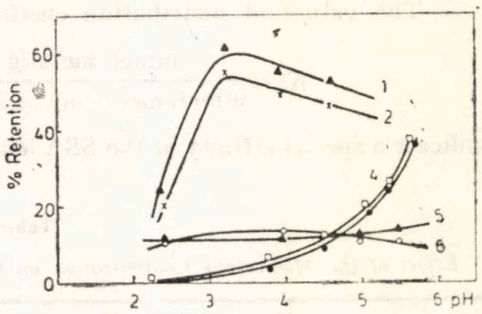

Fig. 4. — Effect of pH on the absorption of: Fe(III) — (*1,2*); Cu(II) — (*3, 4*); Zn(II) —(*5, 6*), on SSA loaded resins: Dowex 2x4 (*1, 3, 5*) and Vionit AT-14 (*2, 4, 6*).

At a constant pH value, i.e. 3.2...3.4, the absorbtion of Fe(III) depends on saturation degree of the resin with SSA (Fig. 5).

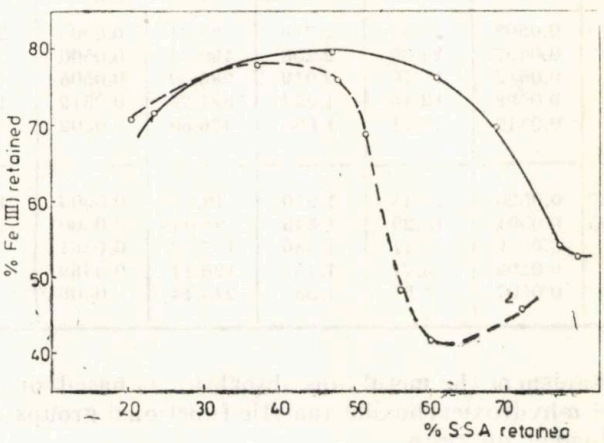

Fig. 5. — Effect of the saturation degree of resins with SSA on the Fe(III) absorbtion: *1* — Dowex 2x4; *2* — Vionit AT-14.

Capacity of the loaded resins to retain Fe(III) becomes lower as saturation degree of the resins with chelating agent increases; these behaviour can be explained as a consequence of the interactions between SSA molecules, in the resin phase, bloking the oxigroups of the reagent.

For a certain saturation degree of resins with SSA (45...50%) in solutions with optimum pH, corresponding to complex formation, the absorbtion depends on metal ions concentration only (Table 2).

The data of Table 2 show comparable values for absorption degree of Fe(III), Cu(II) and Zn(II) of the two investigated resins.

The values of distribution coefficient:

$$K_d = \frac{\text{mmol metal/g modified resin}}{\text{mmol metal/mL solution at equilibrium}},$$

indicate a special affinity of the SSA loaded-resins against Fe(III).

Table 2

Effect of the Metal Ions Concentration on their Absorption on SSA Loaded Resins

	Dowex 2x4 — SSA				Vionit AT-14 — SSA			
	Co μg/25 mL	g ionit	Retention %	lg K_d	Co μg/25 mL	g ionit	Retention %	lg K_d
Fe (III) pH= =3.2... 3.4	98.28	0.0510	94.91	3.961	98.28	0.0503	92.87	3.811
	196.54	0.0503	86.00	3.485	196.54	0.0503	83.46	3.399
	298.84	0.0516	83.02	3.375	294.84	0.0503	77.10	3.223
	393.12	0.0510	79.64	3.328	393.12	0.0506	74.56	3.160
	491.40	0.0507	75.64	3.183	491.40	0.0510	72.89	3.119
Cu (II) pH ≃ 5	95.31	0.0508	27.87	2.279	95.31	0.0503	23.93	2.194
	190.64	0.0497	24.30	2.208	190.64	0.0500	21.31	2.132
	286.00	0.0512	17.70	2.019	286.00	0.0505	15.29	1.968
	381.28	0.0498	12.46	1.854	381.28	0.0512	11.07	1.783
	476.60	0.0510	10.11	1.695	476.60	0.0502	8.77	1.680
Zn (II) pH ≃5	49.027	0.0520	14.48	1.910	49.027	0.0502	12.64	1.858
	98.055	0.0501	13.29	1.845	98.055	0.0500	10.76	1.780
	147.08	0.0519	7.41	1.586	147.08	0.0481	6.66	1.463
	196.11	0.0502	5.71	1.454	196.11	0.0489	5.26	1.453
	245.14	0.0507	4.67	1.383	245.14	0.0506	3.87	1.299

The mechanism of the metal ions absorbtion is based on their complexation with the *o*-hydroxicarboxilic analytic-functional groups of the sulphonated reagent loaded on resin.

The retention percentage is in a good agreement with the stability of metal chelates in aqueous solutions.

Absorption of the metal ions on the SSA loaded resins is not a complete one (about 100%), although the experiments were carried out in dilute solutions, with concentrations much less than entire sorption capacity of the modified resins. This behaviour is in good agreement with the mechanism of SSA absorbtion on anionites and with participation of carboxyl groups simultaneously with diminishing of the complexation capacity against the metal ions.

The entire absorbtion capacity of the loaded resins depends on a series of factors such as the nature of chelating agent adsorpted on resin, availablity of chelating groups, composition of complex compounds with metallic ions, itheir stability, pH, etc.

The performed experiments allow to evidence some possibilities of separation of the mixtures of Fe(III), Cu(II) and Zn(II).

4. Conclusions

From the experimental results presented above, the following conclusions may be drawn.

1. By absorption of SSA on the Dowex 2x4 and Vionit AT-14 anionic resins, the chelating sulphonated agent-loaded ion exchangers is produced, with complexing properties and selectivity against metal ions.

2. Absorbtion of the chelating agent depends on pH solution and takes place by an ion exchange mechanism, SSA behaving as both monovalent and divalent ion, in function of concentration.

3. The anionites loaded with SSA can be employed successfully for selective concentration of Fe(III) and its separation from Cu(II) and Zn(II).

Received, February 7, 1989

Polytechnic Institute, Jassy,
Department of Inorganic and Analytical Chemistry

REFERENCES

1. Мясоедова Г. В., Малофеева Г. И., ЖАХ, **34**, *8*, 1626 (1979).
2. Мясоедова Г. В., Савин С. Б., ЖАХ, **37**, *3*, 499 (1982).
3. Белявская Т. А., Брыкина Г. Д., *Определение малых концентрации элементов*. Изд. Наука, Москва, 1986.
4. Брыкина Г. Д., Марчак Т. В., Белявская Т. А., ЖФХ, **54**, *8*, 2094 (1980).
5. Брыкина Г. Д. Филиппова Н. Л., Крысня Л. С., Белявская Т.А., ЖФХ, **53**, *8*, 2 075 (1979).
6. Брыкина Г. Д., Степанова Н. Л., Белявская Т. А., ЖАХ, **37**, *2*, 208 (1982).
7. Brajter K., Dabek-Zlotorzynska E., Microchim. Acta, **2**, *3—4*, 179 (1985).
8. Chwastowska J., Przygoda D., Chem. Anal., **31**, *4*, 545 (1986).
9. Marina M. L., Gonzales V., Rodrigues A.R., Microchem. J., **33**, *3*, 275 (1986).
10. Lee K.S., Lee W., Lee D.W., Anal. Chem., **50**, *2*, 255 (1978).
11. Chikuma M., Nakayama M., Itoh K.,Talanta, **27**, 807 (1980).
12. Марчак Т. В., Брыкина Г. Д., Белявская Т. А., ЖАХ, **36**, *3*, 513 (1981).
13. Рубалкова Л. Н. М., Егоров А. М., Медина П. М. Ф., ЖПХ, **48**, *11*, 2423 (1975).

SORBȚIA ȘI SEPARAREA UNOR IONI METALICI PE RĂȘINI SCHIMBĂTOARE DE IONI MODIFICATE CU AGENȚI SULFONAȚI DE CHELATIZARE

(Rezumat)

Prin sorbția reactivilor organici (modificatori) pe schimbători de ioni se obțin materiale cu selectivitate înaltă, utilizate pentru preconcentrarea, separarea selectivă și determinarea unor ioni metalici.

Se prezintă rezultatele studiului sorbției acidului sulfosalicilic (ASS) pe diferite rășini anionitice (Dowex 2x4, Vionit AT-14).

S-au stabilit condițiile optime de reținere (concentrație, pH, natura anionitului) a ASS.

Capacitatea schimbătorilor de ioni modificați față de o serie de ioni metalici (Fe(III), Cu(II), Zn(II)) este determinată pentru diferite concentrații ale acestora în soluție precum și în funcție de pH.

Sînt evidențiate concluziile de ordin practic ce rezultă din datele experimentale.

BULETINUL INSTITUTULUI POLITEHNIC DIN IAŞI
Tomul XXXV (XXXIX), Fasc. 3—4, 1989
Secţia II
CHIMIE ŞI INGINERIE CHIMICĂ

D. C. 542.48 ; 546.843 ; 576.8

THE CONCENTRATION OF THORIUM BY MEANS OF MICROBIOLOGICAL COLLECTORS

BY

VIORICA DULMAN, AL. CECAL, TINCA ONOFREI and CONSTANŢA BURCOVEANU

1. Introduction

The concentration of certain ions diluted solutions by means of levuric cells as microbiological collectors is important in the depolluting of residual waters [1]. Various types of microorganisms have proved to be efficient biosorbents in the removal of the radionuclides resulting from the reprocessing of the exhausted nuclear fuel and can be found as radioactive wastes of ligh and medium activity [2]...[4]. Biofilms with immobilized cells have also been used in the removal of uranium and lead from residual waters [5].

The present paper studies the possibility of concentrating thorium with a strain of *Saccharomyces cerevisiae* as microbiological collector, from diluted solutions. The influences of certain physico-chemical parameters upon the optimum concentration has been investigated.

2. Experimental

The microbiological collector employed was a strain of *Saccharomyces cerevisiae*, grown and kept under condition similar to those presented in a previous paper [6],

The dense suspension collected by the washing with physiological serum of the microbiological culture obtained on a solid medium was standardized by drying at 105°C and a constant weight (m). Under sterile conditions, the suspension was introduced into buffer solution of 40 ml acetic acid — acetate sodium, or in bidistilled water and 2 ml of 10% glucose, in the presence of thorium ions. The samples were maintained at 37°C in a thermostat, without being shaken.

The thorium solution was prepared from thorium nitrate and standardized by the gravimetric method with amonium oxalate [7].

The determination of thorium was carried out by the thoron method in the respective supernatant resulting by centrifugation an aliquote of the sample at 6 000 rpm [8].

For determination of the thorium concentration capacity the percentage accumulation and the mg Th/1 g dry levuric mass was calculated.

3. Results and Discussions

3.1. The influence of pH

The levuric mass of standardized *Saccharomyces cerevisiae* was introduced into the buffer solution acetic acid—sodium acetate with pH = 3.6...

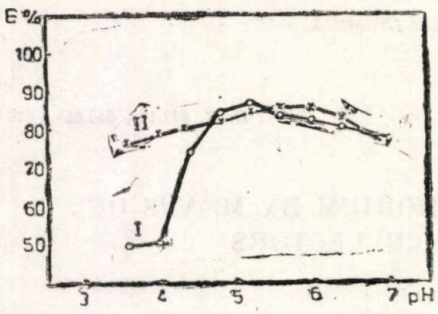

Fig. 1. — The influence of pH vs. thorium ions concentration: *I* — acetic acid — sodium acetate buffer; *II* — bidistilled water (pH corrected with HCl or NaOH); 9.42 μg/ml Th, 0.4 % glucose; time — 24 h; m=0.15 g.

7 or into bidistilled water whose pH had been corrected by means of HCl or NaOH, between the same values. Under the experimental conditions indicated in Fig. 1, a dependence was found as function of the percentage of the accumulation of the pH of the medium, stronger in the case of the acetate buffer, when the maximum obtained is 87 % for pH=5.2 (curve *I*). In distilled water there is a slow variation of biosorbtion, the accumulation percentage coming up to 85 %, for pH= =5.2...6 (curve *II*).

3.2. The Influence of the Time of Contact : Levuric Mass — Solution

The thorium biosorbtion depending on time has been studied in two ways :

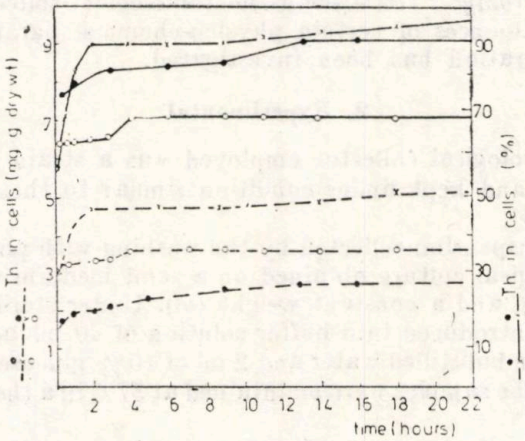

Fig. 2. — Influence of time : • — acetic acid — sodium acetate buffer (pH=5.2; 9.42 μg/ml Th; 0.4 % glucose, m=0.15 g); x — bidistilled water in the presence of 0.4 % glucose; o — bidistilled water in the absence of glucose) (pH=5.6; 9.42 μg/ml Th; m=0.089 g).

a) After certain intervals of time of contact between levuric mass and solution, the thorium quantity left in solution was analyzed. The obtained results (Fig. 2) indicate that accumulation percentage grows with the time of contact. An acetate buffer after 16 hours goes up to 91 %, then this parameter remains constant. In the bidistilled water in the presence of glucose, after two hours, an important quantity of thorium is concentrated (90 %); after that the increase is slow, at the most reaching 97 % in 24 hours. The presence

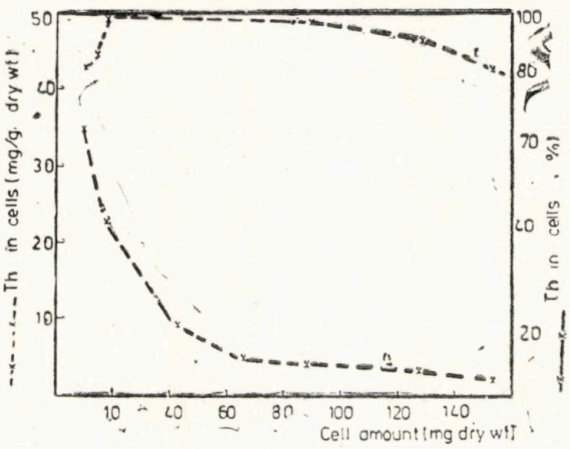

Fig. 5. — The influence of the collector's mass on the thorium concentration in bidistilled water (9.42 μg/ml Th ; 0.4 % glucose ; time — 24 h ; pH=5.6).

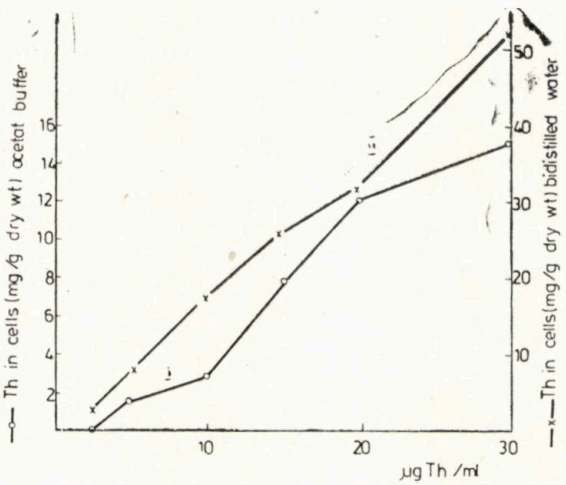

Fig. 6. — The influence of the thorium concentration.

of glucose was found to have little influence on thorium concentration in the case of the acetate buffer but an important role in bidistilled water.

b) Thorium was added after certain intervals of time within the levuric mass in the medium acetate buffer pH=5.2 or bidistilled water pH=5.6 in the presence of 0.4% glucose was maintained constant. The analysis of all samples was made after 24 hours.

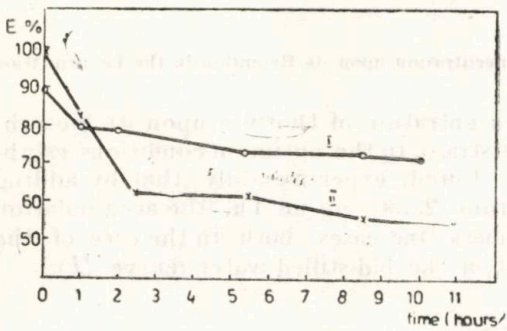

Fig. 3. — Addition of thorium after certain time intervals to the medium containing the levuric mass: *I* — acetate buffer (pH=5.2; 9.42 μg/ml Th; 0.4% glucose; m=0.171 g); *II* — bidistilled water (pH=5.6; 9.42 μg/ml Th; 0.4% glucose, m=0.086 g).

The percentage of accumulation was found to decrease in both cases as the thorium was added after longer intervals of time (Fig. 2). Thorium probably forms compounds with CO_2 or other metabolism products released in the environment and which are not retained on the levuric mass.

3.3. The Influence of the Collector's Mass

The collector was added to the acetate buffer on variable quantity corresponding to 38 ... 380 mg dry mass at 105°C, in the optimum conditions established both for pH and time.

An increase of the accumulation percentage from 81% to 91% was found together with the corresponding increase of the quantity of the levuric mass from 38 to 150 mg. Then, for 300 mg levuric mass the accumulation percentage decreases to 72% (Fig. 3, curve *I*).

The capacity of the levuric mass to retain the thorium ions from the bidistilled water in the presence of glucose is higher than in the case of the acetate buffer, reaching 99.8% for 17 mg collector mass, after which it slowly decreases to 85% for 148 mg collector (Fig. 5). This different behaviour of the levuric mass in larger quantities in the medium, in the presence of the same quantity of thorium ions, might also be explained by the interaction of these ions with the carbon dioxide or others products released by the fermentation of the microbiological collector.

If the results of the biosorbtion achieved in both media, for 1 g cells

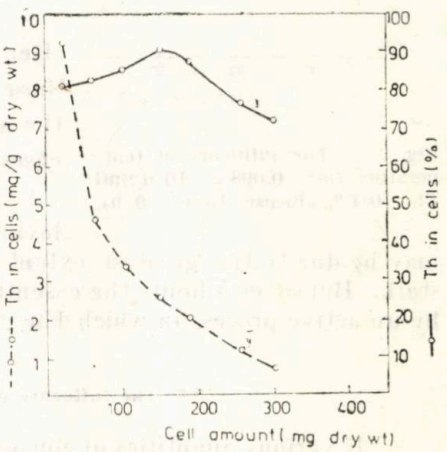

Fig. 4. — The influence of the microbiological collector's mass on the thorium concentration in the acetate buffer (9.42 μg/ml Th; 0.4 % glucose; time — 24 h; pH=5.2).

(dry mass at 105°C) are analyzed, it is obvious that the retained quantity of thorium decreases with the increase in the collector's mass. The maximum of 9.3 mg Th is attained in the acetate buffer and 37 mg Th in bidistilled water, retained on 1 g cells. Consequently, from this point of view, an efficient concentration may be achieved in bidistilled water, in the best condition established, respecting the ratio between collector mass and the concentration of the thorium in the medium.

3.4. The Influence of the Thorium Concentration upon its Retention in the Levuric Mass

The effect of the (external) concentration of thorium upon its biosorbtion by the *Saccharomyces cerevisiae* strain, in the optimum conditions established, was studied (Fig. 6). It was found, experimentally, that by adding different quantities of thorium, from 2...30 μg/ml Th, the accumulation expressed in mg Th/1 g dry levuric mass increases both in the case of the acetate buffer (curve *I*) and in that of the bidistilled water (curve *II*).

3.5. The Influence of Temperature

The levuric mass was kept in bidistilled water in the presence of glucose, at various temperatures between 0°...37°C. The obtained results shown that the accumulation percentage increases slightly with temperature up to 20°C, then it remains constant (Fig. 7).

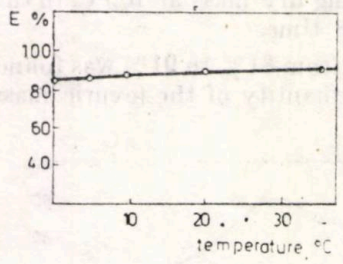

Fig. 7. — The influence of temperature, (m = 0.098 g ; 10 μg/ml Th ; 0.4 % glucose, time — 6 h).

3.6. The Influence of Shaking

At room temperature, the shaken samples after 30 min. accumulate 81% thorium, while those not shaken only 39%. After 5 hours, the accumulation percentage is 85% in both cases (Fig. 8).

In the first hours of contact between the levuric mass and thorium, the concentration may be due to the greatest extent to adsorbtion at the surface of the levuric stalk. But after 5 hours the essential retention role is likely to be played by an active process in which the glucose is also involved.

3.7. The Influence of the Glucose Concentration

If various quantities of glucose (0...2.7%) are introduced into the acetate buffer solution, the presence of glucose (<0.4%) is found not to influence the accumulation percentage. But larger quantities of glucose determine a decrease in the biosorption of thorium ions on the levuric strain (Fig. 9, curve *I*). In bidistilled water, glucose has a stimulating effect. Thus, biosorbtion in-

creases with the growth of the glucose concentration from 0 to 1 % after which a decrease of the retention is recorded (curve *II*).

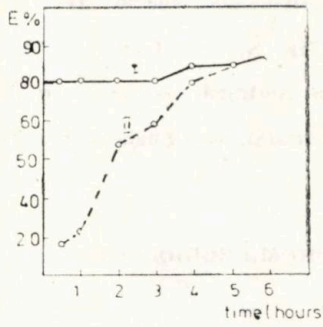

Fig. 8. — The influence of shaking on the biosorbtion of the thorium ions : *I* — shaken samples ; *II* — unshaken samples (m=0.098 g ; 10 μg/ml Th ; 0.4% glucose).

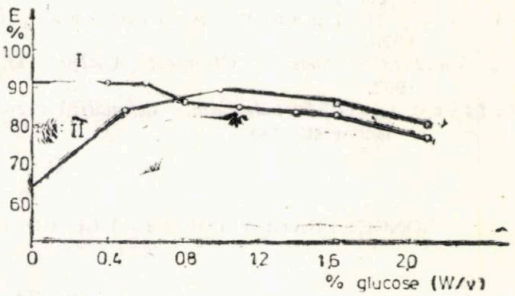

Fig. 9. — The influence of the glucose concentration : *I* — acetate buffer ; *II* — bidistilled water (m=0.15 g ; 10 μg/ml Th ; time — 24 h).

4. Conclusions

1. Thorium can be concentrated from media containing acetate buffer with pH =5.2 or bidistilled water (pH =5.6), in the presence of glucose at the best time interval and a corresponding levuric mass by using a strain of *Saccharomyces cerevisiae* as microbiological collector.

2. The experimental results prove that a certain râtio must be maintained between the levuric mass and the thorium concentration in the medium.

3. The thorium biosorbtion probably takes place owing to adsorbtion at the surface of cells, but when using bidistilled water in a certain stage of the concentration process a certain penetration into the cells can also be supposed to occur.

4. For high thorium concentration, a coprecipitation of this ion is possible.

Received, December 12, 1988

Polytechnic Institute, Jassy,
Department of Inorganic and Analytical Chemistry
and
Medical-Pharmaceutical Institute, Jassy,
The 5th Medical Clinic

REFERENCES

1. Dulman V., Burcoveanu C., Bul. Inst. polit., Iaşi, **33** (**37**), *1—4*, s. II, 23 (1987).
2. Horikshi T., Nakajima A., Sakaguchi T., Eur. J. Appl. Microbiol. Biotechnol., **12**, 90 (1981).

3. Horikshi T. Nakajima A., Sakaguchi T., J. Ferment. Technol. **97**, 191 (1979).
4. Standberg S. W., Shumate S. E., Parrott Jr. Appl. Environ. Microbiol., **41**, 237 (1981).
5. Makaskie L. E., Dean Alastair C. R., Enzyme and Microb. Technol., **1**, 9 (1987).
6. Fișel S., Dulman V., Burcoveanu, C., Sep. Sci. a. Technol., **13**, 835 1978.
7. *** *Standard Methods of Chemicat Analysis.* D. van Nostrand Co. Inc., New York, 1962.
8. Jeffery D. G., *Metode chimice de analiză a rocilor*, (transl. from English). Ed. Tehn., București, 1983.

CONCENTRAREA TORIULUI CU COLECTORI MICROBIOLOGICI

(Rezumat)

Toriul poate fi concentrat cantitativ întrebuințînd un colector microbiologic care constă dintr-o tulpină de *Saccharomyces cerevisiae* suspendată în tampon acetat sau apă bidistilată în prezența glucozei.

S-au studiat condițiile optime pentru o astfel de concentrare în ceea ce privește : pH-ul, timpul, masa colectorului, concentrația ionului toriu, temperatura.

BULETINUL INSTITUTULUI POLITEHNIC DIN IAȘI
Tomul XXXV (XXXIX), Fasc. 3—4, 1989
Secția II
CHIMIE ȘI INGINERIE CHIMICĂ

D. C. 541.8 ; 661.848.511 ; 661.847.2 ; 661.849.511

THE USE OF INTERNAL ISOTOPIC DILUTION FOR THE SOLUBILITY DETERMINATION OF CERTAIN HARD SOLUBLE SULPHIDES

BY

AL. CECAL

1. Introduction

There are several studies concerning the determination of the solubility of certain hard soluble chemical compounds in various solvents [1]...[6]. The corresponding dissolving process is characterized by a series of thermodynamic parameters such as : the effect of the reacting medium upon the dissolving of the given substance, as well as the variation of the standard (G i b b s) free energy. At the same time, attempts have been made to determine the dissolving mechanism of the hard soluble compounds in different experimental conditions [7]...[10].

The present paper continues a study began previously [11], [12] regarding the determination of solubility of certain hard soluble chemical compounds by using internal isotopic dilution [13],]14].

2. Experimental

The three hard soluble sulphides : ZnS, CdS and HgS, were prepared according to known methods [15]...[18]. The hard soluble compounds obtained were separated, by filtering, from given solution, then were introduced into a drying chamber at 130°C, with the aim to eliminating the rest of water. Finally, the respective sulphides were stored for keeping in an exiccator with $CaCl_2$.

Three Erlenmayer glasses were used to receive each 90 ml water, while other 3×8 glasses received each 90 ml mixture of water — organic solvent (methanol, ethanol, or isopropanol), in the volumetric ratios : 80 : 10 ; 70 : 20 ; 60 : 30 ; 50 : 40 ; 40 : 50 ; 30 : 60 ; 20 : 70 and 10 : 80, so that a given ratio should be found in three glasses (water--methanol, water —ethanol and water — isopropanol). 1 g of the hard soluble compounds previously prepared (ZnS, CdS, HgS respectively) was introduced in these glasses, so that a given sulphide should be found in nine glasses (one with water and the rest with the mixture : water — organic solvent).

Then, 10 ml radioactive aqueous solution of $^{65}ZnCl_2$ (for the samples with ZnS), $^{115}CdCl_2$ (for those with CdS) and respectively $^{203}HgCl_2$ (for the samples

with HgS) was introduced into the glasses. The initial radioactive solutions had a specific activity of 1×10^4 Bq/ml and a concentration of 1×10^{-4} g/ml.

The samples, thus prepared, were shaken for 30 min., then left the rest for about 10 min. From each solution over the precipitate 0.5 ml was extracted and decanted into a porcelain crucible. The solutions in these crucibles were subjected to evaporation with an infrared lamp and then the activity of each residuum was determined by means of a scintillation detector (NaI/Tl) connected to a monochanal analyzer NK-150. The value of the previously determined cosmic background was substracted from these readings so that the values of the specific activity R_2, [Bq/ml], could be calculated for each sample.

At the same time three Erlenmayer glasses were used, each for 90 ml water and 10 ml of one of the radioactive solutions : $^{65}ZnCl_2$, $^{115}CdCl_2$ and $^{203}HgCl_2$, respectively. Then 0.5 ml solutions were extracted from each glass and put into three crucibles. Following the same method as in the previous case (evaporating, measuring of the activity, etc.) the values of the specific activity of the initial solution, R_1, [Bq/ml], were determined.

3. Results and Discussion

At the same time with the dissolving of the hard soluble compounds in the given solvent, there takes place, implicitly, an internal isotopic dilution of the radioactive cations initially introduced into the system. If the concentration of these cations is C_1 after the internal isotopic dilution, the concentration of the nonradioactive cations that have passed into the solution after the dissolving process is :

$$C_2 = \frac{(R_1 - R_2)}{R_1} C_1. \tag{1}$$

With this value, the solubility of the hard soluble substance in the given solvent, [mol/l], can be calculated.

For the Zn, Cd and Hg sulphides, the following solid—solution equilibrium is established :

$$MS \rightleftharpoons M^{2+} + S^{2-}. \tag{2}$$

Hence, the solubility product will be :

$$K_s = [M^{2+}][S^{2-}] = s^2, \tag{3}$$

where s is the solubility of the hard soluble compound.

The concentration C_2, [g/ml], of the nonradioactive ions that have passed into the solution, can be considered equal to the solubility, s, of the dissolved substance. At the same time :

$$[M^{2+}] = [S^{2-}]. \tag{4}$$

These reasons justify the existence of the relation of the solubility product.

Every time there is a difference between the values of the solvatation standard free energy ($\Delta_s G_i^0$) and those of hydratation standard free energy ($\Delta_w G_i^0$), which is expressed by :

(5) $$\Delta G_i^0 = \Delta_s G_i^0 - \Delta_w G_i^0 = RT \log \Delta_m \gamma_i = RT(\log \Delta_s K_s - \log \Delta_w K_s).$$

Here $\Delta_m \gamma_i$ represents the medium effect (the activity coefficient of the reactions medium) which influence the process of the dissolving. At the same time, the medium effect represent a measure of the standard free energy of transfer of the solved substance from water to the nonaqueous solvent. The greater the standard free energy, the less soluble the solid substance is.

The experimental data are summarized in Tables 1...3.

Table 1

The Values of the Solubility (s), Solubility Product (K_S), Medium Effect ($\Delta_m \gamma_i$) and the Variation of Standard Free Energy (ΔG^0_i) for ZnS

Dissolv. medium	Water–organic solvent ratio %	s mole/l	K_S	log $\Delta_m \gamma_i$	ΔG_i^0 Y/mole
Water	—	1.56×10^{-13}	2.43×10^{-26}	—	—
Water — methanol	90:10	1.21×10^{-13}	1.46×10^{-26}	0.221	537.2
	80:20	1.08×10^{-13}	1.16×10^{-26}	0.321	779.7
	70:30	9.80×10^{-14}	9.60×10^{-27}	0.403	979.3
	60:40	8.45×10^{-14}	7.14×10^{-27}	0.532	1 291.5
	50:50	7.24×10^{-14}	5.24×10^{-27}	0.665	1 617.7
	40:60	7.56×10^{-14}	5.71×10^{-27}	0.629	1 529.0
	30:70	8.01×10^{-14}	6.41×10^{-27}	0.578	1 405.2
	20:80	8.17×10^{-14}	6.67×10^{-27}	0.560	1 363.3
	10:90	8.23×10^{-14}	6.91×10^{-27}	0.545	1 324.5
Water — ethanol	90:10	1.37×10^{-13}	1.87×10^{-26}	0.113	276.2
	80:20	1.20×10^{-13}	1.44×10^{-26}	0.227	551.7
	70:30	1.07×10^{-13}	1.14×10^{-26}	0.328	798.1
	60:40	9.79×10^{-14}	9.58×10^{-27}	0.404	981.6
	50:50	9.25×10^{-14}	8.55×10^{-27}	0.453	1 100.1
	40:60	9.32×10^{-14}	8.68×10^{-27}	0.447	1 085.5
	30:70	9.56×10^{-14}	9.13×10^{-27}	0.425	1 032.2
	20:80	9.77×10^{-14}	9.54×10^{-27}	0.406	985.9
	10:90	9.92×10^{-14}	9.84×10^{-27}	0.392	953.2
Water — isopropanol	90:10	1.49×10^{-13}	2.22×10^{-26}	0.039	95.1
	80:20	1.38×10^{-13}	1.90×10^{-26}	0.106	259.4
	70:30	1.30×10^{-13}	1.69×10^{-26}	0.157	382.9
	60:40	1.22×10^{-13}	1.48×10^{-26}	0.215	522.8
	50:50	1.09×10^{-13}	1.18×10^{-26}	0.313	761.7
	40:60	1.12×10^{-13}	1.25×10^{-26}	0.236	573.9
	30:70	1.19×10^{-13}	1.41×10^{-26}	0.204	498.9
	20:80	1.27×10^{-13}	1.61×10^{-26}	0.178	434.0
	10:90	1.35×10^{-13}	1.82×10^{-26}	0.125	304.9

Table 2

The Values of the Solubility (s), Solubility Product (K_S), Medium Effect ($\Delta_m\gamma_i$) and the Variation of Standard Free Energy (ΔG_i) for CdS

Dissolv. medium	Water—organic solvent ratio %	s mole/l	K_S	log $\Delta_m\gamma_i$	ΔG_i^0 J/mole
Water	—	3.47×10^{-12}	1.20×10^{-23}	—	—
Water—methanol	90:10	3.22×10^{-12}	1.03×10^{-23}	0.066	161.0
	80:20	2.87×10^{-12}	8.23×10^{-24}	0.163	397.6
	70:30	2.51×10^{-12}	6.30×10^{-24}	0.297	679.4
	60:40	2.33×10^{-12}	5.09×10^{-24}	0.361	867.5
	50:50	2.14×10^{-12}	4.56×10^{-24}	0.418	1 015.6
	40:60	2.45×10^{-12}	6.01×10^{-24}	0.301	729.1
	30:70	2.91×10^{-12}	8.46×10^{-24}	0.153	368.4
	20:80	3.17×10^{-12}	1.01×10^{-23}	0.074	181.7
	10:90	3.29×10^{-12}	1.08×10^{-23}	0.045	111.4
Water—ethanol	90:10	3.31×10^{-12}	1.09×10^{-23}	0.041	101.3
	80:20	3.25×10^{-12}	1.05×10^{-23}	0.061	148.5
	70:30	3.19×10^{-12}	1.02×10^{-23}	0.070	171.3
	60:40	3.07×10^{-12}	9.42×10^{-24}	0.105	255.2
	50:50	2.82×10^{-12}	7.89×10^{-24}	0.184	448.8
	40:60	2.92×10^{-12}	8.52×10^{-24}	0.149	361.7
	30:70	3.09×10^{-12}	9.27×10^{-24}	0.112	272.2
	20:80	3.18×10^{-12}	1.02×10^{-23}	0.070	171.3
	10:90	3.26×10^{-12}	1.07×10^{-23}	0.054	128.6
Water—isopropanol	90:10	3.33×10^{-12}	1.10×10^{-23}	0.037	91.7
	80:20	3.26×10^{-12}	1.07×10^{-23}	0.037	128.6
	70:30	3.17×10^{-12}	1.01×10^{-23}	0.074	181.7
	60:40	3.11×10^{-12}	9.67×10^{-24}	0.093	227.6
	50:50	3.05×10^{-12}	9.30×10^{-24}	0.110	268.7
	40:60	3.07×10^{-12}	9.42×10^{-24}	0.105	255.2
	30:70	3.18×10^{-12}	1.01×10^{-23}	0.074	181.7
	20:80	3.24×10^{-12}	1.05×10^{-23}	0.058	142.2
	10:90	3.30×10^{-12}	1.08×10^{-23}	0.046	111.5

The values of the solubility of the hard soluble compounds calculated by this method are in accordance with those found by other authours [20], [21].

Taking into account the basicity of the solvent and the similar data found by other authors [22], [23], who studied similar systems, we could explain the variation of the respective parameters by reference to the water—organic solvent ratio. The basicity of pure water is known to be lower if compared to that of water organic solvent mixtures, where the hydrogen bonds are weaker. By an addition of organic solvent to pure water, the associated forms of the type $H^+(H_2O)_n$ (of reduced basicity) are distroyed, the result being pre-

Table 3

The Values of the Solubility (s), Solubility Product (K_s), Medium Effect ($\Delta_m\gamma_i$) and the Variation of Standard Free Energy (ΔG_i^0) for HgS

Dissolv. medium	Water—organic solvent ratio %	s mole/l	K_s	log $\Delta_m\gamma_i$	ΔG_i^0 J/mole
Water	—	6.29×10^{-27}	3.95×10^{-53}	—	—
Water—methanol	90:10	6.18×10^{-27}	3.81×10^{-53}	0.015	38.0
	80:20	6.12×10^{-27}	3.74×10^{-53}	0.023	57.1
	70:30	6.03×10^{-27}	3.69×10^{-53}	0.029	71.7
	60:40	5.92×10^{-27}	3.50×10^{-53}	0.053	127.7
	50:50	5.80×10^{-27}	3.36×10^{-53}	0.070	170.6
	40:60	5.95×10^{-27}	3.59×10^{-53}	0.038	101.5
	30:70	6.01×10^{-27}	3.64×10^{-53}	0.035	90.9
	20:80	6.09×10^{-27}	3.71×10^{-53}	0.028	68.8
	10:90	6.15×10^{-27}	3.78×10^{-53}	0.019	46.4
Water—ethanol	90:10	6.22×10^{-27}	3.86×10^{-53}	0.012	28.2
	80:20	6.17×10^{-27}	3.80×10^{-53}	0.017	41.7
	70:30	6.09×10^{-27}	3.71×10^{-53}	0.026	65.3
	60:40	6.02×10^{-27}	3.62×10^{-53}	0.038	92.9
	50:50	5.93×10^{-27}	3.51×10^{-53}	0.051	124.5
	40:60	6.02×10^{-27}	3.61×10^{-53}	0.037	91.9
	30:70	6.08×10^{-27}	3.69×10^{-53}	0.029	71.6
	20:80	6.12×10^{-27}	3.74×10^{-53}	0.023	57.6
	10:90	6.15×10^{-27}	3.78×10^{-53}	0.019	47.4
Water—isopropanol	90:10	6.25×10^{-27}	3.91×10^{-53}	0.004	10.7
	80:20	6.21×10^{-27}	3.85×10^{-53}	0.011	27.0
	70:30	6.18×10^{-27}	3.82×10^{-53}	0.014	35.3
	60:40	6.11×10^{-27}	3.73×10^{-53}	0.026	63.2
	50:50	6.05×10^{-27}	3.66×10^{-53}	0.034	83.3
	40:60	6.08×10^{-27}	3.74×10^{-53}	0.029	71.7
	30:70	6.12×10^{-27}	3.80×10^{-53}	0.026	60.8
	20:80	6.17×10^{-27}	3.84×10^{-53}	0.016	41.7
	10:90	6.23×10^{-27}	3.89×10^{-53}	0.007	18.8

dominantly separate ions of hydronium H_3O^+ and associations with a reduced number of water molecules $(H_2O)_m$ (with a stronger basic character); here $m<n$.

Therefore, the degree of hydratation of the metallic ions in the mixture water—organic solvent is low, and the solubility of that solid compound is a little lower than in pure water.

As the amount of organic solvent in the mixture increases, the hydronium ions, H_3O^+, are gradually replaced by oxonium ions, ROH_2^+, providing a less intense basic medium than that of pure water. Consequently, the sol-

ubility of the given compound (in this medium) will be a little higher than in the previous case.

Received, F bruary 5, 1989

Polytechnic Institute, Jassy,
Department of Inorganic and Analytical Chemistry

REFERENCES

1. Grunwald E., Baughman G., Kohnstan G., J. Amer. Chem. Soc., **82**, 5801 (1960).
2. Popovich O., Anal Chem., **38**, 558 (1966).
3. Alexander R., Parker A. J., J. Amer. Chem. Soc., **89**, 5549 (1967).
4. Millero J., J. Phys. Chem., **75**, 280 (1971).
5. Kim J. I., J. Phys. Chem., **82**, 191 (1978).
6. Kim J. I., Cecal Al., Born H.J., Gomaa E. A., Z. phys. Chem., Neue Folge, **110**, 209 (1978).
7. Marcus Y., Naveh J. N., J. Phys. Chem., **73**, 591 (1969).
8. Popovich O., Crit. Rev. Anal. Chem., **1**, 73 (1970).
9. Strehlov H., Schneider H., Ber. Bunsenges. phys-Chem., **77**, 760 (1973).
10. Coetzee J. F.., Ritichie C. D., *Solute—Solvent Interactions.* Marcel Dekker, New York, 1976.
11. Cecal Al., Ţepeş I., Rev. Chim. (Bucureşti), **37**, 11 (1986).
12. Cecal Al., Ciuchi G. I., Rev. Roumaine de Chimie, **34**, 953 (1989).
13. Cecal Al., Isotopenpraxis, **20**, 9 (1984).
14. Cecal Al., Isotopenpraxis, **20**, 259 (1984).
15. Platz H., Schenk P. W., Angew. Chemie, **49**, 822 (1936).
16. Milligan O., J. Phys. Chem., **38**, 797 (1934).
17. Haussmann O., Ber. dtsch. Chem. Ges., **7**, 1 747 (1974).
18. Brauer G., *Handbook of Preparative Inorganic Chemistry.* Vol. **2**, Sec. Ed., Acad. Press, New York, 1965.
19. Kolthoff M., Chantooni Jr. M. K., Anal. Chem., **44**, 915 (1972).
20. *** *Handbook of Physics and Chemistry.* CRC Press, Chicago, 1974—1975.
21. Alfenaar M., De Ligni C. L., Rev. Trav. Chim., **86**, 929 (1967).
22. Oiwa I. T., Sci. Rep. Tohoku Univ., **42**, 129 (1967).
23. Paabo M., Bates R. G., Robinson R. A., J. Phys. Chem., **70**, 247 (1966).

UTILIZAREA DILUŢIEI IZOTOPICE INTERNE PENTRU DETERMINAREA SOLUBILITĂŢII UNOR SULFURI GREU SOLUBILE

(Rezumat)

Se prezintă o metodă pentru determinarea solubilităţii unor sulfuri greu solubile de zinc, cadmiu şi mercur, utilizînd diluţia izotopică internă. Solubilitatea acestor sulfuri a fost determinată în apă şi în diferite amestecuri de apă—solvent organic (metanol, etanol şi izopropanol), calculîndu-se apoi valorile coeficientului de activitate, produsului de solubilitate şi variaţiei energiei libere Gibbs, care caracterizează desfăşurarea procesului de dizolvare.

BULETINUL INSTITUTULUI POLITEHNIC DIN IAȘI
Tomul XXXV (XXXIX), Fasc. 3—4, 1989
Secția II
CHIMIE ȘI INGINERIE CHIMICĂ

D. C. 544.844 ; 615.45

APPLICATION OF LIQUID HIGH PRESSURE CHROMATOGRAPHY IN THE SEPARATION OF PHARMACEUTICAL PRODUCTS

BY

I. M. POPA, DOINA HRIȚCU and GH. IONESCU

1. Introduction

Separation of the active compounds of pharmaceutical preparations or of the basic products in pharmaceutical industry, as well as their direct dosage from blood, represent a special problem of chemical analysis.

Until recently, the separation and dosage techniques mainly used were : thin-layer chromatography [1] or gas chromatography [2]. The former is a simple and rapid technique, yet quite difficult to be applied to quantitative determinations ; the latter is a sensible and precise method, with the disadvantage that the products to be analyzed must be volatile and thermally stable (or, it is known that a lot of pharmaceutical compounds do not meet these requirements).

High pressure liquid chromatography (HPLC) eliminates the shortcomings of gas chromatography and, more than that, evidences the following advantages : determinations may be performed at room temperature, the compounds involved need not to be volatile, polarity of the mobile, as well as of the stationary phase, may be variable, quite simple sample preparation is possible [3].

HPLC has been successfully applied in the separation of some drugs, either in pharmaceutical industry, or directly from blood, after their administration.

2. Experimental

a) *Equipment.* A Varian 5 000 chromatograph has been used, supplied both with detectors with fix wave length (254 or 280 nm) and with a variable wave length detector. The columns used were of the Micropak type (250 × ×4.7 mm). As mobile phase there have been used—depending on the nature of the analyzed products — water/methanol mixtures, in various rations and different pH-values.

b) *Analysis of Cephalosporine C* : Mixtures — prepared synthetically — have been analyzed by dissolving the product in adequate solvents, as well as directly from the culture media. The mobile phase has been methanol / /buffer solution (0.05 M KH_2PO_4), 1 mL/min. flow, detection being performed in UV (254 nm), sensibility 0.32 AUFS.

c) *Analysis of the Phenylacetic Acid.* It was extracted from the culture media, according to the following technique : to 10 mL culture liquid, 2.5 g anhydrous natrium sulphate, 1 mL sulphuric acid 6 M and 10 mL chloroform are added. The mixture is stirred for 5 min. and, after phase separation, the organic phase is analyzed chromatographically. The mobile phase consisted of methanol/water (80/20 in volume), 1 mL/min. flow. Detection was performed in UV (210 nm), sensibility 0.5 AUFS.

d) *Analysis of Chloramphenicol.* After its oral administration (as tablets), blood samples have been taken at various time intervals. After separation of the serum, 0.2 mL of serum have been mixed with 0.2 mL methanol, in view of deproteinization. The mixture thus obtained was centrifuged (3,500 rpm), for 3 min. The supernatant liquid was analyzed by HPLC. The mobile phase consisted of methanol/water (pH = 2.5, by employing perchloric acid), 50/50 in volume, 0.6 mL/min. flow. Detection was made in UV (280 nm); the detector's sensibility 0.005 AUFS.

e) *Analysis of Adenosine.* Analysis of the blood samples taken was similar to that employed in the case of chloramphenicol. The mobile phase and its flow were, also, the same, while detection was performed at 254 nm; the column's temperature was of 50°C.

3. Results and Discussions

Cephalosporine *C* (I) and two of the main degradation products, having structures (II) and (III), respectively, have been separated from synthetic mixtures or directly from the culture medium employed in the preparation of this antibiotic. One can observe that separation of cephalosporine *C* from the degradation products may be performed, at retention times of 6.8 min. (for compound (I)), 2.3 min. (for compound (II)) and 3.8 min. (for compound (III)), respectively.

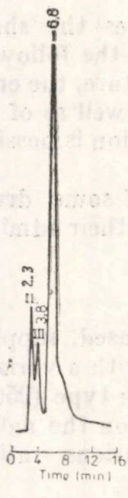

Fig. 1. — Chromatogramme of compounds (I), (II), (III), from the culture liquid.

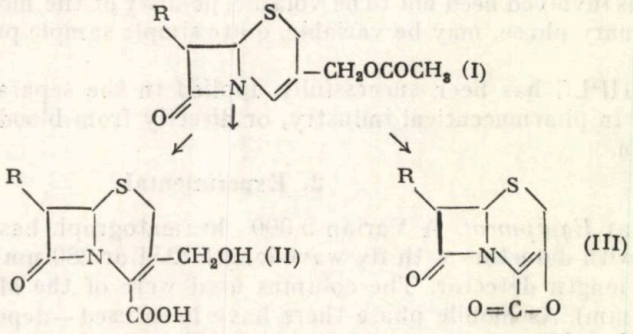

Analysis of the phenylacetic acid is possible after its extraction from the culture liquid (retention time 4.5 min., Fig. 2).

The calibration curve, surface vs. concentration-peak (Fig. 3), obtained for synthetic samples, permits the determination of the acid concentration in the samples taken from the culture mediu m.

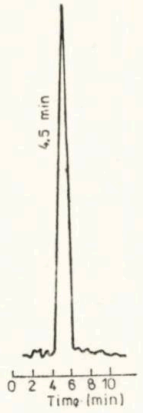

Fig. 2. — Phenylacetic acid chromatogramme.

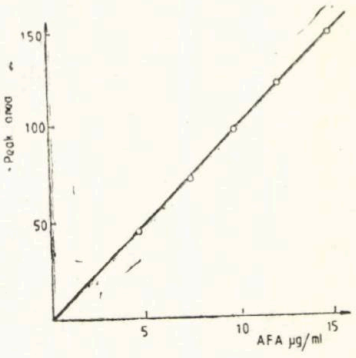

Fig. 3. — Response vs. concentration dependence.

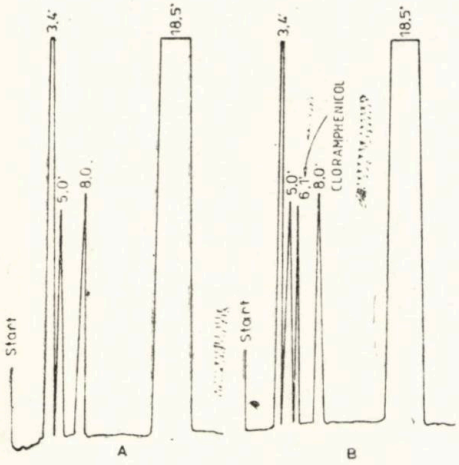

Fig. 4. — Chloramphenicol chromatogrammes from serum; *A* — before drug administration; *B* — after drug administration and sample taken at 2 h.

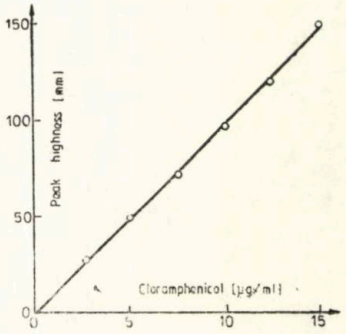

Fig. 5. — Serum chromatogramme:

Fig. 4 plots the chromatogrammes obtained from serum analysis, in the case of oral administration of 50 mg chloramphenicol/kg. All these chromatogrammes are observed as similar with reference to the distribution of compounds. Chloramphenicol's time of retention is of 6.1 min. In the samples analyzed, no metabolization products do appear. The largest part of metabolites, the diacetyl- and 3-glucoronic form [3] are more polar than the drug as such as under conditions of inverse phase separation; they are, probably, elutted more rapidly from the column, no interference with the sample occuring.

The response factors (height of the concentration-peak) lead to a linear dependence and are constant for a given concentration when repeating the analysis several times (Fig. 5).

As to the analysis of adenosine (when the variation of concentration has been followed in myocardium infarct), Fig. 6 evidences that both its identification and the quantitative estimation of the concentration variation in time, are possible. Mention must be made of the fact that, besides the basic product (having a retention time of 6.6 min.), another product appears, too, at a retention time of 5.1 min. It probably results from the proteic mass, after centrifugation. Such products appear also when analysing chloramphenicol samples from blood, they have a low molecular weight and are not removed in the deproteinization process.

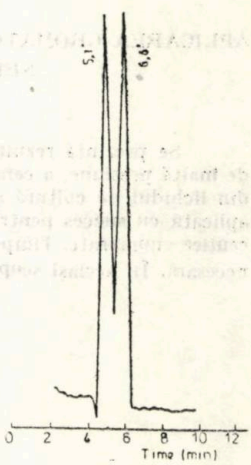

Fig. 6 — Adenosine chromatogramme.

4. Conclusions

Qualitative and quantitative dosing of cephalosporine *C* is possible at concentrations lower than 0.1 mg active substances; in parallel the main degradation products (II) and (III) accompanying the process are evidenced.

In the case of phenylacetic acid, quantitative dosage is possible through HPLC, after a preliminary extraction from the culture liquid.

Chloramphenicol may be dosed directly from blood, up to a concentration of 1 mg, if employing a detector with a sensibility of 0.001 AUFS. Extraction of chloramphenicol from technological samples, by employing organic solvents, may also increase the method's accuracy.

The variation of adenosine's concentration may be followed in time, in myocardium infarct, through HPLC.

Application of HPLC in the analysis of such products results in: a) optimization of the synthesis conditions; b) determination of drug's purity; c) establishment of therapeutic concentrations.

Received, February 15, 1989

Polytechnic Institute, Jassy, Department of Inorganic and Analytical Chemistry

REFERENCES

1. Johnoson E. L., Stevens R., (Ed.), *Basic Liquid Chromatography*, Varian Associates, New York, 1979.
2. Kalàsz H., (Ed.)., *New Approaches in Liquid Chromotography*. Proc. of 2-nd Annual American Eastern European Symp. on Advances in Liquid Chromatography, Hungary, 1982.
3. Popa M. I., *Cercetări în domeniul unor polimeri analogi ai poliozelor și altor compuși macromoleculari hidroxilați cu proprietăți terapeutice*. Ph. D. Thesis, Polyt. Inst., Jassy, 1986.

APLICAREA CROMATOGRAFIEI ÎN FAZĂ LICHIDĂ DE ÎNALTĂ PRESIUNE LA SEPARAREA PRODUSELOR FARMACEUTICE

(Rezumat)

Se prezintă rezultatele obținute la studiul separării prin cromatografie în fază lichidă de înaltă presiune, a cefalosporinei *C*, de principalii produși de degradare, a acidului fenilacetic din lichidul de cultură și a cloramfenicolului și adenozinei direct din sînge. Metoda poate fi aplicată cu succes pentru dozarea cantitativă, după separare prealabilă, a produselor farmaceutice enumerate. Timpul scurt de separare și dozare conferă metodei aplicabilitatea practică necesară. În același scop pledează și sensibilitatea metodei HPLC.

BULETINUL INSTITUTULUI POLITEHNIC DIN IAŞI
Tomul XXXV (XXXIX), Fasc. 3—4, 1989
Secţia II
CHIMIE ŞI INGINERIE CHIMICĂ

D. C. 669.268 ; 621.357.1 ; 621.3.061.1

SOME POSSIBILITIES OF REDUCING THE MATERIAL AND POWER CONSUMPTIONS IN THE PROCESS OF CHROME ELECTRODEPOSITION

BY

ŞT. IVĂŞCAN, FLORIN BANDRABUR and MARIA APOSTOLESCU

1. Introduction

The electrochemical plating of the steel surfaces with chrome layers is widely utilised in the industry due to the fact that it grants to the support a remarcably decorative aspect and a high mechanical wearing resistance.

At the same time, the chrome plating is a difficult and complex process characterised by low current yield (8.14%) and a poor dispersion of the electrolyte requiring high power consumptions.

In the main, the electrochemical process of the chrome deposition on a metallic support consists in reducing the hexavalent chrome ions (resulted from CrO_3 dissolution) to the metallic chrome. Simultaneously, at the two electrodes hydrogen and oxygen, respectively, are released.

The overall reaction taking place at the electrode surface can be written as :

(1) $$H_2CrO_4 + H_2O \rightarrow Cr + 2H_2 + \frac{5}{2}O_2.$$

At the anode the possible processes can be described by the equations :

(2) $$Cr - 3e^- \rightarrow Cr^{3+},$$

(3) $$Cr^{3+} + 16OH^- \rightarrow H_2CrO_4 + 7H_2O + \frac{5}{2}O_2 + 13e^-.$$

The chrome ions occur in the solution as a consequence of the reactions at the cathode :

(4) $$H_2CrO_4 + 6H^+ + 6e^- \rightarrow Cr + 4H_2O,$$

(5) $$H_2CrO_4 + 6H^+ + 3e^- \rightarrow Cr^{3+} + H_2O,$$

(6) $$4H^+ + 4e^- \rightarrow 2H_2.$$

The simultaneous development of the chrome electrodeposition (4) and of the side reactions involves additional power consumption. The purpose of the present paper is to find new potential ways of diminishing the material and power consumptions based on some investigations reported partly in the present paper.

2. Analysis of the Possibilities of Reducing the Specific Consumptions of Materials and Power During the Chromeplating Process

To find potential ways of reducing the specific consumptions in the chrome plating equipment, the main process in the flow sheet — the chrome electroplating — has been investigated.

The calculations have been accomplished for a chrome plating bath with the following characteristics : a) the pan size, $1.96 \times 1 \times 1.15$ m ; b) the electrolyte volume, 1 000 l ; the working temperature, 55°C ; d) the number of lead anodes, $h_A = 20$ (the anode dimensions $0.9 \times 0.1 \times 0.01$ m) ; e) the number of steel cathodes, $n_c = 20$, (the cathode size $0.25 \times 0.1 \times 0.01$ m).

The electroplating pan is built in steel with a wall thickness of 4 mm covered inside with a lead layer. It is provided with a heating jacket with steam (6 ata). The working parameters of the cell are as follows: a) the electrolyte composition, $C^0_{CrO_3} = 250$ g/l, $C^0_{CrO_3}/C^0_{H_2SO_4} = 100/1$; b) the cathodic current density, $i_c = 30...50$ A/dm² ; c) the thickness of chrome layer, $\delta_{Cr} = 20...60$ μm ; d) the actual terminal voltage, 6... 8 V.

The current efficiency, experimentally determined, has values between 12...14%.

To calculate the specific consumption the following balance equations have been used [3]...[4] :

a) The specific consumption of chromic anhydride :

$$C_{CrO_3} = \frac{M_{CrO_3}}{Z.F.} i_c r_c + \frac{m_{CrO_3(losses)}}{S_C}, \quad [kg/dm^2]. \tag{7}$$

b) The steam flowrate for pan heating to the working temperature :

$$V_{steam\ heating} = V_{S\ steam} \frac{Q_{steam} - Q_{caw}}{\Delta i}, \quad [m^3/h]. \tag{8}$$

c) The steam flowrate for maintaining the pan at the working temperature :

$$V_{steam\ losses} = V_{s\ steam} \frac{Q_{pe} - Q_{rc}}{\Delta i}, \quad [m^3/h]. \tag{9}$$

d) The power specific consumption :

$$W_s = i_c U^r_B \tau_t, \qquad [Kwh/dm^2]. \tag{10}$$

e) The calculus equation of the actual terminal voltage :

$$U^r_B = (e^e_A - e^e_K) + \rho_A \frac{e_A}{n_A S_A} + \rho_k \frac{e_k}{n_k S_k} I + \rho_{el} \cdot lI + 0.6(e^e_A - e^e_k). \tag{11}$$

The material balance calculations allowed the settlement of the specific consumptions of chrome anhydride (Table 1) and water as well as the volumes of the gas released (Table 2).

Table 1

Specific Consumptions of Chromic Anhydride

Nr. crt.	Thichness of the chrome layer, δ μm	Calculated specific consumption of CrO_3, [Kg/m²]	Overall consumption of CrO_3 Kg/m²	
1	20	0.2657	0.2907	Anhydride losses in taking out the samples 0.025 Kg/m²
	30	0.3985	0.4235	
2	40	0.5314	0.5564	
	50	0.6643	0.6893	
3	60	0.7971	0.8221	

Table 2

Technological Calculations

Working conditions	Consumed water, [Kg/m²]		Volume of gas released m³/m²	
	Technological	Evaporated	O_2	H_2
r_c=0.13 U_B^r=7 V δ=30 μm i_c=30 A/dm²	74.50	172.33	0.2315	0.9817

The calculated thermal balance allows the settlement of heat losses during the chrome plating as follows :

a) 1% of the heat is lost with the chrome plated pieces, heated at the working temperature ;

b) 15% are lost due to the water evaporation ;

c) 84% are lost by convection and radiation.

By analysing the calculated balance voltage the following conclusions can be drawn :

a) the equilibrium voltage is 2.1 V ;

b) the voltage calculated at the reactor terminals is 5.678 V ;

c) 22% of the voltage value at the terminals represents the voltage drops through contacts, circuits and rheostat ;

d) 18% of the voltage represents the anodic overvoltage ;

e) 13% of the voltage represents the cathodic overvoltage.

In fact, in the chrome plating equipment the working voltage at terminals is comprised between 6 and 8 V. The increase of voltage at the terminals results in an increase of power consumption (Fig. 1).

In Table 3 the specific power consumptions calculated for various thickness of the depositec chrome layer are listed.

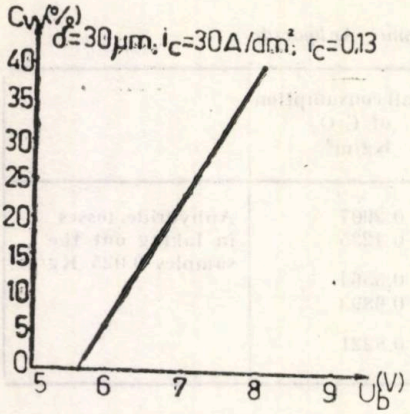

Fig. 1. — Correlation between the specific power consumption (C_w,[%]) and working voltage (U_v,[V]).

Table 3

Power Specific Consumption (r_c=0.13; i_c=30 A/dm²)

Thinkness of chrome layer, δ, [μm]	Voltage at the terminals	
	U_B^r=5.678 V	U_B^r=7 V
20	19.4	23.9
30	29.1	35.9
40	38.8	47.8
50	48.5	59.8
60	58.2	71.8

3. Conclusions

Based on the effectuated analysis, the following ways for obtaining reduced material and power consumptions in chrome electroplating can be considered:

1. The regeneration, to extend the heating duration of the electrolyte for chrome plating. In this connection the elimination from the solution of the Fe^{3+} ions, which conditions the duration of pan heating or the recovery of chromic anhydride from the electrolyte is imposed. This way substantial reductions of the CrO_3 and sulphuric acid consumptions can be obtained.

2. The scientific management of the processes in the whole flowsheet (mechanical working degasing, pickling, duying of pieces, etc.) to remove the inadequate chrome plated pieces, leading to significant reductions of the technological consumptions.

3° The periodical cleaning of the lead anode, by removing the passive layers; an additional resistance is this removed which contributes to the power consumption lowering.

4° By working continuously in the electroplating equipment significant amounts of steam required for pan heating to the working temperature can be saved.

Notations

A_{Cr} — atomic mass of chrome;
τ — time, [s];
$V_{S\ steam}$ — the specific steam volume;
e^e_A, e^e_K — the equilibrium potentials for anode and cathode, respectively, [V];
ρ_A, ρ_K — the anode, respectively the cathode resistivity, [Ωm];
ρ_{el} — the electrolyte resistivity, [Ω m];

$Q_{pevaporation}$ — heat losses with the evaporated losses, [KJ/h] ;
Q_{r_c} — heat losses by radiation and convection, [KJ/h] ;
i — liquid entropy, [KJ/Kg].
Z — number of electrons ;
F — Faraday's number, [C],
Q_{caw} — heat evacuated with the condens, [KJ/Kg].

Received, March 15, 1988

Politechnic Institute, Jassy,
Department of
Inorganic Chemical Technology

REFERENCES

1. Firoiu C., *Tehnologia proceselor electrochimice.* EDP, Bucureşti, 1983.
2. Ivăşcan Şt. et al., Bul. Inst. polit., Iaşi, **XX(XXIV)**, *1—2* (1974).
3. *** Research contract, Polyt. Inst., Jassy, *4350* (1986).
4. Pavlov K. F. et al., *Exerciţii şi probleme de procese şi aparate în industria chimică,* (transl. from Russian). Ed. Tehn., Bucureşti, 1972.

UNELE POSIBILITĂŢI DE REDUCERE A CONSUMURILOR SPECIFICE DE MATERIALE ŞI DE ENERGIE ÎN PROCESUL DE CROMARE ELECTROLITICĂ

(Rezumat)

S-a urmărit stabilirea unor căi posibile de micşorare a consumurilor specifice de materii prime şi de energie în procesul de cromare electrolitică. În acest scop s-a efectuat analiza funcţionării unei celule industriale prin intermediul ecuaţiilor de bilanţ de materiale, de energie termică şi de tensiuni.

Prin compararea consumurilor calculate cu cele reale se evidenţiază unele căi de reducere a acestora, în special a consumului specific de energie electrică.

BULETINUL INSTITUTULUI POLITEHNIC DIN IAȘI
Tomul XXXV (XXXIX), Fasc. 3—4, 1989
Secția II
CHIMIE ȘI INGINERIE CHIMICĂ

D. C. 631.85

NEW SORTS OF PHOSPHOGYPSUM FERTILIZERS

BY

CAROLINA HAGIU and MARIANA MICU

1. Introduction

The manufacture of phosphoric acid by means of dihydrate procedure has, as a main disadvantage, the obtaining of significant phosphogypsum amount, a waste including in $CaSO_4 \cdot 2H_2O$ the whole sulphur amount, as sulphuric acid, used as a raw material. In addition, the sulphur deposition in dumps determines the pollution of the underground waters and takes significant surfaces out of the agricultural circuit. This situation determined the intensification of the researches aimed to find the most efficient procedures for turning to good account the phosphogypsum.

The results obtained so far indicated the possibility of using the phosphogypsum in three significant fields as follows :

a) In the chemical industry, for the obtaining of sulphuric acid or of other sulphur containing compounds [1] ,..., [14], of a pigment for the paper industry [12], [13].

b) In the industry of the construction materials, for obtaining the cements, as a material for building panels, as binding matter, and as an additive to the Portland cement [14], ..., [20].

c) In the agriculture as an amendament for the saline soils and for obtaining the fertilizers [21], ..., [23].

Though the thermal working of phosphogypsum with the obtaining of gypsum and sulphuric acid, wich is recycled in the process, represents a solution of the problem of phosphogypsum waste, it remains, however, a power consuming process.

Since the use of the phosphogypsum in the agriculture is very limited, the requirement occur to intensify the researches in this field.

The phosphogypsum contains calcium and sulphur, significant nutrient elements for plant development as well as important amounts of microelements coming from the phosphatic rock.

By enriching the phosphogypsum with essential macroelements (nitrogen, phosphorus, kalium) various sorts of fertilizers can be obtained.

In the present paper the results in studying the obtaining of some N—P fertilizer sorts from the unwashed phosphogypsum, with variable content of free phosphoric acid, by working it with phosphorite, are reported.

2. Results and Discussion

2.1. Technological Flowsheet. Calculus Equations for the Requirement of Raw Materials

In working out the phosphogypsum, with the aim to obtain some fertilizers, the following method is used : the mixing of washed phosphogypsum with phosphoric acid to obtain some suspensions with various contents of free phosphoric acid followed by the treatment of these suspensions with cal-

culated amounts of phosphorite in view to promote the formation of dicalcium phosphate and the product to contain free phosphoric acid in order to avoid the phosphorus backwardness. The flowsheet of the technological process is depicted in Fig. 1.

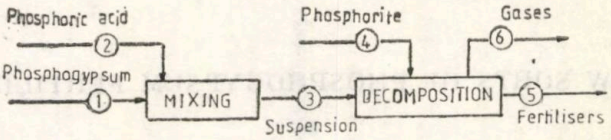

Fig. 1. — Sketch of the technological sheet.

The mixing process is accomplished in such a manner which permit to obtain suspensions of phosphogypsum with the desired content of phosphoric acid. Based on the mass balance, the equations

$$(1) \qquad m_2 = \frac{m_3(\bar{x}^{(3)}_{H_3PO_4} - \bar{x}^{(1)}_{H_3PO_4})}{\bar{x}^{(2)}_{H_3PO_4} - \bar{x}^{(1)}_{H_3PO_4}} \quad \text{and} \quad m_1 = m_3 - m_2$$

are derived for calculus of the requirement of phosphoric acid and phosphogypsum of known composition, to obtain determined amounts of suspensions (m_3) with a prescribed content of phosphoric acid

In the decomposition of phosphatic rock with suspension of phosphogypsum the processes of independent conversion are:

$$(2) \qquad Ca_{10}(PO_4)_6F_2 + 14H_3PO_4 = 10Ca(H_2PO_4)_2 + 2HF,$$

$$(3) \qquad CaCO_3 + 2H_3PO_4 = Ca(H_2PO_4)_2 + CO_2 + H_2O,$$

$$(4) \qquad CO_{2[]_l} \rightleftarrows CO_{2[]_g}, \qquad (5) \qquad HF_{[]_l} \rightleftarrows HF_{[]_g}.$$

Based on the processes (3)...(5) and using the general method [24] the equations of mass balance listed in Table 1 are settled.

By using the equations of mass balance given in Table 1, the equation:

$$(6) \qquad m_4 = \frac{m_3(\bar{x}^{(3)}_{H_3PO_4} - \bar{x}^{(5)}_{H_3PO_4})}{\bar{x}^{(5)}_{H_3PO_4}(2.273\,\bar{x}^{(4)}_{P_2O_5} + 1.273\bar{x}^{(4)}_{CO_2} + \bar{x}^{(4)}_{A''}) + (3.22\bar{x}^{(4)}_{P_2O_5} + 4.454\bar{x}^{(4)}_{CO_2})},$$

is settled, for calculating the phosphorite requirement.

2.2. Obtaining of Various Fertilizer Sorts and their Analysis

The raw materials used have the chemical composition given in Table 2.

Using a reactor with mechanical stirring five fertilizer sorts have been prepared, the variation vs. time of the content of free phosphoric acid, of the P_2O_5 soluble in water and citrate, the moisture content, as well as the overall P_2O_5 content, for the sample taken at 33 min. being determined. The analysis procedures have been the standard ones [25].

Table 1

Equations of Mass Balance

Phase	Component	Equations of mass balance
Suspensions (5)	$Ca(H_2PO_4)_2$	$m^{(5)}_{Ca(H_2PO_4)_2} = m_4(5.493\bar{x}^{(4)}_{P_2O_5} + 5.318\bar{x}^{(4)}_{CO_2})$
	H_3PO_4	$m^{(5)}_{H_3PO_4} = m_3\bar{x}^{(3)}_{H_3PO_4} - m_4(3.22\bar{x}^{(4)}_{P_2O_5} + 4.454\bar{x}^{(4)}_{CO_2})$
	H_2O	$m_{H_2O} = m_3\bar{x}^{(3)}_{H_2O} + 0.409m_4\bar{x}^{(4)}_{CO_2}$
	$CaSO_4 \cdot 2H_2O$	$m_{CaSO_4 \cdot 2H_2O} = m_3\bar{x}^{(3)}_{CaSO_4 \cdot 2H_2O} = m_1\bar{x}^{(1)}_{CaSO_4 \cdot 2H_2O}$
	Inert	$m^{(5)}_{A''} = m_3\bar{x}^{(3)}_{A''} + m_4\bar{x}^{(4)}_{A''}$
	Total suspension (5)	$m_5 = m_3 + m_4(2.273\bar{x}^{(4)}_{P_2O_5} + 1.273\bar{x}^{(4)}_{CO_2} + \bar{x}^{(4)}_{A''})$
Gas (6)	CO_2	$m^{(6)}_{CO_2} = m_4\bar{x}^{(4)}_{CO_2}$
	HF	$m^{(6)}_{HF} = 0.0939m_4\bar{x}^{(4)}_{P_2O_5}$
	Total gas (6)	$m_6 = m_4(0.0939\bar{x}^{(4)}_{P_2O_5} + \bar{x}^{(4)}_{CO_2})$
Total amount		$m_5 + m_6 = m_3 + m_4$

Table 2

Composition of the Raw Materials (% by weight)

Component \ Raw material	Unwashed phospho-gypsum	Technical phosphoric acid	Israel phosphorite
H_3PO_4	13.55	39.27	—
$CaSO_4 \cdot 2H_2O$	62.00	—	—
H_2O	22.1	52.48	—
Inert	2.35	8.25	7.2
P_2O_5	—	—	32.98
CaO	—	—	50.93
F	—	—	2.94
CO_2	—	—	5.95

Table 3

Need of Raw Materials

Sorts	$\bar{x}_{H_3PO_4}$	Phosphogypsum, m_1, [Kg]	Phosphoric acid, m_2, [Kg]	Phosphorite, m_4, [Kg]	m_1 / m_2
I	0.1355	1.0	0.0	0.0779	—
II	0.15	0.9436	0.0564	0.0885	1 : 16.7
III	0.17	0.8659	0.1341	0.1034	1 : 6.45
IV	0.20	0.7492	0.2508	0.1256	1 : 2.98
V	0.23	0.6326	0.3674	0.1477	1 : 1.72

Table 4

Experimental Results. The Composition of Fertilisers (% by weight)

Sort	Time, [min.] / Component	6	12	18	24	28	33
I	Free H_3PO_4	4.49	4.07	3.52	2.75	2.22	1.98
	P_2O_5 soluble in water and citrate solution	8.93	10.05	10.75	11.04	11.42	11.52
	Overall P_2O_5	—	—	—	—	—	11.64
	Moisture	20.02	20.45	20.87	21.06	21.60	21.83
II	Free H_3PO_4	6.38	4.82	4.35	3.80	2.85	2.40
	P_2O_5 soluble in water and citrate solution	9.85	11.32	11.85	12.35	12.45	12.72
	Overall P_2O_5	—	—	—	—	—	12.92
	Moisture	21.13	21.32	21.72	22.04	22.21	22.26
III	Free H_3PO_4	8.42	6.40	5.65	4.58	4.22	3.71
	P_2O_5 soluble in water and citrate solution	11.05	12.92	13.86	14.13	14.31	14.32
	Overall P_2O_5	—	—	—	—	—	14.63
	Moisture	23.32	23.80	24.25	24.31	24.37	24.52
IV	Free H_3PO_4	10.25	7.62	6.75	5.63	5.02	4.01
	P_2O_5 soluble in water and citrate solution	12.85	15.20	15.78	16.25	16.50	16.62
	Overall P_2O_5	—	—	—	—	—	16.84
	Moisture	25.26	25.80	26.04	26.85	27.03	27.42
V	Free H_3PO_4	12.04	8.84	7.64	6.52	5.82	5.30
	P_2O_5 soluble in water and citrate solution	15.50	17.62	18.21	18.45	18.62	18.92
	Overall P_2O_5	—	—	—	—	—	19.31
	Moisture	27.42	28.17	29.46	29.82	29.91	30.15

The need of raw materials calculated with Eqs. (1) and (6), taking $m_3 = 1$ kg for a content of phosphoric acid in suspension (3) of 13...23% and a free acidity of the obtained products of 3%, is listed in Table 3. The obtained experimental results are given in Table 4.

By plotting the variation vs. time of the content P_2O_5 soluble in water and citrate (Fig. 2) a fast solubilization of P_2O_5 in phosphorite is observed. After a residence time of 20...30 min. the increase of the content of the P_2O_5 soluble in water and citrate is unsignificant. After 33 min. almost the whole amount of P_2O_5 has been solubilized, the content of insoluble P_2O_5 being very low in the last samples (0.12... 0.39%).

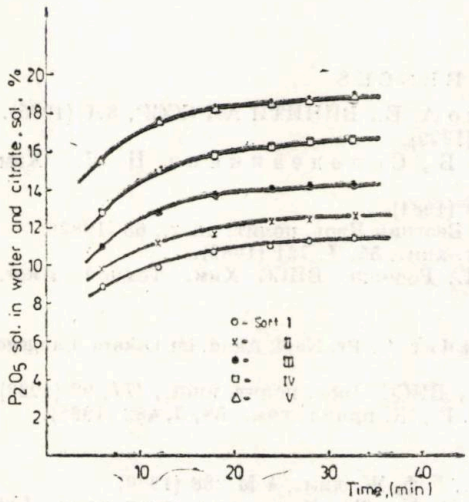

Fig. 2. — Variation vs. time of the P_2O_5 soluble in water and citrate solution.

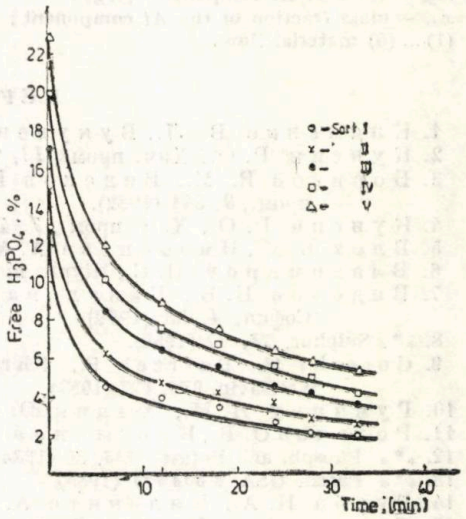

Fig. 3. — Variation vs. time of the content of free phosphoric acid.

The rate of consumption of the free phosphoric acid is higher at the process beginning (Fig. 3), and decrease then after 20...30 min. The content of free phosphoric acid in the final samples varied between 1.98 and 5.30%.

3. Conclusions

A method for using the unwashed phosphogypsum, with a certain content of phosphoric acid, to obtain some fertilizers of superphosphate type, is advanced. By treating the unwashed phosphogypsum with phosphorite the conversion of insoluble P_2O_5 into monocalcic phosphate is accomplished.

By analysing the obtained results it can be noticed that the process duration is of about 30 min. later on, the increase of the content of P_2O_5 soluble in water and citrate being unsignificant.

The sorts of fertilizers obtained by this procedure have a relatively low content of active substances (11.64...19.31% P_2O_5), comparable to that of superphosphate ; they contain also insoluble P_2O_5 (0.12...0.39%) and free phosphoric acid for avoiding the phosphorus backwardness.

It may be appreciated that the valorification of phosphogypsum in this way is efficient only when utilising suspensions with 13...17% H_3PO_4, above this value the mixing ratio, m_1/m_2, in unsuitable large amounts of insoluble P_2O_5 (0.12...0.39%) being required.

Received, November 19, 1987

Polytechnic Institute, Jassy,
Department of Inorganic
Chemical Technology

Notations

m — mass, [Kg];
m_{Ai} — mass of *Ai* component, [Kg];
$\bar{x}_{Ai}$ — mass fraction of the *Ai* component;
(1) ... (6) material flows.

REFERENCES

1. Клименко В. Л., Вукуленко А. Е., ВИНИТИ АН СССР, 870 (1975).
2. Кунсик Р. О., Хим. пром., *12*, 9 (1979).
3. Борисов В. М.. Виденов Н. Б., Солодеанкина Н. Л., Хим. пром., *9*, 541 (1982).
4. Кунсик Р. О., Хим. пром., *7*, 409 (1981).
5. Влох В. М., Низовцева А. А., Вестник Львов. полит. инст., 63 (1982).
6. Владимиров П. С., Журн. прик. хим., **55**, *4*, 721 (1982).
7. Виденов Н. Б., Бакалова И., Годищн. ВИСС Хим. Технол. Инст., София, *4*, 38 (1979).
8. *** Sulphur, **74**, 27 (1968).
9. Gorecki H., Patrzek F., Shroeder J., Pr. Nauk Akad. im Oskara Langego, Wroclavin, *200*, 127 (1982).
10. Гумицку Я. М., Халик Ю. А., ВИСС Львов. полит. инст., *171*, 92 (1983).
11. РогачевО. В., Костылков И. Г., Ж. прикл. хим., **58**, *3*, 482 (1985).
12. *** Phosph. and Potass., *133*, 36 (1984).
13. *** Patent USA, *4 334 925* (1983).
14. Гурба Н. А., Калекитс А. К., Реф, Ж. хим., 4 М 288 (1980)
15. Тимашев В. И., Колбашов В. М., Тр, Моск. хим. техн. инст., *109*, 60 (1979).
16. Andrieux P., Tehn. Equip., *2*, 333 (1978).
17. Меревкова Т. М., Хим. пром. за рубежом, *3*, 14 (1980).
18. Сулейманов А. Т., Тумашев В. В., Сб. труды ВНИИ строит. матер. и констр., **17**, 188 (1981).
19. Сулейманов А. Т., Ванлериа Н. Г., Сб. труды ВНИИ строит. матер. и констр., **17**, 122 (1981).
20. Туганков А. П., Арачев Б. В., Кержаков Б. И., Хим. пром., *3*, 158 (1981).
21. Ruediger L., Patent West-Germany, *1 121 633* (1960).
22. Калмиков С. И., Шевченко А. П., Тр. Инст. Химий АН Каз. ССР, 50, 41 (1979).
23. Uher S., Uwrova M., Patent Czechoslovakia, *108 558* (1963).
24. Calistru C., Leonte C., *Tehnologia substanţelor anorganice*. EDP, Bucureşti, 1972.
25. *** STAS 8 379/1, 1974; 8 379/3, 1969; 8 379/4, 1969.

NOI SORTIMENTE DE ÎNGRĂŞĂMINTE DIN FOSFOGHIPS

(Rezumat)

Fosfoghipsul nespălat — produs secundar în industria acidului fosforic — este utilizat pentru obţinerea de noi sortimente de îngrăşăminte de tip superfosfat prin tratarea lui cu fosforită. Îngrăşămintele obţinute prin acest procedeu au un conţinut relativ mic de substanţă activă (11,6...19,3 % P_2O_5 total), comparativ cu superfosfatul simplu. Prezenţa acidului fosforic liber în produsele finale, în proporţie de 2...3 %, împiedică retrogradarea fosforului.

BULETINUL INSTITUTULUI POLITEHNIC DIN IAŞI
Tomul XXXV (XXXIX), Fasc. 3—4, 1989
Secţia II
CHIMIE ŞI INGINERIE CHIMICĂ

D. C. 661.832.532 ; 532.7

INVESTIGATIONS ABOUT THE KINETICS OF THE OBTAINING PROCESS OF POTASSIUM SULPHATE BY DOUBLE EXCHANGE FROM KCl AND $(NH_4)_2SO_4$

BY

STELIAN PETRESCU and C. CALISTRU

1. Introduction

The obtaining process of potassium sulphate from potassium chloride and ammonium sulphate has a significant importance for the national economy because of the large amounts of ammonium sulphate solution resulted in caprolactam synthesis process. As follows, there was conceived a new technology of potassium sulphate obtaining which has, as fundamental process, the crystallization of potassium sulphate based on double exchange reaction between KCl and $(NH_4)_2SO_4$ [1].

The investigation of the crystallization process of potassium sulphate [1] at equilibrium pointed out its maximum possibilities, showing respectively the conditions when there are obtained maxima transformation degrees for potassium ion and minima transformation degrees for ammonium ion.

The real values for $\eta_{(K^+)_2}$, $\eta_{(NH^+)_2}$ and respectively the phase transformation degree of potassium chloride can be established only by experimental way.

The experimental investigation concerning the kinetics of the obtaining proces of ammonium sulphate was provided only with the purpose to establish the conditions able to ensure high values for the transformation degree of potassium ion and for the phase transformation degree of potassium chloride.

The investigation of the kinetics of the potassium sulphate crystallization process did not aimed at the mathematical modelling of the real course of the process.

2. Macrokinetic Mechanism

The crystallization process of potassium sulphate is part of the unitary process dissolving—reaction—forming and growing of crystalls.

The reactant phases, in this process, are the ammonium sulphate solution and the solid potassium chloride. The reactant liquid phase is a resiauary solution outcoming from caprolactam synthesis which contains 30... 33% $(NH_4)_2SO_4$, and 2...5% solved organic substances. The reactant solid phase, potassium chloride, is composed of 94... 97% KCl, the rest being impurities, most of them soluble.

The crystallization process of potassium sulphate may be expressed by the following characteristic equation:

$$(1)\qquad [(NH_4)_2SO_4+H_2O+A_1'']_L+[KCl+A_2'']_s\rightarrow[K_2SO_4+(NH_4)_2SO_4]_s+ +[(NH_4)_2SO_4+KCl+NH_4Cl+H_2O+A_1''+A_2'']_l.$$

The elementary processes insolved may be written in the following form:

$$(2)\qquad KCl_{\square}\rightarrow KCl_{[]_l},\qquad (3)\qquad 2KCl+(NH_4)_2SO_4\rightleftarrows K_2SO_4+2NH_4Cl,$$

$$(4)\qquad K_2SO_{4[]_l}\rightarrow K_2SO_{4[]_s},\qquad (5)\qquad (NH_4)_2SO_{4[]_l}\rightarrow(NH_4)_2SO_{4[]_s}.$$

The obtaining process of potassium sulphate has the macrokinetic mechanism represented in Fig. 1.

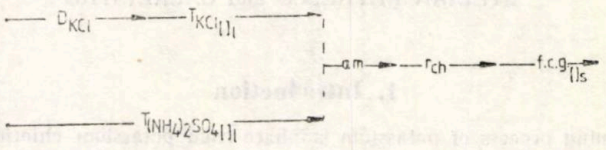

Fig. 1. — The structure of crystallization process of potassium sulphate.

Generally, this process is endothermic; the thermic processes structure is shown in Fig. 2.

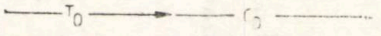

Fig. 2. — The structure of thermic processes.

The initial reaction mass is a two-phase, and, at one time, a three-phase system, made of potassium chloride unchanged grains and of new phase grains $[K_2SO_4+(NH_4)_2SO_4]_s$ dispersed in liquid phase.

3. Experimental Technique

For experimental investigations of the obtaining process kinetics of potassium sulphate there was used a laboratory installation. It consists of a laboratory thermostat, a stirring flask with an anchor type stirrer, made of rustless steel.

The reactor used in experiments has the following technical characteristics: interior diameter, $D_i=110$ mm, total height, $H_T=240$ mm, stirrer diameter, $c=90$ mm, distance from the flask bottom to the stirrer, $z=10$ mm.

On the lid of the reactor is fixed a hydraulic closing and there are five inlets, namely; for the control thermometer, for introducing materials, for connecting the reactor to a refrigerant, the other two being used for collecting samples out of the reaction mass.

The collecting device of the samples is based of an original conception [2] and allows, fast taking over from the suspension, filtering in the same time the sample inside the reactor. The time of taking-over is approximatively 5... 10 sec.

The stirrer of the reactor is acted by an electromotor fixed on a support, with a classical transmission device consisting of a whed coming in contact with a rubber cylinder fixed on the electromotor arbor, two belt wheels and a driving belt. This device has nine different speeds.

Experimentally there was used potassium chloride, p.a., with the granulation d_p=0.0755 mm; 0.255 mm; 0.375 mm. The ammonium sulphate solution, of concentration $\bar{X}^0_{(NH_4)_2SO_4}$=0.30, was prepared from ammonium sulphate p.a. and distilled water. For experimental determinations there was used ammonium sulphate solution of concentration $\bar{X}^0_{(NH_4)_2SO_4}$ =0.30, because the residuary solution in caprolactama synthesis has a concentration close to 0.30.

There were used two values of molar ratio $\dot{X}^0_{(K+)_2}$, respectively 0.4771 and 0.4088. Also, there were varied the temperature (T=25° ; 35° ; 45° ; 60°C) and the speed of the stirrer (n=160 ; 205 ; 295 r.p.m.).

To obtain the kinetics curves $\eta_{(K+)_2}$ vs. τ and $\eta_{KCl_{[]_s}}$ vs. τ it is necessary to knowledge the evolution of the two degrees of transformation in time. According to mathematical pattern of the balance of materials in the crystallization process of potassium sulphate, to determine the values of the transformation degrees $\eta_{(K+)_2}$ and $\eta_{KCl_{[]_s}}$ it is necessary to collect samples at different periods of time and to analyse them in order to find out the concentration of chlorine, ammonium and potassium ions ($\bar{X}_{(Cl^-)_2}$, $\bar{X}_{(NH_4^+)_2}$, $\bar{X}_{(K+)_2}$).

The collecting of the samples was made according to the following program: τ = 5 ; 10 ; 20 ; 40 ; 60 ; 90 ; 120 min. In order to obtain the necessary data for drawing a kinetic curve there was used the following procedure: the thermostat was started and fixed on the prescribed temperature value; in the reactor was introduced a precise amount of ammonium sulphate solution; the stirrer started, the refrigerant has been connected; when the solution atteined the prescribed temperature, the potassium chloride, in a determined amount, was added and there was switched on the chronometer.

According to the program established before there were collected samples of liquid phase from the reactor in order to determinate the concentrations, $\bar{X}_{(Cl^-)_2}$, $\bar{X}_{(NH_4^+)_2}$, $\bar{X}_{(K^+)_2}$.

In regard of analysis methods, for the chlorine ion was used Mohr method [3], for ammonium ion the method with formic aldehyde [4] and the flame-photometric method for potassium ion.

4. Obtained Results and their Interpretation

The obtained experimental data as regards concentrations values of potassium, chlorine and ammonium ions were worked out under the form of kinetic curves $\eta_{(K+)_2}$ vs. τ and $\eta_{KCl_{[]_s}}$ vs. τ. In Figs. 3...10 these curves are graphically represented.

According to Fig. 3, the transformation degree of potassium ion, $\eta_{(K^+)_2}$, decreases with the rise of temperature at any period of time.

In small periods of time, at the beginning of the process, the rise is more significant and over 30 min. it becomes smaller and the $\eta_{(K^+)_2}$ vs. τ dependence is practically linear.

For any value of time period from the beginning of the process, the bigger is the separation degree of potassium, $\eta_{(K^+)_2}$, the lower temperature is. So, decreasing temperature from 60°C to 25°C, $\eta_{(K^+)_2}$ increases with approx. 10%.

From Fig. 4 it may be seen that, the transformation degree of potassium ion increases when the grains of potassium chloride become smaller, its growth being substantial. At $\tau=120$ min., when potassium chloride grains with $d_p=0.375$ mm are used instead of grains with $d_p=0.255$ mm, $\eta_{(K^+)_2}$ decrease from 0.57 to 0.33.

The speed of the stirrer has a negative influence upon crystallization process of potassium sulphate. That fact occurs from Fig. 5.

The maxima values for the transformation degree of potassium ion are obtained in case of small speeds of the stirrer.

For values of the stirrer speed from 160 to 295 r.p.m., the differences between the values of the separation degree of potassium ion are small.

In regard to molar ratio of the reactants ($\dot{X}^0_{(K^+)_2}$), the decrease or the increase of its value leads, as shown, by equilibrium data, to the decrease or the increase of the separation degrees of potassium, $\eta_{(K^+)_2}$. In the present case (Fig. 6), for the value $\dot{X}^0_{(K^+)_2}=0.4088$, close to that which ensures the maximum separation degree of potassium ion (respectively $\dot{X}^0_{(K^+)_2}=0.4771$), was obtained a smaller value for $\eta_{(K^+)_2}$, as resulted from the equilibrium study of the process.

The degree of transformation of potassium chloride or its dissolving degree, $\eta_{KCl_{[]_s}}$, has a very big practical importance because its value determines the purity of the obtained product, concerning the chlorine content.

Therefore, as follows, based on the kinetic study, there has been possible to establish the conditions able to ensure high values for the transformation degree of potassium chloride.

According to Fig. 7 the transformation degree of potassium chloride increases with temperature, the growth being significant by small periods of time from the beginning of the process.

The smaller granulation of potassium chloride is, the more favourable is the influence of temperature, respectively, by increasing temperature, increases the $\eta_{KCl_{[]_s}}$ value (Fig. 8).

For temperature value of 25°C, $\dot{X}^0_{(K^+)_2}=0.4771$, $n=160$ r.p.m., the potassium chloride grains dimension influences appreciably the values of transformation degree, $\eta_{KCl_{[]_s}}$.

For potassium chloride with the granulation $d_p=0.375$ mm, the transformation degree has small values in comparison with potassium chloride with granulation $d_p=0.225$ mm (Fig. 9).

The speed of the stirrer, at the beginning of the process, has a small influence upon the transformation degree of KCl. Significant differences appear

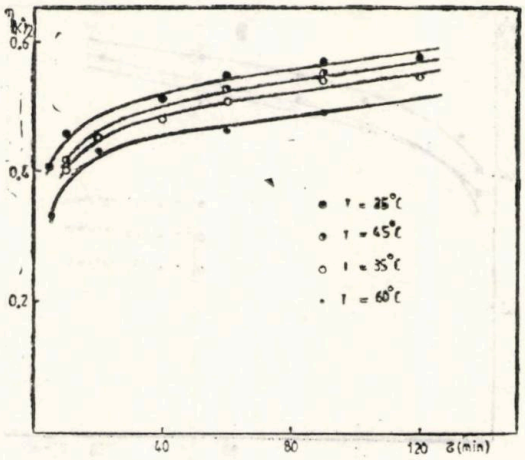

Fig. 3. — The dependence $\eta_{(K+)_2}$ vs. τ; $\bar{X}^0_{(K+)_2} = 0.4771$, $n=160$ r. p. m., $d_p=0,225$ mm ; $\bar{X}^0_{(NH_4)_2SO_4}=0,30$.

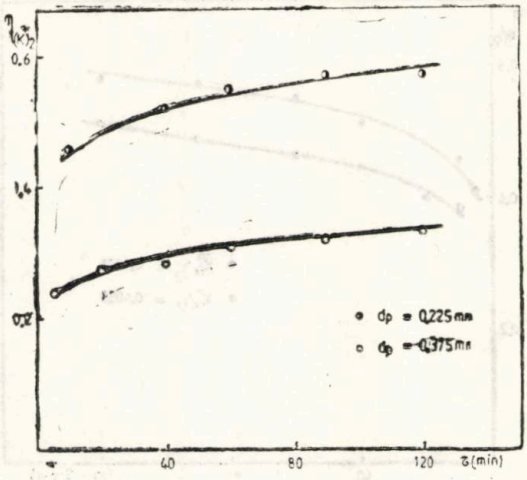

Fig. 4. — The dependence $\eta_{(K+)_2}$ vs. τ; $\bar{X}^0_{(K+)_2}=0.4771$, $T=25°C$. $n=160$ r.p.m.; $\bar{X}^0_{(NH_4)_2SO_4}=0.30$.

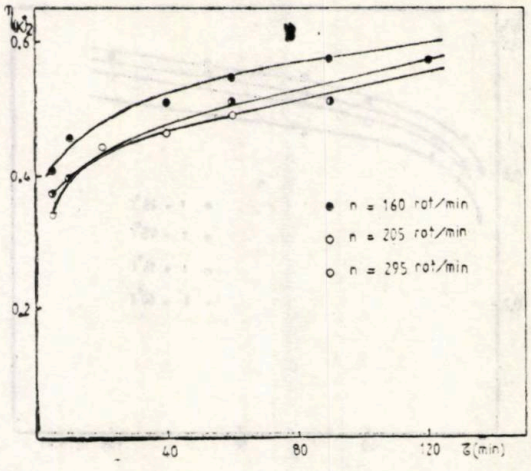

Fig. 5.—The dependence $\eta_{(K^+)_2}$ vs. τ; $\dot{X}^0_{(K^+)_2}=0.4771$, $T=25°C$, $d_p=0\ 225$ mm, $\bar{X}^0_{(NH_4)_2SO_4}=0.30$.

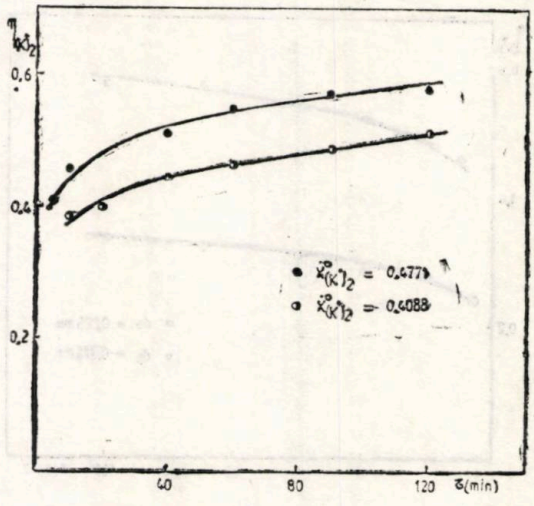

Fig. 6. — The dependence $\eta_{(K^+)_2}$ vs. τ; $T=25°C$, $n=160$ r.p.m., $d_p=0.225$ mm, $\bar{X}^0_{(NH_4)_2SO_4}=0.30$.

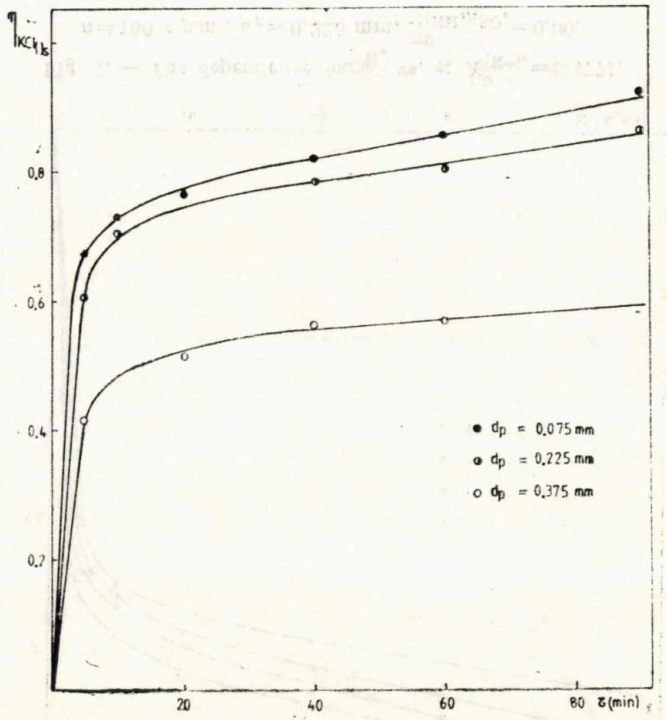

Fig. 9. — The dependence $\eta_{KCl_{[]_s}}$ vs. τ; $T=25°C$, $n=160$ r.p.m., $\dot{X}^0_{(K^+)_2}=0.4771$, $\overline{X}^0_{(NH_4)_2SO_4}=0.30$.

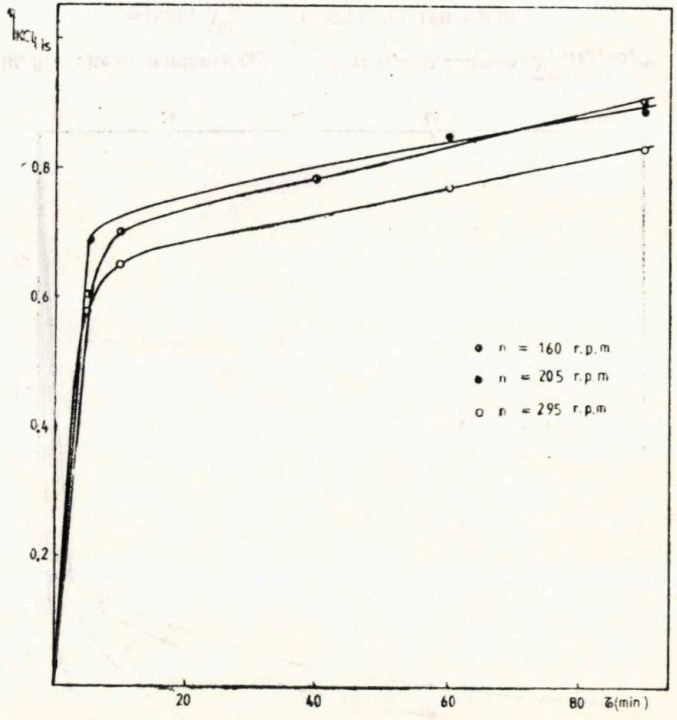

Fig. 10. — The dependence $\eta_{KCl_{[]_s}}$ vs. τ; $T=25°C$, $d_p=0.225$ mm $\dot{X}^0_{(K^+)_2}=0.4771$, $\overline{X}^0_{(NH_4)_2SO_4}=0.30$.

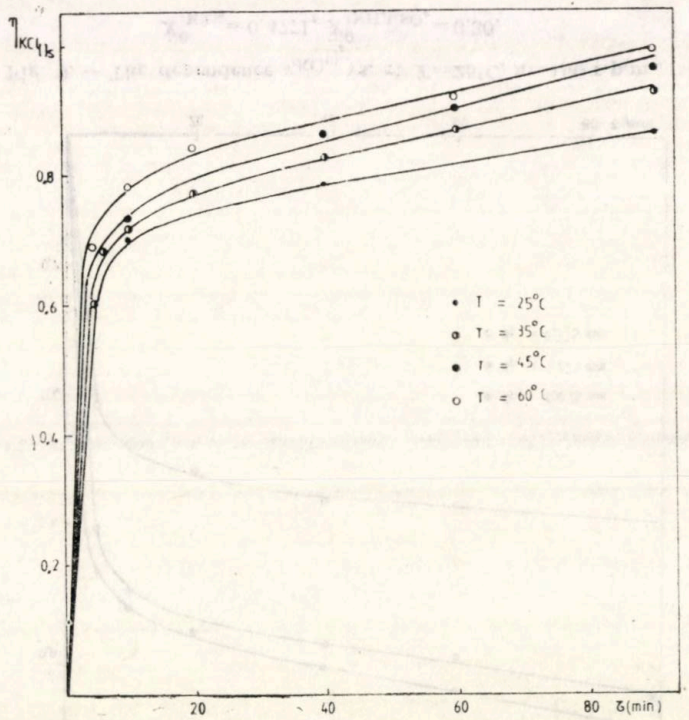

Fig. 7. — The dependence $\eta_{KCl[]_s}$ vs. τ; $\dot{X}^0_{(K+)_2}=0.4771$, $n=160$ r.p.m., $d_p=0.225$ mm, $\bar{X}^0_{(NH_4)_2SO_4}=0.30$.

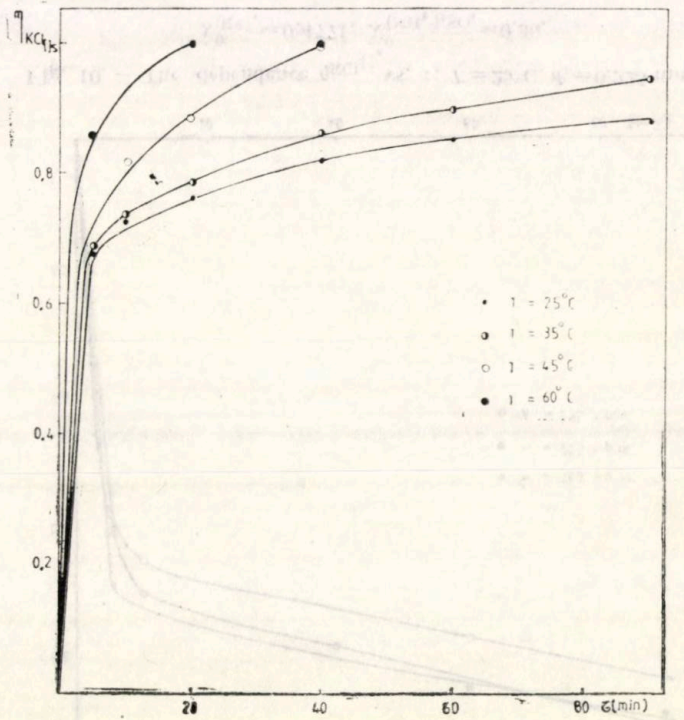

Fig. 8. — The dependence $\eta_{KCl_{[]_s}}$ vs. τ; $d_p=0.225$ mm, $\bar{X}^0_{(NH_4)_2SO_4}=0.30$, $\dot{\bar{X}}^0_{(K^+)_2}=0.4771$, $n=160$ r.p.m.

after 10 min. from the beginning of the process in regard of the transformation degree $\eta_{KCl_{[]_s}}$. Generally, the bigger is the speed of the stirrer, the higher are the values of the transformation degree of KCl, as shown the Fig. 10.

From the undertaken analysis regarding the influence of kinetic parameters upon the values of transformation degree of potassium chloride and separation degree of potassium ion follows that the crystallization process of potassium sulphate may be practically realized in one step or in two.

The one step process requires one reactor, the temperature being maintained at 25°C, the whole duration of the process, in this case, is approximativelly 4 hours.

In case of two steps process, the first step is realized in a reactor provided with a stirrer, at 60°...80°C. The duration of this step is, according to Fig. 8, of 20 min. when using KCl with the granulation d_p =0.0755 mm, and of 90 min. when potassium chloride granulation is d_p =0.225 mm. The second step is realized also in a reactor provided with a stirrer and a cooling casing, and the cooling of the reaction mass is done slowly to ensure the growth of potassium sulphate crystalls. The duration of this step varies between 90 and 120 min.

Because the two steps process requires more equipment and more energy to heat the reaction mass up to 60°...80°C and to maintain this temperature and, also, in the second step, a large amount of water for cooling, there is obvious that the one step process is more efficient even if its duration is bigger.

5. Conclusions

There had been studied the crystallization process of potassium sulphate, based on the double exchange reaction between KCl and $(NH_4)_2SO_4$, establishing the macrokinetic mechanism, the influence of the temperature of the molar ratio of reactants, of the stirrer speed and of potassium chloride granulation exerced upon the transformation degree of KCl.

As result of the investigation, there had been established that an efficient and practically complete transformation of potassium chloride can be obtained using the one step process and a 4 hours duration.

Notations

d_p — the grain diameter;
$\overline{X}_A$ — mass fraction of A component;
τ — process duration;
A_1'', A_2'' — impurities;
D_{KCl} — dissolving potassium chloride;
$T_{A_{[]_l}}$ — A component transfer through liquid phase;
am — molecular mixing;
r. ch. — chemical reaction;
f. c. g. — forming and growth of crystalls;
T_Q — heat transfer;
C_Q — heat consumption;
l, s — liquid (solid);
[ ] — phase;
0 — initial.

Received, February 25, 1988

Polytechnic Institute, Jassy,
Department of Inorganic Chemical Technology

REFERENCES

1. Petrescu S., *Cercetarea de inginerie chimică a procesului de obținere a sulfatului de potasiu prin valorificarea soluției de sulfat de amoniu rezultată la fabricarea caprolactamei.* Ph. D. Diss., Polyt. Inst., Jassy, 1987.
2. Petrescu S. et al., *Aparat pentru preluarea probelor din suspensii.* Patent RSR, *91 136* (1986).
3. Liteanu C., *Chimie analitică cantitativă. Volumetrie.* EDP, București, 1972.
4. Гроше в А. П., *Технический анализ.* Госхимиздат, Москва, 1953.
5. Luca C., Duca A., Crișan I., *Chimie analitică și analiză instrumentală.* EDP, București, 1983.

CERCETAREA CINETICII PROCESULUI DE OBȚINERE A SULFATULUI DE POTASIU PRIN DUBLU SCHIMB DIN KCl și $(NH_4)_2SO_4$

(Rezumat)

Se prezintă rezultatele cercetărilor experimentale ale cineticii procesului de cristalizare a sulfatului de potasiu din cadrul tehnologiei de obținere din clorură de potasiu și soluție de sulfat de amoniu rezultată la fabricarea caprolactamei, stabilindu-se influența specifică a parametrilor cinetici asupra gradului de separare a potasiului, $\eta_{K^+[]_2}$ și a gradului de transformare a clorurii de potasiu, $\eta_{KCl[]_s}$.

BULETINUL INSTITUTULUI POLITEHNIC DIN IAŞI
Tomul XXXV (XXXIX), Fasc. 3—4, 1989
Secţia II
CHIMIE ŞI INGINERIE CHIMICĂ

D. C. 66.02

MIXED-TYPE OPTIMIZING ALGORITM

BY

MATEI MACOVEANU and PAVEL TALPALARU

1. Theoretical Aspects

The number of the direct searching methods for the optimum value of a purpose function with n decision variables is very high and is continually increasing. Generally, the optimum solution is obtained by an iterative process, in which the $\bar{x}^k$ point being given, according to some rules—or in other words, by means of an algorithm— a new point $\bar{x}^{k+1}$ is generated. The used algorithm is characterized both by the manner in which the searching direction is chosen, respectively the way to be covered from the point $\bar{x}^k$ to the point $\bar{x}^{k+1}$, and by the distance on which the displacement between the old point and the new one on the searching direction is accomplished [1]. It is said that the algorithm converges in a finite number of steps if in a finite number of operations, the optimum solution, i.e. $\bar{x}^*$, is obtained.

Z a n g w i l l formalized in a series of works the concept of algorithm and of convergence; sometimes this formalization allows a more direct demonstration of convergence [2].

It is known that algorithms behave differently in the optimizing process; some of them have a greater convergence rate at the beginning of the process, others, as one approaches to the optimum point. For that reason it is natural to use various algorithms in so an order in which they are more efficient, thus composing mixed algorithms. This means that, function of the $\bar{x}^k$ point, different algorithms will be applied.

Generally speaking, one choses a basic convergent algorithm which is applied for certain values of $k \in K = \{0,1,2,...,m\}$. For the other values of k we can even use algorithms for which we have not demonstrated the convergence conditions, but which we know from experience that they behave well [3].

This paper proposes a mixed algorithm in which the H o o k e—J e e v e s method is used as a basic algorithm, this procedure being combined, at a certain moment, with an unidimensional optimizing method.

2. The Presentation of the Proposed Algorithm

The H o o k e - J e e v e s or the Pattern Search method, used as the basic algorithm in the proposed mixed-type algorithm, employs as searching principles both the testing to parallel directions with the coordinate axes and the acceleration in a direction which will be later specified [4], [5].

In the following we suppose that the minimum value of a function $f(\bar{x})$ is searched for, where $\bar{x} = (x_1, x_2, ..., x_n)$ represents the vector of the decision variables in the n-dimensional space R^n.

The H o o k e - J e e v e s method uses two types of points, namely, basic points, of coordinates $\bar{b} = (b_1^k, b_2^k, ..., b_n^k)$, and climaxes with the coordinates $\bar{v} = (v_1^k, v_2^k, ..., v_n^k)$. As part of an iteration, the basic point is a fixed one, while the climax is displaced according to the local search.

A certain iteration k from within a minimizing problem, where f_1 is the least value of the purpose function determined up to a given moment during the local exploration, develops as follows :

a) Successive displacements of the climax on the n directions of the coordinate axes are made as :

$$v_1^{k+1}=v_i^k+\Delta x_i^k,\ k\in K \text{ fixed},\ (i=1,\ 2,\ \ldots\ n). \tag{1}$$

If, for instance,

$$f(v_1^{k+1},\ v_2^k,\ldots,\ v_n^k)<f_1, \tag{2}$$

the new value of f_1 will be :

$$f_1:=f(v_1^{k+1},\ v_2^k,\ \ldots,\ v_n^k).$$

Otherwise, the displacement will be made in an opposite direction, that is

$$v_i^{k+1}=v_i^k-\Delta x_i^k,\ (i=1,\ 2,\ \ldots,\ n). \tag{3}$$

If the relation (2) is verified, then f_1 is accordingly modified. If the two displacement tests of the climax on the i direction are unsuccessful, the respective coordinate remains unmodified, that is $v_i^{k+1}=v_i^k$, and the algorithm is applied up to the complete determination of $\bar{v}^{k+1}=(v_1^{k+1},\ v_2^{k+1},\ \ldots,\ v_n^{k+1})$.

Generally, if we have

$$f(v_1^{k+1},\ v_2^{k+1},\ldots,v_j^{k+1},\ v_{j+1}^k,\ \ldots,\ v_n^k)<f_1,\ j\in\{1,\ 2,\ \ldots,\ n\}, \tag{4}$$

the new value of f_1 will be :

$$f_1:=f(v_1^{k+1},\ v_2^{k+2},\ \ldots,\ v_j^{k}+1,\ v_{j+1}^k,\ \ldots,\ v_n^k),$$

where $v_i^{k+1}=v_i^k\pm\Delta x_i^k$ or $v_i^{k+1}=v_i^k$, $(i=1,\ 2,\ \ldots,\ j)$, $j\in\{1,\ 2,\ \ldots,\ n\}$.

Consequently, if we note with

$$\bar{v}^{k+1}=(v_1^{k+1},\ v_2^{k+1},\ \ldots,\ v_j^{k+1},\ v_{j+1}^k,\ \ldots,\ v_n^k) \tag{5}$$

it results that $f_1:=f(\bar{v}^{k+1})$. The new basic point is chosen $\bar{b}^{k+1}=\bar{v}^{k+1}$.

b) If, at the end of the local explorations

$$f_1=f(\bar{v}^{k+1})<f(\bar{b})^k,$$

then an acceleration of the displacement is made and the displacement of the basic point is in these case :

$$\bar{b}^{k+1}=\bar{v}^{k+1}.$$

The new climax will be on the direction defined by $\bar{b}^{k+1}$ and $\bar{b}^k$, at a distance from $\bar{b}^{k+1}$ equal with that between the two consecutive basic points :

$$\bar{v}^{k+1}=\bar{b}^{k+1}+(\bar{b}^{k+1}-\bar{b}^k)=2\bar{b}^{k+1}-\bar{b}^k. \tag{8}$$

c) If

$$f_1=f(\bar{v}^{k+1})\geqslant f(\bar{b}^k) \tag{9}$$

both the acceleration from the iteration $k-1$ and the local exploration from

the iteration k have been unsuccessful. As a result, the elements of the local exploration vector are reduced either by dividing into halves or by another relation of continuous reduction.

Therefore

$$\Delta\bar{x}^{k+1} = \frac{1}{2}\Delta\bar{x}^{k}. \tag{10}$$

The climax is moved, as well, in the basic point

$$\bar{v}^{k+1} = \bar{b}^{k+1} = \bar{b}^{k}. \tag{11}$$

d) When the elements of the local search vector become smaller than certain pre-established values, i.e. $\Delta x_i^{k+1} < \varepsilon_1$, the evolution of the algorithm is stopped, considering as an optimum value the best coordinate point $\bar{b}_k$ found out up to that moment. Otherwise, the calculations are resumed from stage a).

At the first iteration there must be specified, as well, the initial values of the elements of the local search $\Delta\bar{x}^0$ beside the coordinates of the basic point (which is initially superposed with the climax). The previously exposed principles are shown in Fig. 1.

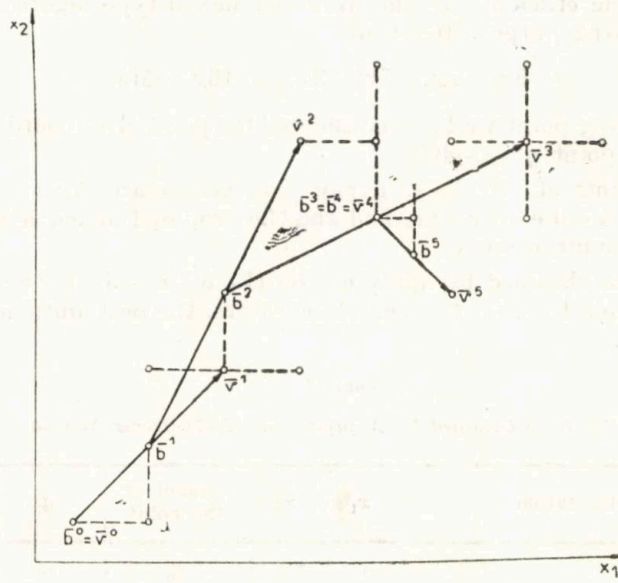

Fig. 1. — The principle of the Hooke-Jeeves method (the points are numbered in the order of their estimation): success ; ∘ failure ; — — — local explorations ; ——— acceleration.

The proposed mixed algorithm replaces the fixed step acceleration in the direction of the successful displacements carried out as part of the exploration movements by an optimum step acceleration.

Having in view these purpose a new climax $\bar{v}^{k+1}$ will be completed, stipulating that

$$f(\bar{v}^{k+1}) = \min_{\lambda} f[\bar{b}^{k+1} + \lambda(\bar{b}^{k+1} - \bar{b}^{k})] \tag{12}$$

by means of an unidimensional optimizing method.

By the proposed modification there will be a local minimum value in $\bar{v}^{k+1}$ in the direction $d = \bar{b}^{k+1} - \bar{b}^{k}$, if the function admits a minimum.

When some restrictions occur, as well, i.e. g_j, where $(j = 1, 2, \ldots, m < n)$, in the acceleration stage, the following condition will be imposed :

$$f(\bar{v}^{k+1}) = \min_{\lambda, \lambda_j} \left\{ f[\bar{b}^{k+1} + \lambda(\bar{b}^{k+1} - \bar{b}^{k})] + \sum_{j=1}^{m} \lambda_j g_j \right\}, \tag{13}$$

In this manner, the new climax $\bar{v}^{k+1}$ will be a permitted local optimum.

3. The Testing of the Mixed-type Algorithm Efficiency

The efficiency of an optimizing algorithm is estimated, in the specialized literature, by means of a test function [3], [5].

To test the efficiency of the proposed mixed-type algorithm, we have used the following purpose function :

$$y = 6x_1 + 7x_2 - 7x_1^2 + 2x_1x_2 - 16x_2^2 = \text{Max.} \tag{14}$$

As a starting point we have considered the point A of coordinates $x_1^A = 5$, $x_2^A = 5$; in this point $y^A = -460$.

The elements of the local exploration vector are $\Delta x_1 = 0.2$, $\Delta x_2 = 0.2$. Both the H o o k e-J e e v e s method and the proposed mixed algorithm have been applied simultaneously.

The results obtained by applying the H o o k e - J e e v e s method are presented in Table 1. After two searching cycles, the best obtained value has been $y = -315$.

Table 1

The Data Obtained by Applying the Hooke-Jeeves Method

Cycle	Operation	x_1	x_2	Symbol of the point	y	Remarks
0	Start	5.0	5.0	$\bar{x}_0^0$	−460	Starting point
1	Testing on the Ox_1 direction	5.2	5.0		−471	Failure
		4.8	5.0	$\bar{x}_1^0$	−449	Success
	Testing on the Ox_2 direction	4.8	4.8	$\bar{x}_2^0 = \bar{x}^1$	−421	Success
	Acceleration	4.6	4.6	$\bar{x}_0^1$	−384	Success
2	Testing on the Ox_1 direction	4.4	4.6	$\bar{x}_1^1$	−375	Success
	Testing on the Ox_2 direction	4.4	4.4	$\bar{x}_2^1 = \bar{x}^2$	−349	Success
	Acceleration	4.2	4.2	$\bar{x}_0^2$	−315	Success

The data obtained by applying the mixed algorithm are presented in Table 2. The acceleration accomplished according to the mixed-type algorithm has used the condition (10); it result :

$$\bar{v}^{k+1}=\bar{b}^{k+1}+\lambda(\bar{b}^{k+1}-\bar{b}^{k}). \tag{15}$$

Table 2

The Data Obtained by Applying the Mixed-type Algorithm

Cycle	Operation	x_1	x_2	Symbol of the point	y	Remarks
0	Start	5.0	5.0	$\bar{x}_0^0$	−460	Starting point
1	Testing on the Ox_1 direction	5.5	5.0		−471	Failure
		4.8	5.0	$\bar{x}_1^0$	−449	Success
	Testing on the Ox_2 direction	4.8	4.8	$\bar{x}_2^0=\bar{x}^1$	−421	Success
	Acceleration	0.31	0.31	$\bar{x}_0^1$	2.01	Success
2	Testing on the Ox_1 direction	0.11	0.31		1.27	Failure
		0.51	0.31	$\bar{x}_1^1$	2.18	Success
	Testing on the Ox_2 direction	0.51	0.51		1.16	Failure
		0.51	0.11		1.92	Failure
	Acceleration	0.31043	0.31	$\bar{x}_0^2$	2.0128	Success

For the considered application, the coordinates of the new point obtained by the acceleration achieved at the end of the cycles *1*, are

$$x_1=4.8+\lambda(4.8-5),\quad x_2=4.8+\lambda(4.8-5).$$

To determine λ, i.e. the displacement point, the coordinates of the new point considered as functions of λ have been introduced in the purpose function (12) resulting :

$$y=-421.44+37.72\,\lambda-0.84\,\lambda^2. \tag{16}$$

Then, the optimum λ has been determined by equaling to zero the derivative $dy/d\lambda$; it result

$$\lambda_{opt}=22.45.$$

Under these conditions, as a result of the acceleration achieved according to the proposed mixed-type algorithm, the new searching point with the following coordinates, is determined :

$$x_1=4.8-0.2\times 22.45=0.31,\quad x_2=4.8-0.2\times 22.45=0.31.$$

If the data given in Tables 1 and 2 are analysed one can easily notice that the proposed mixed-type algorithm converges easier towards the optimum solution even from the beginning. After two searching cycles, the value of the purpose function is improved from −460 to 2.0128, in comparison with the case when the H o o k e-J e e v e s method is used, a case when this improv-

ement is much less remarked. It is true that in the case of the proposed mixed-type algorithm it is necessary to perform an additional calculus, i.e. the computation of the function derivative w.r.t. λ, should be done for each searching cycle.

But considering the total number of calculi having in view to localize with a certain precision the optimum value, the proposed mixed-type algorithm proves to be much more efficient as compared to the Hooke-Jeeves method, requesting the accomplishment of a much more reduced number of searching cycles.

4. Conclusions

a) A mixed-type optimizing algorithm has been proposed, for which the Hooke-Jeeves method has been used as a basic algortihm; at a certain stage, the Hooke-Jeeves method has been combined with an unidimensional optimizing method.

b) The testing of the proposed mixed-type algorithm has proved that this is more powerfully convergent than the Hooke-Jeeves method, and allows the localization of the optimum value with a precision imposed by a reduced number of tests.

Received, September 19, 1988

Polytechnic Institute, Jassy,
Department of Chemical Engineering
and
Department of Mathematics

REFERENCES

1. Curievici I., *Optimizări în industria chimică.* EDP, București, 1980.
2. Zangwill W.I., *Nonlinear Programming. A Unified Approach.* Prentice-Hall, New Jersey, 1969.
3. Dumitru V., *Programare neliniară.* Ed. Acad. RSR, București, 1975.
4. Hooke R., Jeeves T., J. Assoc. Comput. Mach., **8**, *2*, 212 (1961).
5. Hoffmann U., Hoffmann H., *Einführung in die Optimierung.* Verlag Chemie, Weinheim, 1971.

ALGORITM DE OPTIMIZARE DE TIP MIXT

(Rezumat)

Se propune un algoritm de optimizare de tip mixt, în care ca algoritm de bază se folosește metoda Hooke-Jeeves, care la un anumit moment se combină cu o metodă de optimizare unidimensională. Testarea algoritmului propus, comparativ cu metoda Hooke-Jeeves, a arătat că acesta converge mult mai rapid către soluția optimă.

BULETINUL INSTITUTULUI POLITEHNIC DIN IAŞI
Tomul XXXV (XXXIX), Fasc. 3—4, 1989
Secţia II
CHIMIE ŞI INGINERIE CHIMICĂ

C. D. 66.048.37 ; 66

ÉTUDE D'UNE COLONNE À PULSATIONS POUR L'EXTRACTION LIQUIDE—LIQUIDE

I. COMPORTEMENT HYDRODYNAMIQUE : CAPACITÉ DE LA COLONNE

PAR

M. FOURAR et A. ALIANE

1. Introduction

La colonne pulsée est un extracteur utilisé à l'heure actuelle dans le monde entier pour la purification des concentrés uranifères et pour le traitement des combustibles irradiés dans les réacteurs nucléaires.

Dans ces deux domaines, la colonne pulsée, plus particulairement la colonne pulsée à plateaux perforés, a été reconnue comme un appareil réunissant un certain nombre de qualités primordiales : simplicité de fonctionnement, durée de vie plus longue, grande fiabilité, bonne efficacité, faible volume, faible coût de maintenance et grande tolérance quant à la présence d'impuretés solides ou de crasses.

L'accélération des programmes nucléaires a conduit à une augmentation notable des capacités, ce qui a pour effet de faire entrer peu à peu la colonne pulsée dans le champ d'applications industrielles externes au nucléaire.

L'intérêt, ainsi de plus en plus accru, porté à la colonne pulsée, a suscité l'apparition d'un nombre très important de recherches sur ce type d'extracteur. Néanmoins, très peu d'entre elles ont utilisé des plateaux en polytétrafluoroéthylène (Téflon) et une phase organique comme phase continue.

Dans ces circonstances, nous proposons une série de données expérimentales sur le comportement hydrodynamique et les conditions d'engorgement d'une colonne pulsée à plateaux perforés pour un contre-courant de deux liquides immiscibles sans transfert de matière. L'influence de la nature de la phase continue sur la capacité de la colonne est également considérée dans cette étude.

2. Description de l'appareillage

2.1. La colonne à pulsations

La colonne est du type à plateaux perforés équipée d'un système de pulsation qui agite périodiquement les phases. Cette colonne comprend trois parties (Fig. 1): a) une section d'extraction contenant les plateaux, b) deux sections de décantation en haut et en bas de la colonne.

a) *La section d'extraction.* Elle représente la colonne proprement dite en verre, diamètre intérieur 50 mm, hauteur 4 m, avec robinets de prise d'échantillon tous les 50 cm. La colonne dispose de deux types de garnissage qui diffèrent par la nature des plateaux perforés à savoir : α) un garnissage avec pla-

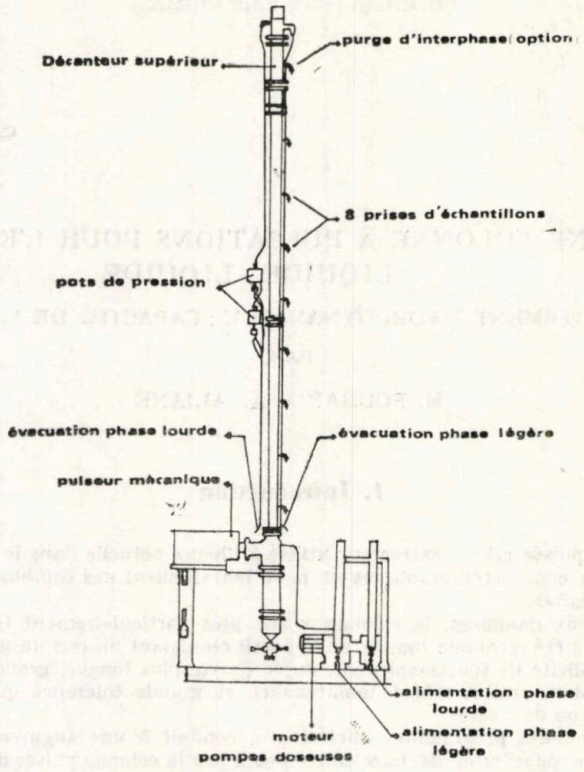

Fig. 1. — Schéma détaillé de la colonne pulsée à plateaux perforés.

teaux perforés en acier inoxydable, utilisé lorsqu'on veut que la colonne fonctionne en phase aqueuse continue; β) un garnissage avec plateaux perforés en téflon, destiné au fonctionnement en phase organique continue. Ces garnissages sont réalisés en éléments de longueur unitaire (1 m) qui peuvent être fixés les uns aux autres par un système vis—écrou.

Les plateaux perforés (diamètres des perforations: 4 mm, surface perforée : 23%) sont placés sur une tige centrale et régulièrement espacés de 5 cm. Ils sont ajustés de manière à recouvrir entièrement la section transversale de la colonne.

b) *Décanteur supérieur.* Il est constitué d'un tube en verre, de diamètre intérieur 100 mm et de hauteur 500 mm environ. Il est muni d'un déversoir phase légère, d'un dispositif d'admission de la phase lourde et de la possibilité de régulation d'interface pour le fonctionnement en phase lourde continue (interphase en haut). Un robinet permet de soutirer les crasses au niveau de l'interface.

c) *Décanteur inférieur.* Il est constitué d'un tube en verre et muni d'un dispositif de pulsion mécanique réglable en fréquence et en amplitude, d'un dispositif d'admission de la phase légère, d'un système de soutirage de la phase lourde et de la possibilité de régulation d'interphase pour le fonctionnement en

phase légère continue (interphase en bas). Un robinet permet de soutirer les crasses au niveau de l'interphase.

2.2. Mécanisme de production des pulsations

Les pulsations sont produites à l'aide d'un piston avec soufflet en téflon (assurant l'étanchéité) actionné par un moteur anti-déflagrant. Les pulsations sont réglables en fréquence et en amplitude. Le réglage de la fréquence s'effectue par action sur le bouton molleté supérieur du variateur de vitesse. Le réglage de l'amplitude s'obtient en faisant varier la course du piston en vissant ou en dévissant le bouton molleté correspondant.

2.3. Alimentation des phases

L'alimentation des phases est assurée par une pompe doseuse à deux têtes en acier inoxydable réglables indépendamment de 0 l/h à 82 l/h pour l'alimentation des phases lourde et légère avec bacs doseurs en verre (2,5 l chacun) pour l'étalonnage.

2.4. Système de régulation pneumatique d'interphase

C'est un système à pots de pression dont le rôle est de maintenir constant le niveau de l'interphase, que cette dernière soit située dans le décanteur supérieur (phase lourde continue), soit dans le décanteur inférieur (marche en phase légère continue).

3. Mode opératoire

Les expériences ont porté sur le système binaire eau — kérosène, ces deux liquides étant complètement immiscibles. L'eau du robinet est directement utilisée, le kérosène provient de la NAFTAL (entreprise nationale). Sa densité et sa viscosité a 20°C sont respectivement de 0,7888 g/cm^3 et 1,369 centipoises.

Le garnissage en téflon a été utilisé. Il est préférentiellement mouillé par le kérosène qui a été pris comme phase continue pour toutes les expériences (interphase en bas de la colonne). Les liquides sont envoyés en contre-courant : le kérosène par le bas, l'eau par le haut de la colonne. Les débits maxima utilisés sont de 11 l/h pour le kérosène et de 15,5 l/h pour l'eau.

Les premières séries d'expériences ont été consacrées à délimiter les zones opératoires qui caractérisent les différents types de fonctionnement de la colonne. Le mode opératoire suivant a été adopté :

a) La colonne est remplie avec la phase aqueuse jusqu'à mi-hauteur du décanteur inférieur indiquant la position de l'interphase choisie.

a) La pulsion mécanique est mise en action et la fréquence des pulsations est ajustée à la valeur voulue, l'amplitude ayant été réglée au préalable pour toute une série d'expériences. On a utilisé les amplitudes suivantes : a=1,0 cm ; a=1,5 cm et a=2,0 cm. Les fréquences étaient comprises entre 0 et 110 mn^{-1}.

c) Le kérosène est admis dans la colonne à un débit suffisamment petit pour que l'engorgement ne se produise pas tandis que le débit de l'eau est ajusté à la valeur voulue. Quant le kérosène passe en haut de la colonne, on en augmente le débit progressivement, en laissant chaque fois s'établir un ré-

gime stable (débits constants, interphase fixe) jusqu'à ce que, un second interphase apparaisse dans la section de décantation supérieure, l'eau s'accumulant en raison de la grande résistance que lui offre la phase continue pour son écoulement. On considère que c'est à ce moment qu'a lieu l'engorgement. On peut également atteindre l'engorgement en laissant le débit de kérosène constant et en faisant croître celui de l'eau.

d) Quand l'engorgement se produit, on lit les débits d'eau et de kérosène. Ce sont ces débits qu'on appelle habituellement les débits d'engorgement et sont ceux qui fixent la capacité de la colonne (débit maximal pouvant transiter dans la colonne).

4. Résultats et discussion

Le but des premières séries d'expériences a été de déterminer la dépendance entre la capacité de la colonne et les variables opératoires. En effet, il est absolument indispensable de connaître le domaine des amplitudes, des fréquences et des débits de phases où la colonne est appelée à mieux fonctionner.

Des mesures ont été effectuées avec des conditions de fonctionnement différentes : énergie de pulsation (produit amplitude×fréquence), débits de phases (leur rapport étant variable). Les résultats obtenus sont regroupés dans le Tableau 1. Il ressort qu'au mêmes conditions de pulsation, pour différents rapports de débits, la capacité de la colonne est pratiquement constante. Sur la base de ces résultats on peut conclure que la capacité de l'extracteur dépend essentiellement des conditions de pulsation.

Les valeurs moyennes de la somme des vitesses de passage des phases (débits rapportés à la section transversale de la colonne) sont représentées dans les Fig. 2...4 en fonction de l'intensité d'agitation et à amplitudes constantes.

Suivant l'intensité de la pulsation, la somme des débits étant fixée, on peut distinguer plusieurs types de fonctionnements hydrodynamiques de la colonne. On peut observer également, que plus l'amplitude de travail augmente, plus la zone mélangeur—décanteur se rétrécit et plus la zone d'émulsion augmente. En d'autres termes, on assiste à une augmentation du rapport de surface entre la zone émulsion et de la zone mélangeur—décanteur en fonction de l'amplitude.

Le comportement hydrodynamique de la colonne est identique à celui qu'ont décrit S e g e et W o o d f i e l d [1]. On distingue trois zones opératoires essentiellement différentes :

a) *Zone mélangeur--décanteur.* C'est celle qu'on obtient avec des pulsations peu intenses ($14\ mn^{-1} \leqslant f \leqslant 30\ mn^{-1}$). Les deux phases sont alternativement dispersées à chaque pulsation et coalescent lorsque celle-ci change de sens ainsi que l'ont indiqué W i e g a n d t et von B e r g [2]. La séparation de phases est réalisée de façon distincte (apparition de couches claires dans l'espace entre plateaux—Fig. 5).

b) *Zone émulsion.* Avec des pulsations plus intense ($f > 30\ mn^{-1}$), les gouttes deviennent plus fines, la répartition de la phase dispersée devient assez uniforme et il n'y a plus de coalescence à chaque pulsation.

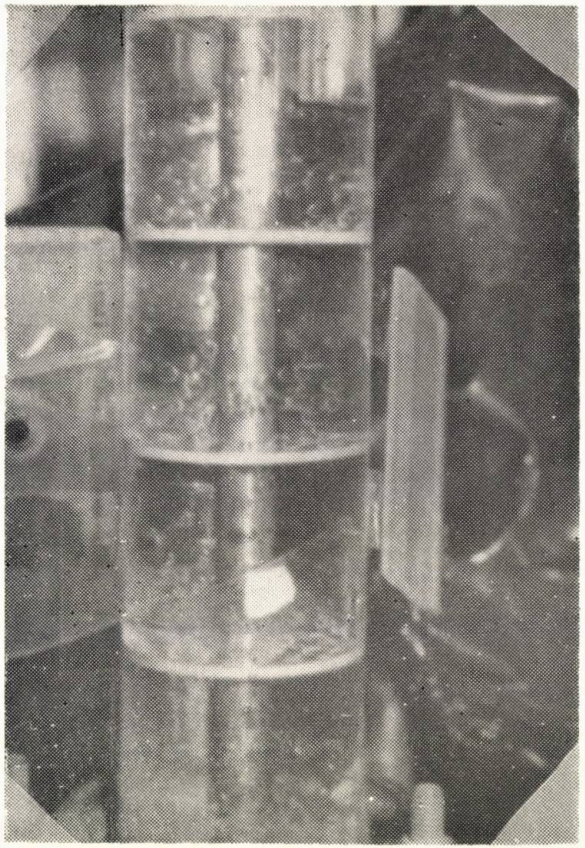

Fig. 5. — La dispersion en régime mélangeur — décanteur pour les conditions : $a=1{,}0$ cm; $f = 14\,\text{mn}^{-1}$; $V_d=0{,}113$ cm/s et $V_c=0{,}085$ cm/s.

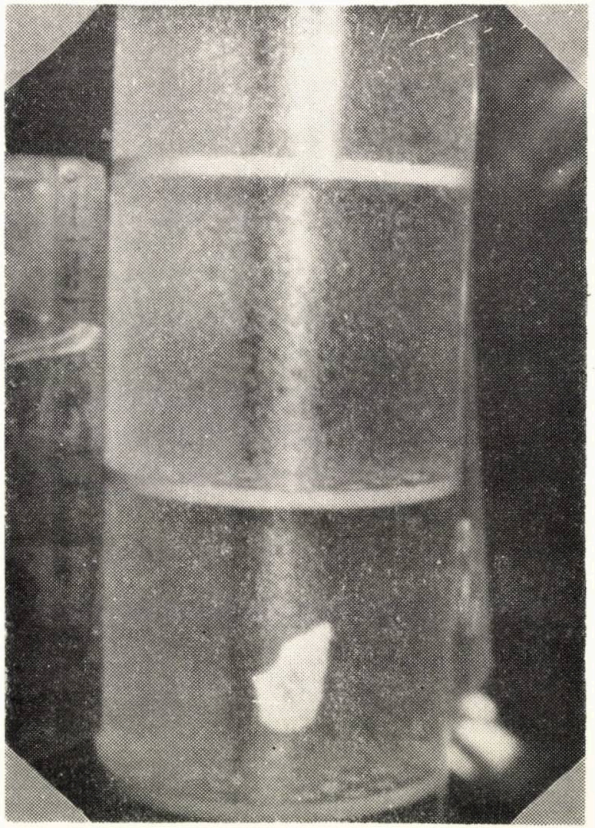

Fig. 6. — La dispersion en régime émulsion pour les conditions : $a=2{,}0$ cm ; $f=95\ \text{mn}^{-1}$; $V_d=0{,}071$ cm/s et $V_c=0{,}014$ cm/s.

Tableau 1

Resultats expérimentaux concernant la capacite de la colonne

a cm	f mn^{-1}	Q_c l/h	Q_d l/h	V_c+V_d cm/s	$\overline{V_c+V_d}$ cm/s	af cm/s
		11,0	11,0	0,311		
		8,0	1 ,5	0,304		
1,0	29	9,5	12,0	0,304	0,309	0,483
		13,0	9,5	0,318		
		9,0	9,5	0,262		
		7,4	10,7	0,256		
1,0	45	5,7	12,5	0,257	0,259	0,75
		8,2	10,3	0,223		
		6,5	9,0	0,219		
		5,2	10,0	0,215		
1,0	60	5,7	9,5	0,215	0,218	1,0
		7,5	8,3	0,223		
		5,0	8,0	0,184		
		9,5	9,0	0,177		
1,0	78	6,4	7,0	0,189	0,187	1,3
		7,5	6,5	0,198		
		2,0	7,0	0,127		
		2,5	6,5	0,127		
1,0	110	4,0	5,5	0,134	0,130	1,83
		3,6	6,0	0,134		
		9,0	9,5	0,262		
		6,5	11,5	0,255		
1,5	29	2,5	15,5	0,255	0,259	0,72
		10,8	8,0	0,266		
		8,5	7,5	0,226		
		7,0	8,5	0,219		
1,5	45	9,5	7,0	0,233	0,226	1,12
		10,0	6,0	0,226		
		8,0	6,0	0,198		
		6,5	7,0	0,191		
1,5	60	9,5	5,0	0,205	0,197	1,5
		7,5	6,2	0,194		
		2,0	7,5	0,134		
		2,5	7,0	0,134		
1,5	78	4,0	6,0	0,141	0,134	1,95
		1,0	8,0	0,127		
		2,5	6,5	0,127		
		1,5	7,3	0,124		
1,5	110	3,0	6,0	0,127	0,128	2,75
		4,5	5,0	0,134		
		8,0	8,0	0,226		
		7,5	8,5	0,226		
2,0	29	10,0	5,5	0,219	0,222	0,97
		9,0	6,5	0,219		
		8,0	5,0	0,184		
		7,5	6,0	0,191		
2,0	45	6,0	8,0	0,198	0,195	2,0
		5,5	9,0	0,205		
		9,0	1,5	0,149		
		7,0	4,0	0,156		
2,0	60	10,0	0,5	0,149	0,153	2,0
		8,0	3,0	0,156		
		2,0	7,0	0,127		
		8,0	2,0	0,141		
2,0	78	6,0	4,0	0.141	0,138	2,6
		9,0	1,0	0,141		
		6,0	2,5	0,120		
		5,5	3,0	0,120		
2,0	110	7,0	1,5	0,120	0,120	3,67
		7,5	1,0	0,120		

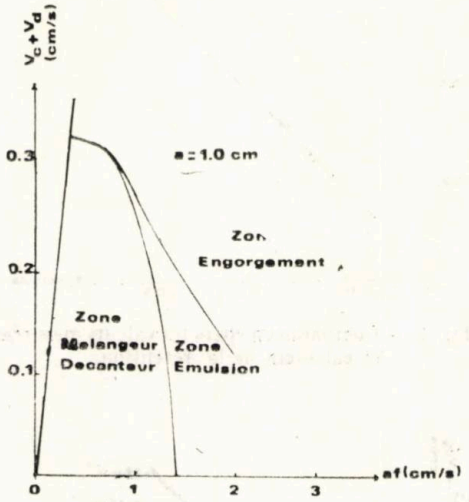

Fig. 2. — Détermination des zones opératoires de la colonne (a=1,0 cm).

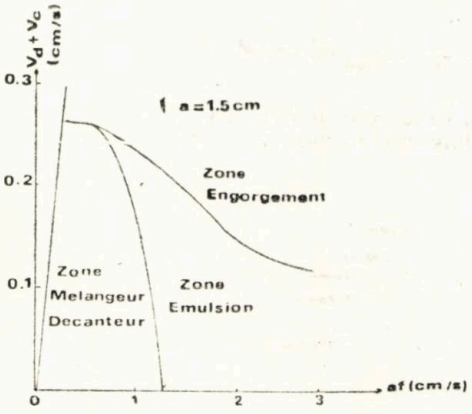

Fig. 3. — Détermination des zones opératoires de la colonne (a=1,5 cm).

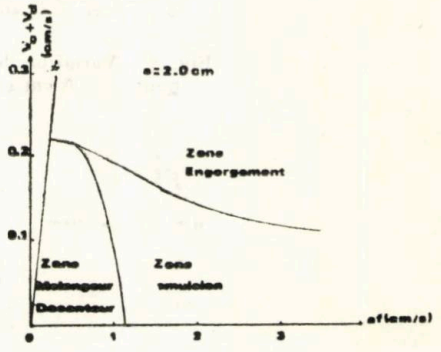

Fig. 4. — Détermination des zones opératoires de la colonne (a=2,0 cm).

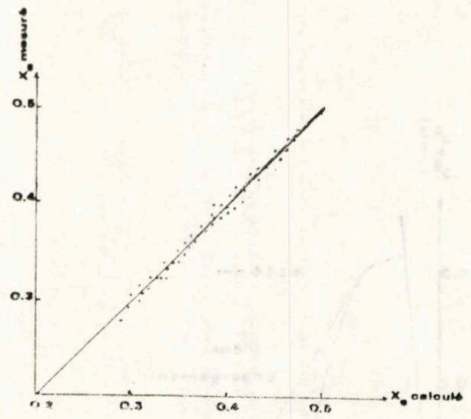

Fig. 7. — Comparaison entre les valeurs mesurées et calculées de la rétention.

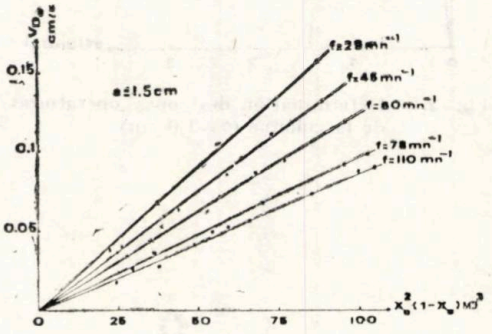

Fig. 8 — Variation de V_{de} en fonction de $x_e^2(1-x_e)$ pour $a=1{,}0$ cm et à différentes fréquences.

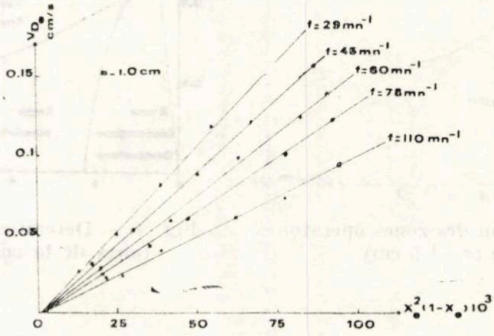

Fig 9 — Variation de V_{de} en fonction de $x_e^2(1-x_e)$ pour $a=1{,}5$ cm et à différentes fréquences.

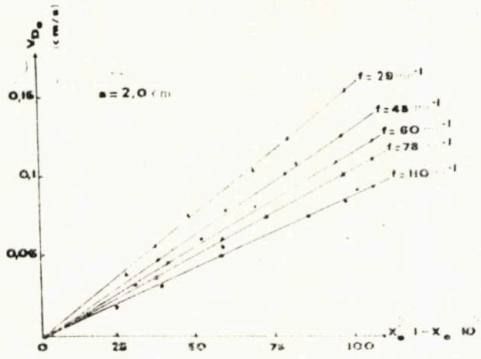

Fig. 10. — Variations de V_{de} en fonction de $x_e^2(1-x_e)$ pour $a=2{,}0$ cm et à différentes fréquences.

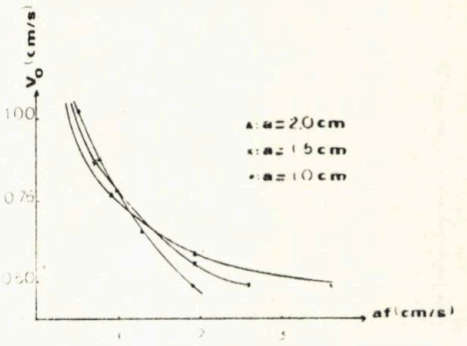

Fig. 11. — Variation de la vitesse caractéristique V_0 en fonction de l'intensité d'agitation af.

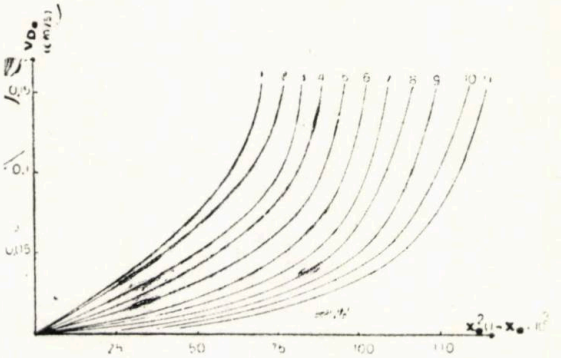

Fig. 12. — Variation de V_{de} en fonction de $x_e^2(1-x_e)$ à $V_{ce}=$const.
1 — $V_{ce}=0{,}162$ cm/s ; *2* — $V_{ce}=0{,}148$ cm/s ; *3* — $V_{ce}=0{,}134$ cm/s ; *4* — $V_{ce}=0{,}120$ cm/s ; *5* — $V_{ce}=0{,}106$ cm/s ; *6* — $V_{ce}=0{,}092$ cm/s ; *7* — $V_{ce}=0{,}078$ cm/s ; *8* — $V_{ce}=0{,}064$ cm/s ; *9* — $V_{ce}=0{,}050$ cm/s ; *10* — $V_{ce}=0{,}036$ cm/s ; *11* — $V_{ce}=0{,}022$ cm/s.

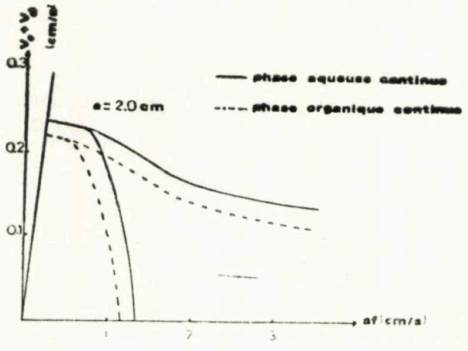

Fig. 13. — Influence de la nature de la phase continue sur la capacité de la colonne.

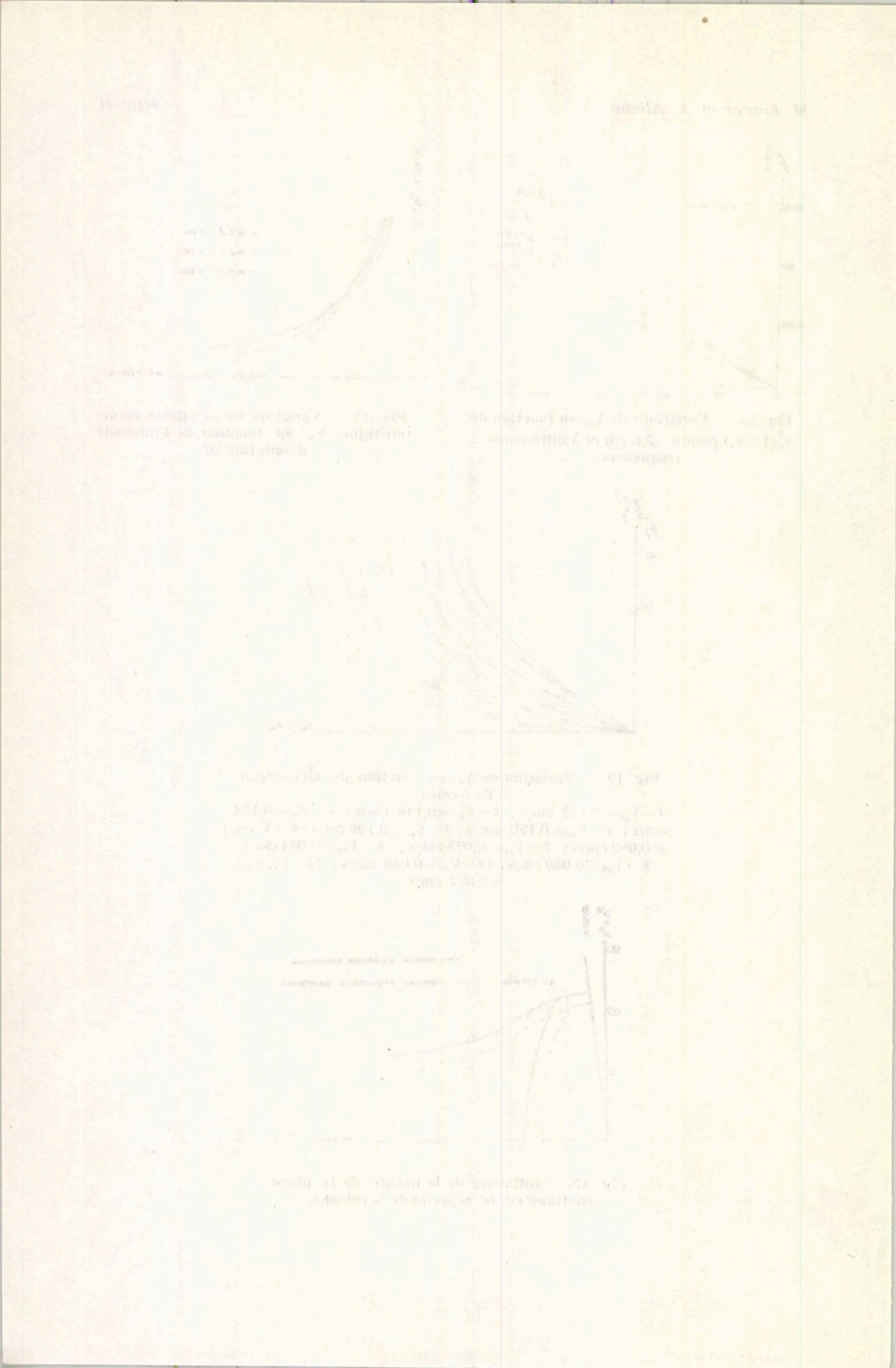

Une augmentation progressive de la fréquence de pulsation se traduit par une agitation de plus en plus forte dans l'extracteur ; l'émulsion entretenue entre les plateaux perforés coalesce dans les sections de décantation de l'appareil. À partir d'une certaine fréquence, la coalescence n'a plus le temps de s'effectuer ; les phases liquides ne sont plus différenciées ; c'est l'engorgement par excès de pulsation. Cette fréquence au-delà de laquelle il n'est plus possible de fonctionner caractérise la capacité de l'appareil (Fig. 6).

Notons en outre qu'on peut également déterminer une fréquence minimum (f=14 mn^{-1}) en deçà de laquelle l'extracteur ne peut fonctionner ; cette fréquence, en général très basse, est celle de l'engorgement par insuffisance de pulsations.

4.1. Étude de l'engorgement

L'engorgement provoqué par une forte emulsion est défini par l'apparition d'un second interface. Il est indispensable de connaître le domaine dans lequel on peut travailler sans qu'il se produise.

La présente étude a utilisé comme point de départ les observations effectuées concernant un grand nombre de mesures experimentales recueillies sur la capacité de la colonne et la rétention à l'engorgement :

a) Le Tableau 1 montre clairement qu'aux mêmes conditions de pulsations, la capacité de la colonne est constante.

b) L'analyse du Tableau 2 montre que pour des rapports de débits constants à différentes conditions de pulsation, la rétention à l'engorgement est pratiquement constante.

Ces observations sont en accord avec les équations basées sur le concept de la vitesse caractéristique établies par Gayler-Roberts et Pratt [3] dans le cas des colonnes à garnissage et reprises par Thornton [4] dans le cas des colonnes á pulsations :

$$(1)\qquad \frac{V_d}{x}+\frac{V_c}{1-x}=V_0(1-x), \qquad (2)\qquad \frac{dV_d}{dx}=0 \text{ et } \frac{dV_c}{dx}=0,$$

$$(3)\qquad V_{de}=2V_0x_e^2(1-x_e) \qquad (4)\qquad V_{ce}=V_0(1-2x_e)(1-x_e)^2,$$

$$(5)\qquad x_e=\frac{2}{3+(1+8V_{ce}/V_{de})^{1/2}}.$$

Dans l'expression de la rétention à l'engorgement on observe que x_e ne dépend que du rapport des débits. Connaissant ce dernier par l'expérience, on peut calculer x_e. La Fig. 7 permet de comparer les valeurs de x_e calculées et mesurées. Les points se répartissent autour de la première bissectrice avec un écart moyen égal à 6,7%.

Tenant compte des expressions de la capacité de la colonne, on observe que si l'on porte sur un graphique V_{de} en fonction de $x_e^2(1-x_e)$, on doit obtenir une droite passant par l'origine, de pente $2V_0$. C'est ce que nous avons vérifié avec le système eau — kérosène utilisé. Les Fig. 8...10 indiquent les droites obtenues avec différentes fréquences et amplitudes. Le débit à l'engor-

gement (capacité de la colonne) dépend directement de la vitesse caractéristique V_0 et par suite des paramètres de pulsation (amplitude, fréquence).

Tableau 2

Résultats expérimentaux concernant la rétention à l'engorgement

af cm/s	V_d/V_c	x_e (exp)	af cm/s	V_d/V_c	x_e (exp)
0,483	1,000	0,320	1,830	1,375	0,36
0,750	1,060	0,340	0,970	1,380	0,36
1,000	1,100	0,340	0,750	1,460	0,365
1,300	1,090	0,340	1,950	1,500	0,365
0,725	1,060	0,340	2,670	1,500	0,362
1,500	1,080	0,340	1,000	1,670	0,380
2,750	1,100	0,320	1,300	1,600	0,380
0,970	1,000	0,280	1,830	1,670	0,380
1,350	1,090	0,340	1,500	1,600	0,380
0,750	1,260	0,360	1,330	1,650	0,380
1,125	1,210	0,340	1,330	2,570	0,400
1,500	1,250	0,360	1,830	2,600	0,400
0,483	1,390	0,360	2,000	2,670	0,400
0,483	1,320	0,360	1,300	2,500	0,400
1,000	1,380	0,340	1,500	2,600	0,420

Nous avons cherché à connaitre les variations de la vitesse caractéristique des gouttes, V_0, en fonction des paramètres de la pulsation. La Fig. 11 montre les variations de V_0 en fonction du produit af pour trois amplitudes différentes. Les valeurs V_0 qui y figurent sont calculées pour chaque expérience. On constate que pour des pulsations peu intenses ($af<0,1$ cm/s) les points s'alignent sensiblement sur une droite. Lorsque le produit af devient supérieur à 0,1 cm/s, les points se répartissent sur des courbes différentes, qui correspond chacune à une amplitude déterminée.

Enfin, au-dela de 3 cm/s, V_0 présente une tendance à être pratiquement constante.

L'étude de l'engorgement de la colonne en phase organique continue a donné des résultats qui sont en bon accord avec les relations de T h o r n t o n dans le cas d'un fonctionnement en phase aqueuse continue (système toluène—eau) et vérifiées par D e f i v e s et collaborateurs [5] dans les mêmes conditions pour le système heptane—eau.

La connaissance des courbes indiquant les variations de la vitesse caractéristique des gouttes, V_0, en fonction du produit de l'amplitude par la fréquence permet de déterminer le domaine où l'engorgement ne se produit pas et où il est possible d'utiliser la colonne d'extraction. En effet, pour une pulsation donnée, V_0 est connue, et on peut tracer la droite correspondante de pente $2V_0$ sur le graphique V_{ae} en fonction de $x_e^2(1-x_e)$. Cette droite coupe les courbes de débit de kérosène constant tracées sur ce même graphique (Fig. 12). Les points d'intersection déterminent les débits limites et les rétentions maximales à ne pas dépasser sous peine d'atteindre l'engorgement.

4.2. Étude de l'influence de la phase continue sur la capacité de la colonne

La deuxième série d'expériences sur la capacité de la colonne a été consacrée à l'étude de l'influence de la nature de la phase continue. Les résultats obtenus (Fig. 13) montrent que la capacité de la colonne en phase aqueuse continue est supérieure à celle déterminée en phase organique continue. En effet, lorsque les plateaux sont mouillés par la phase dispersée (fonctionnement en phase organique dispersée et phase aqueuse continue), les gouttes brisées sous l'influence de l'agitation des phases dans l'appareil se regroupent en mouillant les plateaux, la dispersion est donc moins fine, la rétention de la phase dispersée est moins forte et les gouttes se déplacent plus rapidement dans l'appareil.

Ce type de fonctionnement, quoiqu'il permet d'obtenir des capacités plus élevées, n'est pas bénéfique : d'une part, la coalescence sur les plateaux mouillés par la phase dispersée, en réduisant l'aire de contact entre les phases, peut conduire à une diminution de l'efficacité de l'extracteur. D'autre part les gouttes de grosse dimension qui se forment près des plateaux peuvent provoquer des changements locaux de phase continue ou même amener une inversion totale de l'émulsion. En conséquence, le fonctionnement de la colonne dans de telles conditions est moins stable et le transfert de masse est plus faible.

Tenant compte de ces considérations on comprend aisément pourquoi, dans les procédés d'extraction sur colonne à plateaux, on utilise comme phase continue celle qui mouille préférentiellement les plateaux.

Dans notre cas, l'emploi des plateaux en téflon nous a amené à prendre comme phase continue celle organique pour toutes les expériences. Ce type d'opération, appelé fonctionnement en phase organique continue, présente comme résultat la formation d'un interface en bas de la colonne. Cette situation est très bénéfique en hydrométallurgie nucléaire pour les opérations d'extractions où le soluté est transféré de la phase aqueuse vers celle organique (extraction du nitrate d'uranyl par le tri-*n*-butyl phosphate (TBP)—kérosène) puisqu'elle permet de résoudre l'important problème de la formation de crasse. En effet, dans la colonne pulsée, on a constaté qu'aucun encrassement ne prend naissance dans la partie utile de la colonne et que les crasses se rassemblent à l'interface unique de celle-ci. L'interface étant en bas de la colonne il est plus aisé d'effectuer des soutirages périodiques pour maintenir la quantité de crasse à un niveau convenable sans troubler le fonctionnement de l'extracteur. D'autre part, il arrive souvent que les crasses aient tendance à suivre préférentiellement une des phases. Pour peu que les crasses suivent la phase aqueuse, elles peuvent ainsi être éliminées naturellement en continu avec le raffinat.

5. Conclusions

La présente étude sur le comportement hydrodynamique et les conditions d'engorgement d'une colonne d'extraction à pulsations pour un contre-courant de deux liquides immiscibles a permis de tirer les conclusions suivantes :

1. Il existe trois zones opératoires essentiellement différentes : a) zone mélangeur--décanteur ; b) zone émulsion ; c) zone engorgée par insuffisance ou par excès de pulsations.

2. La capacité de la colonne dépend essentiellement des conditions de pulsations.

3. La rétention à l'engorgement ne dépend que du rapport des débits de phases.

4. Lorsque l'amplitude des pulsations augmente, le rapport des surfaces entre la zone émulsion et la zone mélangeur—décanteur augmente.

5. Pour une intensité de pulsation donnée il est possible de déterminer les débits limites et les rétentions maximales à ne pas dépasser sous peine d'atteindre l'engorgement.

6. Les équations de T h o r n t o n ont été vérifiées pour le fonctionnement de la colonne en phase organique continue avec le système eau — kérosène utilisé.

7. Le fonctionnement en phase aqueuse continue permet d'obtenir une capacité de la colonne plus grande mais ce type de fonctionnement est moins stable et le transfert de masse serait plus faible qu'en marche en phase organique continue.

Notations

a — amplitude de pulsation, [cm] ;
f — fréquence de pulsation, [mn^{-1}],
V_c — vitesse de passage de la phase continue (débit rappoté à la section transversale de la colonne), [cm/s] ;
V_d — vitesse de passage de la phase dispersée, [cm/s] ;
V_0 — vitesse caractéristique des gouttes aux conditions : $V_c=0$ et $V_d \to 0$;
V_{de}, V_{ce} — vitesse de passage à l'engorgement respectivement de la phase dispersée et de la phase continue ;
x_e — rétention de la phase dispersée à l'engorgement (fraction volumique de la phase dispersée à l'engorgement).

Reçue le 1 février 1989

Haut Commissariat à la Recherche,
Centre de Developpement des Matériaux,
Alger, Algérie

BIBLIOGRAPHIE

1. S e g e G., W o o d f i e l d F. W., Chem. Eng. Prog., **50**, 396 (1954).
2. W i e g a n d t H. F., von B e r g R. L., Chem. Eng., **61**, 7, 183 (1954).
3. G a y l e r R., R o b e r t s N. W., P r a t t H. R. C., Trans. Inst. Chem. Eng., **31**, 57 (1953).
4. T h o r n t o n J. D., Trans. Inst. Chem. Eng., **35**, 316 (1957).
5. D e f i v e s D., D u r a n d e t J., G l a d e l Y. I., Revue I.F.P., **11**, *2*, 231 (1956).
6. R o u y e r H., Journées techniques Caen, France, 11—15 Mai 1976, CEA— CONF.3 615.
7. R o u y e r H., L e b o u e l l e c J., H e n r y E., BIST CEA, *184*, 29 (1973).
8. L o g s d a i l D. H., S l a t e r M. J., *Handbook of Solvent Extraction*. Wiley-Interscience, New York, 1983, 355.
9. Y u Y. H.., K i m S. D., Can. J. Chem. Eng., **65**, 752 (1987).

STUDIUL UNEI COLOANE CU PULSAȚII PENTRU EXTRACȚIA LICHID—LICHID

I. Comportarea hidrodinamică ; capacitatea coloanei

(Rezumat)

Se studiază comportarea hidrodinamică și condițiile de înec ale unei coloane pulsate cu talere perforate, din politetrafloretilenă, în absența transferului de masă. Faza continuă a fost cea organică.

Au fost verificate ecuațiile bazate pe conceptul de viteză caracteristică, utilizîndu-se sistemul apă—kerosen.

BULETINUL INSTITUTULUI POLITEHNIC DIN IAŞI
Tomul XXXV (XXXIX), Fasc. 3—4, 1989
Secţia II
CHIMIE ŞI INGINERIE CHIMICĂ

C. D. 67

INVESTIGATIONS CONCERNANT LE COMPORTEMENT DE LA LAINE COMME COMPOSANT DE COPULATION[1])

PAR

SAVEL IFRIM

1. Introduction

La fibre de laine est un produit biologique cellulaire, de nature protéïque, ayant une structure histologique très complexe.

Dans la composition d'une fibre de laine il y a trois couches principales, constituées de kératine à savoir:

1. La couche cuticulaire ou la cuticule, qui se trouve à la surface de la fibre et a un aspect caractéristique; elle est formée par des écailles; la cuticule, ayant une densité plus élevée que la couche corticale, protège la fibre.

2. La couche corticale, nommée également cortex, représente la plus importante partie de la fibre de laine; elle constitue le corps proprement-dit de la fibre et détermine presque exclusivement les propriétés physiques de celle-ci.

3. La couche médulaire, ou le canal médulaire, se trouvant dans l'intérieur de la fibre; pour les laines fines cette couche peut absenter. Dans ce travail elle n'est pas impliquée.

La kératine, qui constitue les deux premières couches, n'est pas identique ni par sa composition en α-aminoacides et par conséquent ni par ses propriétés physiques et chimiques. Ainsi on connait que dans la couche cuticulaire manque la tyrosine et que le pourcentage de 6% en tyrosine contenu dans la fibre de laine se trouve pratiquement dans la constitution du cortex. De point de vue quantitatif le cortex représente environ 90% de la fibre de laine, tandis que la cuticule, seulement 10%.

Compte tenu de la réaction P a u l y [1], qui est une réaction de couleur utilisée à l'identification du début de dégradation de la fibre, dans le présent travail on a poursuivi si la fibre de laine ne peut pas être teintée par un simple traitement avec des sels de diazonium, la macromolécule de kératine ayant le rôle de composant de copulation.

Dans la réaction P a u l y les sels de diazonium copulent avec les noyaux aromatiques, en résultant des colorants azoïques [2]:

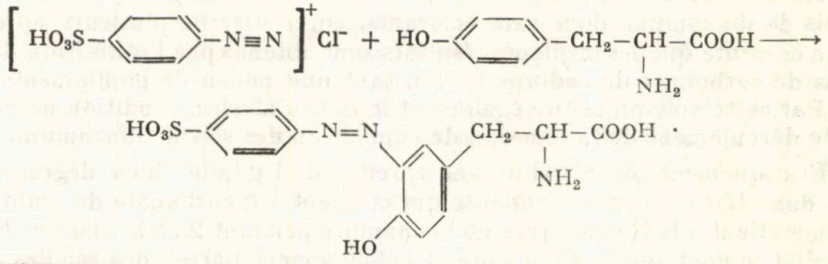

[1]) Communication présentée au III-ème Congrès National de Chimie, 21—24 septembre 1988, Bucarest.

Si la couche écailleuse de la fibre de laine est partiellement détruite, le sel de diazonium peut pénétrer vers la couche corticale où le pourcentage de tyrosine est élevé et par conséquent la fibre est teinte d'une façon plus intense.

Dans le présent travail on prend en considération le fait que non seulement la tyrosine et la histidine peuvent copuler avec les sels de diazonium, mais également la phénylalanine et le tryptophane, compte tenu que ces acides aminiques ont aussi des noyaux aromatiques dans leur structure chimique. De même on considère qu'il n'est pas nécessaire que la couche écailleuse soit détruite pour permettre la pénétration des sels de diazonium a l'intérieur de la fibre, vers le cortex, mais il est suffisant que la fibre de laine soit soumise à un simple processus de gonflement, quand les écailles s'éloignent un peu du cortex, de telle manière que l'accessibilité des réactifs chimiques soit favorisée.

2. Partie expérimentale

Les premières épreuves effectuées dans le laboratoire ont poursuivi à vérifier si les acides aminiques ayant des noyaux aromatiques, utilisés chacun d'eux isolés, copulent avec les sels de diazonium. Ont été soumis à cette vérification la tyrosine, l'histidine, la phenylalanine et le tryptophane. Dans ce but on a dissous 1 g de ces acides aminiques, chacun séparément, dans 50 ml solution diluée de carbonate de sodium 1%. Parallèlement on a préparé les sels de diazonium obtenus par la diazotation de l'acide sulfanilique, de la *p*-nitroaniline, de la β-naphtylamine et de la benzidine, en travaillant selon les méthodes connues. On a soumis à la diazotation 1 g de chaque composant diazotable. Par introduction des ces sels de diazonium dans les solutions alcalines des acides aminiques, refroidies à une température sous 5°C, chacune séparément, on a constaté qu'il se produit, à grande vitesse, la réaction de copulation, parce que dans tous le cas ont apparu rapidement des changements évidents de couleur. Par copulation il apparait de belles colorations de jaune, orange, marron, marron-rougeâtre et rouge. Les colorants résultés sont solubles dans le milieu de copulation.

On a effectué des épreuves de copulation également avec d'autres acides aminiques (proline et hydroxyproline) sans obtenir des résultats positifs ; les solutions alcalines des ces acides aminiques n'ont pas changé leur couleur par l'introduction des sels de diazonium.

Ensuite on a étudié la possibilité de teindre la laine par traitement avec des sels de diazonium, donc sans colorants. On a effectué plusieurs épreuves et on a constaté que les meilleurs résultats sont obtenus par l'utilisation des solutions de carbonate de sodium 1% en tant que milieu de gonflement de la fibre. Par cette voie on assure également le milieu alcalin, condition nécessaire pour le déroulement de la réaction de copulation des sels de diazonium.

Pratiquement on introduit une épreuve de 1 g laine, bien dégraissée et lavée, dans 100 ml solution aqueuse qui contient 1 g carbonate de sodium et on la maintient à la température de la chambre pendant 2...3 h. Dans ce temps se produit le gonflement de la fibre et l'éloignement partiel des écailles de la couche cuticulaire. Ensuite on refroidit à 3...4°C et on introduit le sel de diazonium (bien entendu sous agitation continue), qui a aussi la même tempé-

rature baisse. Au moment de l'introduction du sel de diazonium il apparait un faible coloriage de la laine, mais au fur et à mesure que le temps passe, environ 40...60 min., le coloriage s'intensifie et la laine prend une belle et uniforme nuance.

La quantité d'amine soumise à la diazotation a été prise en excès par rapport à la fibre de laine, en pesant 0,4...0,5 g. Dans ce cas aussi on a soumis à la diazotation l'acide sulfanilique, la *p*-nitroaniline, la β-naphtylamine et la benzidine. On indique ci-dessous les nuances obtenues :

Laine + acide sulfanilique diazoté . . . . . marron-clair
Laine + *p*-nitroaniline diazotée . . . . . marron-rougeâtre
Laine + β-naphtylamine diazotée . . . . . marron
Laine + benzidine diazotée (tetrazotée) . . . rose-foncé

3. Interprétation des résultats

Il est bien connu que le gonflement de la fibre se produit par simple introduction de la laine dans l'eau, parce que la kératine possède un grand nombre de groupements hydrophiles libres, qui peuvent retenir les molécules de l'eau par l'intermédiaire des liaisons hydrogène [3]. Comme résultat du gonflement apparait la croissance du diamètre de la fibre avec 18%. Le gonflement de la fibre a lieu aussi dans les solutions des agents de gonflement (substances avec la structure moléculaire semblable aux détergents); les solutions aqueuses de carbonate de sodium (pH =11) à la température de la chambre favorisent aussi en bonne mesure le gonflement de ce matériel fibreux. Compte tenu que le carbonate de sodium est très accessible et à bon marché, en assurant également les conditions nécessaires à la copulation, il est recommandable pour être utilisé en pratique comme agent de gonflement.

Les épreuves qualitatives effectuées dans ce travail conduisent à la conclusion que dans la structure chimique de la kératine de la laine il y a quatre acides aminiques qui peuvent copuler avec les sels de diazonium. Du point de vue quantitatif ces acides aminiques totalisent plus que 12% du poids de la fibre de laine [4]. Compte tenu du fait que le tryptophane se trouve aussi en plus grande quantité dans le cortex [5], [6], il résulte que dans cette couche le pourcentage en acides aminiques qui peuvent copuler avec les sels de diazonium est d'environ 14%. Ce pourcentage est assez élevé pour conférer à la couche corticale de la fibre de laine la propriété générale de se comporter comme composant de copulation.

Le fait que l'intensification du colorriage a lieu dans un temps plus prolongé conduit à la conclusion qu'il se produit un processus de diffusion des sels de diazonium vers la couche corticale où a lieu la réaction de copulation. Dans ce cas la kératine de la laine manifeste le rôle de composant de copulation. On peut considérer qu'il se forment des colorants macromoléculaires fibreux, qui correspondent aux suivants structures chimiques, où Ar représente le reste d'amine aromatique qui a été soumise à la diazotation :

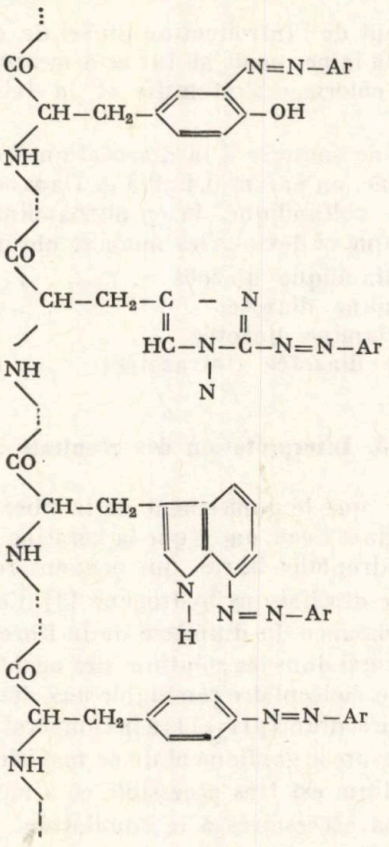

Il n'est pas impossible que dans le cas de la benzidine tétrazotée, par copulation apparaissent de nouveaux ponts transversaux, qui puissent réticuler la kératine.

Une telle teinture de la laine, par simple traitement avec des sels de diazonium à froid, présente plusieurs et importants avantages à savoir : a) on évite la consommation d'énergie nécessaire à apporter la flotte de teinture à l'ébullition; b) la résistance de la teinture est meilleure parce que le colorant a résulté par la formation de liaisons covalentes entre la kératine et les sels de diazonium; c) pour appliquer dans la pratique ce procédé de teinture de la laine ne sont pas nécessaires d'installations spéciales. Compte tenu que dans la pratique on utilise des sels de diazonium stabilisés, ce procédé commode de teinture de la laine devient encore plus important.

5. Conclusions

On étudie la possibilité de teindre la laine par simple traitement à froid avec des sels de diazonium. On montre que les α-aminoacides ayant des noyaux aromatiques dans leur composition. forment des colorants azo-

iques par traitement avec des sels de diazonium. Le pourcentage élevé des ces acides aminiques dans la structure du cortex de la fibre de laine confère à celle-ci la propriété de jouer le rôle de composant de copulation.

Par traitement de la laine avec des solutions de carbonate de sodium, à froid, le processus de pénétration vers le cortex des sels de diazonium est favorisé. Par greffage des sels de diazonium sur les macromolécules de kératine résulte des „colorants macromoléculaires fibreux", la kératine de la laine en se comportant comme un composant de copulation. Ce procédé s'avère commode et très économique pour teindre la laine à froid.

Reçue le 25 novembre 1988

Institut Polytechnique, Jassy,
Chaire de Chimié générale et Technologie

BIBLIOGAPHIE

1. Agster H., *Färberei und Textilchemische Untersuchungen.* Spinger Verlag, Berlin, 1956.
2. Toma I., Giuglea A., Industria textilă, **13**, *3*, 105 (1962).
3. Mauro A., Laniera, *1*, 37 (1977).
4. Ifrim S., *Chimia lînii.* Ed. Tehnică, Bucureşti, 1979, 57.
5. Miró P., Bull. I.T.F., **94**, 65 (1961).
6. Simmonds D.H., Burtulovich J.J., Text. Res. J., **28**, 378 (1958).

CERCETĂRI PRIVIND COMPORTAREA LÎNII DREPT COMPONENTĂ DE CUPLARE

(Rezumat)

Se cercetează posibilitatea vopsirii lînii prin simplă tratare cu săruri de diazoniu, la rece Se pune în evidenţă faptul că acizii aminici care au nuclee aromatice în compoziţia lor formează coloranţi azoici prin tratare cu săruri de diazoniu. Procentul ridicat în aceşti acizi aminici, în componenţa cortexului, conferă lînii proprietatea de a juca rolul de componentă de cuplare.

Prin tratarea lînii cu soluţii de carbonat de sodiu, la rece, procesul pătrunderii către cortex a sărurilor de diazoniu este favorizat.

Grefînd săruri de diazoniu pe cheratină rezultă coloranţi macromoleculari fibroşi. Se pune în evidenţă un procedeu comod şi economic de vopsire a lînii.

BULETINUL INSTITUTULUI POLITEHNIC DIN IAŞI
Tomul XXXV (XXXIX), Fasc. 3—4, 1989
Secţia II
CHIMIE ŞI INGINERIE CHIMICĂ

C. D. 547.53.024 ; 615-015.37

STRUCTURES AMIDIQUES AVEC ACTION SUR LE SYSTÈME NERVEUX CENTRAL.

I. N-(ARYLAMIDOMÉTHYL)-CARBAMATES D'ALKYLE[1])

PAR

CANDIANO LEONTE, EUGENIA CARP, SAVA DUMITRESCU, ŞT. CILIANU et RODICA BOZGA

1. Introduction

Dans les recherches antérieures [1],...,[5] on a montré que la condensation en milieu acide des N-hydroxyméthyl-amides aliphatiques (I) avec l'uréthane — comme réactif nucléophile — conduit aux dérivés N,N'-diacylés de la méthylène-diamine (II) :

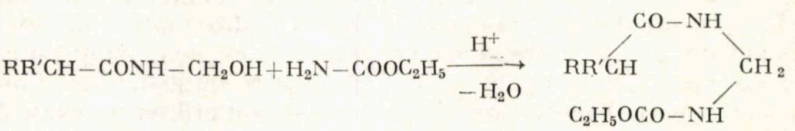

(I) (II)

La conformation quasicyclique des structures (II) présente une évidente similitude avec certains anticonvulsivants cycliques tels les barbituriques ((III), X=O) ou la primidone ((III), X=H_2, R=C_6H_5, R'=C_2H_5).

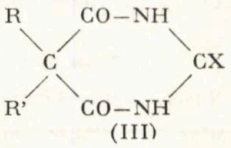

(III)

Les essais pharmacologiques [6],...,[8] ont mis en évidence l'action anticonvulsivante de plusieurs représentants des structures acycliques du type (II), par exemple pour R=H et R'=C_6H_5 respectivement $ClCH_2$ (exception surprenante pourtant pour l'analogue acyclique de la primidone (I), R=C_6H_5, R'=C_2H_5, qui présente une action néurostimulatrice). Une recherche approfondie sur le dérivé (II) (R=H, R'=C_2H_5) a prouvé dans toutes les expériences, l'efficacité de ce produit dans l'administration orale, sa toxicité réduite, l'absence des propriétés hypnotiques, ainsi qu'une faible activité sédative ; la courte durée d'action, conséquence probable d'une métabolisation rapide, représente son principal désavantage. Il paraît que cette classe de composés, facilement accessibles, constitue une interessante source de nouveaux médicaments pour le traitement de l'épilepsie.

2. Recherches théoriques

Dans le but d'obtenir de représentants munis d'une action prolongée, de dépister éventuellement d'autres types d'actions sur le système nerveux

---

[1]) Communication présentée au III-ème Congrès National de Chimie, Bucarest, 21—24 septembre 1988.

et aussi d'élargir la gamme des dérivés de cette classe — comme prémisses de la corrélation entre la structure et l'activité —, on a étudié et préparé, dans ce travail des structures similaires, dérivées de la benzamide, N-(arylamidométhyl)-carbamates d'alkyle (VII). Ces produits ont été obtenus par la condensation en milieu acide de quelques N-hydroxyméthyl-benzamides (V) (celles-ci étant obtenues par l'action du formaldéhyde en catalyse basique sur les benzamides correspondantes, (IV) (v. les Tableaux 1 et 3) avec le carbamate d'éthyle et/ou de méthyle ((VI), $R' = C_2H_5$, CH_3) (v. les Tableaux 2 et 4) :

$$\underset{(IV)}{R-C_6H_4-CONH_2} \xrightarrow{CH_2O/HO^-} \underset{(V)}{R-C_6H_4-CONH-CH_2OH} \xrightarrow[-H_2O]{H_2N-COOR'/H^+ \ (VI)} \underset{(VII)}{R-C_6H_4-CO-NH-CH_2-NH-COOR'}$$

Les benzamides substituées (IV) (R indiqué dans les tableaux), utilisées pour la synthèse des produits (V) et (VII), sont, à l'exception du composé (IV) (R_7), des substances connues. En partant des amides correspondantes, les synthèses des produits (VII) ont été réalisées en conditions douces, un peu différentes de celles utilisées antérieurement pour l'obtention des composés (II) [1],...,[3], [5]. Pour la préparation des N-hydroxyméthyldérivés (V) un rapport molaire de 1 : 1 entre l'amide et le formaldéhyde (appliqué d'habitude dans le cas des amides aliphatiques) s'est montré insatisfaisant, l'amide ne réagissant que partiellement ; on a été donc obligé d'utiliser un excès de 0,4... 0,5 moles de formaldéhyde pour un mole d'amide aromatique (v. le Tableau 3).

Les N-hydroxyméthyl-benzamides obtenues sont, à l'exception des dérivés (V) ($R_{1-3, 5, 8}$), des produits nouveaux, dont la structure est confirmée par les analyses élémentaires et les données spectrométriques (IR).

Tableau 1

N-Hydroxyméthyl-benzamides (V)

Nr.	R	Formule moléculaire	Rendement %	*F* (décomp.) °C
1	H	$C_8H_9NO_2$	98	104...106
2	(*o*) CH_3	$C_9H_{11}NO_2$	93	112...113
3	(*o*) CH_3O	$C_9H_{11}NO_3$	90	100
4	(*o*) Cl	$C_8H_8ClNO_2$*)	91	100...103
5	(*p*) CH_3O	$C_9H_{11}NO_3$	91	130
6	(*p*) CH_3S	$C_9H_{11}NO_2S$*)	99	130
7	(*p*) $(n-C_3H_7)_2N-SO_2$	$C_{14}H_{22}N_2O_4S$*)	93	114
8	(*p*) NO_2	$C_8H_8N_2O_4$	96	136...137
9	(*p*) F	$C_8H_8FNO_2$*)	79	136
10	(*p*) Cl	$C_8H_8ClNO_2$*)	98	145
11	(*p*) Br	$C_8H_8BrNO_2$*)	99	136
12	(*p*) I	$C_8H_8INO_2$*)	88	167...168

*) N-Hydroxyméthyldérivés qui ne sont pas décrits dans la littérature.

Pour les dérivés (V) connus, l'application des conditions indiquées dans le Tableau 3 a conduit à des résultats meilleurs par rapport aux autres procédés décrits dans la littérature.

En ce qui concerne la réaction ultérieure des N-hydroxyméthylamides on a constaté, de même, que, pour un rapport d'équivalence entre les réactifs, le produit de condensation (VII), isolé du milieu réactionnel, est en général plus ou moins contaminé avec de N-hydroxyméthyldérivé non transformé, ce qui a imposé l'utilisation d'un excès de carbamate (VI) (v. le Tableau 4).

À l'exception du dérivé (VII) (R=H, R'=C_2H_5), décrit dans la littérature comme un produit de la transposition de l'hippurazide (selon C u r t i u s) en milieu éthanolique [9], les N-(benzamidométhyl)-carbamates d'alkyle présentés dans le Tableau 2 sont des substances nouvelles, dont la structure est confirmée par les analyses élémentaires, les spectres en IR et, dans le cas du produit (VII) (R=(*p*) Cl, R'=C_2H_5), par la RMN-^{1}H.

Tableau 2

N-(Benzamidométhyl)-carbamates d'alkyle (VII)

Nr.	R	R'	Formule moléculaire, [litt.]	Rendement (rapporté à (V)) %	*F* °C (solvant)
1	H	C_2H_5	$C_{11}H_{14}N_2O_3$ [11]	60	169...171[a]) (éthanol)
2	(*o*) CH_3	C_2H_5	$C_{12}H_{16}N_2O_3$	80	153...154 (éthanol—eau)
3	(*o*) CH_3O	C_2H_5	$C_{12}H_{16}N_2O_4$	77	160 (éthanol—eau)
4	(*o*) Cl	C_2H_5	$C_{11}H_{13}ClN_2O_3$	57	162...163 (éthanol—eau)
5	(*p*) CH_3O	C_2H_5	$C_{12}H_{16}N_2O_4$	68	171 (éthanol)
6	(*p*) CH_3S	C_2H_5	$C_{12}H_{16}N_2O_3S$	36	178...179 (éthanol ; acétate d'éthyle)
7	(*p*) $(n-C_3H_7)_2N-SO_2$	C_2H_5	$C_{17}H_{27}N_2O_5S$	78	144 puis 158 (éthanol—eau)
8	(*p*) NO_2	C_2H_5	$C_{11}H_{13}N_2O_5$	80	180 (éthanol)
9	(*p*) NO_2	CH_3	$C_{10}H_{11}N_3O_5$	95 (brut)	252...253 (acétone)
10	(*p*) F	C_2H_5	$C_{11}H_{13}FN_2O_3$ [12]	42	144...146 (acétate d'éthyle)
11	(*p*) Cl	C_2H_5	$C_{11}H_{13}ClN_2O_3$ [13]	70...75	169...171 (éthanol, méthanol)
12	(*p*) Cl	CH_3	$C_{10}H_{11}ClN_2O_3$ [14]	78	206...207 (méthanol)
13	(*p*) Br	C_2H_5	$C_{11}H_{13}BrN_2O_3$ [11]	88	174...175 (acétone)
14	(*p*) I	C_2H_5	$C_{11}H_{13}IN_2O_3$ [11]	65	196 (acétone)

a) Litt. [9] : 162°C (èthanol) ; [10] : 166°...167°C (benzène).

Tableau 3

Conditions de synthèse des N-hydroxyméthyl-benzamides (V)

Nr.	R	CH_2O*) mol/mol (IV)	Eau**) mol/mol (IV)	K_2CO_3 g/mol (IV)	Acétone***) ml/mol (IV)	Température de reaction °C	Temps de chauffage min	Purification
1	H	1,5	100	10	—	40	10...15	*a*
2	(*o*) CH_3	1,5	100	10	—	52	5	*b*
3	(*o*) CH_3O	1,5	100	10	—	52...55	10	*b*
4	(*o*) Cl	1,5	100	10	—	54	5	*b*
5	(*p*) CH_3O	1,8	100	10	—	52	16	*b*
6	(*p*) CH_3S	4,3	100	17	—	59	7	*c*
7	(*p*) $(n-C_3H_7)_2\ N-SO_2$	1,5	0...100	12	—	65	15	*c*
8	(*p*) NO_2	2,7	700	14	47	60...62	12	*c*
9	(*p*) F	2,7	700	14	47	50...70[d])	12	*a*
10	(*p*) Cl	2,7	700	14	47	50...70[d])	10...11	*c*
11	(*p*) Br	5	1 000	20	60	50...70[d])	12	*a*
12	(*p*) I	4	1 000	20	155	50...70[d])	12	*a*

*) Solution aqueuse 35 %.
**) Ajoutée au formol sous forme de solution de K_2CO_3.
***) Ajoutée après l'introduction de l'amide, pour humectation.

a — Trituration avec d'acétate d'éthyle, 4 ml/g.
b — Précipitation du produit dissous en acétone par le CCl_4.
c — Produit utilisé sans purification supplémentaire.
d — Augmentation de la température entre les limites indiquées.

Tableau 4

Conditions de synthèse des N-(benzamidométhyl)-carbamates d'alkyle (VII)

Nr.	R′	R′	Carbamate d'alkyle mol/0,1 mol V	HCl conc. ml/0,1 mol V	Solvant ml/0,1 mol V	Température de réaction °C	Temps de chauffage min.
1	H	C_2H_5	0,3	15	eau : 100	55	5
2	(*o*) CH_3	C_2H_5	0,6	14	eau : 30 ; dioxane : 75	60	15
3	(*o*) CH_3O	C_2H_5	0,6	5	eau : 22	60	8
4	(*o*) Cl	C_2H_5	0,6	9	eau : 22	60	3...4
5	(*p*) CH_3O	C_2H_5	0,7	10	eau : 25	60	4
6	(*p*) CH_3S	C_2H_5	0,6	8	eau : 22	60	1...2
7	(*p*) $(n-C_3H_7)_2N-SO_2$	C_2H_5	0,6	28	eau : 40 ; dioxane : 460	60	20
8	(*p*) NO_2	C_2H_5	0,6	H_2SO_4 conc. : 3 ml	acide acétique : 37	57...60	5
9	(*p*) NO_2	CH_3	0,6	H_2SO_4 conc. : 3 ml	acide acétique : 37	56...60	2
10	(*p*) F	C_2H_5	0,3	10	eau : 60	55	8
11	(*p*) Cl	C_2H_5	0,6	28	eau : 37 ; dioxane : 167	55	15
			0,6	H_2SO_4 12 N : 26	eau : 37 ; acétone : 167	65	15
12	(*p*) Cl	CH_3	0,6	H_2SO_4 12 N : 13	eau : 56*)	66...67	8...9
13	(*p*) Br	C_2H_5	0,7	H_2SO_4 12 N : 33	eau : 33 ; acétone : 207	65	15
14	(*p*) I	C_2H_5	0,7	H_2SO_4 12 N : 33	eau : 62 ; acétone : 202	60...61	13...14

*) Masse de réaction humectée avec de l'acétone (10 ml).

Les expériences effectuées sur des souris blanches et des rats indiquent, pour certains produits du type (VII), une action anticonvulsivante prolongée ; les structures *p*-halogénées sont les plus intéressantes du point de vue pharmacologique. Le dérivé *p*-fluoré est le plus actif ; les produits *p*-chlorosubstitués avec R=(*p*) Cl, R′ = C_2H_5 ou CH_3 présentent des activités comparables, le dernier étant moins toxique. Les études cliniques sur le dérivé R=(*p*) Cl, R′=C_2H_5 ont confirmé l'activité anticonvulsivante chez l'homme et ont dépisté un effet décontracturant chez des malades présentant des lésions nerveuses centrales [15]. Il nous semble très probable que le produit de métabolisation de ce composé soit l'acide *p*-chlorohippurique, hypothèse qui reste à verifier. L'acide lui-même s'est montré, dans les essais effectués, inactif sur le SNC. Le composé *p*-nitrosubstitué ((VII), R=(*p*)NO_2, R′=C_2H_5) ne présente aucune activité anticonvulsivante. En ce qui concerne les autres dérivés indiqués dans le Tableau 2, leur action anticonvulsivante est sans intérêt. D'autres résultats de l'étude pharmacologique des produits du type (VII) seront communiqués ultérieurement.

Même les *p*-halogénobenzamides de départ ne sont pas privées d'action sur le SNC, mais leurs effets inhibiteurs sont moins sélectifs et la toxicité plus importante par rapport à ceux des dérivés (VII).

3. Partie expérimentale

3.1. Produits de départ et intermédiaires

A. *Amides (IV)*. La préparation des benzamides substituées, en tant que connues, a été effectuée selon la littérature, parfois avec des modifications, ou suivant les méthodes générales.

a) *p-(N,N-di-n-propyl-sulfamoyl)-benzamide* ((IV), R=(*p*)($n-C_3H_7)_2N-SO_2$). On chauffe à reflux sur un bain d'eau, pendant une heure, un mélange de 0,1 mol d'acide *p*-(N,N-di-*n*-propyl-sulfamoyl)-benzoïque (probénécide) et de 0,17 mol de chlorure de thionyle. On ajoute ensuite 40 ml de benzène anhydre et on distille sous pression réduite l'excès de chlorure de thionyle et le benzène. Après refroidissement on dissout le solide résiduel (chlorure acide) dans 190 ml de dioxane anhydre et à cette solution on ajoute goutte à goutte, en secouant vigoureusement, 19 ml d'ammoniaque concentré. On verse le mélange réactionné dans un excès d'eau froide. L'amide brute, isolée par filtration, lavée avec de l'eau et séchée à l'air, est ensuite recristallisée dans l'éthanol (environ 12 ml/g). Rendement 86 %; *F*=181°C. La structure est confirmée par les analyses élémentaires (C, H, N) et le spectre IR.

B. *N-Hydroxyméthyl-benzamides* (V) (Tableau 3) [16].

a) *Mode opératoire général*. On introduit la benzamide (IV), recristallisée et finement pulvérisée, dans une solution aqueuse de formaldéhyde (1,5...5 mol/mol amide), la quantité d'eau étant en général comprise entre 100 et 1 000 ml/mol amide, solution alcalinisée au préalable avec du K_2CO_3 (10...20 g/mol amide) ; dans le cas des amides fortement hydrophobes ($R_{8...12}$) on en favorise l'humectation par addition d'acétone. Le mélange est chauffé sur un bain d'eau, avec légère agitation, à 50°...70°C, pendant 5...15 min., selon la concentration du formol et la température de réaction. Après refroidissement on dilue avec de l'eau le mélange réactionnel (si celui-ci est trop consistant) et le produit précipité (solide ou huile qui cristallise) est isolé par filtration sous vide, lavage répété avec de l'eau froide jusqu'à la disparition de l'alcalinité dans le filtrat et séchage à l'air ou sous vide sur $CaCl_2$. Compte tenu de l'instabilité thermique des N-hydroxyméthylamides (scission de CH_2O), la recristallisation par chauffage des composés de ce type est en général évitée. Dans certains cas la substance est purifiée par dissolution en acétone et précipitation avec de CCl_4. Une pureté analytique satisfaisante est atteinte quelquefois par simple trituration de la substance sèche avec d'acétate d'éthyle (4 ml/g).

3.2. N-(Arylamidométhyl)-carbamates d'alkyle (VII) (Tableau 4)

Le tableau 4, qui résume les conditions de la synthèse des produits de condensation en catalyse acide des N-hydroxyméthyl-benzamides (V) avec les carbamates d'alkyle (VI), nécessite quelques commentaires. Dans la plupart des cas la réaction s'effectue en milieu aqueux, par l'introduction de la N-hydroxyméthylamide pulvérisée dans la solution acide de l'uréthane (l'addition d'un peu d'acétone (v. Nr. 12) favorise l'humectation du solide), suivie de quelques minutes de chauffage sur un bain d'eau, sous légère agitation. Pendant cet intervalle se produit le passage du solide en solution et la précipitation du produit, accompagnée en général de la formation d'une masse consistante. Dans ce cas le mélange est d'abord dilué avec de l'eau, puis tamponné avec d'acétate de sodium (sous forme de cristaux ou de solution concentrée) et refroidi. Le produit est ensuite isolé par filtration sous vide, lavage avec de l'eau jusqu'à la disparition dans le filtrat de l'anion du catalyseur acide et séchage à l'air. Quelquefois la condensation a été effectuée en ajoutant à la solution aqueuse acide de l'uréthane une solution (ou suspension) chaude (environ 60°...65°C) du dérivé N-hydroxyméthylique dans dioxane ou acétone ; dans ces cas (Tableau 4, Nr. 2, 7, 11, 13 et 14), pour une précipitation quantitative du produit, le mélange doit être finalement dilué avec une quantité plus importante d'eau. Comme milieu de condensation on a utilisé aussi une solution de H_2SO_4 concentré en acide acétique glacial (Tableau 4, Nr. 8, 9), lorsque la séparation du composé se produit après l'alcalinisation du mélange final avec une solution de soude.

Les solvants utilisés pour recristallisation et les températures de fusion de produits (VII) sont présentées dans le Tableau 2. Le composé (VII) (Nr.7) se comporte, entre 144°...158°C, comme un cristal liquide. Les produits de condensations (VII) avec $R'=CH_3$ exigent pour recrystallisation des volumes excessivement grands de solvant. Les rendements (rapportés aux N-hydroxyméthylamides) sont en général satisfaisants. Les substances obtenues sont cristallines, incolores, peu solubles dans l'eau.

On présente, ci-dessous, la synthèse du N-(*p*-chlorobenzamidométhyl)-carbamate d'éthyle (VII), R=(*p*) Cl, $R'=C_2H_5$) en partant de la *p*-chlorobenzamide, dans une variante qui implique une succession continuelle d'opérations, dont la durée totale est inférieure à 8 heures.

À une solution de 67 ml de formol 35%, 233 ml d'eau et 4,5 g de K_2CO_3, on ajoute 50 g de *p*-chlorobenzamide recristallisée et pulvérisée. Apres humectation avec 15 ml d'acétone, on chauffe sur un bain d'eau, sous agitation, en augmentant la température, pendant 8...9 min., de 50° à 70°C. Aprés la formation d'une masse pâteuse on continue le chauffage et l'agitation encore 1...2 min., le mélange est ensuite refroidi, dilué avec 110 ml d'eau et gardé à froid pendant une heure et puis filtré sous vide. La tourte, bien lavée avec de l'eau et pressée sur le filtre, est ensuite introduite dans un balon de 2 l. On ajoute une solution de 164 g d'uréthane dans 400... 500 ml d'acétone, 24 ml d'eau et 82 ml de H_2SO_4 12 N et on chauffe à reflux, pendant 15 min. à 65°C, en secouant légèrement le balon. On refroidit et on tamponne l'acidité minérale avec une solution aqueuse 9...10% d'acétate de sodium. On conserve à froid pendant quelques heures et on sépare ensuite le produit par filtration sous vide. On lave avec de l'eau distillée jusqu'à la disparition dans le filtrat de l'ion sulfate ($BaCl_2$ 6%). On continue le lavage avec du méthanol froid (au total 100...150 ml) et, sans séchage préalable, on recristallise la substance en utilisant la quantité nécessaire de méthanol (environ 12,5 ml/g produit sec). $F=170$°C ; rendement (par rapport à l'amide) environ 75%.

Reçue le 12 janvier 1989

Institut Polytechnique, Jassy,
Chaire de Chimie et Technologie Organique
et Macromoleculaire

BIBLIOGAPHIE

1. Zugrăvescu I., Leonte C., Petrovanu O., Anal. Şt. Univ. „Al. I. Cuza", Iaşi, S.I, **VI**, *4*, 1 045 (1960).
2. Zugrăvescu I., Leonte C., Petrovanu O., Anal. Şt. Univ. „Al. I. Cuza", Iaşi, S.I, **IX**, *1*, 219 (1963).
3. Petrovanu O., Zugrăvescu I., Anal. Şt. Univ. „Al. I. Cuza", Iaşi, S.Ic, **XIV**, *1*, 59 (1986).
4. Zugrăvescu I., Petrovanu O., Leonte C., Melianu E., Brevet RSR., *57 363*, 23 janvier 1970.

5. Petrovanu O., *Cercetări privind condensarea unor N-hidroximetilamide cu reactanţi nucleofili*. Thèse de doctorat, Univ. „Al. I. Cuza", Iaşi, 1971.
6. Brînzei P., *Premiers essais pharmacologiques sur II (R=H, R'=C_6H_5)* non, (publié).
7. Moisă L., *Studiul farmacologic al unor substanţe anticonvulsivante noi, de sinteză din clasa diacilmetilen diaminazelor*. Thèse de doctorat, Univ. „Al. I. Cuza", Iaşi, 1969.
8. Chiosa L., Dumitrescu S., Manolescu V., Nicolescu-Catargi A., Neurologia, Psihiatria, Neurochirurgia (Buc.), **15**, 201 (1970).
9. Curtius Th., J. pr. (2), **52**, 266 (1985).
10. Neher R., Wettstein A., Miescher K., Helv., **29**, 1 824 (1946).
11. Leonte C., Carp E., Dumitrescu S., Cilianu Şt., Bozga R., Bobulescu V., Brevet R.S.R., *86 563*, 15 janvier 1985.
12. Carp E., Leonte C., Cilianu Şt., Bogza R., Brevet R.S.R., *87 212*, 25 janvier 1985.
13. Leonte C., Carp E., Cilianu Şt., Neubauer G., Dumitrescu S., Bobulescu V., Brevet R.S.R., *73 870*, 15 fevrier 1980.
14. Leonte C., Carp E., Cilianu Şt., Dumitrescu S., Bobulescu V., Brevet R.S.R. nr. *86 612*, 15 janvier 1985.
15. Nemţeanu E., Popescu C.D., Dumitrecu S., Pathologie du Système Nerveux Péripherique, Symp. Roum.-Bulg., juin 1987.
16. Leonte C., Carp E., Cilianu Şt., Bogza R., Brevet R.S.R., *94 551*, février 1988.

STRUCTURI AMIDICE CU ACŢIUNE ASUPRA SISTEMULUI NERVOS CENTRAL

I. N-(Arilamidometil)-carbamaţi de alchil

(Rezumat)

Prin condensarea în cataliză acidă a unor N-hidroximetil-benzamide (V) (obţinute prin acţiunea formaldehidei în mediu bazic asupra benzamidelor corespunzătoare) cu carbamaţii de etil şi metil, s-au obţinut structuri noi de tipul N-(benzamidometil)-carbamaţilor de alchil (VII), produşi cu acţiune anticonvulsivantă, de interes farmacologic fiind mai ales derivaţii *p*-halogenosubstituiţi.

BULETINUL INSTITUTULUI POLITEHNIC DIN IAȘI
Tomul XXXV (XXXIX), Fasc. 3—4, 1989
Secția II
CHIMIE ȘI INGINERIE CHIMICĂ

C.D. 547.53.0.24 ; 615—015.3

STRUCTURES AMIDIQUES AVEC ACTION SUR LE SYSTÈME NERVEUX CENTRAL

II. N-BENZYL-ARYLAMIDES[1])

PAR

EUGENIA CARP, CANDIANO LEONTE, SAVA DUMITRESCU, ȘT. CILIANU et RODICA BOGZA

1. Introduction

Il est connu que l'action anticonvulsivante d'un composé à fonction amide ne dépend pas rigoureusement d'une structure cyclique. Dans l'article précédent [1] nous avons montré que certains dérivés diacylés de la méthylène-diamine, comme les N-(arylamidométhyl)-carbamates d'alkyle (I) :

(I) $X-C_6H_4-CO-NH-CH_2-NH-COOR$

surtout les structures *p*-halogénées, présentent des propriétés anticonvulsivantes (ainsi que d'autre types d'action sur le SNC). Le N-(*p*-chlorobenzamidométhyl)-carbamate d'éthyle ((I), $X=(p)$ Cl, $R=C_2H_5$) a été soumis à des études pharmacologiques approfondies, en se trouvant actuellement en recherche clinique. On connaît aussi l'activité anticonvulsivante d'un autre produit acyclique, la N-benzyl-β-chloropropionamide (béclamide, (II)) [2]...[4] :

(II) $Cl-CH_2CH_2CO-NH-CH_2-C_6H_5$

2. Considérations théoriques

Dans ce travail on a préparé, afin d'effectuer des études pharmacologiques, des benzylamines acylées du type (III) (v. le Tableau 1) :

(III) $(p)\ R-C_6H_4-CH_2-NH-CO-C_6H_4-R'(p)$

des produits amidiques relativement simples qui réunissent dans leurs molécules des groupements constitutifs des structures (I) et (II). Parmi ces produits on a trouvé des représentants intéressants du point de vue de l'action sur le SNC.

Les dérivés (III) ont été préparés par le traitement des benzylamines correspondantes ($R=H$, Cl, NO_2) avec les chlorures de benzoyle *p*-substitués ($R'=F$, Cl, NO_2), en effectuant l'acylation dans un système à deux phases : benzène (chlorure acide) — eau (benzylamine, hydroxyde alcalin), mode opératoire commode qui s'est montré plus avantageux que la variante conventionelle de Schotten-Baumann en ce qui concerne les rendements et la pureté des produits. Les structures (III), qui, à l'exception du produit avec $R=H$, $R'=NO_2$, sont des substances nouvelles, ont été caractérisées par les analyses élémentaires et les données spectrales en IR.

[1]) Communication présentée au III-ème Congrès National de Chimie, Bucarest, 21—24 septembre 1988.

Tableau 1

N-Benzyl-benzamides (III)

Nr.	R	R′	Formule moléculaire	Rendement en produit brut*), [%]	*F* °C (solvant)
1	H	F	$C_{14}H_{12}FNO$	(76)	114...146 (éthanol)
2	H	Cl	$C_{14}H_{12}ClNO$	93 (87)	168...169 (méthanol ou éthanol)
3	H	NO_2	$C_{14}H_{12}N_2O_3$	88 (46)	141,5...142,5 (éthanol ou acétone**))
4	Cl	Cl	$C_{14}H_{11}Cl_2NO$	74	174,5...175,5 (méthanol ou éthanol)
5	Cl	NO_2	$C_{14}H_{11}ClN_2O_3$	86,4	177...178 (éthanol)
6	NO_2	Cl	$C_{14}H_{11}ClN_2O_3$	92,5	165 (méthanol ou acétone)
7	NO_2	NO_2	$C_{14}H_{11}N_3O_5$	80	217,5...218,5 (décomp.) ; 220...221 (décomp.) (acétone***))

*) On indique, entre paranthèses, le rendement en produit brut obtenu par l'application de la variante conventionnalle de Schotten-Baumann.
**) Litt. [5] : 141°....143°C (éthanol).
***) Purification par traitement avec de l'acétone à chaud, sans dissolution totale. *F* (décomp.) est variable, selon la vitesse de chauffage.

En ce qui concerne les benzylamines soumises à l'acylation, la *p*-chlorobenzylamine a été obtenue par la réaction de Delépine de l'adduit chlorure de *p*-chlorobenzyle — urotropine, avec un rendement supérieur à celui indiqué dans la littérature [6]. La *p*-nitrobenzylamine a été préparée par l'hydrolyse acide du N-(*p*-nitrobenzyl)-carbamate de méthyle, obtenu à son tour de N-benzyl-carbamate de méthyle (produit aisément accéssible par carbométhoxylation de la benzylamine par le chloroformiate de méthyle), par nitration en conditions différentes et plus précises que celles indiquées dans le travail [7], dont les prescriptions ne nous ont pas conduit à des résultats reproductibles :

$$C_6H_5CH_2NH_2 \rightarrow C_6H_5CH_2-NH-COOCH_3 \rightarrow (p)\ O_2N-C_6H_4CH_2-NH-COOCH_3$$

$$\rightarrow (p)\ O_2N-C_6H_4-CH_2-NH_2$$

Du mélange résultant de la nitration on a réussi à isoler l'isomère *para*, qui est le seul produit difficilement soluble en benzène. Bien que le rendement de la nitration soit relativement faible, l'obtention de la *p*-nitrobenzylamine par cette voie nous semble plus convenable par rapport aux autres possibilités offertes par les informations de la littérature.

Les essais sur des animaux ont mis en évidence des effets généraux anticonvulsivants et antiamphétamine des produits (III). Intérêt pharmacologique présentent surtout les dérivés avec R=H, R′=NO_2 et R=Cl, R′=Cl. Le premier est nettement supérieur au produit (I) (X=(*p*) Cl, R=C_2H_5) en

ce qui concerne l'action envers l'effet létal de la strychnine (l'apparition des convulsions n'étant pas empêchée). Il présente aussi une action antispastique sans diminution de la tonicité normale et sa toxicité est très réduite. Ce composé est soumis à présent à des études pharmacologiques approfondies. Le second produit, possédant une action anticonvulsivante moyenne, exerce en même temps une forte action antiamphétamine et présente une très faible toxicité (5 g/kg souris). Bien qu'avec une intensité pus faible, les autres produits (III) manifestent les mêmes types d'action.

3. Partie expérimentale

3.1. Produits de départ

a) *p-Chlorobenzylamine*

Le chlorure de *p*-chlorobenzyle a été obtenu par la chloration du *p*-chlorotoluène avec le chlorure de sulfuryle en présence de péroxyde de benzoyle [8], d'une manière analogue à la chloration du toluène [9]. Rendement 64% (par rapport au SO_2Cl_2) ; F=29°C.

Le *chlorure de N-(p-chlorobenzyl)-hexaméthylétraminium* a été préparé selon la méthode générale Indiquée dans [10]. Rendement 90%, F (avec décomp.) =203°C [11].

p-Chlorobenzylamine. Selon les indications de la littérature on peut effectuer la scission du composé précédent soit avec SO_2 [12], procédé impliquant l'isolement du sulfite acide de (*p*-chlorobenzylamino)-méthyle, intérmédiare qui est ensuite soumis à l'hydrolyse, soit avec un mélange d'acide chlorhydrique—méthanol [6], variante de la réaction de D e l é p i n e offrant un rendement modéré (60,7%). C'est pourquoi on a préféré à appliquer les conditions originaires de la réaction de D e l é p i n e [13], [14] qui ont conduit à l'amine avec un rendement supérieur (83,7%) [15] ; Eb_6=83...84°C.

b) *p-Nitrobenzylamine*

N-(p-Nitrobenzyl)-carbamate de métyle. À 70 ml (103 g, 1,34 mol) d'acide nitrique, incolore à 82%, refroidi à —2°C, on ajoute en portions 20 g (0,12 mol) de N-benzyl-carbamate de méthyle finement pulvérisé, en agitant continuellement, de sorte que la température, après l'addition de chaque portion, ne dépasse pas 5...7°C, une nouvelle portion étant ajoutée seulement après que la température baisse à 0...2°C. La durée totale de l'introduction du carbamate est d'environ 10...15 min. Le mélange homogène, jaunâtre, est encore agité pendant 30...40 min. sans refroidissement, en évitant pourtant de dépasser la température de 20°C par l'introduction occasionelle du vaisseau dans l'eau glacée. Le liquide est ensuite versé sous agitation sur environ 200 g de glace broyée. On alcalinise avec une solution de soude 18%. Après filtration sous vide, le précipité est dissous dans 150 ml de chloroforme et le résidu obtenu par l'évaporation de la solution lavée avec de l'eau et séchée sur Na_2SO_4 est trituré avec un peu de benzène froid. Le solide est isolé par filtration sous vide, lavage sur le filtre avec du benzène froid et séchage à l'air. On obtient 13 g (51,5%) de produit brut qui est purifié par recristallisation dans le benzène (2 ml/g) et puis dans le méthanol (2 ml/g). Il en résulte 9,4 g (37%) de produit pur, F=109°C, identique avec les substances de référence obtenues par la carbométhoxylation de la *p*-nitrobenzylamine avec du chloformiate de méthyle [7] ou par la transposition de la *p*-nitrophenylacetylazide en méthanol [16], selon C u r t i u s.

p-Nitrobenzylamine. L'hydrolyse du composé précédent a été effectuée en milieu acide, selon la méthode générale appliquée aux uréthanes [17], [18]. Dans un ballon de 250 ml on dissout en chauffant légèrement 21 g (0,1 mol) de N-(*p*-nitrobenzyl)-carbamate de méthyle dans 53 ml d'acide acétique glacial. On ajoute 82 ml d'acide chlorhydrique 20% et on porte à reflux pendant 15 heures. On distille ensuite jusqu'à la formation, à la surface de la masse de réaction, d'une croûte de cristaux. Le résidu, transvasé dans un cristalliseur, et refroidi en bain de glace et le chlorhydrate de la *p*-nitrobenzylamine est isolé par filtration sous vide, sur une frite. On garde à part les eaux et on continue à laver le solide avec de l'acétone. Les cristaux incolores sont séchés sous vide sur NaOH. Rendement 16,5 g (78,3%). Les premières eaux de filtration, après l'évaporation et la trituration du résidu avec de l'acétone pour l'éloignement du matériel non saponifié, fournissent une quantité supplémentaire de sel légèrement coloré, qui est purifié par recristallisation dans l'acidé chlorhydrique dilué 1:1 (10 ml/g). F=250°C(avec décomp.).

3.2. Mode opératoire général d'acylation des benzylamines avec les chlorures de benzoyle dans un système à deux phase benzène—eau [19]

À une solution aqueuse 10% contenant 0,15 mol de NaOH on ajoute 0,1 mol de benzylamine soumise à l'acylation (si celle-ci est utilisée sous forme de chlorhydrate, la solution alcaline 10% doit contenir 0,25 mol de NaOH). En refroidissant avec de l'eau glacée on ajoute graduellement, en agitant légèrement, 0,1 mol de chlorure acide dissout dans 40...60 ml de benzène Le mélange est secoué vigoureusement pendant 15...20 min., intervalle de temps pendant lequel a lieu la précipitation de l'amide (III). Le produit est isolé par filtration sous vide sur une frite, lavage avec de l'eau jusqu'à la disparition de l'alcalinité dans le filtrat et séchage à l'air ou sous vide sur $CaCl_2$. La plupart des impuretés et très petites quantités de produit sont retenues dans la phase organique. Les amides (III), purifiées supplémentairement par recristallisation (v. le Tableau 1), sont des substances incolores ou, dans le cas où R=NO_2, faiblement jaunâtres. Les dérivés (III) (R=H, R'=Cl et NO_2) ont été aussi préparés, mais avec des rendements inférieurs, selon la variante classique de Schotten-Baumann, procédé qu'on a uniquement appliqué pour le produit (III) (R=H, R'=F).

Reçue le 12 janvier 1989

Institut Polytechnique, Jassy,
Chaire de Chimie et Technologie Organique
et Macromoléculaire

BIBLIOGRAPHIE

1. Leonte C., Carp E., Dumitrescu S., Cilianu Şt., Bogza R., Bul. Inst. Polit. Iaşi, **XXXV (XXXIX)**, *1—2*, s. II 67—72 (1989).
2. Kushner S., Cassel R.T., Marton J., Williams J.H., J. Organ. Chem., **16**, 1 283 (1951).
3. Zugrăvescu I., Leonte C., Petrovanu O., Brevet R.S.R., *46 224*, 21 octobre 1966.
4. Leonte C., Petrovanu O., Zugrăvescu I., An. Şt. Univ. „Al. I. Cuza", Iaşi, s.I., **IX**, *2*, 561 (1963).
5. Rügheimer L., Ber., **49**, 596 (1916)
6. Кочетков Н. К., Дудыкина Н. В., ЖОХ, **26**, 2 612 (1956).
7. Baker J.W., Soc., 568, 570 (1927).
8. Karasch M.S., Brown H.C., A.P. 2 302 228 (1940) (Du Pont); J. Am. Chem. Soc., **61**, 2 146 (1939).
9. Curtter H.B., Brown H.C., J. Chem. Educ., **21**, 445 (1944); dans Houben-Weyl, vol. **V/3** ,IV-ème édition, 892 (1962).
10. Angyal S.J., Org. Reactions, **VIII**, 205 (1954).
11. Mayer F., English F.A., Ann., *417*, 78 (1918).
12. Reichert B., Dornis W., Ar., *282*, 100 (1944).
13. Delépine M., Jaffeux P., Bl. [4], **31**, 108 (1922).
14. Delépine M., C.R. Ac. Sci., Paris, **120**, 501 (1895); C.R. Ac. Sci., Paris, **124**, 292 (1897); Bl. [3], **17**, 290 (1987).
15. Carp E., Leonte C., Cilianu Şt., Bozga R., Brevet R.S.R., Nr. enreg. OSIM, *126 260*, 29 décembre 1986.
16. Shriner R.L., Cross J.M., J. Am. Chem. Soc., **60**, 2 338 (1938).
17. Smith P., Org. Reactions, **III**, 380, 383 (1959).
18. Moller F., dans Houben-Weyl, vol **11**/1, IV-ème édition, 948 (1957).
19. Carp E., Leonte C., Cilianu Şt., Bogza R., Dumitrescu S., Bobulescu V., Brevet R.S.R., Nr. enreg. OSIM, *126 259*, 29 décembre 1986.

STRUCTURI AMIDICE CU ACŢIUNE ASUPRA SISTEMULUI NERVOS CENTRAL

II. N-Benzil-arilamide

(Rezumat)

S-au obţinut structuri noi de tipul N-benzil-benzamidelor (III), din benzilaminele corespunzătoare, prin acilare cu cloruri de benzoil, într-un sistem bifazic benzen—apă, procedeu ce oferă randamente mai ridicate decît varianta Schotten-Baumann convenţională. A fost cercetată acţiunea acestor produşi asupra sistemului nervos central.

BULETINUL INSTITUTULUI POLITEHNIC DIN IAŞI
Tomul XXXV (XXXIX), Fasc. 3—4, 1989
Secţia II
CHIMIE ŞI INGINERIE CHIMICĂ

D.C. 547.587.52

NEW MANNICH BASES OF 3-*n* BUTHYL-4-METHYLUMBELLIFERONE

BY

AL. CAŞCAVAL, TATIANA NICOLAESCU, ŞT. BIBIAN-CILIANU and CRISTINEL V. ZĂNOAGĂ

1. Introduction

4-Methylumbelliferone (1) is one of the coumarin derivatives which afforded in Mannich reaction exclusively 8-dialkylaminomethylderivatives [1]. Many of these exhibit very promising properties as stimulating agent for central nervous system (CNS) [2] also remarcable antimicrobial and antifungal activities [3].

2. Theoretical Considerations

Our interest in the synthesis of various oxygen containing heterocycles with marked physiological activities by using different substituted alkyl-hydroxycoumarins led us to undertaken an intensive study concerning the synthesis and reactivity of 3-*n*buthyl-4-methylumbelliferone (2) starting off from then following arguments : the coumarin nucleus is one of the most important component of a variety of pharmacological high active compounds both naturally like VISNADIN [4] (coronary vasodilator and angioprotective agent) or MESHUAGIN [5] (a new plant antibiotic from Meshua Ferrea Linn) and synthetic like CARBOCROMEN (with useful coronary dilatory activity also antifibrilant and antiarhythmic actions [4]).

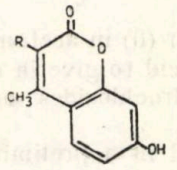

1 : R = H
2 : R = nC_4H_9

We wish here to report our newly results related to modified von Pechmann synthesis of coumarin derivatives [6] of 3-*n*buthyl-4-methylumbelliferone and its reactivity in the Mannich reaction conditions also for

the parent compound 4-methyl-umbelliferone which give the M a n n i c h bases in very mild reaction conditions.

4-Methylumbelliferone (1) and its 3-*n*buthyl derivative (2) react with aqueous formaldehyde solution and cyclic secondary amines (3) at room temperature (15 days) to affors the coresponding 8-cycl-aminomethyl derivatives (4) and (5) :

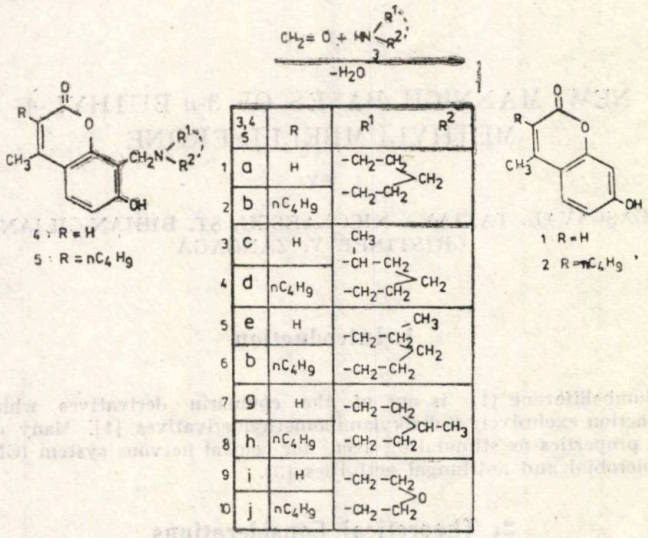

4 : R = H
5 : R = nC_4H_9

1 R = H
2 R = nC_4H_9

3,4 5	R	R^1 R^2
1 a	H	$-CH_2-CH_2$ > CH_2 $-CH_2-CH_2$
2 b	nC_4H_9	
3 c	H	CH_3 $-CH-CH_2$ > CH_2 $-CH_2-CH_2$
4 d	nC_4H_9	
5 e	H	CH_3 $-CH_2-CH_2$ > CH_2 $-CH_2-CH_2$
6 b	nC_4H_9	
7 g	H	$-CH_2-CH_2$ > $CH-CH_3$ $-CH_2-CH_2$
8 h	nC_4H_9	
9 i	H	$-CH_2-CH_2$ > O $-CH_2-CH_2$
10 j	nC_4H_9	

It is interesting to note that by refluxing for a 5 hr. of a mixture of (2) with morpholine and paraformaldehyde results a bis-M a n n i c h base (6) with a good yield :

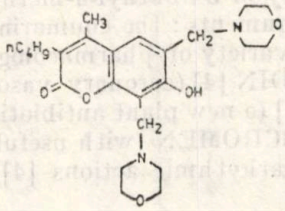

6

A suspension of (4), (5) or (6) in acetone was treated with concentrated hydrochloric or hydrobromic acid to give in near quantitative yields the corresponding water soluble hydrochlorides or hydrobromides also dihydrobromide of (6).

These new salts showed in a preliminary pharmacological screening antihypertensive activity and we hope that the present clinical screenings will offer a new series of drugs interesting from a practical point of view.

We thank Dr. V. B ă r b o i u, Gh. Z. S t o i c a, Z. C i o b a n u and C. B e r n i c from Institute of Macromolecular Chemistry „Petru Poni", Iaşi, Romania, for microanalysis and NMR also IR spectra. One of us (Al. C a ş c a v a l) thank to „Alexander von Humboldt", Bonn-Bad Godesberg, for financial assistance and help during your fellowship also BASF-Ludwigshafen (West Germany) for gift a series of useful intermediates.

Table 1

New Mannich Bases of 4-Methylumbelliferone and its 3-n Buthyl Derivative

Prod.	Yield %	m. p. °C	I. R. ν,[cm^{-1}]	^{1}H—N.M.R. (CDCl$_3$, TMS$_{int.}$) δ,[ppm]
2	45	135...137	3 400 ; 1 720; 1 600 ; 1 210	0.9(*t*, 3H, CH_3) ; 1.45(*s*, 4H, $2CH_2$) ; 2.35(*s*, 3H, CH_3—4) ; 2.75(*t*, 2H, CH_2) ; 6.95(*d*, 1H, H6) ; 7.45(*d*, 1H, H5) ; 8.1(*s*, 1H, OH).
4_a	57	137...138	3 350... 1 720	1.55(*m*, 6H, $3CH_2$) ; 2.35(*s*, 3H, CH_3—4) ; 2.60(*m*, 4H, $2CH_2N$); 4.0(*s*, 2H, CH_2—8); 6.01(*s*, 1H, H—3) ; 6.7(*d*, 1H, H_6) ; 7.4(*d*, 1H, H—5) ; 12.7(*s*, 1H, OH).
4_c	62	156...157	3 400 1 730 ; 1 595 ; 1 210	1.3(d, 3H, CH_3) ; 1.7(*m*, 6H, $3CH_2$) ; 2.35(*s*, 3H, CH_3—4) ; 2.7(*m*, 3H, CH+CH_2) ; 4.2(*m*, 2H, CH_2N) 6.0(*s*, 1H, H—3); 6.6(*d*, 1H, H—6); 7.3(*d*, 1H, H—5); 13.2(*s*, 1H, OH).
4_e	49	104...106	3 350 ; 1 715 1 590 ; 1 200	1.0(*d*, 3H, CH_3) ; 1.8(*m*, 4H, $2CH_2$) ; 2.4(*s*, 3H, CH_3—4) ; 3.0(*m*, 3H, CH+CH_2) ; 4.1(*m*, 4H, $2CH_2$) 6.0(*s*, 1H, H—3) ; 6.6(*d*, 1H, H—6) ; 7.3(*d*, 1H, H—5) ; 13.1 (*s*, 1H, OH).
4_g	64	128...129	3 450 ; 1 715 ; 1 600 ; 1 210	1.0(*d*, 3H, CH_3) ; 1.4(*m*, 7H, $3CH_2$+CH) ; 2.6(*m*, 9H, $2CHN_2$+$2CH_2C$+CH_3) ; 4.0(*s*, 2H, CH_2—8) ; 6.6(*d*, 1H, H—6) ; 7.3(*d*, 1H, H—5) ; 10.7(*s*, 1H).
4_f	59	138...139	3 250 ; 1 740 ; 1 600 ; 1 200	2.4(*s*, 3H, CH_3—4) ; 2.6(*t*, 4H, $2CH_2$) ; 3.8(*t*, 4H, $2CH_2O$) ; 4.1(*s*, 2H, CH_2—N) ; 6,1(*s*, 1H, H—3) ; 6.7(*d*, 1H, H—6) ; 7.4(*d*, 1H, H—5) ; 11.9(*s*, 1H, OH).
5_b	83	105...107	3 400 ; 1 720 ; 1 610 ; 1 200	1.4(*t*, 3H, CH_3) ; 1.7(4H, $2CH_2$) ; 1.55(*m*, 4H, 6H, $3CH_2$) ; 4.0(*s*, 2H, CH_2—8) ; 6.01(*s*, 1H, H—3) ; 6.7(*d*, 1H, H—6) ; 7.5(*d*, 1H, H—5) ; 12.1(*s*, 1H).
5_d	90	117...119	3 400 ; 1 720	1.0(*t*, 3H, CH_3) ; 1.3(*t*, 3H, CH_3) ; 1.4(*m*, 4H, $2CH_2$) ; 1.7(*m*, 6H, $3CH_2$) ; 2.4(*s*, 3H, CH_3—4) ; 2.7(*m*, 3H, CH+CH_2N) ; 4.2(*m*, 2H, CH_2N) ; 6.0(*s*, 1H, H—3) ; 6.6(*d*, 1H, H—6) ; 7.4(*d*, 1H, H—5) ; 12.3(*s*, 1H, OH).
5_f	85	132...134	3 450 ; 1 710 ; 1 600 ; 1 210	1.0(*t*, 6H, $2CH_3$) ; 1.8(*m*, 8H, $4CH_2$) ; 2.4(*s*, 3H, CH_3—4) ; 3.0(*m*, 3H, CH+CH_2) ; 4.1(*m*, 4H, $2CH_2N$); 6.0(*s*, 1H, H—3); 6.6(*d*, 1H, H—6) ; 7.3(*d*, 1H, H—5); 13.2(*s*, 1H, OH).
5_h	57	119...120	3 300 ; 1 725 ; 1 600 ; 1 200	1.0(*d*, 3H, CH_3) ; 1.45(*m*, 7H, $3CH_2C$+CH) ; 2.6(*m*, 9H, $2CH_2C$+$2CH_2N$+CH_3) ; 4.0(*s*, 2H, CH_2—8) ; 6.6(*d*, 1H, H—6) ; 7.3(*d*, 1H, H—5) ; 10.7(*s*, 1H, OH).
5_j	54	92...94	3 400 ; 1 710 ; 1 600 ; 1 200	1.05(*m*, 3H, CH_3); 1.5(*m*,4H, $2CH_2$); 2.4(*s*, 3H,CH_3—4). 2.7(*m*, 6H, $2CH_2N$+CH_2—3); 3.8(*m*, 4H, $2CH_2O$); 4.1(*s*, 2H, CH_2); 6.7(*d*, 1H, H—6) ; 7.4(*d*, 1H, H—5); 10.2(*s*, 1H, OH).
6	59	118...119	3 450 ; 1 710 1 600 ; 1 210	0.9(*t*, 3H, CH_3) ; 1.4(*m*, 4H, $2CH_2$) ; 2.4(*s*, 3H, CH_3); 2.6(*m*, 10H, CH_2—3+$4CH_2N$) ; 3.7(*m*, 8H, $4CH_2O$); 3.9(*s*, 4H, $2CH_2N$); 6.1(*s*, 1H, OH); 7.4(*s*, 1H, H—5).

3. Experimental Results

M. p. : Uncorr., IR spectra : KBr pellets on Perkin Elmer 577 spectrophotometer, NMR spectra : 60 MHz, JEOL C-60 HL, TMS-reference.

a) *1.3.-nButhyl-4-methylumbelliferone (2)*

11 g resorcine with 17 ml methyl 2-*n*buthylacetoacetate at 50°C was stirred with 3 ml concentrated sulphuric acid during 15 min. then was treated with 100 ml water. After crystallization from methanol obtained 9.7 g white prisms m. p. 135°...137°C. All data are presented in Table 1.

b) *2.4 Methyl-8-cycl-aminomethylumbeliferone (4). General Procedure*

To a solution of 4-methylumbelliferone (0.1 mol) and secondary cyclic amine (technical grade, 0.15 mol) in methanol (10 ml) is added aqueous 37% formaldehyde (0.15 mol) and the mixture is allowed to stand at room temperature for 15 days. Cold water is added and the product (4) is recrystallized from acetone (Table 1).

c) *3.3-nButhyl-4-methyl-8-cycl-aminomethylumbelliferone (5). General Procedure*

In a similar manner was been prepared and Mannich bases (5). All experimental data are presented in Table 1.

Received, November 18, 1988

Polytechnic Institute Jassy,
Department of Organic and Macromolecular Chemistry and Technology,
Central Research Institute of Pharmaceutical Chemistry, Bucharest
and
Biological Research Center, Jassy

REFERENCES

1. Desai R.B., J. Org. Chem., **26**, 5 251 (1961).
2. Molho D., Boschetti E., Fr. *1 310 535*, 30. 11. 1962 ; C. A., **58**, 12 517 e (1963).
3. Rao A.K., Raju M.S., Raju K.M., J. Indian Chem. Soc., **58**, 1 021 (1981).
4. Negwer M., *Organisch-chemische Arzneimittel und ihre Synonyma*. Akademie Verlag, Berlin, 1978, 4 389, 4 586.
5. Bhattacharyya P., Chatterjee D., Chakrabarti A., Chakrabarti D. P., Indian J. Chem., **17 B**,, 111 (1979).
6. Caşcaval Al., Nicolaescu T., Cilianu Şt., Petition Patent, OSIM, Bucureşti, *128 838*, 01.07.1987.

NOI BAZE MANNICH ALE 3-*n*BUTIL-4-METILUMBELIFERONEI

(Rezumat)

Sînt prezentate cele mai recente sinteze ale unor mono- şi bis-baze Mannich derivate ale 3-*n*butil-4-metilumbeliferonei, sinteze care constituie o extindere a gamei derivaţilor alchilaţi ai cumarinei hidroxilate în poziţia 7 în vederea testării activităţilor farmacologice. Noile substanţe sînt caracterizate din punct de vedere analitic şi spectral (IR, RMN) şi se obţin în condiţii experimentale blînde.

BULETINUL INSTITUTULUI POLITEHNIC DIN IAȘI
Tomul XXXV (XXXIX), Fasc. 3—4, 1989
Secția II
CHIMIE ȘI INGINERIE CHIMICĂ

D.C. 547.566.6

NEW DERIVATIVES OF *L*-ASPARAGIC ACID WITH POTENTIAL ANTITUMOURAL ACTIVITY

BY

VALERIU ȘUNEL and C. CIUGUREANU

1. Introduction

Among the compounds applied in antitumoral therapy some alkylating derivatives are particularly important.

Their selectivity much depends on the support nature. For instance, the aminoacids, the metabolites, etc., improve the chemiotherapic indices when used as supports.

The *L*-asparagic acid, *L*-asparagine and their acylated derivatives with *p*-substituted benzene ring are known to decrease the toxicity of some drugs and to facilitate their transport at the cell level due their participation to the metabolism of the animal organisms [1]...[19].

Taking these facts into account, the authors of the present paper have synthesized alkylating agents containing di-(β-chloroethyl)-amine as an active component on derivatives of N-[*p*-N′-acylamino)-benzoyl]-*DL*-asparagic acid as supports.

2. Results and Discussions

In the present paper, new di-(β-chloroethyl)-amides with active group supported by N-[*p*-(nicotinoylamino)-benzoyl]-*DL*-asparagic acid and N-[*p*-(nicotinoylamino)-benzoil]-*DL*-asparagine are synthesized.

The intermediates involved in their preparation, such as the N-(aminobenzoyl)-*L*-asparagic acid (I) and the N-(*p*-aminobenzoyl)-*L*-asparagine (II), were obtained by the reduction of the N-(*p*-nitrobenzoyl)-*L*-asparagic acid and the N-(*p*-nitrobenzoyl)-*L*-asparagine by ammonium sulphide [20], [21].

By the acylation of the N-(*p*-aminobenzoyl)-*L*-asparagic acid (I) and the N-(*p*-aminobenzoyl)-*L*-asparagine (II) by the nicotinic acid chloride the N-[*p*-(nicotinoylamino)-benzoyl]-*L*-asparagic acid (III) and the N-[*p*-nicotinoylamino)-benzoyl]-*L*-asparagine (IV) were obtained. These compounds show a potential antitumoural activity acting as metabolites [22].

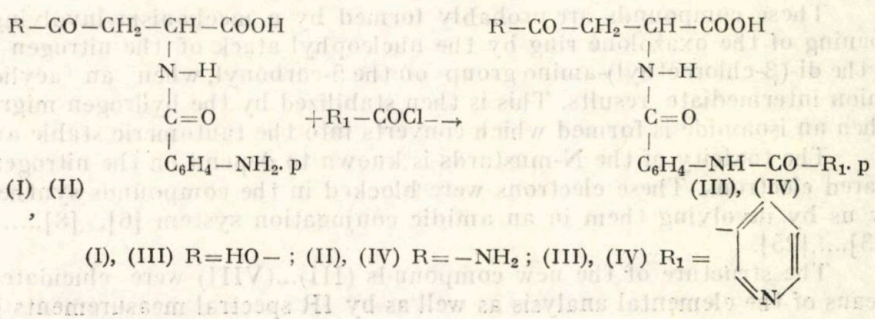

By treating the compounds (III) and (IV) with acetic anhydride under heating, Δ^2-oxazolinones-5 are formed by elimination of an water molecule and cyclization at the α-carboxy group, namely the 2-[*p*-(nicotinoylamino)-phenyl]-4-(β-carboxymethyl)-Δ^2-oxazolinone-5 (V) and the 2-[*p*-(nicotinoyl-amino)-phenyl]-4-(-β-amidomethyl)-Δ^2-oxazolinone-5 (VI) :

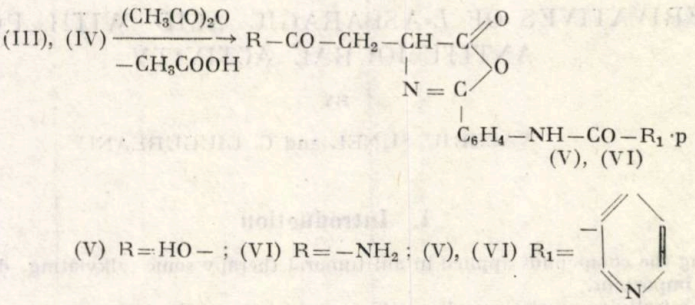

(V) R=HO– ; (VI) R=–NH_2 ; (V), (VI) R_1=

The cyclization is assumed to proceed as given in literature for other Δ^2-oxazolinone-5 types [23].

The reaction of Δ^2-oxazolinones-5 (V) and (VI) with di-(β-chloroethyl)-amine in anhydrous dioxane resulted in formation of N-mustards with the acylated derivatives of the N-(*p*-aminobenzoyl)-*DL*-asparagic acid and the N-(*p*-aminobenzoyl)-*DL*-asparagine as supports. The α-[Di-(β-chloroethyl)-amide] of the N-[*p*-(nicotinoylamino)-benzoyl]-*DL*-asparagic acid (VII) and the α-[Di-(β-chloroetyl)-diamide] of the N-[*p*-nicotinoylamino)-benzoyl]-*DL*-asparagic acid (VIII) were thus obtained :

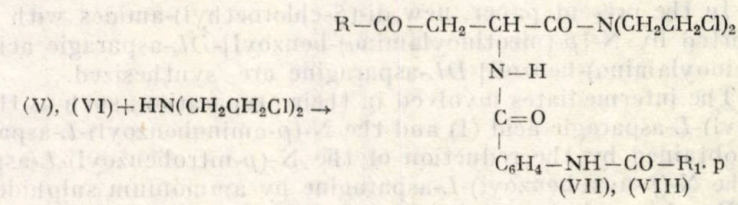

(VII) R=HO– ; (VIII) R=–NH_2 ; (VII), (VIII) R_1=

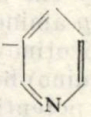

These compounds are probably formed by a mechanism involving the opening of the oxazolone ring by the nucleophyl atack of the nitrogen atom in the di-(β-chloroethyl)-amino group on the 5-carbonyl, when an acylic amphion intermediate results. This is then stabilized by the hydrogen migration when an isoamide is formed which converts into the tautomeric stable amide.

The toxicity of the N-mustards is known to depend on the nitrogen unstared electrons. These electrons were blocked in the compounds synthesized by us by involving them in an amidic conjugation system [6], [8],..., [10], [23],...,[25].

The structure of the new compounds (III)...(VIII) were elucidated by means of the elemental analysis as well as by IR spectral measurements [26].

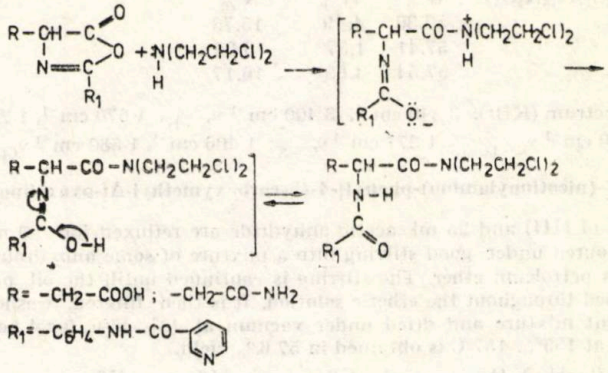

By grafting the N-mustard group on derivatives of the N-[*p*-(N-acyl-amino)-benzoil-*DL*-asparagic acid the improving of the biological properties of the synthesized alkylating agents as well as their toxicity decrease were followed.

3. Experimental

3.1. N-(*p*-aminobenzoyl)-*L*-asparagic acid (I)

It was obtained the reduction of the N-(*p*-nitrobenzoyl)-*L*-asparagic acid by ammonium sulphide [20].

3.2. N-*p*-(aminobenzoyl)-*L*-asparagine (II)

It was obtained by the reduction of the N-(*p*-nitrobenzoyl)-*L*-asparagine by ammonium sulphide [21].

3.3. N-[*p*-(nicotinoylamino)-benzoyl]-*L*-asparagic acid (III)

0.04 moles of N-(*p*-aminobenzoyl)-*L*-asparagic acid in 100 ml water are introduced into a reaction vessel provided with a stirring device and treated with 0.14 moles sodium bicarbonate. 0.04 moles of nicotinic acid chloride are then added stepwise during 30...45 min. The reaction mass is then stirred for another 30 min.

The aqueous solution is acidified by hydrogen chloride (1:1) till pH=2, when a light-yellow solid product separates. It is solved in ethylic alcohol, purified with charcoal and dryied on anhydrous sodium sulphate. The ethanol excess is distilled under vacuum. A colorless solid product separates by cooling which is finally filtred and dried melts at 188°...190°C. Reaction yield 72.8%.

Analyses ($C_{17}H_{15}N_3O_6$)	C%	H%	N%
Calculated :	57.14	4.20	11.76
Found :	57.30	4.62	11.88
	57.35	4.58	11.96

The IR spectrum (KBr): 3 200 cm^{-1}, 3 245 cm^{-1} ν_{N-H}; 1 290 cm^{-1} ν_{C-N}; 1 408 cm^{-1}, 1 582 cm^{-1} ν_{COO}; 860 cm^{-1} $\nu_{C-H\ aromatic}$, 1 190 cm^{-1} ν_{C-O-C}; 1 628 cm^{-1} $\nu_{C=O\ amidic}$.

3.4. N-[*p*-(nicotinoylamino)-benzoyl-*L*]-asparagine (IV)

It was obtained similarly to the compound (III) starting from 0.04 moles N-(*p*-amino-benzoyl)-*L*-asparagine, 0.01 moles sodium bicarbonate and 0.04 moles nicotinic acid chloride. A colorless, solid product, melting at 177°...180°C, was obtained in a yield of 73.6%.

Analyses ($C_{17}H_{16}N_4O_5$)	C%	H%	N%
Calculated :	57.30	4.49	15.73
Found :	57.41	4.57	16.09
	57.54	4.63	16.17

The IR spectrum (KBr): 3 340 cm^{-1}, 3 400 cm^{-1} ν_{N-H}; 1 670 cm^{-1}, 1 728 cm^{-1} $\nu_{C=O\ amidic}$ 1 156cm^{-1}, 1 180 cm^{-1} ν_{C-O-C}; 1 277 cm^{-1} ν_{C-N}; 1 406 cm^{-1}, 1 580 cm^{-1} ν_{COO^-} 860 cm^{-1}.

3.5. 2-[*p*-(nicotinoylamino)-phenyl]-4-(β-carboxymethyl-Δ^2-oxazolinone-5 (V)

0.02 moles of (III) and 25 ml acetic anhydride are refluxed for 90 min. After cooling, the solution is poured under good stirring into a mixture of some anhydrous ethylic ether and 80 ml anhydrous petroleum ether. The stirring is continued untill the oil product precipitates as a solid dispersed throughout the etheric solution. It is then filtered, washed with the above mentioned solvent mixture and dried under vacuum at 40°...45°C for 4 hours. A light-yellow product melting at 155°... 157°C is obtained in 57.6% yield.

Analyses ($C_{17}H_{13}N_3O_5$)	C%	H%	N%
Calculated :	60.17	3.83	12.38
Found :	60.53	4.11	12.60
	60.42	4.18	12.78

The IR spectrum (KBr): 3 285 cm^{-1}, 3350 cm^{-1} ν_{N-H}; 1 154 cm^{-1}, 1180 cm^{-1} ν_{C-O-C} 1 280 cm^{-1} ν_{C-H}; 1 620 cm^{-1} ν_{C-N}; 1 406 cm^{-1} ν_{COO^-}; 880 cm^{-1} $\nu_{C-H\ aromatic}$.

3.6. 2-[*p*-(nicotinoylamino)-phenyl]-4-(β-amidomethyl)-Δ^2-oxazolinone-5 (VI)

0.02 moles of (IV) and 25 ml acetic anhydride are refluxed for 45 min. in a flask on a water both.

The reaction mass is then cooled and poured under stirring into a mixture of 50 ml anhydrous ethylic ether and 60 ml anhydrous petroleum ether. The solvent mixture is then separated by decanting and the remaining viscous mass washed repeatedly with anhydrous ethylic ether till its transformation into a fine powder. It is filtered, washed repeatedly with anhydrous ethylic ether and dried under vacuum for an hours at 45°C. The obtained light-yellow product melts at 164°... 166°C Reaction yield 55.7%.

Analyses ($C_{17}H_{11}N_4O_4$)	C%	H%	N%
Calculated :	60.35	4.14	16.56
Found :	60.43	4.32	16.96
	60.48	4.40	17.01

The IR spectrum (KBr): 3 320 cm^{-1}, 3 520 cm^{-1} ν_{N-H}; 1645 cm^{-1} $\nu_{C-O\ amidic}$ 1 080 cm^{-1} 1 170 cm^{-1} ν_{C-O-C}; 1 306 cm^{-1} ν_{C-N}; 1 620 cm^{-1} ν_{C-N}; 828 cm^{-1} $\nu_{C-H\ aromatic}$.

3.7.. α-[Di-(β-chloroethyl)-amide] of the [*p*-(nicotinoyl-amino)-benzoyl]-*DL*-asparagic acid (VII)

A suspension of 0.01 moles (V) in 50 ml anhydrous dioxan is introduced into a reaction vessel and 0.02 moles of di-(β-chloroethyl)-amine added. The reaction mixture is heated for 90 min. at 60°...70°C The dioxan is then distilled of under vacuum, at 45°...50°C.

The viscous residue is washed repeatedly with anhydrous ethylic ether and then solved in 30 ml ethanol (cooled at +5°C) then anhydrous ethylic ether added under stirring till opalescence appears. The mixture is allowed to stay for 6 hours when gray cristals are formed. After washing with anhydrous ethylic ether the product is dried under vacuum at 40°...45°C for 5 hours.

Melting 190°...192°C. Reaction yield 51.2%.

Analyses ($C_{21}H_{22}Cl_2N_4O_5$)	C%	H%	Cl%	N%
Calculated :	52.39	4.57	14.76	11.64
Found :	52.51	4.68	15.06	11.86
		4.77	15.17	11.94

The IR spectrum (KBr): 3 306 cm^{-1}, 3 350 cm^{-1} ν_{N-H}; 1 680 cm^{-1} $\nu_{C-O\ amidic}$; 1 190 cm^{-1}, 1 204 cm^{-1} ν_{C-O-C}; 1 289 cm^{-1} ν_{C-N}; 1 410 cm^{-1} ν_{COO^-}; 856 cm^{-1} $\nu_{C-H\ aromatic}$ 770 cm^{-1} ν_{C-Cl}.

3.8. α-[Di-(β-chloroethyl)-diamide] of the N-[*p*-(nicotinoyl-amino)-benzoyl]-*DL*-asparagic acid (VIII)

It was obtained similarly to the compound (VII), starting from 0.01 moles product (VI), 50 ml anhydrous dioxan and 0.02 moles di-(β-chloroethyl)-amine. The product is purified by solving it in 20 ml acetone at +10°C and precipitating in 25 ml distilled water. The obtained colorless product melts at 170°...172°C. Reaction yield 51.4%.

Analyses ($C_{21}H_{23}Cl_2N_5O_4$)	C%	H%	Cl%	N%
Calculated :	52.50	4.79	14.79	14.58
Found :	52.66	5.02	15.04	15.00
	52.71	5.15	15.21	14.96

The IR spectrum (KBr): 3 250 cm^{-1}, 3 345 cm^{-1} ν_{NH}; 1 665 cm^{-1} $\nu_{C-O\ amidic}$; 1 152 cm^{-1}, 1 190^{-1} ν_{C-O-C}; 1 320 cm^{-1} ν_{C-N}; 860 cm^{-1} $\nu_{C-H\ aromatic}$; 740 cm^{-1} ν_{C-Cl}.

4. Conclusions

Six new compounds were synthesized by the transformation of both carboxy and amino groups in the N-(*p*-aminobenzoyl)-*L*-asparagic acid and the N-(*p*-aminobenzoyl)-*L*-asparagine.

The amino group in some compounds was acylated with the nicotinic acid chloride, the N-acyl-derivatives (III) and (IV), with potential biological action, acting as antimetabolites, being thus obtained.

The Δ^2-oxazolinones-5 (V) and (VI) were synthesized by the dehydrating action of the acetic anhydride on the N-acyl-derivatives (III) and (IV).

By the decyclization of the Δ^2-oxazolinones-5 (V) and (VI) with di-(β-chloroethyl)-amine new N-mustards (VII) and VIII) of a biological interest were obtained.

The structures of the synthesized products were confirmed by elemental analysis and by IR spectral measurements.

Received, March 15, 1989

Polytechnic Institute, Jassy,
Department of Macromolecular and
Organic Chemistry and Technology

REFERENCES

1. Пушкарева В. Э., Ларйонов Ф. Л., Альфеева В. Е., Крупенова В. А., ЖОХ, **33**, 3379 (1963).
2. Родина В. Л., Уварова М., Пушкарева В. Э., ЖОХ, **34**, 2140 (1964).
3. Паулюконис А., Карпавичюс Ж., Килдишева Б., Кнунянц И., ИАН СССР, ОХН, 133 (1969).
4. Bergel P., Stock A.J., J. Chem. Soc. 4563 (1957).
5. Кнунянц И., Голубева Н. Е., Килдишева В., ДАН СССР, **132** 836 (1960).
6. Budeanu C. H., Şunel V., An. şt. Univ. „Al. I. Cuza", Iaşi, s. Ic, **17**, 207 (1971).
7. Budeanu C. H., Şunel V., An. şt. Univ. „Al. I. Cuza", Iaşi, s. Ic, **18**, 169 (1972).
8. Budeanu C. H., Şunel V., An. şt. Univ. „A.l I. Cuza", Iaşi, s. Ic, **20**, 59 (1974).
9. Budeanu C. H., Şunel V., Iancu I., Dăneţ R., Rev. Medico-Chirurgicală, Iaşi, **77**, 817 (1973).
10. Budeanu C. H., Şunel V., Bul. Inst. polit., Iaşi, **24(28)**, *1—2*, s. II, 95 (1978).
11. Şunel V., Budeanu C. H., Mazilu I., Apostolescu M., Bul Inst. polit, Iaşi, **25(29)**, *1—2*, s. II, 85 (1979).
12. Budeanu C.H., Şunel V., Iorga T., Cecal A., Rev. Farmacia, Bucureşti, **28**, 1 (1980).
13. Budeanu C. H., Şunel V., Ciugureanu C., Rev. de Chimie, **33**, 325 (1982).
14. Şunel V,. Apostolescu M., Budeanu C. H., Dăneţ R., Rev. de Chimie, **3** , 1 099 (1982).

15. Năstase V., Şunel V., Dăneţ R., Rev. Medico-Chirurgicală, Iaşi, **87**, 619 (1983).
16. Şunel C., Cecal Al., Rev. de Chimie, **34**, 394 (1984).
17. Şunel V., Ciugureanu C., Budeanu C.H., Antohe N., Rev. de Chimie, **36**, 397 (1985).
18. Şunel V., Ivas E., Budeanu C.H., Bul. Inst. polit., Iaşi. **33(37)**, *1—4*, s. II, 57 (1987).
19. Şunel V., Ciugureanu C., Budeanu C.H., Rev. de Chimie, **37**, 855 (1986).
20. Budeanu C.H., Şunel V., An. şt. Univ. „Al. I. Cuza", Iaşi, s. Ic, **15**, 67 (1969).
21. Budeanu C.H., Şunel V., An. şt. Univ. „Al.I. Cuza", Iaşi, s. Ic, **20**, 207 (1974).
22. Oiţă N., Şunel V., Surpăţeanu G., Patent R.S.R., Nr. *80 029* (1982).
23. Budeanu C. H., Şunel V., An. şt. Univ. „Al. I. Cuza" Iaşi, s. Ic, **20**, 199 (1974).
24. Şunel V., Ciugureanu C., Budeanu C. H., Antohe N., Popa M., Rev. de Chimie, **39**, 577 (1988).
25. Arnold H., Bourceaux F., Angew. Chem., **70**, 539 (1958).
26. Avram M., Mateescu C. D., *Spectroscopia în infraroşu. Aplicaţii în chimia organică.* Ed. Tehn., Bucureşti, 1966.

NOI DERIVAŢI AI ACIDULUI *L*-ASPARAGIC CU ACTIVITATE ANTITUMORALĂ POTENŢIALĂ

(Rezumat)

În scopul obţinerii de noi substanţe cu posibilă acţiune antitumorală s-a preparat acidul N-[*p*-(nicotinoil-amino)-benzoil]-*L*-asparagic şi N-[*p*-(nicotinoilamino)-benzoil]-*L*-asparagină. Aceştia au fost trecuţi în 2-[*p*-(nicotinoilamino)-fenil]-4-(β-carboximetil)-Δ^2-oxazolinona-5 şi 2-[*p*-(nicotinoilamino)-fenil]-4-(β-amidometil)-Δ^2-oxazolinona-5, care la rîndul lor au fost cuplate cu di-(β-cloretil)-amina.

S-au sintetizat astfel azotiperite cu atomul de azot amidic derivat de la grupa α-carboxilică a acidului N-(*p*-aminobenzoil)-*L*-asparagic şi N-(*p*-aminobenzoil)-*L*-asparaginei.

BULETINUL INSTITUTULUI POLITEHNIC DIN IAŞI
Tomul XXXV (XXXIX), Fasc. 3—4, 1989
Secţia II
CHIMIE ŞI INGINERIE CHIMICĂ

D.C. 66.095.2 ; 678.745 ; 541.459

POLYMERIZATION OF ACRYLONITRILE INITIATED BY THE PEROXYDISULFATE—DI BUNTE SALT REDOX COUPLE

BY

CRISTOFOR I. SIMIONESCU,
Member of the Academy of the Romanian Socialist Republic

VICTOR BULACOVSCHI and CAMELIA MIHĂILESCU

1. Introduction

The peroxydisulfate—thiosulfate redox couple has been intensively studied as an initiation system for free radical polymerization of vinylic monomers, and several transient initiator species were assumed to result from the consumption of the peroxydisulfate and thiosulfate ions throughout the course of the polymerization [1], [2].

In acrylamide redox polymerization Riggs and Rodriguez [2] have found that the thiosulfate radical-ion is unreactive in initiating the process and that at sufficiently high concentrations of this radical, it may complete with monomer in consumption of SO_4 species. Within the studied ranges of peroxydisulfate and thiosulfate concentrations, a half-order dependence of the initial rate on peroxydisulfate and a first-order dependence on initial monomer concentration was reported. However, with other redox systems (chlorate—sulfite [3] and peroxydisulfate—metabisulfite [4]) although initial rates depended on the first power of monomer concentration, the conversion—time data were best fitted by a fivehalves power on the monomer concentration. Recently, Misra et al. [5] have reported a second order dependence on monomer concentration in polymerization of acrylonitrile with cyclohexanone—$KBrO_3$ initiation system.

These results point out on disputable problems in redox free radical polymerization, mainly on the mechanism of inorganic interaction, nature of the initiating species when thiosulfate is a component of the redox couple, and on apparent order with respect to monomer.

The present paper reports data obtained in polymerization of acrylonitrile (AN) initiated by the peroxydisulfate (PDS) — di Bunte salt (DBS) redox system. This study was undertaken particularly to examine if the kinetics and other features of polymerization induced by the mentioned couple of salts would differ from those reported with simple redox vinyl polymerizations. The feature of the above system is that from interaction of PDS and DBS ions, a biradical of di Bunte molecule is expected, which is assumed to be responsable for initiation.

2. Experimental

The di Bunte salt was prepared from sodium thiosulfate and 3,3′-bis (chloromethyl) oxetane in aqueous ethanol [6]. The water soluble product, crystallized from 85% ethanol with three molecules of water of crystallization corresponds to the formula (I) (by IR and elemental analysis).

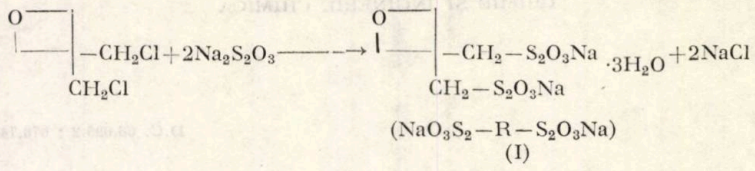

(I)

Solutions of desired concentration from DBS and ammonium PDS (analytical grade) were prepared before every polymerization. Acrylonitrile was purified by normal pressure distillation in atmosphere of dry nitrogen, and fresh aqueous solution was prepared for each run. In all situations a single distilled water was used. Polymerization was carried out in ground-joint conical flasks. Appropiate quantities of a reaction mixture that contained solutions of AN, PDS and DBS were placed in clean conical flasks mounted in a thermostated bath. The mixture was deaerated by bubbling pure nitrogen and polymerization was allowed to proceed at a fixed temperature (± 0.5°C). After an induction period the reaction mixture turns cloudy, thus indicating the onset of polymerization. After definite intervals the flasks were removed from the bath, opened and quenched into a large excess of water containing hydroquinone and HCl. The polymer was filtered off, washed with water and dried to constant weight. The rate of polymerization (R_p) was determined gravimetrically from runs at different initial monomer concentrations.

The average molecular weight of polyacrylonitrile formed was calculated using the formula [7] :

$$[\eta]=39.2\times10^{-3}\overline{M}_n^{0.75},$$

where $[\eta]$ — intrinsic viscosity determined by single point method [8] in DMF at 25°C.

3. Results and Discussion

Polymerization of AN initiated by PDS—DBS redox system at 51°C reveal a short induction period, which becomes longer when low temperatures and low initiator concentrations are employed. As a consequence graphs were ploted after eliminating the induction period.

From preliminary experimental data it was found that $[M]^{-3/2}$ varies linearly in time, suggesting a 2.5 order in monomer for the reaction rate :

$$(1) \qquad -\frac{d[M]}{dt}=R_p=k_2[M]^{5/2}.$$

Subsequently, the rate of polymerization, R_p, was measured within the range of monomer concentration of 0.4055 and 1.0138 M at 51°C. The plot of ln R_p vs. ln $[M]$ gave a straight line with a slope of 2.5 and the plot of R_p vs. $[M]^{2.5}$ was linear passing through origin (Fig. 1), thereby confirming the five-halves order dependence of R_p vs. monomer concentration. A similar conclusion was drawn from time — conversion data obtained for different other polymerization temperatures.

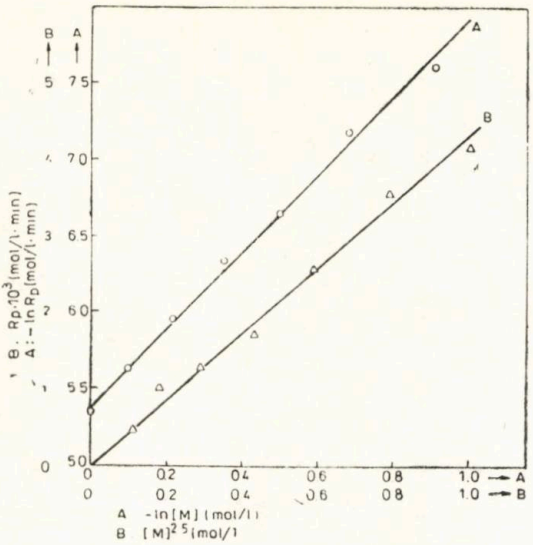

Fig.1. — Plots of $\ln R_p$ vs. $\ln[M]$ (A) and R_p vs. $[M]^{2.5}$ (B), for polymerization of AN at $T=51°C$; $[PDS]=[DBS]=1.66\times10^{-3}$ M.

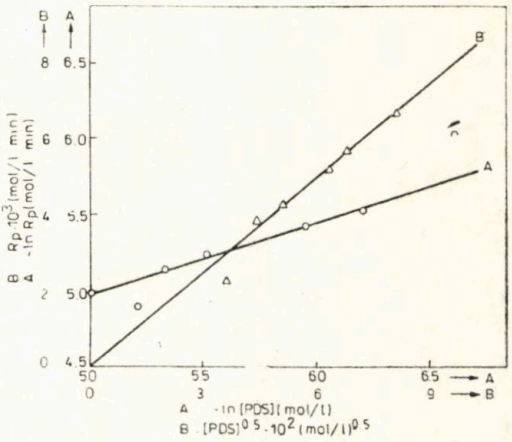

Fig. 2. — Plots of $\ln R_p$ vs. $\ln$ [PDS] (A) and R_p vs. $[PDS]^{0.5}$ (B) for a polymerization with PDS—DBS redox couple; [AN]=1.0138 M; [DSB] $= 1.66\times10^{-3}$ M; $T=51°C$; time=75 min.

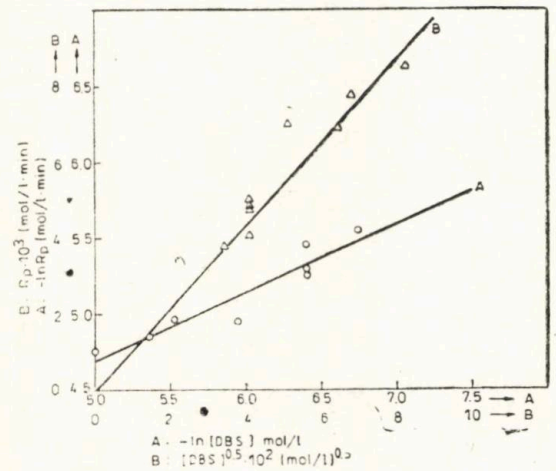

Fig. 3.— Plots of $\ln R_p$ vs. $\ln$ [DBS] (A) and R_p vs. $[DBS]^{0.5}$ (B); [AN]=1.0138 M; $[PDS]=1.66\times10^{-3}$ M; time=75 min.; $T=51°C$.

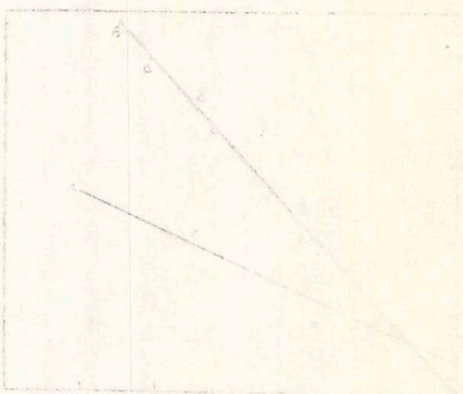

The experimental data show that the rate of polymerization, R_p, increases linearly with the increase of the [PDS] (1.66×10^{-3} ... 6.66×10^{-3} M). Thus, when ln R_p is ploted vs. ln[PDS] a straight line is obtained with a slope of 0.48 (Fig. 2 *A*), and the plot of R_p vs. $[PDS]^{0.5}$ results in a line passing through the origin (Fig. 2 *B*). This shows that the order with respect to [PDS] should be 0.5.

A similar variation of R_p was also noticed with the increase in [DBS] (1.66×10^{-3}... 6.66×10^{-3} M). A plot of ln R_p vs. ln [DBS] is linear having a slope of 0.46 (Fig. 3 *A*), however, when the plot of R_p vs. $[DBS]^{0.5}$ is represented, a straight line passing through the origin is obtained (Fig. 3 *B*), indicating that the order with respect to [DBS] might be 0.5 in these limits of concentrations.

From the above findings it results that R_p is proportional to $[PDS] \times [DBS]^{1/2}$.

Varying the temperature within the 30°... 51°C range, the activation energy could be evaluated using the Arrhenius plot. In such a manner it was calculated to be of 60.65 Kj/mol, a typical value for a free-radical polymerization.

The five-halves order dependence of R_p on monomer concentration contrasts with usual observations that initial polymerization rates are of first order in monomer. Polymerization of AN being a heterogeneous process, it must be considered that between PAN and AN, the formation of organized arrays is possible [9], which reduce the accesible monomer for polymerization:

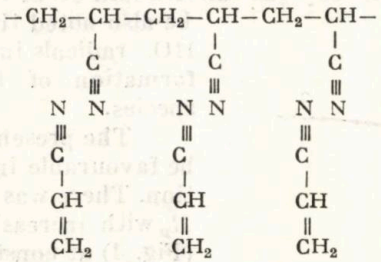

In such conditions the polymerization rate will be of first order in concentration of free monomer $[M]_f$ [3]:

$$R_p \sim [PDS]\,[DBS]^{1/2}\,[M_f]. \tag{2}$$

Provided fraction of the monomer free to participate in the polymerization reaction will depend on the polymer concentration $[P]$ namely:

$$\frac{[M_f]}{[M]} = \left(\frac{[M]}{[M]+[P]}\right)^{3/2}. \tag{3}$$

Since there is no polymer at the beginning of reaction, the sum $[M]+[P]$ is equal to the initial concentration of the monomer ($[M]+[P]=[M]_0$) and from Eqs. (2) and (3) results:

$$R_p = K[PDS][DBS[^{1/2}[M]^{5/2}, \tag{4}$$

where $K \sim [M]_0^{-3/2}$.

Thermal polymerization of AN initiated by PDS alone point out that in the selected conditions, the thermal decomposition of the initiator is almost negligible, so that the $[SO_4^{\cdot-}]$ is very low. As a consequence in the PDS—DBS redox system the free radical initiating species result essentially from the induced decomposition of PDS and they will be of biradical nature :

$$S_2O_8^{2-} + -O_3S_2-R-S_2O_3^- \rightarrow (S_2O_8.O_3S_2-R-S_2O_3)^{4-} \rightarrow \quad (5)$$
$$\rightarrow 2SO_4^{2-} + O_3^{\cdot}S_2-R-S_2O_3^{\cdot} \quad (\text{or .R.})$$

which will promote the polymerization :

$$.R. + (n+m)M \rightarrow .M_n-R-M_m. \quad (6)$$

Several other reactions might be possible if one considers also the thermal decomposition of PDS :

$$S_2O_8^{2-} \rightarrow 2SO_4^{\cdot-}, \quad (7)$$

$$SO_4^{\cdot-} + H_2O \rightarrow HSO_4^- + HO. \quad (8)$$

$$2HO. + {}^-O_3S_2-R-S_2O_3^- \rightarrow 2HO^- + .O_3S_2-R-S_2O_3. \quad (9)$$

or

$$2SO_4^{\cdot-} + .O_3S_2-R-S_2O_3. \rightarrow {}^-O_4S.O_3S_2-R-S_2O_3.SO_4^- \quad (10)$$

The above development show that the free biradicals are consumed in reactions (6) and (10). In presence of monomer, which is highly reactive toward the free radicals, it is unlikely the latter would occur to some extent. It should be also noted that the consumption of HO. radicals in reaction (9) results in formation of the desired initiating species.

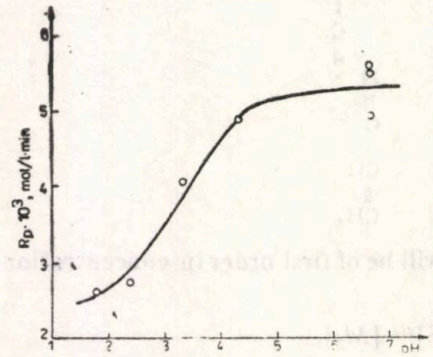

Fig. 4. — Dependence of polymerization rate, R_p, vs. pH.

The presence of HO^- ions seems to be favourable in carrying out the reaction. There was noticed a decrease of R_p with increasing of H^+ concentration (Fig. 4) at constant ionic strength, so that the reactions were run at pH ~ ~6.5...7.

The general expression for the degree of polymerization $\bar{X}_n$ is :

$$\frac{1}{\bar{X}_n} = \frac{R_t}{R_p} + \frac{R_{tr}}{R_p}, \quad (11)$$

where : R_t, $R_.$ and R_{tr} are reaction rates for termination, propagation and transfer, respectively.

Supposing that propagation rate is proportional to first power of monomer concentration, one may write :

$$\frac{1}{\bar{X}_n} = \frac{R_t}{R_p} + C_M + \frac{R_{tr}}{R_p}, \quad (12)$$

where C_M denotes the transfer constant to monomer.

A plot of $1/\bar{X}_n$ vs. R_p gives a curve (Fig. 5), first part of which is a straight line having an interception point with the $\bar{X}_n$ axis offering $C_M = 7.5 \times 10^{-5}$. This denotes that chain transfer reaction to monomer may be ignored. In such conditions several other chain transfer reactions may occur and one of them may involve the reducing agent :

(13) $$.M_n . + {}^{-}O_3S_2-R-S_2O_3^{-} \rightarrow$$
$$\rightarrow S-M_n- S + {}^{-}O_3S-R-SO_3^{-}.$$

The basic assumption in this study was that the initiating species in AN polymerization should be the resulting biradicals. If that is true, then the macromolecular chains should bear units of the type

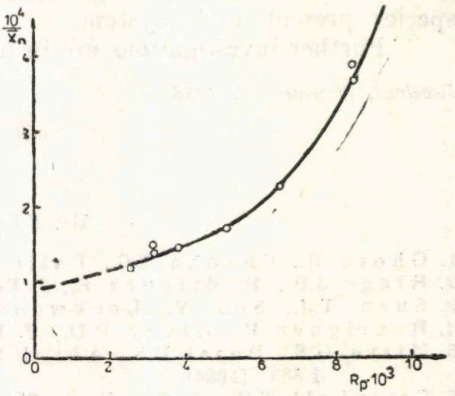

Fig. 5. — Plots of $1/\bar{X}$ vs. R_p; [PDS] = = [DBS] = 1.0×10^{-3}...6.66×10^{-3} M; T = = 51°C; [M] = 1.0138 M.

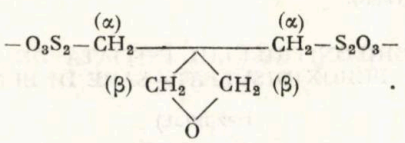

(II)

The ^1H-NMR spectrum of the poly(acrylonitrile) prepared in presence of large ammount of initiator ([PDS] = [DBS] = 6×10^{-2} M) have showed a weak maximum at 4.2 ... 4.5 ppm, which was assigned to $(\alpha)-CH_2-$ protons (Fig. 6). This assignement is supported by the spectra of compounds where $-CH_2-$ protons are in a similar vicinity and which give a signal at 4.2 ppm.

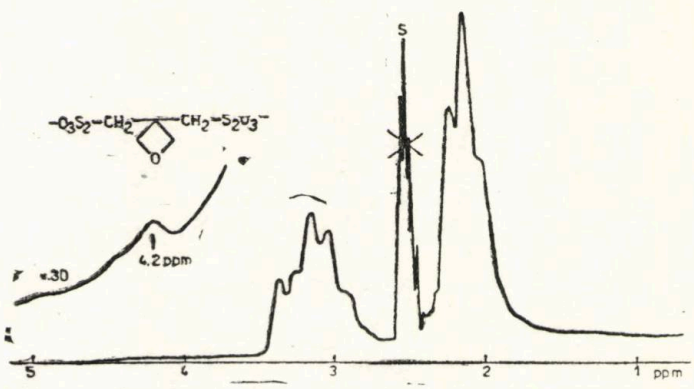

Fig. 6 . — ^1H-NMR spectrum of the polyacrilonitrile prepared by free-radical polymerization wiht PDS—DBS redox system; solvent DMSO—d_6, T = 100°C.

It is worth mentioning that the polymerization of AN with PDS—DBS redox system results in obtaining high molecular weight polymers ($\overline{M}$ = 250,000 ... 300,000). This might be also a consequence of the specific initiating species present in the system.

Further investigations are in progress on this redox couple.

Received, December 5, 1988

Polytechnic Institute, Jassy.
Department of Organic and Macromoleculair Chemisty and Technology

REFERENCES

1. Ghosh P., Chadha S.C., Palit S.R., J. Polym. Sci., **A-2**, 4 441 (1964).
2. Riggs J.P., Rodriguez F., J. Polym. Sci., **A-1**, *5*, 3 167 (1967).
3. Suen T.J., Sen Y., Lockwood J.V., J. Polym. Sci., **31**, 481 (1958).
4. Rodriguez F., Givey R.D., J. Polym. Sci., **55**, 713 (1961).
5. Misra G.S., Bassi P.S., Abrol S.L., J. Polym. Sci., Polym. Chem. Ed., **22**, 1 883 (1984).
6. Campbell T.W., J. Org. Chem., **22**, 1 029 (1957).
7. Lenka S., Nayak P.L., Ray S., J. Polym. Sci., Polym. Chem Ed., **22**, 959 (1984).
8. Rusu M., Bulacovschi V., Mater. plastice (R), **24**, 198 (1987).
9. Burillo G., Chapiro A., Mankowski Z., J. Polym. Sci., Polym. Chem. Ed., **18**, 327 (1980).

POLIMERIZAREA ACRILONITRILULUI INIŢIATĂ DE SISTEMUL REDOX PEROXIDISULFAT—SARE DI BUNTE

(Rezumat)

Se studiază polimerizarea acrilonitrilului (AN) iniţiată de sistemul oxido-reducător peroxidisulfat—sare di Bunte în intervalul de temperatură 30°...51°C.

S-a urmărit efectul variaţiei concentraţiei monomerului, peroxidisulfatului, sării di Bunte şi a ionilor de hidrogen asupra vitezei de consum a monomerului. S-a sugerat că procesul de polimerizare este iniţiat de biradicalii rezultaţi în procesul de oxido-reducere, iar întreruperea decurge prin transfer la agentul reducător.

BULETINUL INSTITUTULUI POLITEHNIC DIN IAŞI
Tomul XXXV (XXXIX), Fasc. 3—4, 1989
Secţia II
CHIMIE ŞI INGINERIE CHIMICĂ

D. C. 66.063.8 ; 678 ; 744.322

POLY(VINYL CHLORIDE) BLENDS

IV. PHYSICO-MECHANICAL PROPERTIES

BY

M. RUSU

1. Introduction

The opportunity of introducing the impact modifiers in unplastified Poly(vinyl chloride) (PVC) blends was so far demonstrated [1], [2]. Also the manner in which they influence the main blend characteristics is known[3]. But there are few studies on the action and the influence of impact modifiers on the unplastified PVC blends, containing filling materials [4]... [7].

Taking into account the special importance of the necessity of using filling materials in the processing of PVC blends [8]...[10] and the possibility of improving their characteristics by adding impact modifiers[4]...[7],[11]...[13], the influence of the chlorinated polyethylene (CPE) type 3 614 A (impact modifier for filled blends) on some physical and mechanical characteristics of the unplastified PVC blends, with and without kaolin as filling materials, is revealed.

2. Experimental Part

In order to find out the influence of adding CPE on physical and mechanical characteristics of the unplastified PVC blends, with and without kaolin, the following formulation was used (parts by weight) : PVC S 67 D— 100 ; tribasic lead sulphate — 2 ; lead soap — 2 ; calcium stearate — 0.3 ; stearin —0.15 ; 0 to 10 parts kaolin and 0 to 10 parts CPE. All materials used and their characteristics, as well as the technique of blend preparation, were the sames as in the previous papers [5] ...[7].

The obtained blends were then mixed on a laboratory two-rolls mixer for 7 min. at a roll temperature of 175°...180°C, drawn in sheets and these transformed in plates of 1... 4 mm in thickness by pressing. Sheets pressing was carried out by the following procedure: 170 daN/cm² for 10 min. and cooling under pressure for 15 min. From the plates, test specimens were cut out and tested for physical and mechanical characteristics (tensile strength, elasticity. modulus, bending strength, Vicat softening point, Shore *D* hardness, density and water absorption).

On the basis of the experimental data concerning the tensile strength of the blends and using the method implemented by Sekisui Chemical Company Ltd. (Japan) for tubes of ELSON type [14], B a r l o w (P_{11}) and N a d a y

(P_{12}) bursting pressure, B a r l o w (P_{21}) and N a d a y (P_{22}) working pressure and minima thickness of the tube walls were calculated for some types of tubes manufactured usually by IPMP, Iaşi (heavy tubes of 50 and 110 mm outer diameter, light type tubes of 50 and 110 mm outer diameter). B a r l o w burst strength means short time stress but N a d a y burst strength refers to a long time stress to pressure.

3. Results and Discussion

The manner in which the CPE and kaolin influence the tensile strength and elasticity modulus of the unplastified PVC blends is represented in Fig. 1. The curves from this figure show that the tensile strength decreases as the content impact modifier increases. The decrease is less at low contents of CPE and becomes appreciable for larger proportions of impact modifier introduced in the system (up to 22% for 10 parts CPE). This behaviour could be explained by the fact that, as the content in CPE increases, the heterogeneity of the system increases too, a fact which unfavourably influences the tensile strength of the blends.

Introduction of 10 parts kaolin into the blends, determines a change in the curve trends. In case of these blends, although the introduction of impact modifier determines a decrease of the tensile strength, the decrease is larger at low contents of CPE and becomes unsignificant as the proportion of CPE in the blends increases.

Taking into account that, due to the greater liophily of the CPE towards the filling material, this concentrates on the surface of its particles changing the structure of the boundary layer [15], [16], the explanation for the manner in variation of the tensile strength vs. content of the impact modifier from the blends, containing 10 parts kaolin could be as following. Low proportions of CPE in the blends determine only a partial modification of the boundary layer from the surface of the kaolin particles, fact which leads to a decrease of the tensile strength. At a certain proportion of the CPE in the blends, the modification of the boundary layer at the particle surface reaches a certain determined level, fact which implies that an additional increase of the CPE content in the blends does not change the tensile strength.

At the same CPE content, the tensile strength of the blends containing 10 parts kaolin is lower than in the case of the blends without filling material, excepting the blends with 10 parts CPE and 10 parts kaolin which the tensile strength is the same as that for the blends without filling material.

The curve that reveals the variation of elasticity modulus against CPE content, for the blends without kaolin, shows a broad maximum corresponding to a domain of 4.0...4.5 parts impact modifier content in the system. The trend is totaly different for the blends with 10 parts filling material, the elasticity modulus decreasing as the CPE content increase in the blends. In the case of this type of blends, the decrease in elasticity modulus is considerable at low CPE content and become less important beyond 4.0 parts impact modifier.

For values exceeding 2.0 parts CPE, the elasticity modulus for the blends containing kaolin is larger than in the case of those without filling material ;

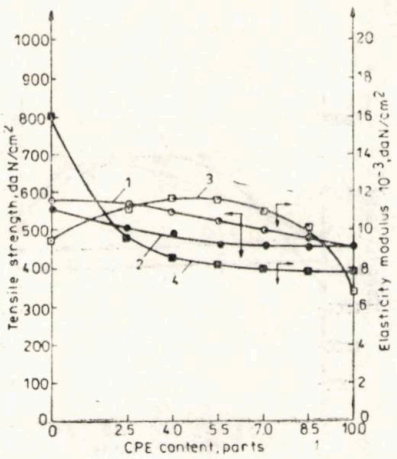

Fig. 1.—Variation of tensile strength and elasticity modulus versus CPE content from the blends : *1, 3*—without kaolin ; *2, 4*—with 10 parts kaolin.

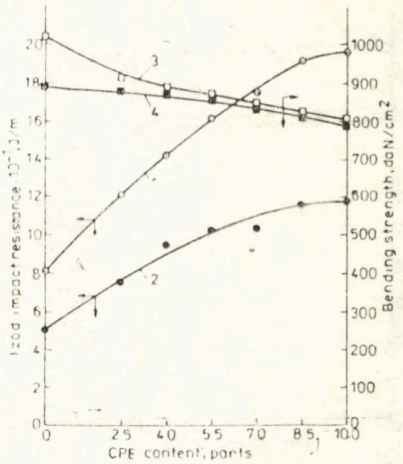

Fig. 2.—Variation of Izod impact resistance and bending strenght versus CPE content from the blends : *1, 3*—without kaolin ; *2, 4*—with 10 parts kaolin.

but at impact modifier content beyond the above mentioned proportion, the trend is reversed.

The impact Izod resistance continuously increases as the content of impact modifier from the blends increases (Fig. 2). The increase is more significant for the blends without kaolin, these, at the same content of CPE, possessing values of impact Izod resistance much larger than for the blends containing filling material.

All the blends containing 10 parts kaolin and more than 3.0 parts CPE have impact resistance larger than control sample (without kaolin and impact modifier). This implies that, by adding more than 3.0 parts CPE in the blends containing kaolin, the decrease of the impact Izod resistance determined by the introduction of the filling material might be avoided.

For the both types of the blends, the bending strength continuously decreases as the proportion of impact modifier increases (Fig. 2). The observed decrease is larger in case of the blends without kaolin (Fig. 2, curve *3*) and low CPE content. For the blends containing more than 4.0 parts impact modifier the bending strength is about the same for the two types of the blends.

Vicat softening point decreases with the increase of the impact modifier for both the blends with and without filling material (Fig. 3). The decrease is linear, about 2.5° for each 5.0 parts CPE added in the system. At any CPE contents, the blends containing 10 parts kaolin show Vicat softening point values larger then for the blends without filling material (the difference being about 3°).

As expected, the Shore *D* hardness of the compunds containing 10 parts kaolin is higher than for the blends without filling material. The difference is larger at low CPE content and decreases as the proportion of impact modifier from the blends increases (Fig. 3).

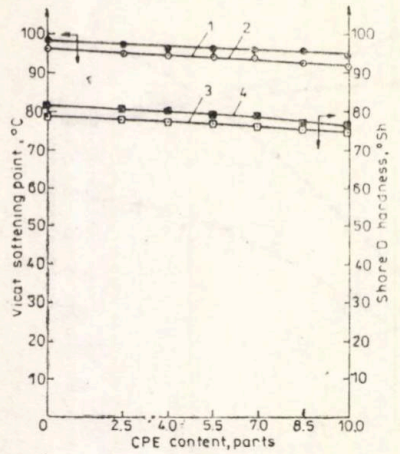

Fig. 3. — Variation of Vicat softening point and Shore *D* hardness versus CPE content from the blends; *1*, *3*— without kaolin; *2*, *4*— with 10 parts kaolin.

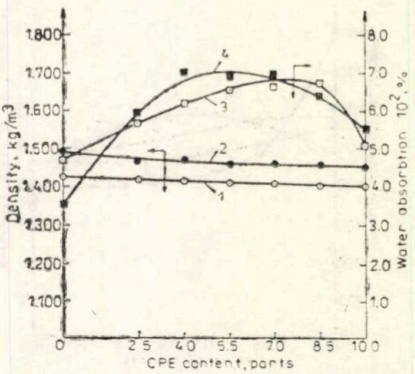

Fig. 4. — Variation of density and water absorption versus CPE content from the beends: *1*, *3*— without kaolin; *2*, *4*— with 10 parts kaolin.

The introduction and the increase of the impact modifier content from the blends, determines a decrease of their hardness. In order to make the blend with 10 parts kaolin, to have the same hardness as the control sample, there must be added about 5.5 parts CPE.

As in the case regarding the hardness characteristic, the density decreases linearly with the increase of the impact modifier content from the blends (Fig. 4). The blends containing kaolin have a larger density as compared with those without filling material; by the introduction of 10 parts CPE, only about 50% of the density increase brought about by the kaolin addition is compensated.

The curves which reveal the variation of water absorption versus CPE content from the blends show maxima at different positions, depending on the blend type. In case of the blends without kaolin, the maximum of water absorption is recorded at 8.0...8.5 parts CPE. The introduction of 10 parts kaolin in the blends determines a shifting of the maximum towards lower CPE content, of about 4.5...7.0 parts (Fig. 4).

The bursting pressure, calculated for heavy pipes of 110 mm outer diameter (*D*), correspounding to blends without filling material, decreases as the CPE content increases. The decrease is less significant at low impact modifier content and becomes appreciable for larger CPE proportions, introduced in the blends (Fig. 5).

By the addition of 10 parts filling material in the blends, the trend of the curves showing the variation of the bursting pressure against the CPE content considerably changes. Although for these blends the bursting pressure decreases too, as the impact modifier content from the blends increases, the decreases is larger at lower CPE content and almost unsignificant, for high proportions of its addition (Fig. 5).

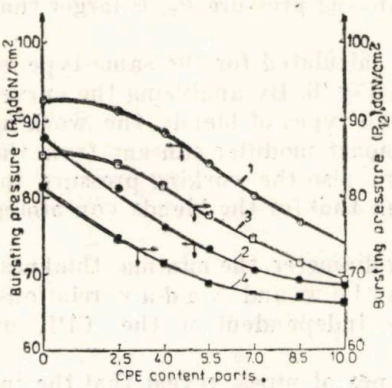

Fig. 5. — Variation of bursting pressures versus CPE content from the blends: *1*, *3* — without kaolin; *2*, *4* — with 10 parts kaolin.

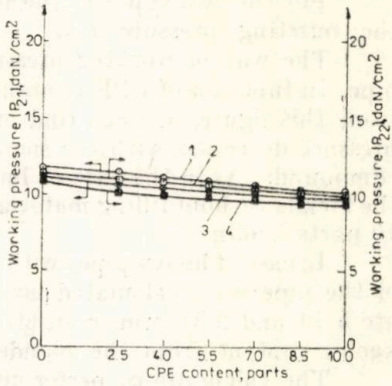

Fig. 6. — Variation of working pressures versus CPE content from the blends: *1*, *3* — without kaolin; *2*, *4* — with 10 parts kaolin.

Table 1

Pressures, [daN/cm²] / CPE content, parts by weight	Blends without kaolin				Blends with 10 parts kaolin			
	P_{11}	P_{12}	P_{21}	P_{22}	P_{11}	P_{12}	P_{21}	P_{22}
Heavy pipes of 50 mm outer diameter, $p^*=3.7$.								
0.0	102.1	93.7	14.6	13.4	128.6	118.0	17.4	16.9
2.5	100.6	92.4	14.3	13.2	95.3	93.2	13.5	13.2
4.0	97.4	89.5	13.9	12.8	89.0	81.8	12.7	11.5
5.5	92.4	85.0	13.2	12.2	81.9	75.2	11.9	10.9
7.0	88.2	80.9	12.6	11.7	81.6	74.9	11.7	10.7
8.5	84.9	78.0	12.1	11.1	81.2	74.6	11.6	10.6
10.0	81.9	75.1	11.7	10.7	80.5	74.0	11.5	10.5
Light pipes of 110 mm outer diameter, $p^*=2.2$ mm								
0.0	23.9	23.4	3.5	3.4	29.9	29.2	4.3	4.2
2.5	23.7	23.1	3.4	3.3	25.3	24.1	3.4	3.2
4.0	22.8	22.3	3.3	3.2	20.9	20.4	2.9	2.9
5.5	21.7	21.2	3.1	3.0	19.6	19.8	2.8	2.8
7.5	20.6	20.2	2.9	2.9	19.2	18.9	2.7	2.7
8.5	19.9	19.5	2.8	2.8	18.9	18.7	2.6	2.6
10.0	19.1	18.8	2.7	2.7	18.7	18.5	2.5	2.5
Light pipes of 50 mm outer diameter, $p^*=1.8$ mm								
0.0	45.1	43.4	6.5	6.4	56.4	54.3	8.1	7.8
2.5	44.5	42.8	6.3	6.1	44.5	43.1	6.5	6.6
4.0	43.0	41.4	6.1	5.9	39.3	37.8	5.6	5.4
5.5	40.1	39.4	5.8	5.6	37.2	35.3	5.4	5.0
7.0	38.9	37.5	5.6	5.4	36.2	34.9	5.2	4.8
8.5	37.5	36.1	5.4	5.2	35.6	34.2	5.1	4.7
10.0	36.1	35.7	5.2	4.9	35.3	34.1	5.0	4.6

For the two types of the blends, the bursting pressure P_{11} is larger that the bursting pressure P_{12}.

The way of working pressure variation calculated for the same type of pipe, in function of CPE content, is shown in Fig. 6. By analyzing the curves from this figure, one can find out that by both types of blends, the working pressure decreases with the increase of the impact modifier content from the compounds. As in the case of bursting pressure, also the working pressure for the blends without filling material is larger than that for the blends containing 10 parts kaolin.

In case of heavy pipes with 110 mm outer diameter, the minima thickness of the pipe wall, calculated according to B a r l o w and N a d a y relations, are 5.74 and 5.31 mm, respectively, and are independent of the CPE or kaolin content from the blends.

The calculations, performed for other types of pipes, reveal that the influence of CPE content on bursting and working pressures is about the same, but the values of these characteristics are different for each type of pipe taken into account (Table 1).

The minima thickness of the pipe walls, calculated with B a r l o w and N a d a y relations, are 2.59 and 2.38 mm for heavy pipes of 50 mm outer diameter, 1.54 and 1.51 mm for light pipes of 110 mm outer diameter and 1.26 and 1.21 mm for light pipes of 50 mm outer diameter.

4. Conclusions

By the analysis of the influence of te kaolin content and the additions of chlorinated polyethylene on the characteristics of the unplastified PVC blends, it was found out that the compounds containing 2.0...4.0 parts impact modifier have the most favourable physical and mechanical properties. The decrease of the physicul and mechanical characteristics, brought about by the kaolin introduction, is somewhat compensated by the addition of the chlotinated polyethylene.

Received, October 28, 1988

Polytechnic Institute, Jassy,
Department of Organic and
Macromolecular Chemistry and Technology

REFERENCES

1. G ä c h t e r R., M ü l l e r H., *Plastics Additives Handbook.* Hanser Publishers, New York, 1985, 361.
2. H o r u n S., *Aditivi pentru prelucrarea polimerilor.* Ed. Tehnică, Bucureşti, 1978, 172.
3. B u c k n a l l C.B., *Toughened Plastics.* Applied Science Publ. Ltd., London, 1977.
4. *** *CPE Resines for Impact Modification of Rigid PVC.* Dow Chemical Prospectus, SUA.
5. R u s u M., P e t r a r u F., G r ă m e s c u L., Angew. Makromol. Chem., **144**, 193 (1986).
6. R u s u M., P e t r a r u F., G r ă m e s c u L., L u n g u M., Acta Polymerica, **38**, *5*, 286 (1987)
7. R u s u M., L u n g u M., P e t r a r u F., G r ă m e s c u L., N i c u M., Acta Polymerica, **39**, *5*, 248 (1988).
8. R i t c h i e P.D., *Plasticisers, Stabilisers and Fillers.* Iliffe Book Ltd., London, 1972.
9. K a t z H.S., M i l e w s k i V., *Handbook of Fillers and Reinforcement for Plastics.* Van Nostrad Reinhold Co., New York, 1978, 107.

10. Titow W.V., Lanham B.J., *Reinforced Thermoplastics*. Applied Science Publ. Ltd., London, 1975.
11. Rusu M., Petraru F., Grămescu L., Mater. Plastice, **23**, *2*, 99 (1986).
12. Rusu M., Petraru F., Grămescu L., Lungu M., Mater. Plastice, **24**, *1*, 23 (1987).
13. Lungu M., Rusu M., Petraru F., Grămescu L., Mater. Plastice, **24**, *4*, 206 (1987).
14. *** Sekisui Chemical Company Ltd. Prospectus, Japan,
15. Липатов Ю. С., Пластические массы, *11*, 6 (1976).
16. Сагалаев Г. В., Пластические массы, *11*, 17 (1976).

AMESTECURI DE POLICLORURĂ DE VINIL

VI. Proprietăţi fizico-mecanice

(Rezumat)

S-a studiat influenţa adaosurilor de polietilenă clorurată asupra caracteristicilor fizico-mecanice ale amestecurilor neplastifiate de PVC, cu şi fără ados de caolin.

Rezultatele obţinute evidenţiază faptul că cele mai favorabile caracteristici le au compoundurile conţinînd între 2,0...4,0 părţi polietilenă clorurată. Pentru aceste compounduri, modificarea nefavorabilă a proprietăţii fizico-mecanice, determinată de introducerea caolinului, este, în parte, compensată de adaosul de polietilenă clorurată.

THE ANTIBIOTICS PLANT, JASSY
RO — 6647, JASSY, ROMANIA

Established more than three decades ago the antibiotics plant in Jassy has got a good reputation for its production programm which incorporates the most important antibiotics obtained by biosynthesis, semisynthesis and chemical modification, steroidic hormons, extracts from plants and pure substances obtained from plants toghether with numerous galenic forms, veterinary drugs and growing stimulants for animals.

All fabricaton processes, equipment and personnel comply with GMP rules. The development, production and tests providing the quality of our pharmaceutical products, represent important components of one of the most complex and advanced industries of the world. The necessary intelligence for maintaining these functions calls for a high calification in several technical and scientific branches of knowledge. As well known the quality control is an important request for a high quality of products, and becomes still more important in the fabrication of antibiotics.

A set of requests for the Good Medical Practice (GMP) and Good Laboratory Practices (GLP) has been worked out and published, under the care of Experts Commitee OMS, which has recomanded to all member countries to adopt and to apply the proposed rules, also the schemes of certification. The Antibiotics Plant from Jassy complies with all GMP and GLP requests in the drug control, promoting „the general effort of the OMS in obtaining the highest level of health in the world". By doing this we export our products in more than 30 countries all over the world.

Among the exported drugs let us mention : G, K and Na-Penicilline, Penicilline V, Tetracicline, HCl-Tetracicline, Oxitetracicline, Nystatine, Grizeofulvine, Streptomicine, Meticilline, Ampicilline $3H_2O$, injectable Na-Ampicilline, peroral and injectable Oxacilline, Eritromicine, Lactobionate, Propionil Eritromicine, Carbenicilline, Aminocaproic acid and numerous ointments, creams and suppositoires.

As specialities realised in our plant we can mention : Amaxilline, Cefalotine, Zn-Pacitracine, Calcium Gluconate, Hemoterp, Metronidazol suppositories, Indometacin as ointment, Trimagant, Rutin S, Brofimen, Lenatozid C, Metilergometrine, Ergotamine tartrate, Ergometrine, Scobutil, Cornhidral, Ergoceps, Variterp, Clofedin suppositories, Piroxipam suppositories, Nitroglycerine ointment, Rombalsam ointment, Propifenazone suppositories and some instant type teas e.g. Instamixt, Sedinstant, Ticiverol, Tarbedol, Diurocist, etc.

Tiparul executat sub cd. 107
la Întreprinderea Poligrafică Iași
str. 7 Noiembrie nr. 49

1990 JUN - 8

40822